Kingston University London

FACULTY OF SCIENCE, ENGINEERING AND COMPUTING

School of Life Sciences and Pharmacy and Chemistry

Implication of Polymer Properties on The Manufacture and Absorption of Soft Contact Lenses Used as Drug Carrier Systems

Shelan Mustafa K0846770

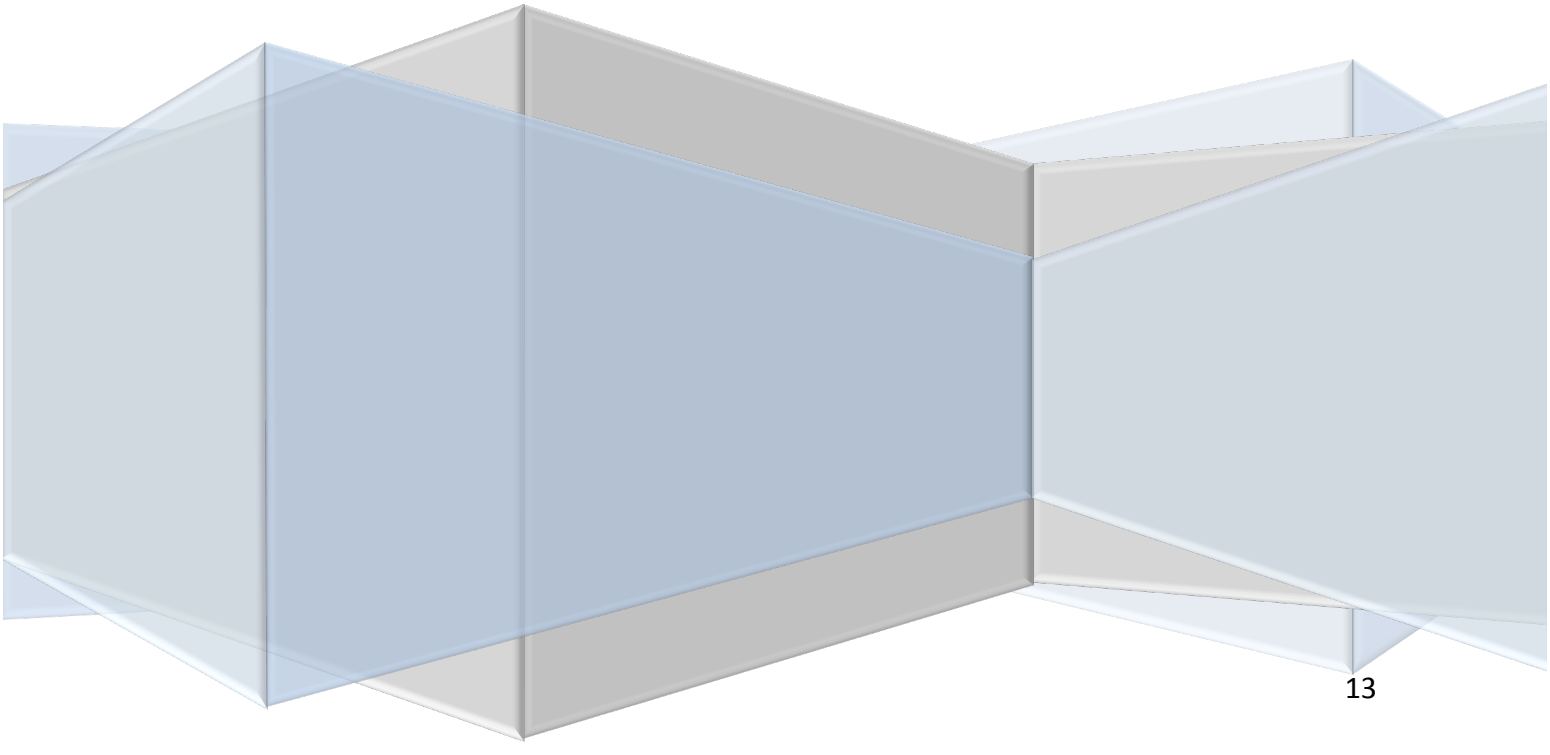

Acknowledgment

Firstly, I would like to express my sincere gratitude to Prof. Raid Alany and Dr Amr Elshaer for their continuous support of my Ph.D study and related research, for their patience, motivation, and immense knowledge. Their guidance helped me in all the time of research and writing of this thesis. I could not have imagined having a better advisors and mentors for my Ph.D study.

My sincere thanks also goes to Dr. Simon Gould and Dr.Simon Demars, who gave access to the laboratory and research facilities. Without they're precious support it would not be possible to conduct this research.

I would like to thank my fellow lab mates Dr Sharan Asher, Dr Amanda Dandagama and Dr Aryan Stanley for the stimulating discussions, and late night working in the lab together before deadlines, and for all the fun we have had in the last four years.

I would like to express my deepest gratitude to husband Raman. This dissertation would not have been possible without his warm love, continued patience, and endless support. Thank you for always encouraging me to work harder and inspiring me to be the best I can be at all times.

Last but not the least, I would like to thank my family: my parents Rashed and Awaz for always encouraging me to pursue my dreams, and being there when I needed motivation and support. Thank you for always reminding me how much I have achieved and how proud I should be. To my sibling Ahmed

and Deren for almost unbelievable support throughout my Ph D journey and life in general. Thank you for always being so positive during stressful times. My family are the most important people in the world and I dedicate this thesis to them.

Abstract

Background: Glaucoma is one of the leading causes of vision loss, where it is found in 2% of the population over the age of 40. It is estimated that more than 500,000 people suffer from glaucoma in England and Wales alone, with more than 70 million affected across the world**.** Conventional treatments start with topical anti-glaucoma medications such as eye drops. Soft contact lenses (SCLs) can substitute eye drops and ocular ointments. They help improve drug bioavailability, residence time and drug delivery to the targeted site, leading to compromised patient compliance.

Aim: This study focused on developing new SCLs using hydrophilic and hydrophobic polymers; which were further investigated as potential carriers for drozolamide hydrochloride (DZH). Surfactants to modulate drug release as well as improve SCL properties.

Experimental: Si-Hy SCLs were prepared via UV-polymerisation. PAA NPs were prepared via ionic gelation using calcium chloride a cross-linking agent; they were incorporated into SCLs. A bacterial adherence study was conducted on the SCLs. The two pathogenic microorganisms investigated were *Staphylococci epidermidis* and *Pseudomonas aeruginosa.* Post SCLs polymerisation characterisation studies were carried out to investigate EWC, CA, TM, YM and in vitro drug release. Ocular toxicity studies (HETCAM and BCOP assays) were undertaken to identify any potential ocular irritation associated with these SCLs.

Results: PDMS-AS displayed the highest EWC% followed by TFMS, PDMS-VT and TRIS. All of these silicones based polymers possessed promising qualities that could be of benefit when preparing SCLs. F-S/A gave rise to the transparent SCLs, whilst PDMS-AS had the highest EWC%. Combining the silicone based polymers with HEMA hydrogel, could potentially eliminate lens-induced hypoxia for SCL wearers, due to the high oxygen permeable nature of siloxane and the hydrophilic HEMA hydrogel will provide the required hydration and comfort for SCL wearers. It was found that polyacrylic acid (PAA) concentration affected the NP size, low PAA concentration proved to be the most promising to achieve the smallest particle size (200nm) and PDI values (0.048). Incorporation of DZH into NPs increased their mean particle size. Entrapment efficiency of DZH was 81%, which is sufficient to achieve a therapeutic dose. *In vitro* drug release studies have demonstrated that this new platform could potentially sustain DZH release, lowering IOP over extended periods of time, beyond what is achieved with conventional eye drops. Bacterial adherence studies revealed that incorporation of P407 aided the resistance of both gram negative and gram-positive bacteria when compared to the controls. Both irritation assays (HET-CAM and BCOP) revealed that the developed SCLs were devoid of potential conjunctiva and corneal irritation.

Conclusion: modified SCLs could be formulated using a blend of silicon and HEMA with improved properties. The carbonic anhydrase inhibitor (DZH) can be loaded into these modified SCLs to achieve sustained drug release and potentially improve patient compliance. Polymeric NPs can be loaded into these SCLs with minimal effect on their properties. P407 surfactant has been shown to be essential to minimise bacterial adherence to the surface of SCLs, hence minimise the chance of microbial keratitis.

Keywords: *IOP, EWC, SCL, DZH, PAA nanoparticles, bacterial adherence, ocular drug delivery, HET-CAM and BCOP.*

Table of Contents

List of abbreviations

Al^{2+}	Aluminum ions
AP	Adenosine monophosphate
API	Active pharmaceutical ingredient
ATP	Adenosine triphosphate
BCOP	Bovine corneal opacity
CA	Contact angle
Ca^{2+}	Calcium ions
$CaCl_2$	Calcium chloride
CaP-NP	Methazolamide calcium phosphate nanoparticles
CL	Contact Lens
CLMK	Contact lens- related microbial keratitis
Dk	Oxygen permeability
DSC	Differential Scanning Calorimetry
EE	Entrapment efficiency
EGDMA	Ethylene glycol dimethacrylate
EWC	Equilibrium water content
FDA	Food and Drugs Administration
Fe^{2+}	Iron ions
FSA	3,3,3-trifluoropropylsilane
GMA	Glycidyl methacrylate
HEMA	2-hydroxyethyl methacrylate
HET-CAM	Hen's Egg test-chorioallantoic membrane

HMPP	2-hydroxy-2-methylproiophenone
IOP	Intraocular pressure
MAA	Methacrylic acid
Mg^{2+}	Magnesium ions
min	Minute
MK	Microbial keratitis
mL	Millilitre
MMA	Methylmethacrylate
nm	Nanometer
MPa	Megapascal
mN/m	Newton-meter
mV	Millivolts
NaOH	Sodium Hydroxide
NPs	Nanoparticles
NVP	N-vinyl pyrrolidone
OD_{600}	Optical density
PAA	Polyacrylic acid
PBS	Phosphate buffered saline
PDI	Polydispersity index
PDMS-AS	Poly(dimethoxysilane) co-alkyl siloxane
PDMS-VT	Poly(dimethylsiloxane) vinyl terminated
PDMS	Poly(dimethoxysilane)
PEO	Poly (ethylene oxide)

pHEMA	Poly (2-hydroxyethyl methacrylate)
pM	Picomolar
PMMA	Poly methylmethacrylate
POE	Poly (oxyethylene)
PP_i	pyrophosphate
PPO	Poly (propylene oxide)
P407	Poloxamer 407
RLU	Relative Light Units
SCL	Soft contact lens
Si-Hy	Silicone hydrogel
SEM	Scanning Electron Microscopy
TEGDMA	Tetraethylene glycol dimethacrylate
TMFS	3,3,3 trifluoromethoxysilane
TGA	Thermogravimetric Analysis
TM	Transmission
TRIS	Trimethylsiloxy saline
UV	Ultraviolet
v/v	Volume per volume
w/v	Weight per volume
w/w	Weight per weight
YM	Young's modulus
ZN^{2+}	Zinc ions
µL	Microliter

µg	Microgram
λ	Lambda max

Introduction

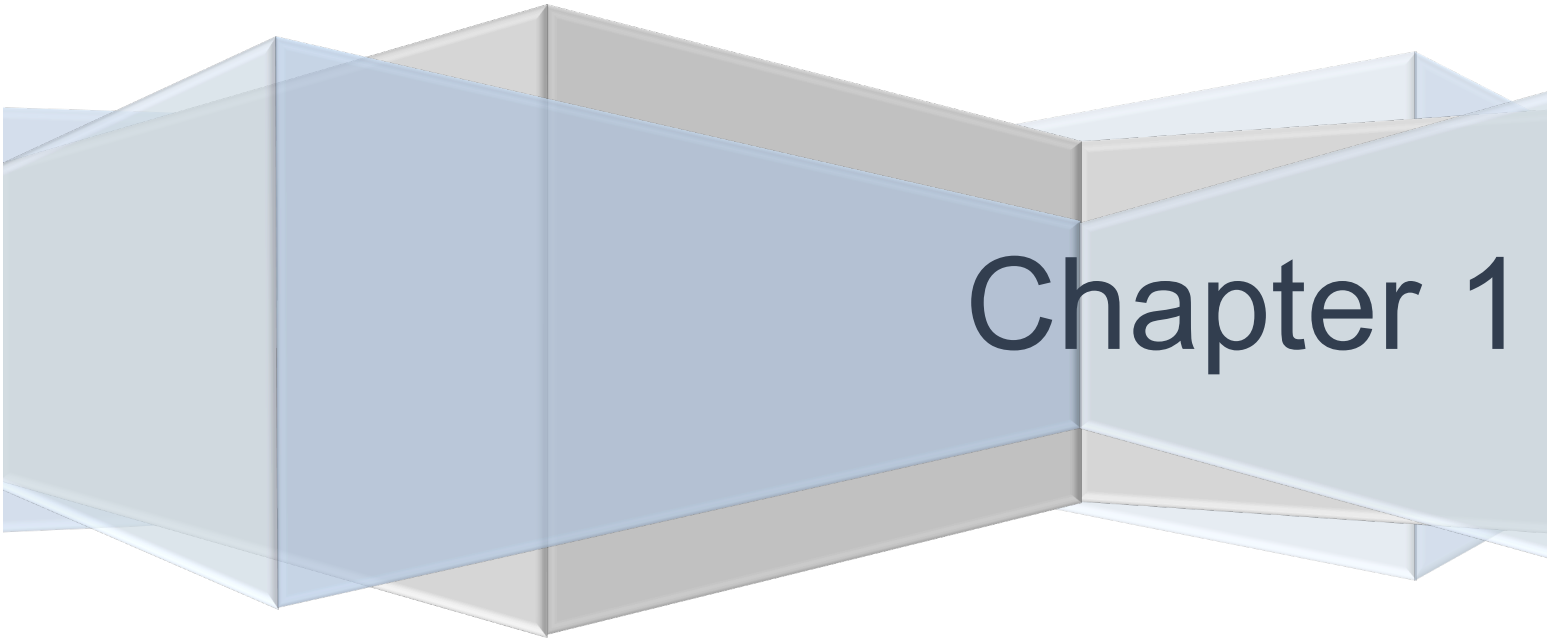

Chapter 1: Introduction

1.1. Anatomy of the human eye

The eye is a very unique and valuable organ that is made of vital components that plays a substantial role in sight. The protective structure of the eye composed of eyelid and sclera, the anterior segment of the eye composed of cornea, iris, aqueous humour, crystalline lens and ciliary muscle. The posterior segment of the eye composed of, retina, vitreous humour and finally optical pathway to the brain composed of the optic nerves (Figure 1.1) (1).

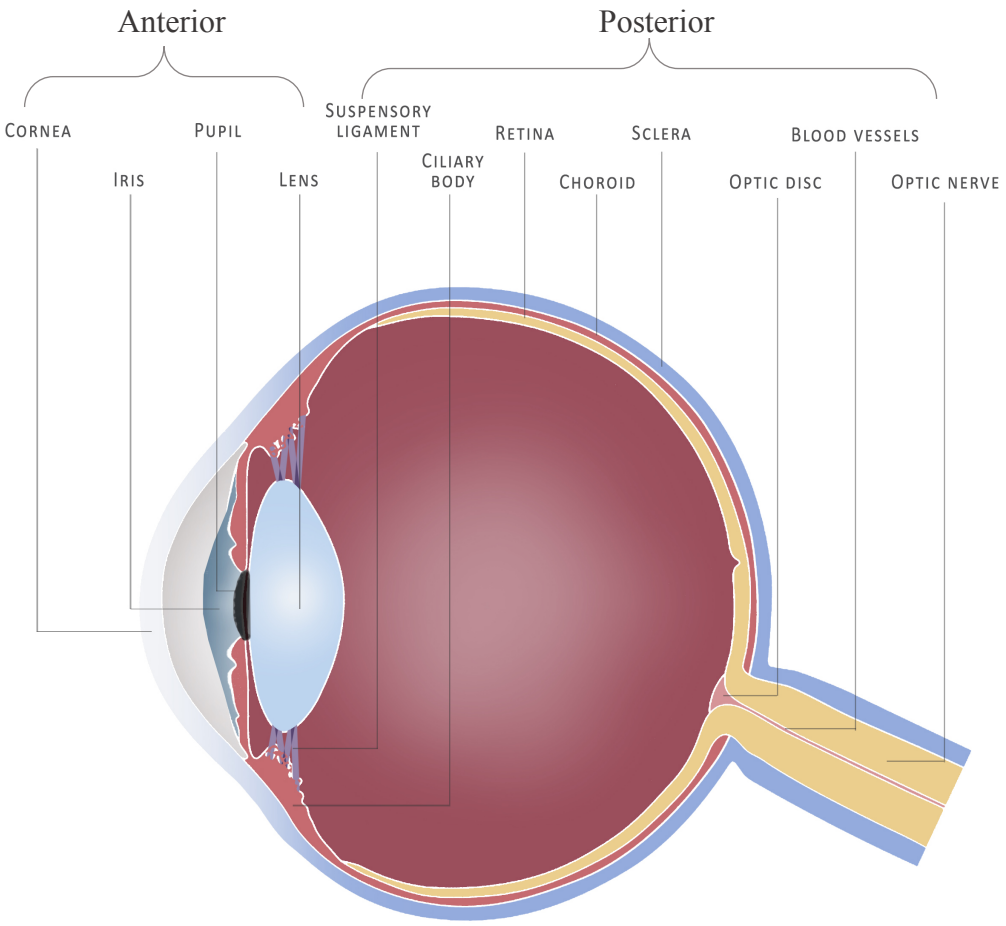

Figure 1.1: Cross section Anatomy of the human eye, adapted from allaboutvision.com (27).

1.1.1. The protective structure of the eye

The upper and lower lids of the eye are composed of tarsal plates, which are cartilage like structure. Together they form an aperture, which is about 30mm, they help provide shape, structure and protection to the eye. Each eyelid has a row of cilia that helps to prevent any foreign particle entering the eye, they also have tear gland that maintain the tear film within the eye. The exposed section of the eye is covered in precorneal tear film of about 10μL and pH 7.4. The sclera is a thick white opaque protective outer layer extending from the cornea to the optic nerve that covers 95% of the eye's surface. Towards the anterior segment of the eye the sclera thins and this gradually thickens towards the posterior segment forming a net like structure at which the optic nerve passes (1,2).

1.1.2. The anterior segment of the eye

Is responsible for focusing images onto the retina, the retina provides the majority of the focusing power and the crystalline lens provides the rest as well as further refining the focus allowing the eye to focus on different objects at different distance. The aqueous humour is a clear fluid that fills the anterior chamber of the eye that lies between the cornea and the crystalline lens; it is produced by the ciliary body. Within the aqueous humour there are blood plasma which helps provide nutrients to the cornea and the crystalline lens (1).

1.1.3. The posterior segment of the eye and optical pathway to the brain

Is lined with a thin tissue layer called the retina that is specialised sensory tissue, also vitreous humour is a transparent gel that is located at the posterior segment of the eye and helps to provide structure and hold the eye in shape. It also provides nutrients to the retina from the ciliary body and the aqueous humour. The optical pathway to the brain is where transmitted chemical and electrical signals initially processed by the retina travels via the ganglion cells that run through the optic nerves and further passed on to the optic tracts which is then transmitted to the visual cortex where the visual process occurs (1,2).

When light rays enter the eye through the cornea a transparent outer layer with a dome shape helps to protect the eye from elements that could cause damage to the inner parts of the eye. The cornea refracts the rays and passes through the pupil, where the iris (coloured part of the eye) contracts and retracts regulating the amount of light taken in, assisting the eye to focus on the objects in line. The light then passes through the crystalline lens (located directly behind the pupil), which changes in shape further bending the rays in order to be transmitted onto the retina. The retina is made up of millions of photoreceptors called rods and cones (3,4). The centre of the retina is known as the macula where all the cones are located, rods on the other had are located on the external part of the macula. Rods help provide a vision in dim light while cones provide sharp vision and detect fine colour and details in the light. The photoreceptors help convert these light rays into chemical and electrical impulses are transmitted onto the optic nerve

whereby it is sent to the visual cortex where by the visual processing takes place (2)(5).

1.2. Anterior segment drug delivery barriers

As a unique organ, the eye (Figure 1.1) is somewhat isolated from the rest of the body due to blood-ocular barriers. The eye is protected by many tissues that act as barriers and prevent substances such as protein and large drug molecules from entering the aqueous humour. The roles of blood-ocular barriers are discussed in detail in following sections.

1.2.1. Conjunctiva- Epithelial tight junction as barrier

The conjunctiva is a thin, transparent vascular tissue that covers majority of the ocular surface. Composed of two layers made of 2-10 sub-layers of stratified epithelial cells and substantia propria (6). Within the conjunctiva there are goblet cells and glands responsible for mucin and tear formation (7,8). The stroma located between the conjunctiva and sclera is rich with lymph nerves and blood posing barrier to hydrophobic drugs (8). The outer epithelial cells form intercellular tight junctions (known as *zonula occlundens*). The tight junctions act as a barrier for high molecular weight hydrophilic drug molecules permeating via paracellular channels (6,8). The conjunctiva possesses efflux pumps P-glycoprotein (P-gp), located on the cell membrane (9). The efflux pumps continuously remove drug from the cell cytoplasm causing a decline in drug concentration thus inhibiting drug transport (8).

1.2.1.1. Tear film turnover / Nasolacrimal drainage

Tear film acts as a protecting layer covering the conjunctiva and cornea preventing dehydration of corneal epithelium layer. The tear film turnover acts as another impeding factor for topical drug permeation (6). Scherz et al, reported that the average tear volume within the cul-de-sac is 7μL, with flow rate of 1.2μL/ min^{-1} (10). Upon topical administration of drug, Bachu et al reported that drug contact time is limited to 1-2 minutes due to the dose high tear efflux, the bioavailability of the drug is significantly reduced (6,8,11). Leaving 10-20% of the drug, some of which can be lost through the nasolacrimal drainage and pre-corneal drainage. Nasolacrimal drainage of the drug occurs via transnasal absorption and further exposure to the systemic circulation (6).Only 5% of the drug available for absorption (8,11).

1.2.2. Cornea as barrier

The cornea is multi-layered and highly sensitive tissue within the eye; it is composed of 5 layers; outer epithelium (lipophilic), bowman's layer, stroma (hydrophilic), descemet's membrane and the endothelium (8). The epithelial cells form tight junctions restricting even small molecular hydrophilic drugs upon topical application (12). Hydrophobic drugs are able to permeate through the lipophilic tight junction channels but will not be able to seep further into the ocular tissues, due to the hydrophilic nature of stroma (8). The endothelium is located between the aqueous humour and stroma allows movements of molecules between the neighbouring compartments (8,13,14). Drug absorption into the aqueous humour occurs via trans-corneal diffusion (Figure 1.2) (8,13). Efflux pumps located on the corneal surface expresses

significant barrier within ocular drug delivery. The efflux pumps present restriction of drug permeation are P-glycoprotein (P-gp), multidrug resistant protein (MRP and ABCC) (6,9). Dey et al, carried out transport studies across human and rabbit cornea as well as rabbit corneal cell line. They confirmed the presence of P-gp efflux pump to be active on cell surface preventing drug diffusion into ocular tissue (9).

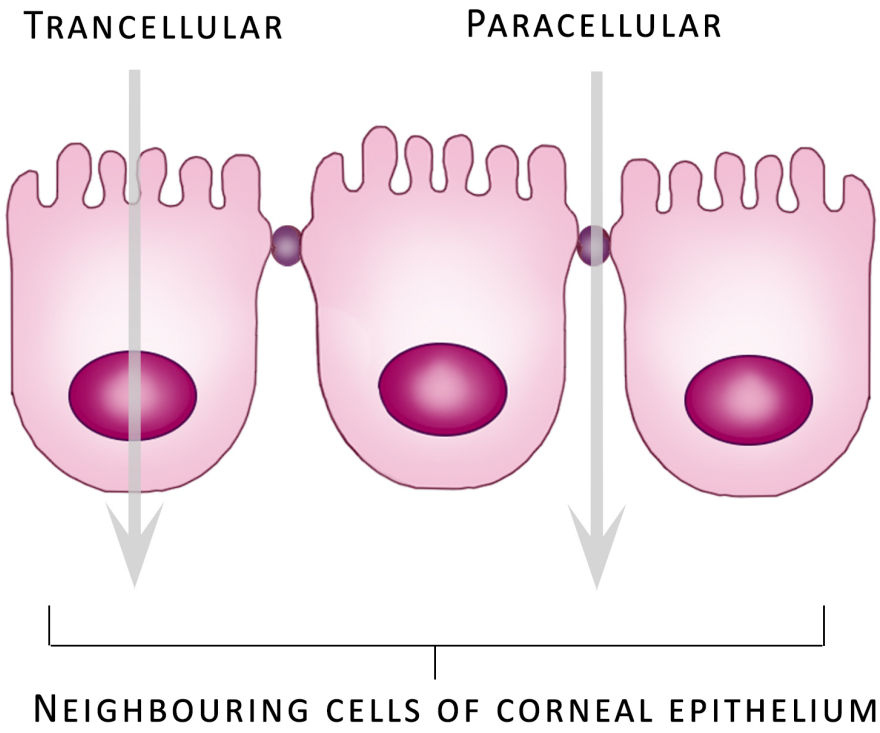

Figure 1. 2: Passive Trancellular and Paracellular transport through tight epithelium junctions (8,13).

When developing ocular drug delivery system, the formulation should possess hydrophilic properties increasing ocular contact time and the bioavailability of the drug within the pre-corneal tear film to improve the permeability of the drug across the various ocular tissues. This is discussed through different approaches within the following sections.

1.3. Diseases of the human Eye

There are many diseases related to the eye some of which have a minor short-term effect while others have long-term effects that could potentially lead to loss of vision. Refractive errors for instance is when the two most focusing structures do not function very well this could be due to the shape of the eye, changes in cornea shape as well as aging of the lens. The most common refractive errors are myopia, hypermetropia, astigmatism and presbyopia. The most common symptom would be blurred vision, eyestrain, halos around bright light and headaches. The ways of correcting these refractive errors would be through laser eye surgery or by wearing contact lenses/ glasses (15). Most common disorders that affect the anterior segment of the eye are including cataract, glaucoma and conjunctivitis. These conditions are mainly treated with topical applications such as eye drops, suspensions and ointments. Within ocular drug delivery topically administered drugs should be able to penetrate through the corneal barrier and into the aqueous humour (8).

1.3.1. Glaucoma

Glaucoma one of the most leading causes of vision loss and it is found in 2% of the population over the age 40. It is estimated that more than 500,000 people suffer from glaucoma in England and wales alone, with more than 70 million people affected across the world (16). Patients with a family history of primary open angle glaucoma are at four times as likely at increased risk compared to those without a family history. There are two main types of glaucoma, primary open angle glaucoma and angle closure glaucoma (16) (17). This type of eye disorder is progressive in nature with no cure, however if detected early current treatment could prevent the disease from advancing.

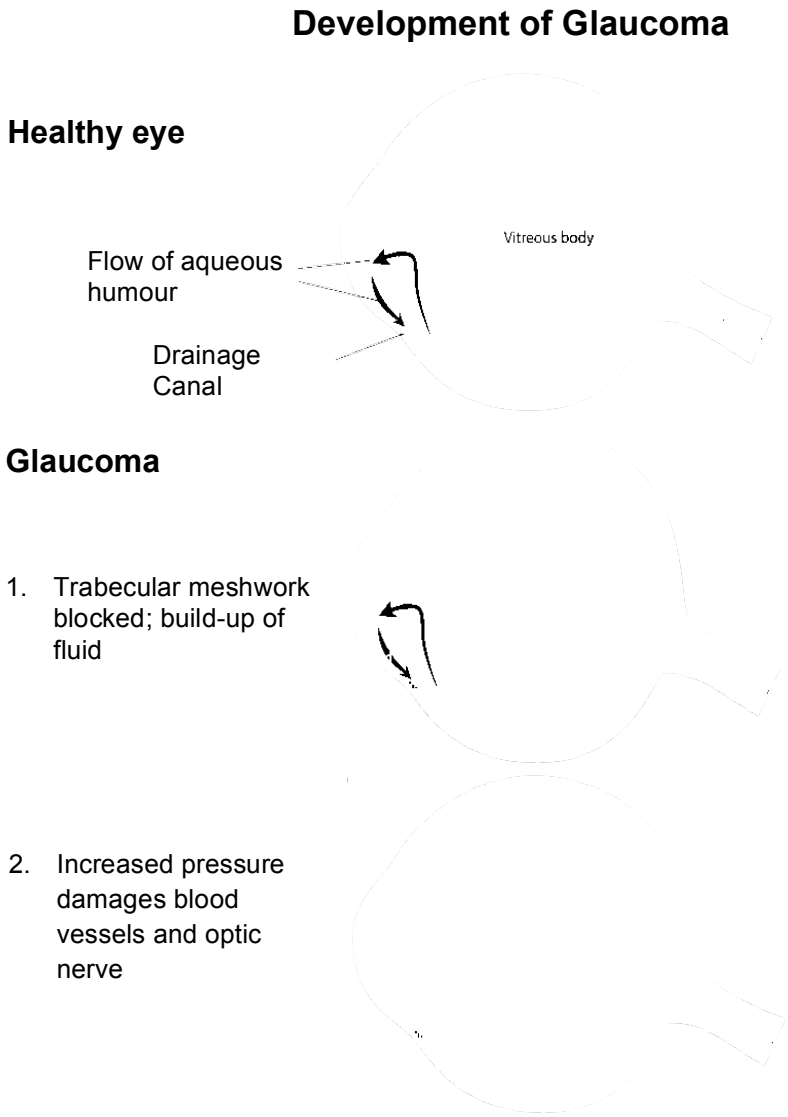

Figure1.3: Represents the development of Glaucoma within the eye. Credit: thelondoneyespecialists.co.uk (17).

Waiting for copyright permission.

1.3.1.1. Primary Open angle glaucoma

Nutrients are drawn from the aqueous humour into the cornea the aqueous humour circulated out of the eye through the trabecular meshwork (drainage), which is between the cornea and iris and replaced by newly formed aqueous fluid. In primary open angle glaucoma, the trabecular meshwork is moderately blocked causing a resistance to the outflow of the circulating aqueous fluid (Figure 1.3). With increase in resistance there will be an increase in pressure due to fluid build-up in the eye, as a result this will cause damage to the optic nerve. Usually there is no pain involved therefore there are no symptoms, and when it does occur it could lead to loss of vision (1,2).

1.3.1.2. Angle closure glaucoma

Also, known as closed angle glaucoma, occurs by the presence of pupillary block causing the iris swell and block the trabecular meshwork between the cornea and the iris, this therefore prevents the out flow of aqueous fluid, and very quickly increasing the intraocular pressure. Some patients are born with narrow trabecular meshwork (drainage angle), which would increase their risk of developing closed angle glaucoma. There are two types of closed angle glaucoma; acute angle-closure glaucoma which occurs abruptly and chronic angle-closure glaucoma which occurs gradually. The symptoms of angle-closure glaucoma are sudden pupil dilation (18)(19).

1.4. Glaucoma treatment option

In America, about 1.1 million people suffer from open-angle glaucoma (20), in England, about 480,000 suffer from chronic open-angle glaucoma (21). Most of these patients are unaware of their disease due to no sign of ocular or systemic symptoms (20). As previously mentioned if left untreated glaucoma could lead to irreversible loss of vision (22). Would lead to increased costs due to both vision rehabilitation and continuous ophthalmology care (23). Glaucoma patients are also at risk of depression, which increases the cost of care and management of the disease (24). Therefore, early detection and immediate treatment is a successful way of preserving sight and avoiding additional costs (25). The current treatment options for the most common type of glaucoma also known as open-angle glaucoma (POAG) will be discussed.

The main role of current glaucoma treatment options is directed at lowering intraocular pressure (IOP). Conventional treatments offered by medical practitioners usually start with topical anti-glaucoma medications. There are multiple types of anti-glaucoma mediations used to reduce IOP. Examples of topical eye drops used as anti-glaucoma therapy include beta-blockers (Timoptic XE®), alpha-agonists (Lopidine®), carbonic anhydrase inhibitors (Trusopt®), and prostaglandin analogues (Lumigan®) (26–28).Table 1.1 presents a summary of various topical eye drops for the treatment of glaucoma (22,29–32). Beta-blockers, reduce IOP by obstructing sympathetic nerve ending in the cilliary epithelium, causing a decline in aqueous humour production (33). Beta-blockers are effective at lowering IOP, they can be

used once or twice a day and they do not affect the size of pupil (20). Beta-blockers are associated with some systemic side effects such as, respiratory, cardiac side effects indicating; decline in heart rate, exacerbation of heart failure, and ocular side effects of decreased ocular blood flow and corneal sensation (27). *Brook et al*, suggested Betaxolol is the beta-blocker of first choice for use due to decreased side effects, however this dose related and should be used with extreme caution with glaucoma patients especially those with a history of respiratory illness (33). Prostaglandin analogues are ocular hypotensive drugs developed for treating POAG. They reduce IOP by increasing the uveoscleral outflow without affecting the aqueous inflow (34). The optimal dose is once a day; prostaglandin analogues are as effective as beta-blockers. They possess ocular side effects such as change in periocular skin pigmentation, and change in iris colour and hyperaemia (20,27).

Table 1.1: Summary of the various topical ophthalmic formulations (29).

Topical Glaucoma Medication Class	Trade name (API)	Mechanism of action	Side effects	Manufacture	References
Beta-blockers	**Timoptic XE®** **(Timolol)**	Reduce aqueous humour production	• Decline in heart rate • Depression • Ocular discomfort • Decrease ocular blood flow and corneal sensation	MERK &CO (New jersey, USA)	(27,33,35)
Prostaglandin analogues	**Lumigan®** **(Bimatoprost)**	Increasing the uveoscleral outflow without affecting the aqueous inflow	• Hyperaemia • Change in colour of iris • Change in pre-ocular skin pigmentation	Allergan (Dublin, Ireland)	(27,34)
Alpha-2 agonists	**Iopidine®** **(Apraclonidine)**	Decreasing aqueous humour secretion and increasing uveoscleral outflow	• Hypotension • Fatigue • Lid retraction • Ocular redness • Pupillary dilatation	NOVARTIS (Surrey, UK)	(27,36)
Carbonic anhydrase inhibitors	**Trusopt®** **(Dorzolamide)**	Reducing aqueous humour formation and lowering IOP	• Ocular discomfort • Irritation • Red eyes	Santen (St Albans, UK)	(27,37)

Alpha-agonists lower IOP by decreasing aqueous humour secretion and increasing uveoscleral outflow (36). They are typically applied 2-3 times a day, however, it is not recommended for long term use due systemic side effects such as hypotension, respiratory and central nervous system depression. Ocular side effects consist of redness of the eye, itching, pupillary dilatation and lid retraction (27). Carbonic anhydrase inhibitors (CAI) are sulphonamide derivatives which inhibit the activity of an enzyme carbonic anhydrase in the ciliary processes of the eye, reducing aqueous humour formation and lowering IOP (37). Examples of CAI are Dorzolmide hydrochloride (DZH) (Trusopt®) and Brinzolamide (Azopt®). Possible side effect includes tingling sensation in fingers and toes as well as recurrent urination. There are many benefits to using DZH, such as having hydrophilic nature also its currently available in the market as ophthalmic eye drops of 2% (31,38). DZH topical CAI have limited side effects (Table 1) (37). They are typically applied twice daily (20). These anti-glaucoma medications are also used as combination drugs to improve compliance (20,34,37).

1.5. Limitations of eye drops as ocular drug delivery systems

Topical ophthalmic administration accounts for 90% of the ocular drug delivery market. These ophthalmic formulations have short residence time and limited bioavailability where only 5% of the administered drug is administered into the cul-de-sac, the rest is drained away due to rapid tear flow and the nasolacrimal drainage, and it can also reach systemic circulation causing some side effects (6,11,39). Soft contact lenses (SCL) have received an enormous amount of attention due to their ability to act as a geometric barrier preventing drug diffusion into the tear fluid, thus prolonged drug action as well as residence time and increasing drug bioavailability, patient compliance and finally reducing the number if any of the side-effects (40,41).

Patel et al, studied several types of ocular drug delivery systems. They mentioned the most convenient, non-invasive mode of ocular administration being topical eye drops. The eye drop solution provides pulse drug permeation post administration and the concentration of the drug rapidly declines decreasing in pre-corneal residence time and drug bioavailability (39). *Joseph et al,* conducted a study of *in vivo* performance of drug loaded SCL used to treat glaucoma. They developed a drug eluting SCLs for enhanced delivery of Latanoprost for the treatment of glaucoma. The study concluded that Latanoprost easily degrades when exposed to environmental conditions as it has difficulty to penetrate the corneal barriers. *In vivo* results

have demonstrated that the drug loaded SCLs were capable of sustained drug release for four weeks, exceeding drug delivery by eye drops (42). Administration of drug solution to the targeted ocular tissue via conventional topical eye drop has demonstrated some drawbacks initiating the introduction of various carrier systems. Many research has been carried out on ocular delivery using SCL and NPs (39,42). Developing a novel ocular drug delivery system that improves drug residence time in the pre-corneal fluid and drug bioavailability as well as increasing patient compliance.

1.6. Ocular drug delivery via contact lenses

SCLs are medical devices worn directly on the eye, floating on tear film layer on the corneal surface. SCLs are designed to correct refractive errors, and maintain a healthy vision(43,44). SCLs have been widely researched for other applications such as ocular drug delivery.

There are several approaches to drug loading into contact lenses to treat anterior ocular diseases which includes the soaking approach, particle-laden contact lens; nanoparticle encapsulated contact lens, liposome, surfactant laden contact lens and cylcodextrins (44–47). Research studies suggest that controlled and sustained drug release over a long period of time can be achieved via SCL. However, the SCL material must be optimised first before incorporating active drug, in order not to compromise properties such as equilibrium water content (EWC), optical clarity (transmittance) (TM), surface wettability (contact angle) (CA) and material elasticity (Young's modulus) (YM) (48). A detailed discussion on the different methodologies is provided in

a review article displayed in the appendix (contact lenses as drug reservoirs and delivery systems: the successes and challenges) (49).

Contact lenses (CL) could be used to improve the bioavailability of ophthalmic drugs. Many hydrogels have been developed in order to improve the properties of contact lenses. Nevertheless, most of the commercial contact lenses can prolong the drug delivery only for few hours and in order to manufacture a successful contact lens that could sustain the drug release for days, addition of diffusion barriers would be necessary.

1.6.1. Nanoparticle laden soft contact lenses

Nanoparticle systems were described to be in the rage of 10-1000 nm (49), these systems are made of either polymers or lipids, where the active drug is incorporated into the nanoparticles by attaching to surface or integrating into the carrier. The nanoparticles then deliver the active drug to the target site in the body. This section will emphasise the importance of nanoparticles as carrier system for a more effective ocular drug delivery. Nanoparticles could be used to encapsulate an active drug that is then dispersed into the SCL material (Figure 1.4). This will help overcome the limitations associated with conventional ophthalmic formulations, such as poor bioavailability, poor solubility, short residence time due to increased tear influx and lack of drug delivery to the targeted site. The idea is that the nanoparticle carrier protects the drug from SCL material during polymerisation as well as providing resistance during drug release period.

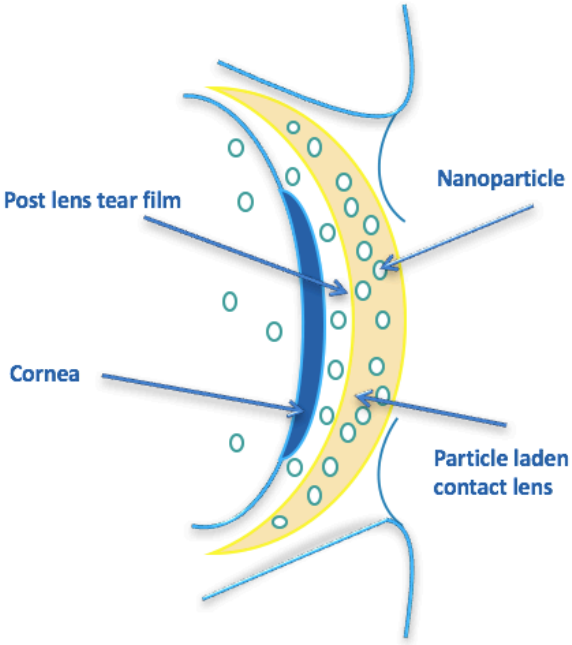

Figure 1.4: Schematic illustration of particle-lade SCL inserted into the eye.

A mixture of hydrogel and silicone polymers, 2-hydroxyethyl methacrylate (HEMA) and Poly (dimethylsiloxane) was used to synthesise the SCLs material via free-radical polymerisation in the presence of cross-linker 2-hydroxy-2-methylproiophenone (HMPP, 97%). Polyacrylic acid (PAA) polymer was used to formulate nanoparticles. The addition of drug-loaded nanoparticles in the polymerisation material will produce particle dispersion in SCL material. Once the SCLs are placed onto the eye the active drug is expected to diffuse from the nanoparticles through the SCL material and into the post-lens tear film located between the cornea and the lens (46). *Creech et al,* reported that use of contact lenses will increase the residence time of the drug in the post-lens tear film, also increasing the drug flux through the cornea (50). The use of nanoparticle laden SCLs provide resistance leading to slow diffusion rates this way continuous drug release is maintained for a long period of time.

Most research has been done on soaking of SCL in drug solution, and insertion into the eye. It can be argued that this approach could improve drug delivery when compared to eye drops, however there are some drawbacks for instance drug loading into the SCL material is limited due the solubility of

the drug. There is limited resistance when delivering the drug, as the drug is only required to diffuse through the SCL material thus decreasing the residence time. Soluri et al used 14 different commercially available contact lenses, to investigate the uptake and delivery of Ketotifen Fumarate. After 24 hours of soaking, the SCLs displayed a burst release and reached plateau within 4 hours. Another study by *Schultz et al*, studied the uptake and release of Timolol Maleate and Brimonidine tartrate via soaking of SCLs in drug solution. *In vitro* release studies displayed an initial burst release of the drug and reaching plateau within 1 hour (51). Even though soaking method is simple and cost effective there are many drawbacks, SCLs have low affinity to the drugs thus hence the burst release leading to poor therapeutic effect (48).

Many researchers proposed encapsulating the active drug within the SCL material, by dissolving the drug in the polymerisation mixture. There are many limitations to this method for instance; hydrophobic drugs possess restricted solubility within HEMA/PDMS-AS polymer mixture. Gulsen et al, suggested that there is no control over drug release timescale when drugs freely dispersed in SCLs, and there is a possibility that the drugs could lose their functionality being involved in the polymerisation reaction (46). In order to overcome these limitations, the drug must be entrapped within a carrier preventing any interaction with the polymerisation material.

Jung et al, developed extended wear SCLs, dispersed with propoxylated glyceryl triacrylate (PGT) nanoparticles loaded with Timolol. *In vitro* release studies display presence of Timolol for a month; also preliminary animal studies in Beagle dogs displayed a decline in intra-ocular pressure (IOP).

This Nano-particulate system showed sustained drug release for a period of time with effective therapeutic effects. However, nanoparticles incorporated into the silicone contact lens material displayed lower ion and oxygen permeability and an increase in YM (52). Another study by *Jung* and *Chauhan*, focused on delivering Timolol via ethylene glycol dimethacrylate (EGDMA) and PGT nanoparticles dispersed in HEMA SCLs. SCLs displayed timolol drug release in phosphate buffered saline (PBS) for 4 weeks. They suggested Timolol delivery was due to the ester bonds linking the drug to the lens material. The results displayed promising effects for extended drug release applications. However a change in YM and EWC was observed with increase in drug loading (53). Thus, optimisation of the SCL and nanoparticle material is crucial in order to avoid compromising any critical properties of the SCL.

1.7. Polymers used to prepare SCL and nanoparticles

1.7.1. Hydrophilic polymers

2-hydroxyethylmethacrylate (HEMA) (Figure 1.5), possesses a hydroxyl functional group as well as a polar ketone group, these functional groups are responsible for the hydrophilic nature of HEMA increasing hydrogen bonding with water molecules thus drawing them into the lens material. Therefore, contact lenses formulated using this polymer will approximately contain 38% water in hydrated state. Since the 1960's HEMA gained extreme popularity and interest in ocular drug delivery research (29,54,55). As already mentioned SCLs were prepared using hydrophilic polymer HEMA, that been successfully used to prepare many of the current marketed SCLs, such as Polymacon by Cooper Vision, Bausch & Lomb and Etafilcon by Vistakon (56). SCLs were formed via free radical polymerisation of different types of polymer combinations producing repeating units of crosslinked polymer chain (57). The SCL material is known to be very soft with little mechanical strength (such as Young's modulus), due to increased equilibrium water content capacity (EWC) (57).

Different polymer combination were used to improve the SCL material, polymers such as methacrylic acid (MAA) and glycidyl methacrylate (GMA) are used to improve properties such as resistance to lipid deposits and increase YM (mechanical strength). MAA was very successful when used in combination of different polymers to form SCLs. The carboxylic acid

functional group was responsible for its hydrophilic nature. It has the ability to obtain approximately 55% EWC thus increasing oxygen permeability rapidly (58). Due to the hydrophilic nature of this polymer it is most likely used to copolymerise with more hydrophobic polymers in order to increase EWC as well as comfort of contact lens.

A series of imprinted hydrogels were introduced HEMA/MAA (59). MAA was used a functional polymer while HEMA acted as the backbone also Dorzolamide hydrochloride (DZH) was used as template drug different MAA with 400 mM molar ratio had the most beneficial effect on loading and releasing properties of hydrogels. Another study evaluated the influence of composition and application of imprinting; soft contact lenses were prepared with and without MAA and Timolol, which was the template drug. They discovered that MAA incorporation increased the loading capacity of Timolol as well as increasing sustained drug release (55,60).

GMA (Figure 1.5) is also a hydrophilic polymer as it has an epoxy side group, methacrylic acid making it the main domain at which hydrogen bonding occurs. *Maldonado-Codina et al*, suggested that this polymer material is stronger than HEMA hydrogels, and when copolymerised with hydrophobic polymer EWC of 30-42% was achieved (54). The EWC of GMA is dependent on the type of copolymerisation, for instance *Rajeev et al,* prepared pH sensitive hydrogels by grafting GMA with anti-inflammatory drugs, such as diclofenac sodium onto chitosan in order to control drug

release. *In vitro* drug release studies showed that GMA had an increasingly positive results for sustained drug release (55,61–63).

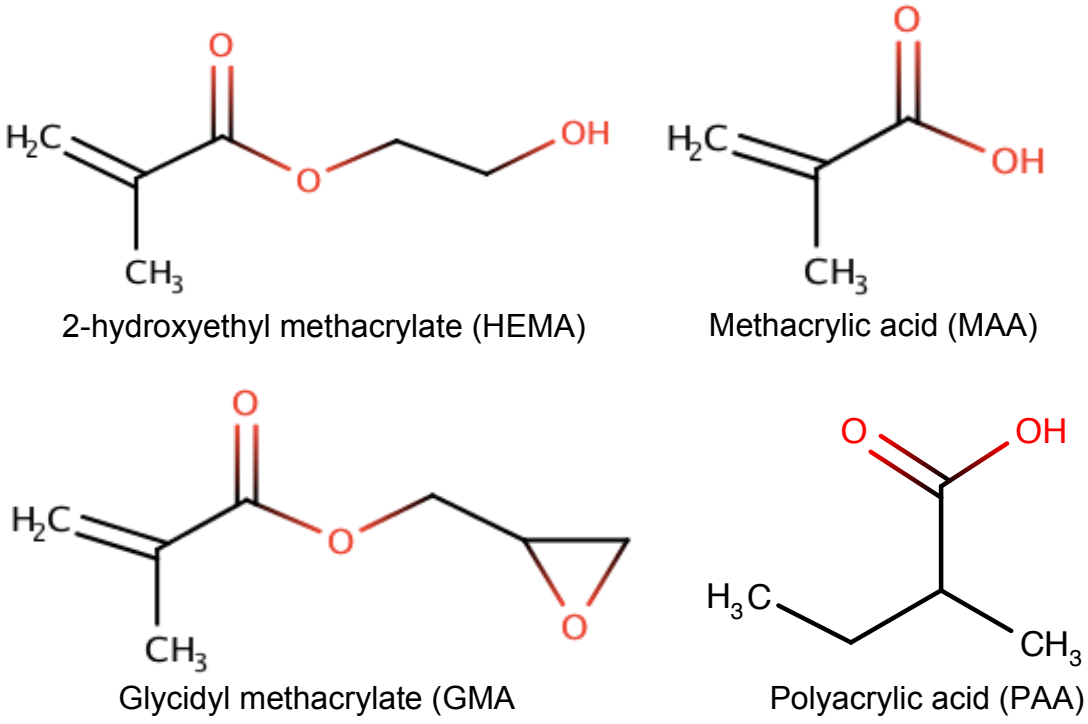

Figure 1. 5: Chemical structures of hydrophilic polymers that are used in the manufacturing of SCLs.

Polyacrylic acid polymer was chosen to formulate nanoparticle carries in this study, due to the many advantages that this polymer possesses. This hydrogel polymer has hydrophilic properties increasing its EWC. PAA is also known as bio-adhesive polymer that can control the permeability within epithelial tissues by relaxing the intercellular junctions (64). Bio-adhesion occurs when polymeric chains interact with epithelial cells forming intermolecular interactions between the entangles chains thus increasing contact time as well as drug concentration in the target site (64). *Greindl et al*, prepared thioloated PAA nanoparticles via ionic gelation. They discovered that the use of Ca^{+2} cross-linker achieved desirable particle size results (220-

300nm), also concluded that PAA nanoparticles remained firm and stable making it promising carrier for ocular drug administration (65).

All the chemical structures of CLs presented in Figure 1.5 possess a double bond C=C, which initiates polymerisation, forming hydrogen and covalent bonds making them increasingly hydrophilic thus highly desirable when preparing SCLs.

1.7.2. Hydrophobic polymers

Hydrophobic polymers are well known for their early use in semi rigid, oxygen impermeable contact lenses, due to their tough nature (66). Hydrophobic polymers are used to increase the strength and elasticity of the contact lens material. However, this will not overcome the lack of oxygen permeability as demonstrated by *Riberio et al* (67). Figure 1.6 below displays a popular hydrophobic polymer used to prepare contact lenses methyl methacrylate (MMA). MMA is used to increase the strength modulus of the contact lens, the methyl groups keep the polymeric chains tight and rigid (68,69). The EWC% of MMA is dependent on the various concentrations used. *Maldonado-Codina et al*, suggested MMA copolymerised with polymer N-vinyl pyrrolidone (VP), showed VP is a hydrophilic monomer this is because of amide side chain enabling many hydrogen bonds thus the EWC of 60-85% (54,68,70). Oxygen permeability is essential to prevent hypoxia. Bausch & Lomb launched silicone hydrogel CLs for daily wear, later Johnson & Johnson's launched Acuvue® Advance silicone hydrogel CLs for extended wear use (58). The idea is to combine both silicone and hydrogel polymers

for more comfortable SCL, increasing the hydration and oxygen permeability of the lens.

1.7.3. Silicone polymers

In order to increase wear time and oxygen permeability, silicone based polymers were used to prepare SCLs. Silicone polymers used on their own are deemed highly uncomfortable due to their tough hydrophobic nature. However, this can be overcome by combining silicone polymers such as Poly (dimethyl siloxane) (PDMS), 3,3,3-trifluoromethoxysilane (TFMS) and Trimethylsiloxy silane (TRIS) with hydrophilic polymers such as HEMA, forming block co-polymers that increase the EWC of the SCLs (58,69,71). All of these silicone based polymers have siloxane groups which interact with oxygen forming Si-O-Si bonds(71). Silicon oxides (Si-O-Si) are the most stable when compared to Si-Si bonds and therefore are most present.

One of the advantages of using silicone hydrogels in SCL is due to the high oxygen permeability, and when wearing CLs it is essential that the eye receives an adequate amount of oxygen from the air and this requires diffusion. However regardless of the high oxygen permeability the polymer is highly hydrophobic and this will instantly cause the patient discomfort and lipid deposition occurs in the eye. Nicolson et al reported that one disadvantages to silicone-based contact lenses would be the build-up of lipids from the tear film. The study suggested that multipurpose solution or surfactants are efficient in preventing and removing lipid deposition on contact lenses (72,73).

A more novel approach is the combination of fluorine and silicone polymers when preparing SCLs. Fluoro-silicone polymers are known to be lipid resistant due to their slippery surface, transparent and is able to reduce the hydrophobic effects displayed by pure silicone polymers (72,74). Lruzubieta et al, tested Lotrafilcon SCLs on 85 patients for 6 months with follow up visits at 1 week, 1, 3 and 6 months. The data collected after each visit had shown minimum surface deposits and patients had highly rated comfort, vision and handling of Lotrafilcon SCLs. The study also concluded that most practitioners would recommend that their patients wearing these SCLs for 1 month extended wear (75).

Xu et al, used silicone hydrogels SCLs to deliver Ketotifen fumarate, they discovered that there was an increased amount of drug loading within the hydrophilic regions and slow drug release from the hydrophobic regions. In *vivo* results displayed sustained drug release for more than 24 hours (55,76–79).

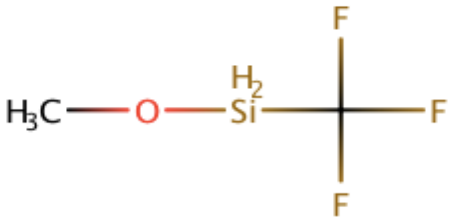

3,3,3-trifluoromethoxysilane
(TFMS)

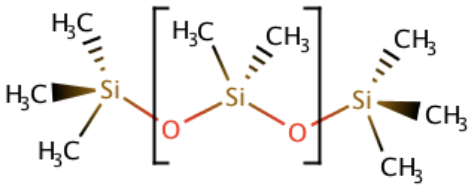

Poly (dimethyl siloxane)
(PDMS)

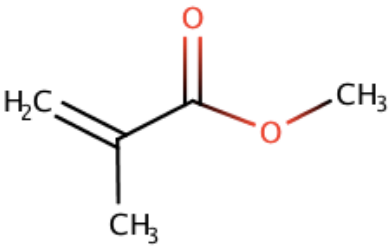

Methyl methacrylate
(MMA)

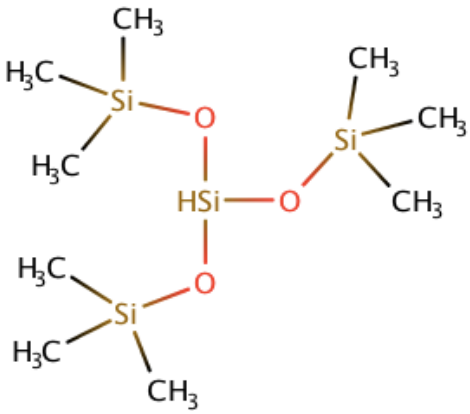

Trimethylsiloxy silane
(TRIS)

Figure 1.6: Chemical structures of different silicone- based and hydrophobic polymer methyl methacrylate (MMA).

1.8. The advantages and disadvantages of CLs as drug delivery systems

Even with current popularity of surgical advances such as laser eye corrections, contact lenses remain to be safe, effective and inexpensive way of improving eyesight. There are many benefits offered by contact lenses over spectacle lenses and refractive surgery due to current advances in technology allowing contact lenses to be increasingly comfortable (79). Thus, contact lenses provide long-term comfort over a long period of time. Contact lenses are also used as potential drug carrier systems, drug loaded contact lenses are able to release active drug over a long period of time. *Kakisu et al* used SCLs to release antibiotics Gatifloxacin and Moxifloxacin, the uptake amount and sustained-release kinetics were monitored. Due to the presence of SCLs antibiotics were released over several days, showing improved penetration into the eye as well as preventing bacterial proliferation. This suggests that use of SCLs prolongs drug residence time as well as drug absorption through the cornea, due to decrease in tear film turnover (80,81).

Guidi et al studied the relationship between dexamethasone absorption using different concentrations of hydrogel and silicone hydrogel SCL material. It was found that silicone hydrogel SCLs had the ability to load more dexamethasone from soaking solutions compared to hydrogel SCLs, as well as extending the drug release duration over 16-days period. The study provided further insight on the optimisation of polymer concentration on

SCL material before drug loading, and this could affect the drug release studies (82)(83).

As discussed contact lenses present far more benefits when compared to conventional ophthalmic formulations, however that is not to say there is no disadvantages to using contact lenses. These impediments are more often due to the lack of knowledge on how to correctly use and store contact lenses. Poor hygiene and maintenance regime, is known to lead to a number of complications such as eye infections, corneal abrasions and loss of sight within contact lens wearers (84,85).

1.9. Microbial Keratitis among contact lens wearers

Microbial keratitis (MK), is a severe inflammation of the cornea with sight threatening potential, if untreated this will result in loss of sight (86). This condition is very rare to the normal eye due to the cornea's natural resistance. None the less the predisposing factors are the following; ocular trauma, contact lens (CL) wear, dry eye, ocular surface disorders and ocular surgery. CL wear is a major predisposition factor for CLMK (contact lens related microbial keratitis); many patients have poor clinical knowledge and understanding of hygiene regimes (87). A study by Bourcier *et al,* discovered that MK was associated with ocular trauma and ocular surface diseases (87). It was discovered that the use of contact lenses had increased the risk of MK by 50%. Bacterial pathogens responsible MK are *Pseudomonas aeruginosa, Staphylococcus aureus (S. aureus) and Staphylococcus epidermidis (S. epidermidis).*

Madhu et al discovered that CL related MK increased over time with increase in soft contact lens wear (SCL). About 45% of corneal ulcers are caused by SCL wear. MK varied tremendously with geographical location, for instance the incidence of this condition varies from 11 per 100,000 for MK to 799 per 100,000 for MK in developing countries such as Nepal (86).

Teo et al carried out an investigation on complications associated with contact lens (CL) wears in Singapore hospital the data was collected between 1999-2001. A total of 953 cases was recorded, 676 of which were

CL wearer (93.7%). The study concluded that out of 73% of CL wearer reported infective keratitis, 24% epithelial keratitis and 18.8% allergic conjunctivitis (88).

Mohamed et al carried out a study analysing 37 patients with MK over a 5-years period, it was discovered that CL wear presents a major predisposing factor for MK. *Pseudomonas aeruginosa (P. aeruginosa)* was widely recognised to cause MK within patient cultures (89). Among the risk factors related to MK CL's wearers constituted the highest number of cases with 35% (Figure 1.7).

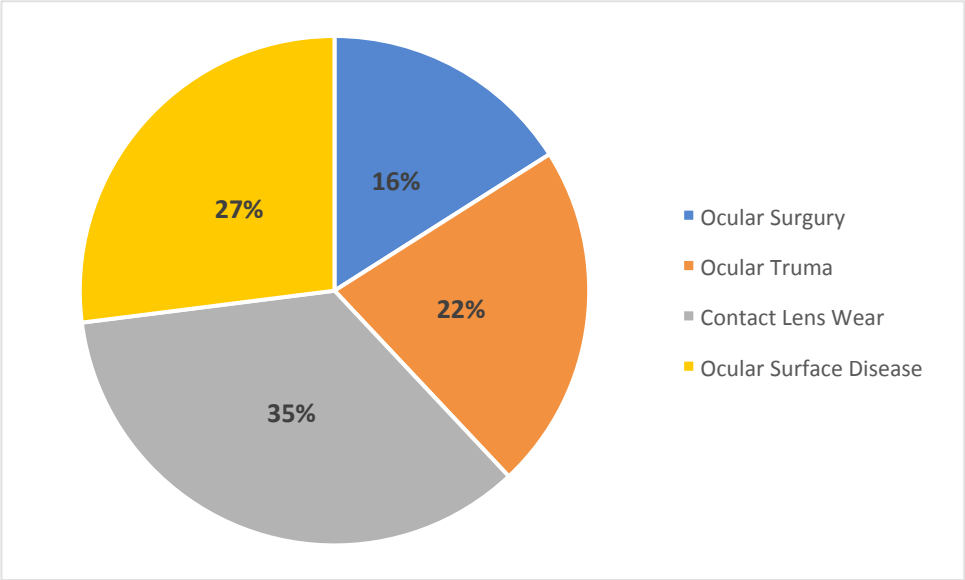

Figure1.7: Predisposing factors associated with microbial keratitis (89).

According to Bruinsma et al, organic matter of bacteria diffuses to the surface of CL immediately after CL becomes in contact with tear fluid. The organic matter that is generally known as conditioning film is where the bacteria will adhere most. Increase in bacterial adherence will eventually

lead to formation of biofilm. *Bruinsma et al* later concluded that CL surfaces dictates the composition of the adsorbed tear fluid based on the hydrophobicity of the CL, and therefore determines bacterial adhesion to CL's (90). Hydrophobic *P. aeruginosa* had the highest number of bacterial adherence to the CL. Dutta et al, came to similar findings, Initial bacterial adhesion is reversible due Van der waals forces and then becomes irreversible as the bacteria has grown to colonize (90,91).

Dutta et al also identified important characteristics that increases bacterial adherence to the ocular surface. Different bacterial strains, hydrophobicity of the bacteria, and the different types of suspension media used in other studies (91). While *Bruinsma et al* studied the roles of hydrophobicity, composition and surface roughness and protein composition of tear films adsorbed on the CL would affect bacterial adherence onto the CL surface (90). As well as characterising bacterial cell surface and its role on bacterial adhesion it is stated that *P. aeruginosa* has hydrophobic surface due to the long polysaccharide chain forming hydrophobic interactions thus adhering to CLs. Bacterial adherence can be reduced if the environment is made less hydrophobic.

Wilcox et al studied the role of bacterial surface on adhesion of both *P. aeruginosa* and *S. epidermidis,* and discovered that even though adhesion of hydrophobic *P. aeruginosa* is more tenacious and that *S. epidermidis* has a similar adherence mechanism to *P. aeruginosa,* expressing polysaccharide adhesion responsible for biofilm formation and adhesion on the ocular surface.

1.10. Role of surfactants to prevent CLMK

Surface-active agents also known as surfactants are composed of both polar (hydrophilic) segment also known as the head and non-polar (hydrophobic) segment also known as the tail these characteristics are illustrated in Figure 1.8. In the perspective of SCL, surfactants are used to reduce surface tension between liquid and solid, and acting as a lubricant in order to minimise discomfort for SCL wearers, acting as a buffer between the finger tips and SCL minimising contamination, it also allows even distribution of tear volume over the SCL. According to *Tran et al*, silicone-based contact lenses are most likely to possess a hydrophobic surface, which is the most suitable environment for bacterial adherence, thus developing ocular infections such as MK (92). By incorporating surfactants into the polymer composition of SCLs, the hydrophobic part of the surfactant would bind to the surface to the SCL, making it hydrophilic and acting as lubricant. Therefore, surfactants are used to improve the stability, biocompatibility and surface wettability of SCL; they could also be used as antibacterial buffer and preventing bacterial adhesion to SCL surface.

Figure 1.8: Schematic structure of surfactants. Showing a hydrophilic head made of polar chemical group and hydrophobic tail made of aliphatic hydrocarbon chain (92).

According to *Sekhon,* there are many uses of surfactants within the pharmaceutical industry such as, solubilisation of hydrophobic drugs in aqueous media, surfactant used for oral and transdermal drug delivery, and as agents to improve drug absorption and penetration, surfactants are also capable of possessing antibacterial properties by disrupting the bacterial cell membrane (93). Mishra et al studied the pharmaceutical applications of several types of surfactants, non-ionic, anionic, cationic, and zwitterionic surfactants (94). Non-ionic surfactants have no electrical charge making them resist water, the hydrophilic head is mainly composed of polyoxyethylene or polyoxypropylene and the hydrophobic tail contains fatty alcohols. Non-ionic surfactants are widely used in ophthalmic formulation due to low toxicity and non-irritant nature. Examples of non-ionic surfactants are Poloxamers, Triton and Polysorbate (94). Anionic surfactants possess a negatively charged head within solution. The hydrophilic head composed of phosphate, sulfonate, sulfate and carboxylates. The hydrophobic tale is a C12-C18 chain. Anionic surfactants are generally used to prepare soaps and shampoos (94).

Cationic surfactants are comprised of a positively charged head, and they work best at low pH as they form a straight hydrophobic chain. Most cationic surfactants are used to prepare disinfectants and preservatives due to their anti-microbial and anti-fungal properties, such as benzalkonium chloride (BAC) and cetylpyridinium chloride (CPC). Zwitterionic surfactants also known as amphoteric possess both anionic and cationic characteristics that

will change depending on the pH of the solution. Due to their mild nature they're commonly used in dermatological products such as cosmetics (94).

Poloxamers 407 (Pluronic® F127) and Poloxamer 188 (Pluronic® F68) are very common non-ionic surfactants used in ophthalmic formulation. Poloxamers are composed of hydrophilic ethylene oxide (PEO) and hydrophobic propylene oxide (PPO) co-polymerised to from tri-block co-polymer (Figure 1.9). Poloxamers share the same chemical structure with difference in the number in PEO and PPO. Research studies have shown many advantages of using Poloxamer 407 (P407) surfactant within ophthalmic preparations, for instance P407 are known to increase the hydrophilicity, prevent bacterial adhesion to SCLs, they are also known as muco-adhesive polymers increasing the bioavailability of the drug in the pre-corneal tissue and finally P407 formulations have shown increased solubility of poorly soluble drugs (6,95,96).

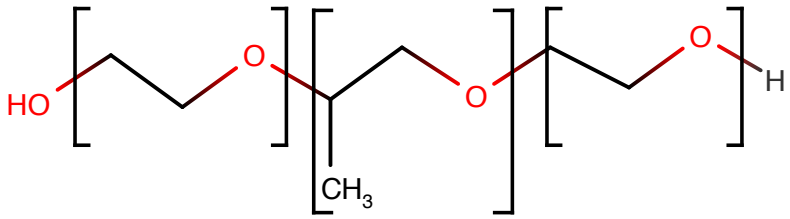

Figure 1.9: Non-ionic surfactant Poloxamer 407 (Pluronic F127), made of ethylene oxide (PEO) and propylene oxide (PPO).

Dumortier et al suggested that P407 displayed thermo reversible properties (liquid state at room temperature and gel state at body temperature) that would help prolong drug release. Pharmaceutical evaluations imply P407

formulation led to increased solubility of poorly water-soluble drugs and prolonged drug release for many applications such as oral, topical, ophthalmic and nasal preparations (96). *Gan et al,* prepared self-assembled liquid crystalline nanoparticles as ophthalmic delivery system of dexamethasone. Ethyl rhodamine B (Rh B) was prepared using monoolein (primary emulsifier for oil in water system) and P407, pre-corneal studies displayed significantly increased pre-ocular retention time and ocular bioavailability of dexamethasone administered Rh B nanoparticles compared to dexamethasone eye drops and carbopol gel (97). *El-Kamel,* carried out *in vivo* and *in vitro* studies to evaluate P407 based ocular delivery system for Timolol maleate. *In vitro* release studies that increases the concentration of P407 used a slow drug release was achieved, *in vivo data* also displayed increased bioavailability by 2.4 fold of the drug in albino rabbits (98).

Conferring *Portoles et al*, a characteristic of P407 polymer is its ability to prevent gram-positive and gram-negative bacteria from adhering to SCLs. The results show that P407 successfully inhibited 90-99% of *Pseudomonas aeruginosa* and 50-60% for *Staphylococcus* strains from adhering to hydrophilic SCLs(95). P407 could also prevent microbial keratitis associated with contact lens wear. *Tran et al*, approves that non-ionic surfactant could prevent bacterial of *Pseudomonas aeruginosa* on silicone-hydrogel SCLs, however they advised that the level of bacterial adhesion was dependent on surface wettability (92). *Garcia-Saenz et al*, supports the findings of *Tran et al*, as it was concluded that bacterial adherence of *Staphylococcus*

epidermidis was most significant for hydrophobic lenses (99). *Miller et al,* and *Cook et al,* had similar findings for *Pseudomonas aeruginosa* (100–102).

1.11. Aim and Objectives of the Thesis

The aim of this doctoral project was to develop a novel ocular delivery system. Using non-ionic surfactants in order to prevent bacterial adherence and improve ocular properties. And disperse drug loaded nanoparticle into the SCLs material to prolong drug release for long period of time and improving drug bioavailability within pre-corneal tear fluid. The specific objectives include:

- To develop and validate a simple, selective and sensitive HPLC method for the quantification of Dorzolamide Hydrochloride in simulated tear fluid. This study is described in ***chapter 3***.
- Study the effect of cross-linker concentration on the properties of SCLs. Evaluate the effect of different hydrogel types and concentrations on the characteristics of SCLs. This study is described in ***chapter 3***.
- Prepare and optimise SCL material using different concentrations and types of silicone-based polymers. In order to understand the level of influence the silicone based polymers possess over SCL properties characterisation studies such as EWC, TM, YM and CA. This study is described in ***chapter 4***.
- Optimise the formulation of PAA nanoparticle, using different concentrations of Ca^{+2} cross-linking agent. Examine the formulated nanoparticle for particle size, surface charge and assess the effect of various variables on the formulation outcome. This study is described in ***chapter 5***.

- Identify the parameters that could affect the PAA nanoparticle preparation. Further assess the potential of the optimised PAA nanoparticle for the particle size, surface charge, loading capacity and *in vitro* release of Dorzolamide Hydrochloride (DZH), as a carrier for anti-glaucoma drug (DZH) dispersed into the SCL material. Quantify the *in vitro* drug release from the nanoparticle loaded SCL. This study is described in ***chapter 5***.
- Evaluate the effect of non-ionic surfactant P407 on the adherence of bacteria *Pseudomonas aeruginosa and Staphylococcus epidermidis* on the surface of SCLs. This study is described in ***chapter 6.***
- Assess the ocular tolerability of the formulated delivery systems, SCLs with and without P407, DZH solution, PAA solution, DZH encapsulated PAA nanoparticles in SCL, via HET-CAM and BCOP assays. This study is described in ***chapter 5 and 6.***

Experimental

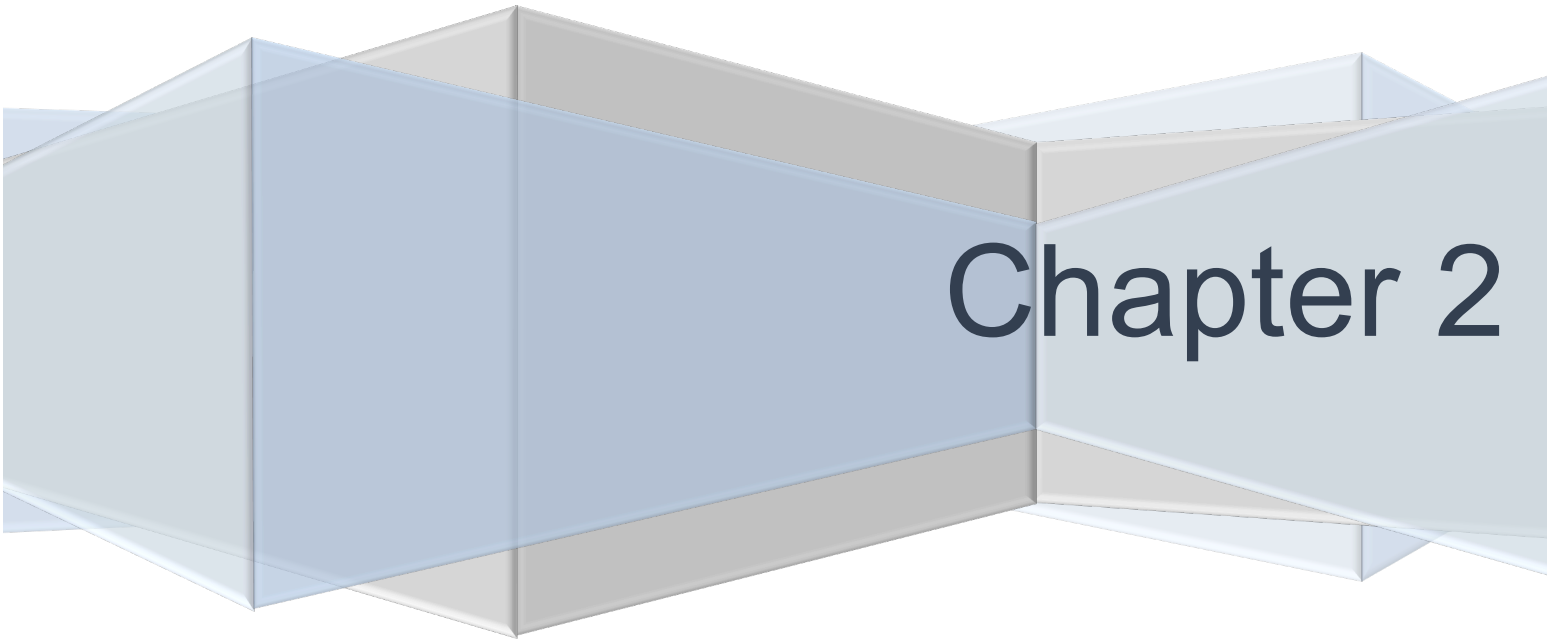

Chapter 2: Experimental

2.1. Reagents and Materials:

Glycidyl methacrylate (GMA),2-hydroxyethyl methacrylate (HEMA), Ethylene glycol dimethacrylate (EGDMA), Poly (dimethylsiloxane), vinyl terminated (PDMS) and (3,3,3- trifluoropropyltrimethoxysilane) (FSA), all were purchased from Tokyo Chemical Industry (TCI, UK). Tetraethylene glycol dimethacrylate (TEGDMA, > 90%) and 2-hydroxy-2- methylproiophenone (HMPP, 97%) were used as cross-linker and photoinitator respectively and were purchased from Sigma Aldrich chemicals (pool, Dorset, united Kingdom). Dorzolamide hydrochloride (DZH) and Poloxamer 407 were purchased from Sigma Aldrich chemicals (pool, Dorset, United Kingdom). For HET-CAM assay: White fertilised hen's eggs were purchased from (Med Eggs (Norfolk, UK), Industrial Methylated Spirit (IMS) ≥ 99% (VWR, Leicestershire, UK), propylene glycol and sodium hydroxide (Fisher Scientific, Loughborough, UK). For BECOP assay: Freshly excised bovine eye was purchased from ABP Food Group, Guilford, UK, sodium hydroxide was purchased from Fisher Scientific, (Loughborough, UK), whilst sodium chloride and fluorescein sodium salt were purchased from Sigma Aldrich (Dorset, UK).

2.2. Dorzolamide hydrochloride quantification:

2.2.1. Chromatographic Condition:

The column used for separation was a Chromolith® Performance RP-18e, 100-4.6 mm column. The mobile phase consisted of mixture of acetonitrile and distilled water (60:40 v/v) respectively. The flow rate of the mobile phase was 1.0 mL/ min. ultraviolet (UV) detection was set to 254nm and the HPLC system was operated at room temperature (25 ± 3°C).

2.2.2. Preparation of mobile phase:

The mobile phase was composed of acetonitrile and distilled water (60:40 v/v). 600 mL of acetonitrile and distilled water were placed into their relevant compartments. An isocratic condition is set whereby the mobile phase was mixed 60:40 ratios upon injection. And this way the mobile phase remains constant throughout the complete HPLC run.

2.2.3. Preparation of stock solution:

A stock solution of Dorzolamide hydrochloride 1mg/ mL was prepared in distilled water as the drug is freely soluble. 25 mg of DZH was weighed and transferred into a 25 mL volumetric flask containing 10mL distilled water. The mixture was sonicated for 15 mins, the rest of the volume is then made up with more distilled water to give the desired concentration of 1mg/mL. The solution was further sonicated for 10mins and was filtered using a what-mann filter paper.

2.2.4. Preparation of standard solution:

A series of diluted solution containing DZH were prepared using the stock solution. DZH with concentrations ranging between 5-200 μg/mL were prepared, these solutions were assayed and quantified using the HPLC.

2.3. HPLC Method Validation- ICH Guidelines

The HPLC validation was conducted as per ICH'S guidance; the developed method was validated in terms of its specificity, linearity, accuracy, precision, detection limit, quantification limit and robustness.

2.3.1. Specificity

Specificity was investigated in order to test the ability of the method to accurately measure, separate and quantify the analyte solutions without any interference from compounds of closely related structures.

2.3.2. Limit of Detection and Limit of Quantification

In order to calculate the limit of detection (LOD) and limit of quantification (LOQ) values, serial dilutions were prepared and analysed by the selected method. The LOD and LOQ was established by evaluating the level of signal to noise ratio of 3:1 and 10:1 respectively, where analytes can be quantified.

2.3.3. Linearity

Linearity of the method was evaluated at different concentration levels of DZH giving analyte solutions over the range of 5-200 μg/ mL. These samples were injected in triplicate and the peak area ratio value of DZH against their respective concentration were inputted and plot calibration curves was generated via Excel® spreadsheet program. LOD and LOQ were calculated at 95% confidence level using "Regression statistics analysis" in Excel with the use of the ICH guideline equations based on the calibration curve: LOD=

3.3*σ/S and LOQ=10*σ/S, where σ is the standard deviation of the response and S is the slope of the calibration curve.

2.3.4. Accuracy

In order to demonstrate accuracy of the recommended method recovery studies were employed. Known concentration of DZH was selected within quality control (QC's) range. Each solution was injected 5 times and the peak area ratio was used to determine the percentage deviation of each concentration.

2.3.5. Precision

Precision was studied in terms of intra-day repeatability and inter-day reproducibility. Both of which were investigated using three different analyte solutions of 7.5, 45 and 150 μg/ mL. The intra-day repeatability was evaluated by injecting the sample solutions 5 times (n=5) from which the peak ratio was calculated. Inter-day reproducibility was tested on three different days by analysing the analyte solutions (n=5) from which the % RSD values were calculated.

2.4. Drug-laden nanoparticle preparation; particle size, zeta potential and morphology of the nanoparticles

2.4.1. Preparation of poly acrylic acid nanoparticles

20 mL of poly acrylic acid (PAA) were formulated at 0.1%, 0.5%, 1.0% and 2% (w/v). The pH of PAA solutions was adjusted to pH8 using 2.25M of sodium hydroxide solution. PAA nanoparticles were produced using $CaCl_2$ as a cross-linker. $CaCl_2$ solutions were prepared at (50 mg/ mL) in 10 mL. The $CaCl_2$ solution was added drop wise to the PAA solution with consistent stirring, until the solution turned turbid, at which the amount of $CaCl_2$ was measured. This was repeated for all four PAA solutions.

The prepared nanoparticles were characterised using scanning electron microscopy (SEM). 0.1% of PAA observed the best results and therefore was further optimised by titration against 4mL, 8mL and 10mL of $CaCl_2$. Using different concentrations of $CaCl_2$ to formulate PAA nanoparticles allowed us to further analyse changes in particle size, and surface charge of PAA nanoparticles.

2.4.2. Preparation of DZH loaded poly acrylic acid (PAA) nanoparticles

0.1% of PAA solution was prepared using 57μL of PAA in 20mL of distilled water; the solution was left stirring at room temperature until it was completely homogenous. NaOH (2.25M) was added drop wise to adjust the

solution to pH8. The solution was then split into 2×10 mL in each beaker, 10 mg of Dorzolamide hydrochloride was weighed carefully and added to one of the 10 mL beaker, the mixture was thoroughly stirred for approximately 30 mins, later 2 mL of $CaCl_2$ was added drop wise while the mixture was under constant stirring at room temperature. The second beaker was used as a control the same procedure was repeated however no drug was added.

2.4.3. Preparation of contact lenses with DZH loaded nanoparticles

Three formulations were prepared with Group A SCLs are control lenses which contained PAA nanoparticle solution, group B contained the drug loaded PAA nanoparticles in the lens matrix and finally group C contained drug in the SCL matrix. Carefully 95% of HEMA, 3% PDMS, 1% TEGDMA and 1% HMPP was pipetted into 50mL beaker with continuous stirring at 1000rpm for 30 mins at Room temperature. 600 μL of the homogenous mixture was then injected into the moulds and placed under UV light for 72 hours at 120 mm height to polymerise.

2.4.4. Nanoparticle Particle Size and Zeta Potential Measured

The particle size and zeta potential of the produced nanoparticles were determined using particle size analyser (DLS and ELS system; Malvern Instruments zetasizer Ultra, Malvern Instruments LTD, Malvern, UK). Samples were diluted prior and analysed at 25 °C, the results were then presented at mean value ± (SD) n = 3.

2.4.5. Encapsulation Efficiency Measurement

The percentage (%) of drug encapsulation efficiency within the prepared nanoparticles (NP's) were quantified via HPLC method. The NP's were centrifuged at 20000rpm for 30 mins (ELMI Model: Skyline CM-6MT, ELMI Ltd, Latvia), the supernatant was then weighed. 10 μL of the supernatant was diluted in approximately 5 mL of distilled water, and analysed at 25 °C using HPLC method. The results were presented as mean value ± (SD) n = 3. Percentage entrapment efficiency of drug will help determine how much DZH was loaded into the NP's. Equation (1) was used to calculate % DZH encapsulation efficiency.

$$\textit{DZH Encapsulation Efficiency (\%)} = \frac{(Total\ amount\ of\ Drug - Free\ amount\ of\ Drug)}{(Total\ amount\ of\ Drug)} \times 100$$

Equation 1

2.4.6. Scanning Electron Microscopy (SEM)

The surface morphology of the formulated NP's was studied using scanning electron microscope (SEM, Zeiss Evo50-oxford Instrument, Cambridge, UK). Samples were prepared by spreading a drop of NP suspension onto the specimen stubs, samples were left to dry for 24 hours. Once dried the stubs were then loaded onto a universal specimen holder. The stubs were then coated in a fine layer of gold via sputter coater (polaron SC500, Polaron Equipment, Watford, UK) at 20 mA for approximately 3 minutes under low vacuum with the presence of argon gas, this step helps enable electricity conduction.

2.4.7. Thermal Analysis

Differential scanning calorimeter (Metter Toledo Instrument (Model: DSC822^{e}-, Mettler-Toledo Ltd., Leicester, UK) was used to study polymorphism and phase change behaviour of DZH and NP's in its solid state. 2-3 mg of the sample was weighed and transferred onto an aluminium pan (50 μL), also an empty pan was used as reference both pans were then covered with an aluminium lid. A small hole was pierced through the lid before the samples were subjected to 250 °C heat at a constant rate of 10 °C / min. Each sample was investigated in triplicates (n=3), the thermograms were then analysed using STAR^{e}SW 10.00 software.

2.5. Nanoparticle-Loaded Soft Contact Lens

2.5.1. Preparation of contact lens via thermal polymerisation.

Contact lenses were prepared using 4 different polymers and cross-linker; each polymer was used to prepare approximately 3-11 different composition percentages of polymer and cross-linker, Ethylene glycol dimethacrylate (EGDMA). The different monomer compositions ranged from 10-99% (v/v) such a wide range is used in order to cover as many different part of the polymer as possible. EDGMA cross-linker was used in order to provide both mechanical strength and thermal stability. 6mg of Benzyl Peroxide (BP) was also used in the formulation, as it helps remove or fade the tint on contact lenses increasing optical clarity. Hydration and biotolernce of all the prepared polymers were recorded after 24hr hydration. The polymers that were used; 2-Hydroxyethyl methacrylate (HEMA), methyl methacrylate (MMA), methacrylic Acid (MAA), and glyceryl methacrylate (GMA). This polymer selection provided a variety ranging from non-ionic/ ionic hydrophilic to non-ionic hydrophobic polymers.

Below is a procedure outline with an example of a single polymer composition;

Stage 1: 1 mL and 4 mL (V/V) of EDGMA and HEMA, were measured respectively and transferred into a 50 mL glass beaker and 6 mg benzyl peroxide was then measured and added to the to the solution mixture. The mixture is was left to stir for approximately 10 mins until all benzyl peroxide has dissolved. Once the mixture was completely homogenous the mixture was injected into the cast wells, shown in Figure 2.1 below.

Stage 2: The reaction tray was transferred into thermostatically controlled oven at a set temperature of 80 °C for 3 hours which was further incubated for an extra hour at 100 °C to remove any excess benzyl peroxide.

Stage 3: After incubation the reaction tray was removed from the oven and left to cool for 2 minutes and the samples are then removed from the casting wells. Finally the samples are stored in tight air bags to prevent any swelling, which was later used for testing.

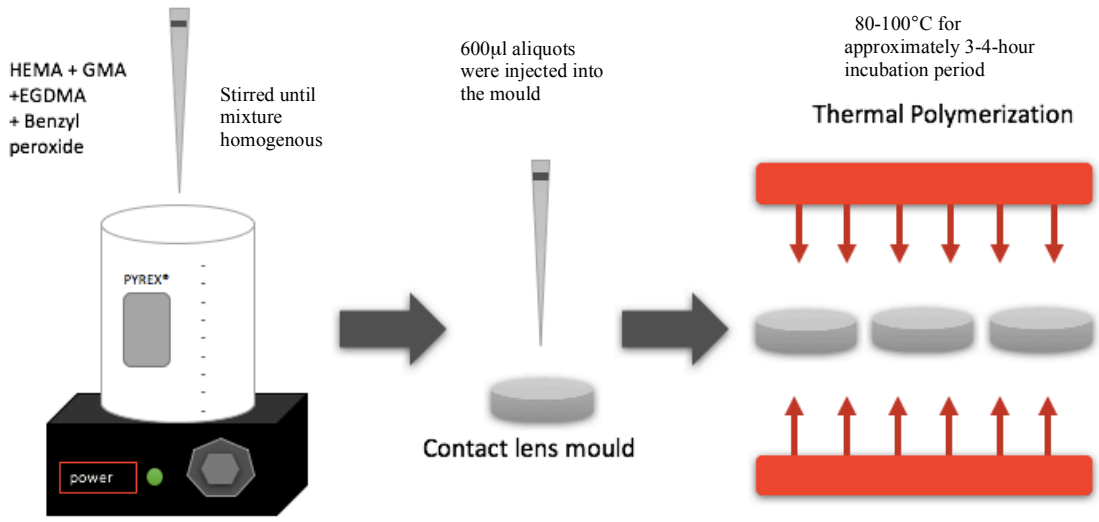

Figure 2.1: Illustration of contact lens formulation via thermal polymerisation.

2.5.2. Contact lens preparation via UV-polymerisation.

Below is a procedure outline with an example of multiple polymer co-polymerisation; 4.5 mL of HEMA, 0.4 mL of GMA, 0.03 mL F-S/A, the cross-linker and photo-initiator were kept constant at 0.5 mL of HMPP and TEGDMA, was all measured and transferred into 50 mL glass beaker the mixture was left to stir for approximately 30 mins. Once the mixture was completely homogenous than 600 µL of the mixture is injected into lens moulds. The sample tray was placed under a UV light at 120 mm height, left to polymerize for approximately 24-48 hours as illustration shown in Figure 2.2.

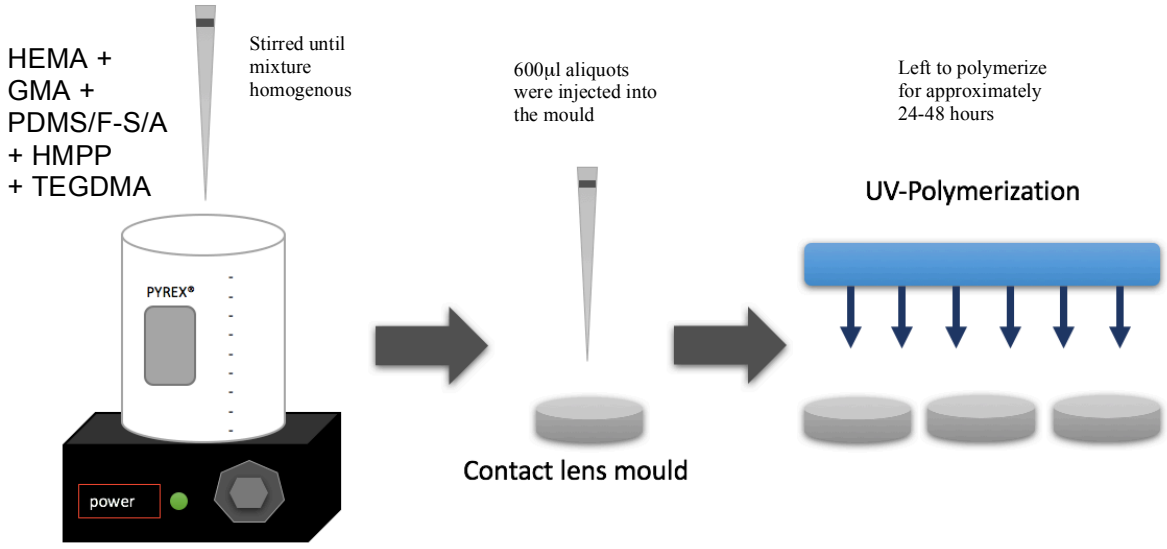

Figure 2.2: Preparation of contact lenses via UV-Polymerization.

Post UV-polymerization the sample tray is removed and the samples are then removed from the lens moulds the samples are stored in tight air bags. A summary of the percentage composition is tabulated in table below for the following results chapter.

2.6. Characterization study of SCL's

2.6.1. Equilibrium Water Content (EWC)

Post SCL polymerisation, hydration testing was carried out via soaking the SCL's in distilled water for approximately 24 hours at room temperature. A record of both dry and wet weights was recorded. The results were presented as a mean value of ± (SD), n = 3. Equation (2) was used to calculate the hydration % within the CL's.

$$\textit{Equilibrium Water Content (\%)} = \frac{Lens\ Wet\ Weight - Lens\ Dry\ Weight}{Lens\ Dry\ Weight} \times 100$$

Equation 2

2.6.2. Contact Angle Measurement

The contact angle measurements were performed using KRUSS DSA30S, (KRÜSS GmbH, Brorsteler Chaussee 85, 22453 Hamburg, Germany). The contact angle was measured using a static sissile drop, after vertically dispensing droplets of deionised water of a specified volume (8 µL), and using a high-tech optical camera the angle from the baseline of the drop to the tangent at drop boundary is easily determined (Figure 2.3). The beauty of using contact angle θ it is efficiently provided solid-vapour and solid-liquid interfacial tensions, due to the ease with which contact angles can be measured on suitably prepared solid surfaces.

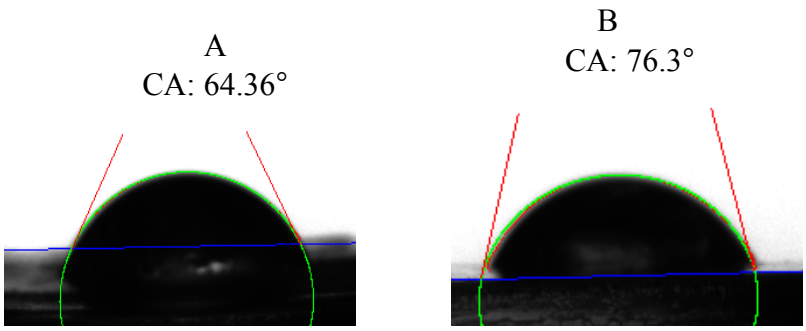

Figure 2.3: Images of CA measurement of DZH within the CL matrix and DHZ NP in CL using sessile drop assay.

2.6.3. Elasticity of Hydrogel Contact Lenses (Young's Modulus)

2.6.3.1. Texture Analysis

TA.XT.plus Texture Analyser (Stable Microsystems LTD, Surrey, UK) was used to measure the tensile strength as well as the elasticity of the SCLs. Post CL hydration the SCL's were then cut into precise dimensions of 25 mm (length), 15 mm (width) and 2 mm (thickness). The sample was then fit in between the mini tensile grip (A/MTG- Mini tensile grip, Stable Microsystems LTD, Surrey, UK), the sample is then stretched vertically until breaking point, each sample was tested three times. The recorded data was analysed on Exponent software (Lite, Stable Micro Systems LTD, Surrey, UK), stress (MPa) and strain (%) of all the tested samples were calculated, those values were then used to calculate the Young's modulus via equation (3) and (4).

$$\textbf{Young's Modulus} = \frac{Stress\ (MPa)}{Strain\ (\%)} \qquad \textit{Equation 3}$$

$$\textbf{Tensile Strength} = \frac{Force\ at\ breaking\ point\ (N)}{Cross\text{-}Sectional\ area\ (mm^2)} \qquad \text{Equation 4}$$

2.6.4. Optical Clarity of Hydrogel Contact Lenses

2.6.4.1. Light Transmission

The transparency of all the SCLs was measured through the extent of light that could travel through the lens, using UV-Spectrometer (UV-VIS (Thermo Scientific, Model: GENESYS^{TM} 10S UV-VIS Spectrometer, Thermo Scientific^{TM}, UK)). The hydrated SCLs were cut into specific measurements of 22 mm (length) and 9 mm (width), that way it would fit precisely inside a UV-cuvette. Light transmission was measured at a visible wavelength of 600 nm (103), as reported by *Gulsen et al,* (46). All the measurements were done in triplicate and data were presented as mean ±SD.

2.7. Bioluminescence ATP Assay

A bacterial adherence study to SCLs was conducted through a method originally proposed by Ludwicka et al (104). The two pathogenic microorganisms used are *Staphylococci epidermidis* and *Pseudomonas aeruginosa* NCTC00950.

2.7.1. Preparation of bacterial suspension

A 100 mL flask of nutrient broth was inoculated with a single colony of the required microorganism. The flask was incubated at 37 °C and continuously shaken using an orbital shaking platform (150 rpm) for 18 hours. After incubation, the culture was then decanted into two 50 mL centrifuge tubes and centrifuged at room temperature for 10 minutes. The supernatant was discarded and the pellet in each cell was suspended in 50 mL of Ringers solution.

2.7.2. Bacterial calibration graph against optical density

In order to produce a bacterial calibration graph, the bacterial density was measured as the optical density (OD_{600}). The bacterial concentration spectrophotometrically adjusted to a high inoculum of 2×10^8 colony forming units (CFU) per millilitre (mL). The bacterial calibration graph is generated by measuring the bacterial density at different dilutions, through optical density (OD_{600}) against bacterial count (CFU/mL). 1 mL of the bacterial suspension was transferred into a UV-quarts cuvette through which the optical density was measured using spectrometer (ThermoSpectronic, UK).

2.7.3. Bacterial plate count

A serial dilution was carried out using well plates, the first six wells were labelled as the following dilutions 10^{-1}, 10^{-2}, 10^{-3}, 10^{-4}, 10^{-5} and 10^{-6}. Each well was injected with a 180 μL Ringers solution and 20 μL of the bacterial solution was injected into the first well. Then 20 μL of the of the solution mixture was transferred into the adjacent wells. Finally, 10 μL of the dilutions were inoculated onto nutrient agar using spread plate method that was then incubated for 24 hours at 37 °C. Plate counts represents the number of bacteria growing into single colonies and are reported as the number of colony forming units (CFU). The CFU were then counted after incubation period.

2.7.4. Standard calibration graph for standard ATP

Within the bioluminescence kit a standard ATP was provided (Sigma, Roche, Germany). The standard ATP was diluted to 990 μL using dilution buffer provided within the bioluminescence kit. A serial dilution was prepared within the range 10^{-6} to 10^{-14} M ATP. A micro-well plate was used to carry out the dilutions where 10 μL of the ATP solution was added to 90 μL of dilution buffer for each dilution. Finally, 10 μL of the luciferase agent was added to each micro-well plate containing the dilutions, which was then immediately subjected to the luminometer (infinite M200 Pro, Tecan) where the luminescence was measured and was represented as the relative light units (RLU).

2.7.5. Bioluminescence and quantification of adherence

The bacterial suspension was then adjusted to 2×10^8 CFU/mL using ringer's solution. The contact lenses were then placed in sterile 6 well-plate with 2 mL of the bacterial solution. the contact lenses were then incubated at 37 °C and continuously shaken for 3 different time points (30 mins, 6 and 16 hour). For every time point a fresh bacterial suspension was prepared. After the incubation period the contact lenses were rinsed repeatedly with ringer's solution in order to detach any unbound bacteria. Using the highly quantitative and sensitive ATP Bioluminescence kit (ATP Bioluminescence kit HS II, Roche diagnostics, Germany), the contact lenses were then soaked in 500 μL of cell lysis reagent, the contact lenses were left soaking in the solution for 1 min, the purpose of this step was to unbound and extract bacterial ATP from the bacteria attached to the contact lenses. The samples were collected after 1 min and subjected to centrifugation for 4 min at 8000 rpm. Bacterial ATP was measured by adding 40 μL of the Luciferase reagent to 160 μL of the supernatant. The light emitted by the system bacterial ATP-Luciferase was measured by luminometer (infinite M200 Pro, Tecan), the data was presented in RLU value from which Log-Log calibration graph of RLU and bacterial ATP concentration (M) was generated to determine the bacterial ATP concentration.

2.7.6. Statistical analysis

Graph-Pad statistical analysis soft wear was used to carry out one-way analysis of variance (ANOVA) followed by paired t-test to analyse the results.

On-way ANOVA tests were carried out to evaluate the difference in bacterial adherence between the different types of contact lenses and to determine a *p* value of <0.05 presenting a significant difference.

2.8. Ocular Tolerability Assay: Hen's Egg Test Chorioallantoic Membrane (HET-CAM) and Bovine Corneal Opacity and Permeability (BCOP).

In vitro Ocular toxicity study

There are many hazards to materials and drugs used in the pharmaceutical industry, that could potentially damage the cornea and even result in irreversible blindness (105). Therefore, ocular toxicity study is required to investigate the risks associated with these materials and Drugs used. Previously *in vivo* Draize testing was developed and used to govern ocular toxicity by applying the test material to a live rabbit's eye and evaluating the biological reaction (2). Originally the Draize testing was approved by the Food and Drugs Administration (FDA) Organisation for Economic Co-oeration and Development (OECD)during the 1940's (105). Over the recent years' alternative *in vitro* studies have been introduced in order to replace live animal testing, which was classed as being inhumane by *Russell et al. In vitro* organotypic models such as the Bovine Corneal Opacity and permeability (BCOP) and the Hen's Egg Test chorioallantoic membrane (HET-CAM) are isolated systems that claims to maintain short term physiological and biological function of human conjunctiva/ cornea (105,108).

Barile, 2010 suggested that results obtained from both HET-CAM and BCOP assays are comparable to those of *in vivo* Draize eye test (108).

The HET-CAM model mimics the conjunctiva within the eye, testing provides information of test Drugs/ materials. According to *Parish, 1985* the CAM is a vascularised mucosal tissue comparable to that of human eye (109). *Barile, 2010* suggested that HET-CAM model was authorised to determine ocular sensitivity and corrosion by U.S EPA (1996), E.U (2001) and UN (2003) (108). The CAM is composed to chorion and allantois (Figure 2.4); the chorion protects the embryo, yolk and other membranes as well as facilitating gas exchange with exterior. Allantois operates by maintaining the viability of the embryos well as facilitating gas exchange (110). Within the HET-CAM model test materials and Drugs are applied onto the CAM where the endpoint is observed based on the changes of the blood vessels in the CAM and scored using HET-CAM irritation score system (Table 2.1). The HET-CAM assay is fast, reproducible and inexpensive way of assessing slight and strong irritants (107,108,111).

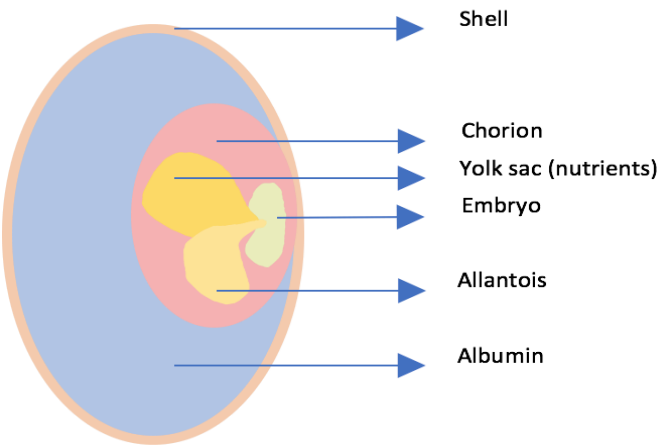

Figure 2.4: Embryonic membranes of chick (110).

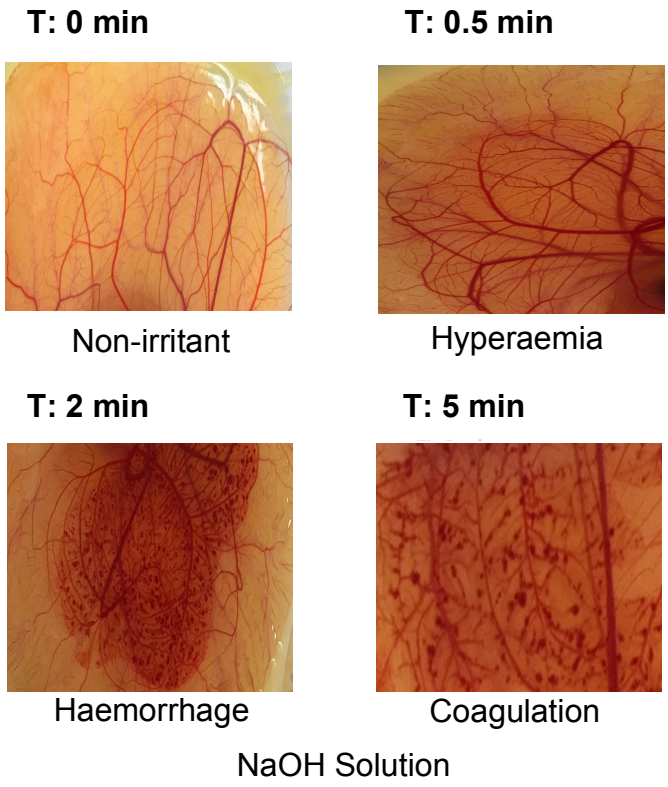

Figure 2.5: CAM Vascular end points to NaOH (0.5 M) strong irritant (+VE control) score irritation within the current formulations at 0,0.5, 2 and 5 mins.

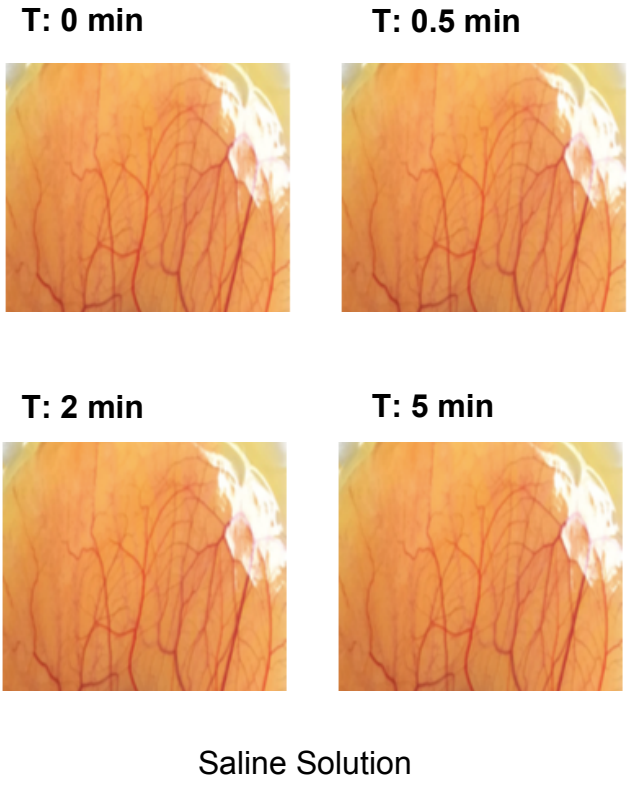

Figure 2.6: CAM Vascular end points of saline solution (0.9%) (-VE control) score irritation within the current formulations at 0,0.5, 2 and 5 mins.

Table 1.1: numerical time-dependent scores for each of the irritant responses (adapted from Alany et al, 2006). (112).

Effect	Time (min)		
	0.5	2.0	5.0
Non- irritant	0	0	0
Hyperaemia	5	3	1
Hemorrhage	7	5	3
Coagulation	9	7	5

Table 2.2: HET-CAM values for classification of irritants.

Cumulative Scores	Inference	Effect
0.0-0.9	Non-irritant	No visible hemorrhage
1.0-4.9	Mild irritant	Visible membrane discoloration
5.0-8.9	Moderately irritant	Structures are covered partially due to membrane discoloration or hemorrhage
9-21	Severe irritant	Structures covered totally due to membrane discoloration or hemorrhages

The BCOP assay also known as the organotypic model that uses isolated whole eyes from cattle. This assay relies on the cornea as an indicator when exposed to drugs/ materials that could cause visual impairment. According to *Gautheron et al,* BCOP assay measures ocular opacity and permeability both of which are very important within ocular irritation testing (113). The cornea is responsible for refracting light through the lens and onto the retina (2). Corneal opacity is an indicator of damaged corneal epithelial layers or protein denaturation, and its therefore thought to be an endpoint for many *in*

vivo ocular irritancy tests (114). Permeability is determined by the amount of fluorescein dye that penetrates through the cornea (108). The test materials are assigned to specific categories based on the irritancy score system (Table 2.3). For controls NaOH is used as a strong irritant, and saline as non-irritant (Figure 2.7).

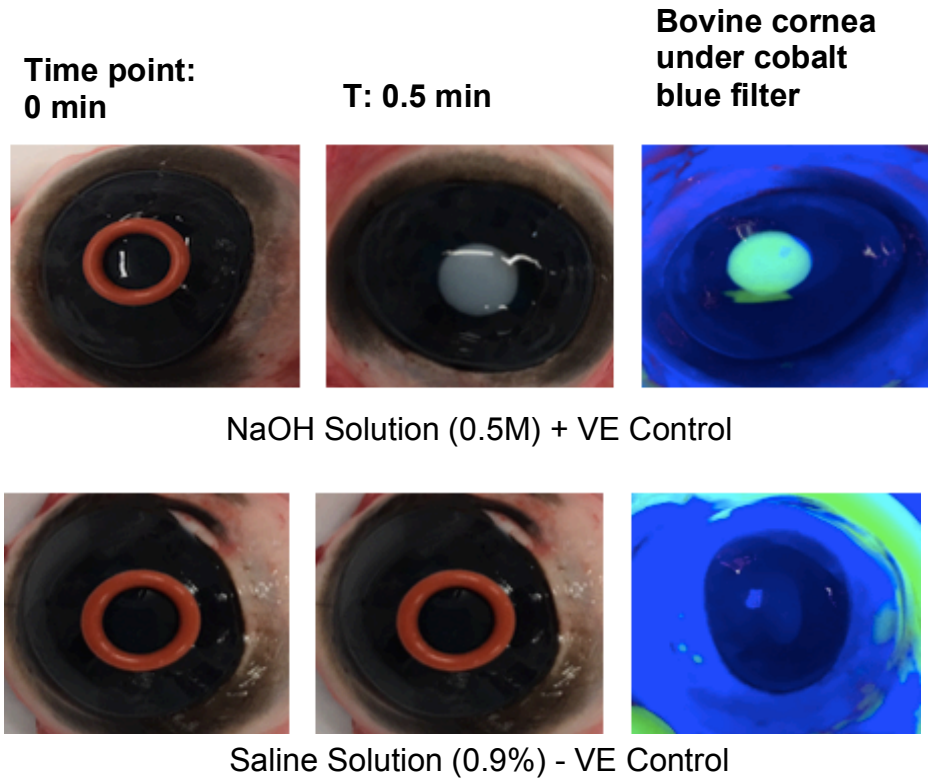

Figure 2.7: BCOP images with corresponding fluorescence images of freshly excised bovine cornea treated with positive control and negative control.

Table 2.3: BCOP irritation test scoring system.

Damage	Degree	Score
Opacity	None	0
	Slight	1
	Marked	2
	Sever	3
	Opaque	4
Epithelial integrity	None	0
	Diffuse and weak	0.5
	Confluent and weak	1
	Confluent and intense	1.5

Table 2.4: BCOP in vitro test score classification system.

Effect	Cumulative score
Non- irritant	≤0.5
Slight irritant	0.6-1.9
Moderate irritant	2.0-4.0
Strong irritant	>4

A comprehensive analysis of the formulations and test materials using several ocular tolerability assays was adopted via the regulatory bodies are displayed within this section. HET-CAM and BCOP were used to assess the ocular tolerability of the formulations and test material.

2.8.1. HET-CAM assay

Freshly collected fertilised hen's eggs were thoroughly checked for cracks and sprayed with 70% IMS, they were later incubated for 3 days at control temperature and humidity of 37 ± 0.5°C and 66 ± 5% respectively. The eggs were placed horizontally in the tray and were gently rotated 5-8 times a day. Meanwhile the growing chambers were prepared according to HET-CAM assay reported by *Alany et al* (112) with slight modification. The chamber consisted of a glass (10 cm internal diameter), inside the beaker about 5-6 cm a pocket was formed using cling film this was then fully secured. These chambers were then further sterilised with 70% IMS, on day 4 the eggs were cracked and opened gently keeping the egg yolk intact when poured into the chambers. The growing embryos with intact yolk sack, CAM were covered with a glass petri dish, theses chambers were further incubated at the same conditions already mentioned above, this is optimum condition for the embryo and CAM to develop.

DZH encapsulated NP's, as well as a number of silicone SCL's with and without surfactants were all tested for their potential ocular irritation effect. The positive control used was NaOH (0.5 M) as a strong irritant and saline (0.9%) was used as a negative control was non-irritant by the 10^{th} day the embryo and CAM were ready for the study, 150 μL of the test materials was placed onto the CAM, post exposure of CAM's blood vessels and capillaries were analysed for hyperaemia, haemorrhage and coagulation at the

following time points 0.5, 2 and 5 minutes. Table 2.1 shows a guideline to help score the level irritant of the test material on the CAM, and Figure 2.5 and 2.6 demonstrates vascular end points used to score irritation.

2.8.2. BCOP ASSAY

The freshly excised bovine eyes were immediately collected from the slaughter farm, in a thermal vessel containing normal saline at 6-7 °C; the eyes were used for testing on the same day of collection. The selecting process of the bovine is very important; we looked out for corneal vascularisation, corneal opacity, subconjunctival damage and epithelium detachment. The following controls were used; sodium hydroxide (NaOH 0.5 M) was used as strong irritant for positive control, saline was used as negative control (Figure 2.7).

DZH encapsulated NP's, control SCL's, as well as surfactant and silicone SCL's were studied for any potential irritation to the corneal surface of the eye. The bovine eyes were placed into large plastic weighing boat with the cornea facing upwards, initially the eyes were transferred into a water bath with a lid (Grant OLS 200, UK), the eyes were incubated in this humid environment for 10 minutes at 37 ± 0.5 °C, with shaking motion at 90 rpm. The eyes were removed after incubation period, a silicon ring was placed onto the centre of the eye, this will prevent any spillage, as well as direct the test materials to the desired location (cornea). A drop of saline was placed onto the centre of the O-ring; the eye was then subjected to a further 5 minutes of incubation in the water bath. The saline solution was later

removed and was replaced with 100 μL of the test material; the eye was further incubated for 30 seconds. The eye was then removed and was thoroughly washed with 15 mL of saline solution; it was then incubated one final time for 10 minutes before it is fully assessed for visually for corneal opacity. A cobalt blue filter (465-490 nm) was used to analyse the corneal epithelium after 0.5 mL of fluorescein solution (2% w/v, pH 7.4). Figure 2.7 and Table 2.2 demonstrates the degree of corneal opacity and fluorescein permeability used to score test materials.

2.9. Drug Release study

An *in vitro* drug release study was conducted over 24 hours, phosphate buffer saline (PBS) was used as a release medium. This study was carried out at temperatures 37 °C. The CL's with A) DZH within the lens matrix and B) DZH NP's loaded CL's were soaked in 10 mL of PBS and the two controls C) DZH in distilled water (1 mg / mL) and D) DZH encapsulated NP solution 1mL were filled into a dialysis bag and immersed in PBS, all off the samples were placed into a mechanical shaking water bath set to 80 cycles/ min at 35.5 °C. Aliquots of 0.5 mL were withdrawn from the test samples at different set time intervals of 15, 30 minutes, 1, 1.5, 22 and 24 hours. every sample withdraw was replaced with 0.5 mL of PBS.

Analytical Methods And Development, Validation, Preparation And Characterisation Of SCLs

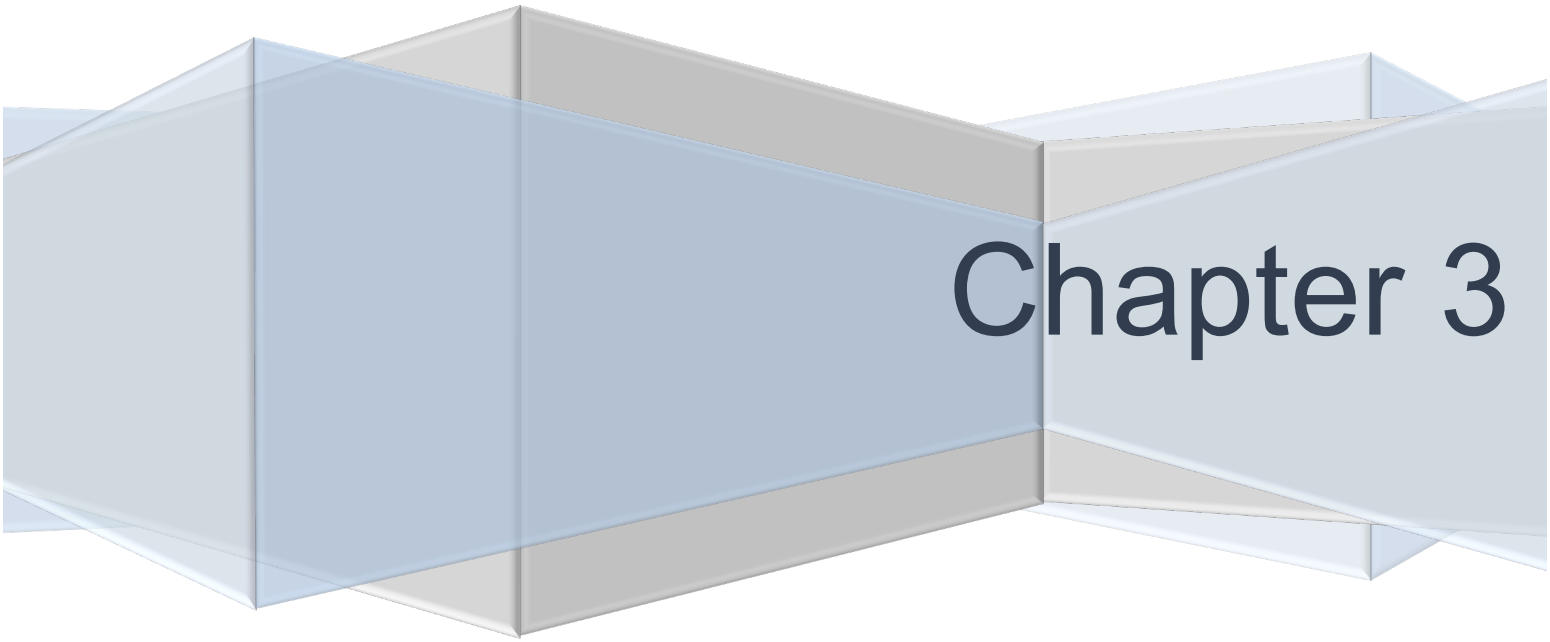

Chapter 3: Development and validation of Dorzolamide Hydrochloride analytical method

3. Introduction

DZH displayed in (Figure 3.1) is a carbonic anhydrase inhibitor used to decrease increased intraocular pressure within open-angle glaucoma and ocular hypertension. This anti-glaucoma drug is currently topically applied in the form of eye drops. Drug stability is an important process of drug development, evaluated during pre-formulation studies. Stability testing helps us to understand the quality and quantitatively monitor the drug under various different environmental conditions, such as temperature, light and humidity.

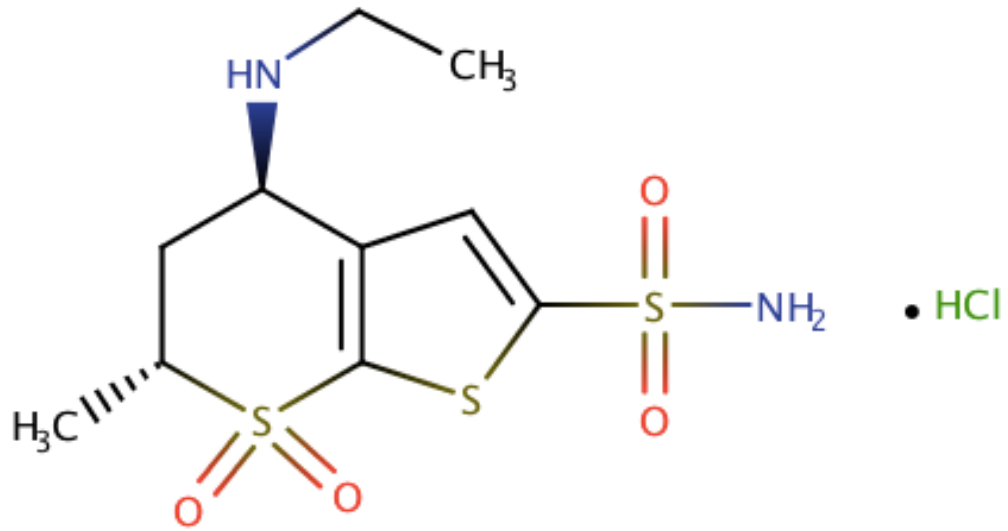

Figure 3.1: Structural formula of DZH.

Therefore, preforming a stability testing requires selecting or developing a valid, reproducible and stable analytical assay that could quantify the drug and the degradation products generated accurately.

High-performance liquid chromatography (HPLC) is a widely used analytical technique for drug analysis within pharmaceutical development; such as formulation, quality control and stability testing. HPLC is a highly efficient, reliable and precise method for quantifying and separating drugs in pharmaceutical formulations. Development of HPLC validation method for the simultaneous determination of DZH was adopted as per international council for harmonisation (ICH) guidelines. The main goal of ICH was to promote international harmonisation bringing together representatives from EU, Japan and USA, to establish joint guidelines. Making ICH-guidelines available globally, thus strengthening the capacity of pharmaceutical industry to utilise the information available (115,116)(117).

Therefore, HPLC method was chosen over various other analytical techniques for drug separation. The liquid mobile phase allows for the transformation of mobilized polarity during chromatography and depending on drug characteristics modification to the mobile phase was possible. Stationary phase was another advantage as it would enable good separation as the separation line was connected to a highly sensitive detector systems such as, diode detector, spectrafluorimeter etc. HPLC is an extremely quick and efficient way of separating analytes; which was achieved by forcing the analytes through a solid absorbent material with different chemical components separating out as they are moving at different speed. A high resolution of the results was then generated, the results presented are accurate and reproducible (116,118).

Mathrusri et al, developed an HPLC method for determining DZH and Timolol Maleate. The study used HPLC as it was fast, sensitive and accurate with wide linearity range, under 10 mins with high resolution chromatograms. The method utilized Inertsil ODS 3V column with acetonitrile and 1-octane sulphonic acid buffer (36: 64 v/v) (run at isocratic condition) at pH of 3.6 as mobile phase was validated as per ICH-guidelines. The retention time for DZH was 6.02 minutes and a LOD and LOQ were found to be of 0.6951 and 2.3214 µg/mL respectively. It was suggested that the proposed method was highly reproducible and reliable (119). *Narendra et al,* also conducted a HPLC validation study to determine DZH within eye drops. Reverse phase HPLC was adopted using Inertsil ODS 3V column with Acetonitrile: (0.02 M) 1, Octane sulphonic acid buffer (pH 3.5) (36:64 v/v) (run at isocratic condition) as a mobile phase. DZH LOD and LOQ were 0.7041 and 2.3483 µg/mL respectively. The method was simple, fast, reproducible for the analysis of DZH in pharmaceutical formulations (120).

Method validation is very important for the measurements of the following parameters, linearity, accuracy, precision, repeatability, specificity and robustness. Within this chapter, the method development and validation is described, in agreement with ICH guidelines. This rapid, accurate, precise isocratic HPLC assay for DZH analysis in the presence of its degradation products. Linearity assay has the ability to form a response that's directly proportional to the increase and decease in the analyte concentration, which is displayed in a linear graph, from which the accuracy and precision was determined (120–122). The lower limit of detection (LLOD) defines the lowest concentration of analyte. The lower limit of quantification (LLOQ) also defines

the lower concentration of analyte which can be quantified through accuracy and precision assay (115). Assay accuracy is explained as the closeness between the experimental mean results with the actual concentration value of the analyte. Accuracy is recognised when triplicate samples of known analyte are analysed (115,119). However, precision of assay looks at the closeness of a series of measured value of analyte to the true value under set conditions, precision assay considered at both repeatability and reproducibility assay (123). Robustness assay is the ability of the procedure to measure the capacity of the sample analyte to remain unaffected when put through various different parameters thus indicating the reliability of the analyte (120,123). For the second part of this chapter several different concentrations of the polymers against cross-linker were prepared, and the different compositions are displayed in table 3.1 and Figure 3.2 displays the polymers used in this study.

Table 3.1: Different polymer concentrations against cross-linker prepared. All polymer formulations had 0.6% benzyl peroxide initiator.

Polymer concentration (v/v)	Cross-linker (EDGMA) (v/v)
HEMA(**99%**), MMA(**99%**), MAA(**99%**), GMA(**99%**)	EGDMA **1%**
HEMA(**95%**), MMA(**95%**), MAA(**95%**), GMA(**95%**)	EGDMA **5%**
HEMA(**90%**), MMA(**90%**), MAA(**90%**), GMA(**90%**)	EGDMA **10%**
HEMA(**80%**), MMA(**80%**), MAA(**80%**), GMA(**80%**)	EGDMA **20%**
HEMA(**70%**), MMA(**70%**), MAA(**70%**), GMA(**70%**)	EGDMA **30%**
HEMA(**60%**), MMA(**60%**), MAA(**60%**), GMA(**60%**)	EGDMA **40%**
HEMA(**55%**), MMA(**55%**), MAA(**55%**), GMA(**55%**)	EGDMA **45%**
HEMA(**50%**), MMA(**50%**), MAA(**50%**), GMA(**50%**)	EGDMA **50%**
HEMA(**30%**), MMA(**30%**), MAA(**30%**), GMA(**30%**)	EGDMA **70%**
HEMA(**20%**), MMA(**20%**), MAA(**20%**), GMA(**20%**)	EGDMA **80%**
HEMA(**10%**), MMA(**10%**), MAA(**10%**), GMA(**10%**)	EGDMA **90%**

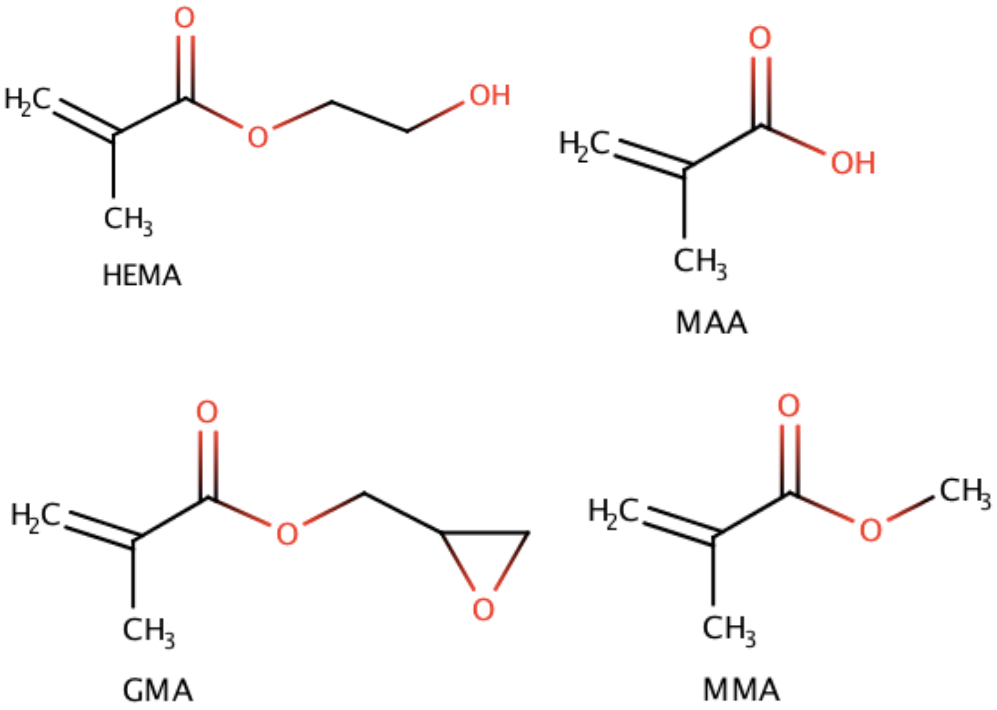

Figure 3.2: Chemical structures of polymers, used to formulate SCLs. 2-hydroxyethyl methacrylate (HEMA), methacrylic acid (MAA), methyl methacrylate (MMA) and glycidyl methacrylate (GMA).

In this chapter, we analysed the effect of the cross-linker EDGMA on equilibrium water content (EWC), contact angle (CA), optical transmission and Young's modulus (YM) of SCLs. Several different concentrations were used, also a variety of different polymers were used of which possessed hydrophilic and hydrophobic properties. EWC properties and CA measurements were recorded. Thermal analysis was carried out in order to aid our understanding of the polymers being used.

Within the final part of this chapter the polymer concentration that possessed the highest EWC% was used and co-polymerised with the following polymers MMA, MAA and GMA. This study was carried out in order to help us understand and come to a conclusion as to what polymer concentration possesses the highest hydration with high surface wettability at the same time have the highest transmission, the result of all these properties help

achieve an ideal SCL base which can be used as a vehicle for ocular drug delivery. These SCLs were then subjected to characterisation testing, such as EWC, CA, optical transmission (TM) and YM.

The first part consists of method development and validation of an analytical method for DZH as per ICH guidelines. The second part of this chapter displays the studied effect of cross-linker EDGMA against the polymers used and how it affected the mechanical structure and EWC of SCLs. The final part of this chapter is based on the results of the effect of cross-linker on SCLs. The polymer with the highest EWC% was selected and copolymerised with the rest of the polymers at several different concentrations, once again these lenses are subjected to several characterisation techniques as already mentioned previously.

3.1. Aim and objectives

The aims of the chapter are to develop an analytical method for DZH as well as to prepare and characterise SCLs. The specific objectives include:

- To develop and validate an HPLC analytical method to quantify DZH
- Prepare SCLs using different concentration (%) of EDGMA as a cross-linker.
- To investigate the effect of cross-linking ratio on EWC% in CLs.
- Investigate the effect of different polymer concentrations on the following properties EWC, CA, transmission and YM of SCLs.
- Prepare co-polymerised SCLs, using HEMA in combination with MMA, GMA and MAA.
- To evaluate the mechanical and optical properties of the co-polymerised SCLs by studying EWC, CA, transmission and YM of the lenses.

3.2. HPLC method development and validation for Dorzolamide - International Conference of Harmonisation Guidelines

Results & Discussion:

DZH was analysed using reverse phase HPLC method where Chromolith® Performance RP-18e was used as a stationary phase. DZH was eluted using a mixture of acetonitrile and distilled water at (60:40 v/v). The mobile phase was pumped at a flow rate of 1.0 mL/ min. The λ was determined using UV scanning spectrophotometer and was found to be 254 nm, therefore the HPLC detector was set at 254 nm and the HPLC system was operated at room temperature (25 °C). DZH was eluted at 1.66 min.

DZH have been simultaneously analysed via sensitive HPLC with a wide linearity range, with high resolution where running time was less then 5 mins. The method was validated as per ICH guidelines (120,123). ICH-guidelines cover linearity, accuracy, precision, specificity, detection limit and repeatability testing (115,120,123).

3.2.1. Specificity

Specificity is the ability of the analytical method to accurately separate, measure and quantify the concentration of analyte without any interference from other components present in the sample. Simulated tear fluid and analyte solution were injected into the HPLC and the chromatogram is displayed in figure 3.3.

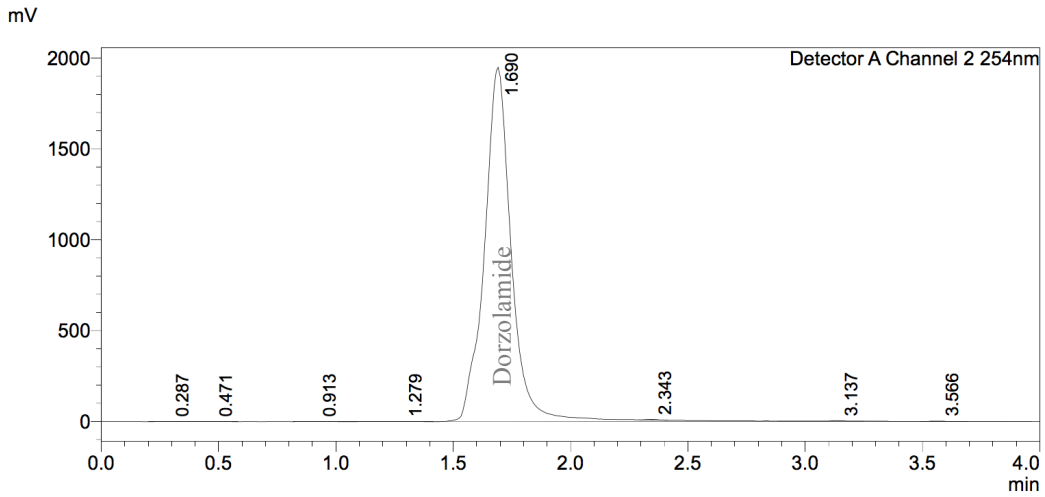

Figure 3.3: Chromatogram of DZH with simulated tear fluid shows no interference between the matrix peak and analyte peak.

3.2.2. Linearity

Linearity of an analytical procedure is its ability to stimulate test results that are directly proportional to the concentration of analyte in samples within a range. A serial dilution of six analyte concentrations of DZH were prepared and studied. Figure 3.4 shows linear calibration plots for the suggested method that were obtained in the concentration range of 5-200 μg/ mL for DZH.

Peak area ratio of DZH was measured, from which a representative calibration graph plotted of peak area versus concentration in the range of 5,10,20,50,100,200 μg/ mL (Figure 3.4). The linear regression equation of DZH was found as Y= 22865 X + 9117.9, where Y is the peak area and X is the value of the various concentrations of the standard solution, with correlation coefficient of R^2= 0.99995. The results have demonstrated a good linearity between peak areas versus concentration.

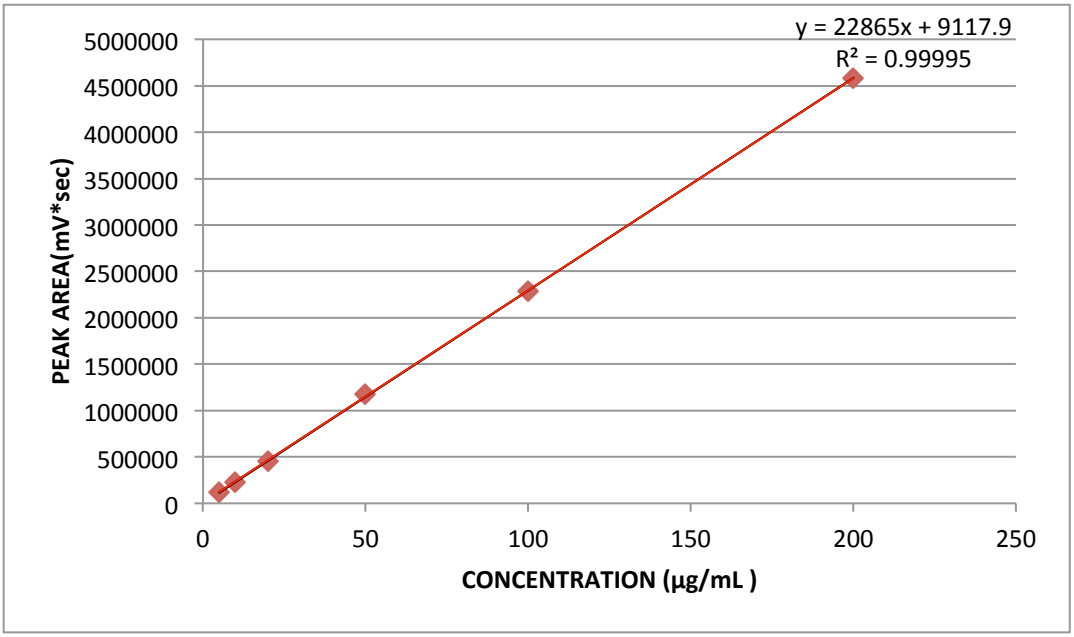

*Figure 3.4: Dorzolamide HCl peak area (mV*sec) Vs concentration (µg/mL) calibration curve. Results are expressed as mean value ± SD (n=3)*

3.2.3. Accuracy

Accuracy refers to the closeness of a measured mean value to a standard or known value. The accuracy of the HPLC method was demonstrated by selecting three sample analytes (QC'S) within the range (7.4, 45 and 150 µg/ mL). Each sample analyte was measured using five determinations. The obtained concentrations were used to re-fit into the derived regression equation giving us the calculated concentration. Then both concentrations (obtained & calculated) were used to determine the percentage deviation at each concentration of the standard solutions. The mean value should be within 15% of the LLOQ and not deviate by more than 20% (124). The percentage recovery and coefficient variance (%) for 7.5, 45, 150 µg/ mL are show in table 3.2. Recovery % (Table 3.2) was within the specified limits that

suggest this method is highly accurate and suitable for the proposed validation method.

Table 3.2: Accuracy for the simultaneous analysis of DZH (n=5).

Drug	Conc. (μg/ mL)	Amount recovered ± SD (μg/ mL)	Recovery (%)	CV (%)
DZH	7.5	7.47 ± 0.02	99.60	0.24
	45	44.78 ± 0.04	99.51	0.10
	150	144.23 ± 0.04	99.15	0.03

3.2.4. Precision

Precision states the closeness of individual measures of three selected analytes within the range of an analytical procedure(123). Table 3.3 displays intra-day precision, which was measured by injecting five determinations per analyte of three different concentrations on the same day (n=5). Inter-day precision was carried out by injecting the same set of 3 different analyte concentrations for 5 consecutive days (119). Each analyte concentration should not exceed 15% of the coefficient of variation (CV), the LLOQ should not exceed 20% of CV (124). The precision of the HPLC methodology was determined as the coefficient of variation (%CV) of inter-day and intra-day. The concentrations were calculated by re-fitting peak areas obtained with different analyte solutions into a derived regression equation. CV for 7.5, 45, 150 μg/ mL – 0.20, 0.18, 0.11 respectively (Table 3.3).

Table 3.3: Intra-day and Inter-day Precision for the simultaneous analysis of DZH (n=5).

Drug	Conc. (μg/ mL)	Intra-day precision		Inter-day precision	
		Amount recovered ± SD (μg/ mL)	**CV (%)**	**Amount recovered ± SD** (μg/ mL)	**CV (%)**
DZH	7.5	7.43 ± 0.01	0.20	7.52 ± 0.11	1.48
	45	44.84± 0.08	0.18	44.83 ± 0.08	0.19
	150	144.37 ± 0.15	0.11	144.23 ± 0.20	0.14

3.2.5. Limit of detection and limit of quantitation

Detection limit of an analytical methodology is represented as the lowest amount of analyte within a sample, which can be detected but not quantified as exact value.

Quantification limit of an analytical methodology is represented at the lowest amount of analyte within a sample, which is quantified using appropriate precision and accuracy. Quantification limit also presented as a parameter for quantitative assays for low levels of analytes within a sample matrices.

LOD and LOQ were calculated at 95% confidence level using “Regression statistics analysis” in Excel with the use of the ICH guideline equations based on the calibration curve: LOD= 3.3*σ/S and LOQ=10*σ/S, where σ is the standard deviation of the response and S is the slope of the calibration curve. The LOD was found to be 2.00 μg/ mL and the LOQ was found to be 6.05 μg/ mL.

Table 3.4: Summary of validation parameters used throughout the stability assay.

Validation parameters		Dorzolamide-Hydrochloride
Specificity		**% Interference**
Range (µg/ mL)	**Linear range**	5-200
	Working range	5-200
	Target range	7.5,45,150
	Target Conc	150
Precision (%CV)	**Repeatability**	
	Intra-day	0.11
	Inter-day	0.05
Accuracy (% recovery)		
LLOD		2.00
LLOQ		6.05

3.3. Effect of different cross-linker concentration on polymers used to prepare SCLs

3.3.1. Preparation of CLs using hydrophilic HEMA polymer polymerised with EDGMA crosslinking agent at different concentrations

Hydrophilic HEMA CLs were prepared at a range of concentration (%) ranging from 10-99% (v/v) HEMA. CLs with high concentrations of HEMA (99%) displayed visually clearer CLs compared to those of lower concentrations HEMA (10-30%) (Figure 3.5). The concentration shown in Figure 3.5 represents combinations that have yielded SCLs, which were taken further to undergo characterisation studies. All other formulation was unsuccessful. EDGMA/HEMA with 1/99% (v/v) concentration, yielded a more transparent CL in comparison with EDGMA/HEMA at 10/ 90% (v/v) shown in Figure 3.5. CLs that were prepared with 80-99% (v/v) HEMA, possessed the highest EWC% values as displayed in Figure 3.4. CLs made of 99% HEMA concentration possessed the highest EWC% of 34.80 ± 0.1%, with the presence of hydroxyl groups results in the formation of hydrogen bonds with the water. The functional groups are responsible for the hydrophilic nature of the polymer, as they form hydrogen bonding with water molecules thus drawing them into the polymer matrix. Figure 3.5 also shows that increasing the concentration (%) of HEMA, EWC% and surface wettability of CLs also increased. HEMA/EDGMA (99/1 v/v %) displays a CA 55.6 ± 2.97° which increased to 105 ± 0.99° for HEMA/EDGMA (20/80% v/v). Statistical analysis has showed significant difference between the two concentrations for both EWC% and CA at $p=<0.0001$. Lower CA values

demonstrate higher surface wettability. Higher concentration of HEMA exhibits low surface wettability supporting the hydration testing.

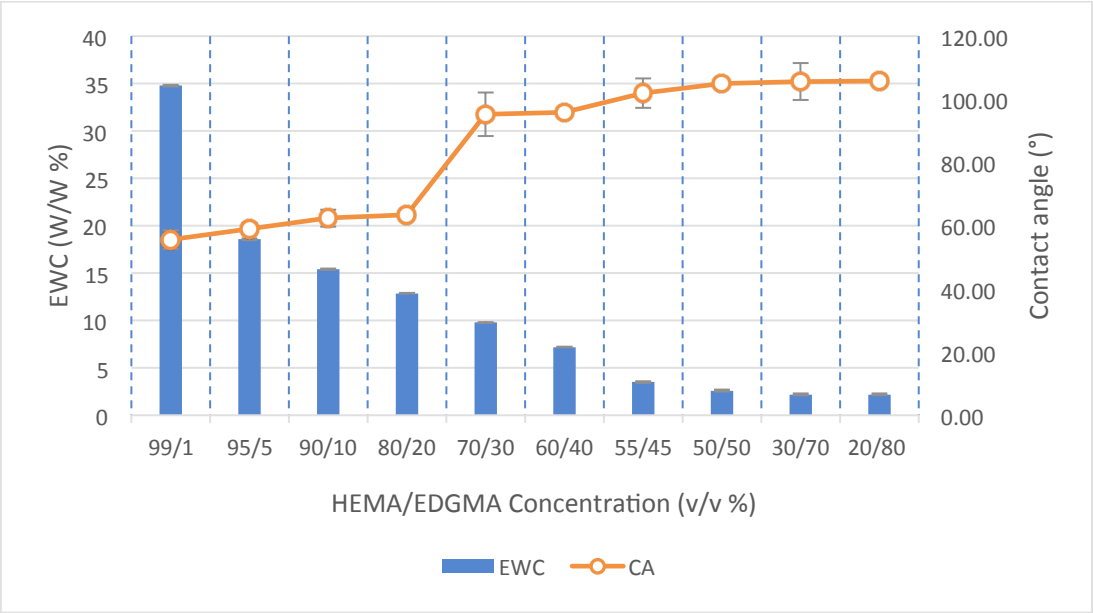

Figure 3.5: Equilibrium water content (%) and contact angle for HEMA polymer co-polymerised with cross-linker (EDGMA) results are expressed as mean ± SD, (n=3).

3.3.2. Preparation of CLs using hydrophilic MAA polymer polymerised with EDGMA crosslinking agent at different concentrations.

MAA is a Hydrophilic polymer that was used to formulate CLs at different concentrations with EDGMA. MMA was used at concentrations ranging between 10-80% (v/v). It was noticed that with an increase in MAA concentration, the opacity and surface roughness of the CLs increases (Figure 3.6). This could be attributed to phase separation (82). Phase separation occurs when polymer blends do not form homogenous mixtures, this is largely triggered by change in temperature or molecular weight (125). Polymer blend miscibility vary depending on concentration (% v/v) and their Gibb's free energy curve (125), polymers with a negative free energy tend to be more miscible as suggested by (126). The concentration shown in Figure 3.7 represents combination that have yielded SCLs, which were taken further to undergo characterisation studies. All other formulation was unsuccessful. EWC% and CA for the prepared EDGMA/MAA CLs are summarized in Figure 3.7. Increasing the MAA concentration has shown the highest EWC% with 6.70 ± 0.01%, with CA of 97 ± 1.20° for EDGMA/MAA (20/80% v/v). This could be attributed to the hydrophilic nature of MAA polymer (127) due to the presence of carboxylic acid functional group (Figure 3.2) that can form hydrogen bonds with water.

The EWC % results compliment with that of CA results. CA showed an increased surface wettability with the increase in MAA concentration. For instance, the CA of MAA/EDGMA at (10/90% v/v) was (2.85 ± 0.12%) and increased to (6.70 ± 0.09 %) when the MAA/EDGMA increased to (80/20%

v/v). Overall, statistical analysis has shown that significant difference with *p=<0.0001* for MAA/EDGMA (80/20%) and (10/90%) (v/v).

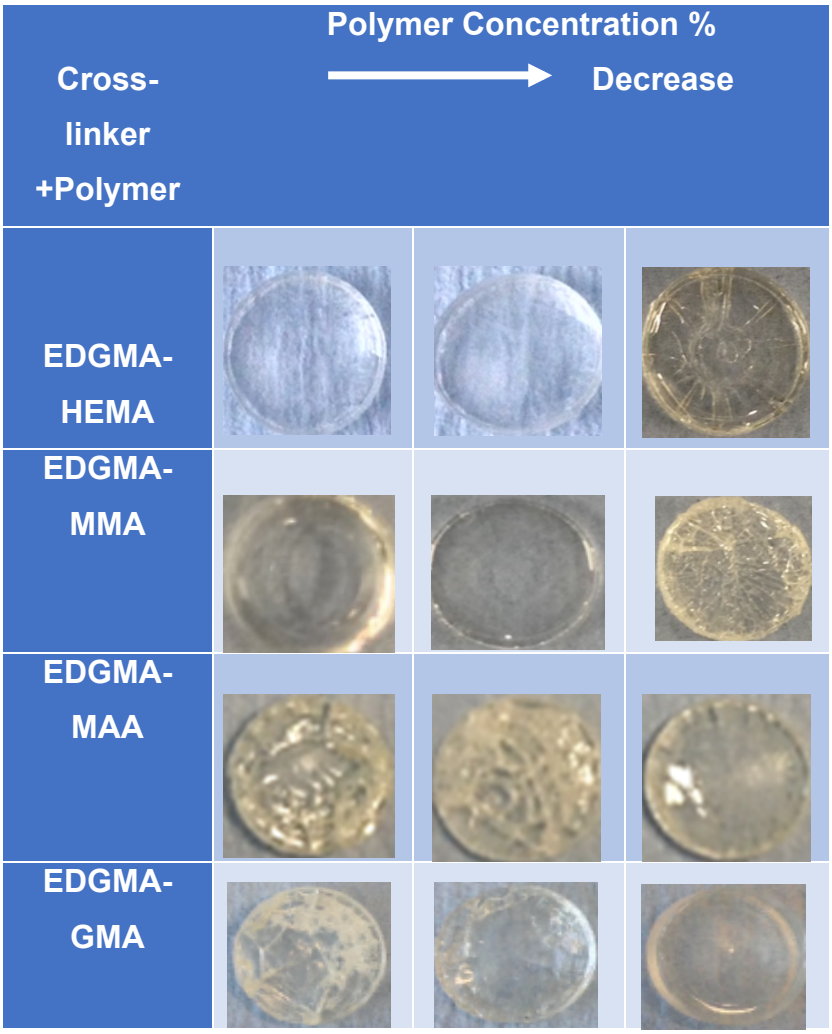

Figure 3.6: Visual representation of the prepared CLs at an increase and decrease concentration %.

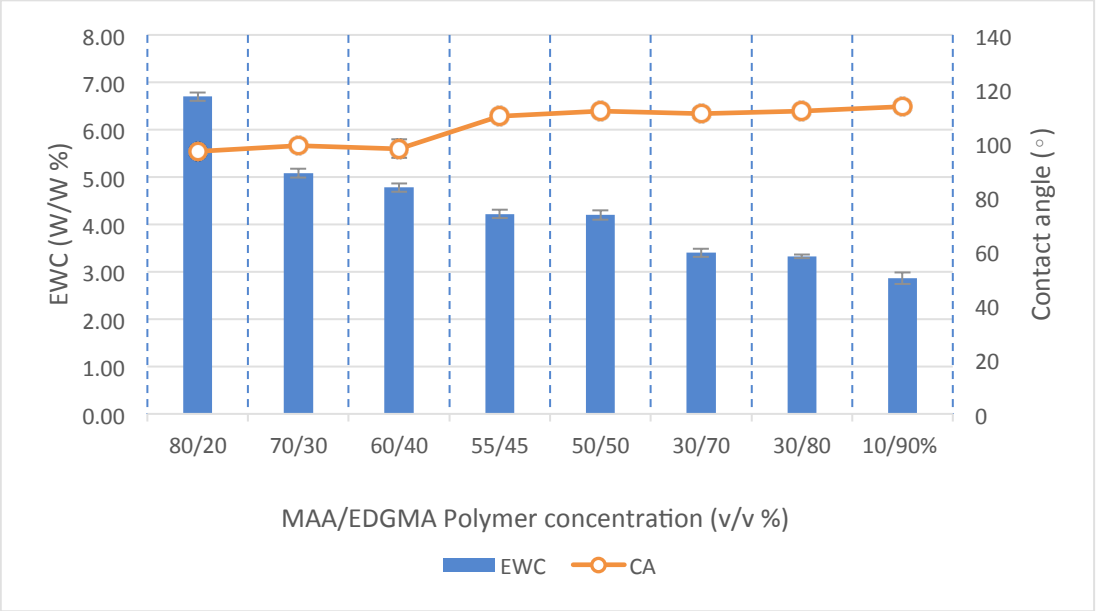

Figure 3.7: Equilibrium water content (%) and contact angle for MAA polymer co-polymerised with cross-linker (EDGMA) results are expressed as mean ± SD, (n=3).

3.3.3. Preparation of CLs using hydrophobic MMA polymer polymerised with EDGMA crosslinking agent at different concentrations.

MMA is a hydrophobic polymer used to prepare CLs; MMA is co-polymerized with EDGMA at concentrations ranging from 10-95% (v/v). MMA consists of both hydrophilic and hydrophobic regions and when hydrated the water molecules will form hydrogen bonds at hydrophilic regions (carbonyl groups) around hydrophobic regions. Therefore, MMA is widely used within a composition of polymers to increase the strength modulus of the contact lens, due to the stiff nature of the polymer. The concentration shown in Figure 3.8 represents combination that have yielded SCLs, which were taken further to undergo characterization studies. All other formulation was unsuccessful. Figure 3.8, shows that with increase in MMA concentration, the EWC% and surface wettability increased slightly. This could be because

EDGMA is a more hydrophobic than MMA (128). The highest EWC% obtained for EDGMA/MMA was at 17.85 ± 0.09% however this is not considered adequate enough to be used to formulate a SCL. EDGMA/MMA 90/10% & 5/95% (v/v) has EWC% of 0.90 ± 0.13% and 17.85 ± 0.09% also a CA of 110 ± 0.30° and 65 ± 1.13° respectively. Statistical analysis has shown that there is a significant difference for EDGMA/MMA between 90/10% & 5/95% (v/v). There is an increased decline in EWC% with increase in hydrophobic EDGMA (cross-linker), this is due to the formation of more hydrophobic regions (129). *Fehim et al,* carried out a case study on the selection of materials for CLs, and reported that MMA polymer was most desirable for eye lenses, as the material is non-toxic and recyclable (130).

When comparing both MAA and MMA results, it showed hydrophilic MAA with a lower EWC% compared to hydrophobic MMA. From the results obtained (Figure 3.6) it was difficult to obtain whole smooth CLs when formulating CLs using EDGMA/MAA, this could be because the mixture was not homogenous or because thermal polymerization was used.

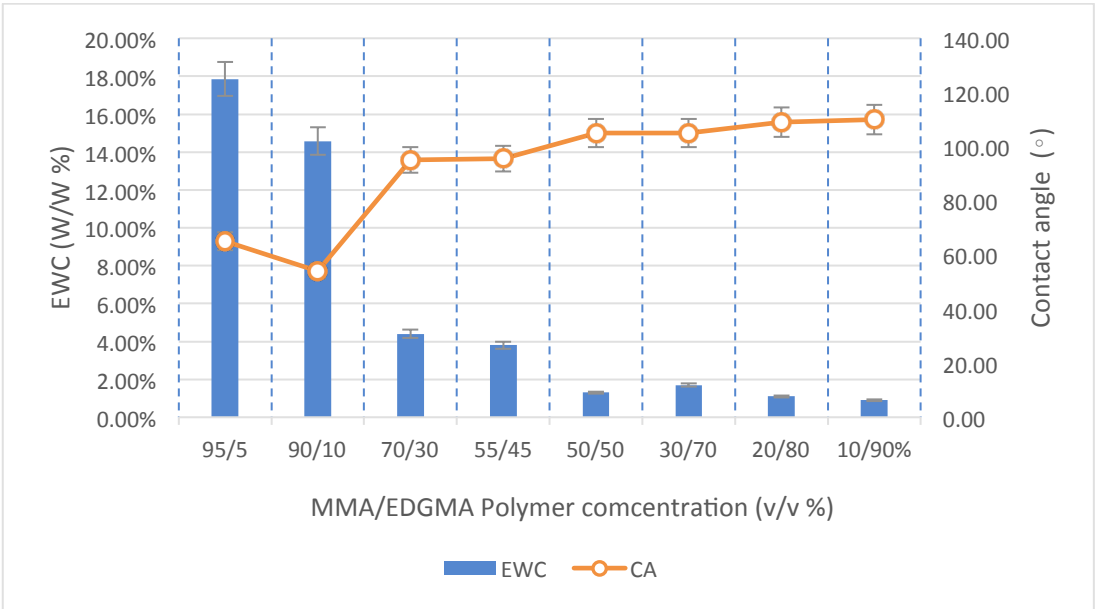

Figure 3.8: Equilibrium water content (%) and contact angle for MMA polymer co-polymerised with cross-linker (EDGMA) results are expressed as mean ± SD, (n=3).

GMA polymer was also used to prepare CLs at concentration % ranging from 10-90% (v/v), however we only obtained whole CLs at concentration % of 90, 70, 50% (v/v). The concentration shown in Figure 3.9 represents combination that have yielded SCLs, which were taken further to undergo characterisation studies. All other formulation was unsuccessful. The other prepared CLs were damaged, this could have been due to the type of polymerisation used, the type of mould used, or that the mixture of EDGMA/GMA was not homogenous causing phase separation to occur (125). Decrease in GMA concentration % presents visually clear CLs as shown in Figure 3.6. GMA; possess an epoxy side group, ester methacrylic acid functional groups, there are strong polar bonds present due to the epoxy side group making it the main hydrophilic domain at which hydrogen bonding occurs. Figure 3.9 shows that a decrease in GMA concentration % results in an increase of EWC%. At EDGMA/GMA 50/50% and 10/90% (v/v) EWC% of 3.30 ± 0.011% and 2.96 ± 0.01% and CA of 109 ± 0.50° and 110 ± 0.01° is achieved. Statistical analysis displayed significant difference between the EWC% with $p=<0.0001$, and no major significant difference between both sets of results for CA with $p=0.0002$.

Magda Carrilho, studied the effect of polymer composition within hydrogel contact lenses on drug release behaviour and their properties, the results show that with an increase in EGDMA cross-linker hydrogels displayed smaller pores, producing a decline in diclofenac release, swelling properties

of CL on the other had YM increased (131). Therefore, optimisation of CL material is essential in order to avoid compromising the CL properties and a achieving a CL material that has the potential to be used as drug carries.

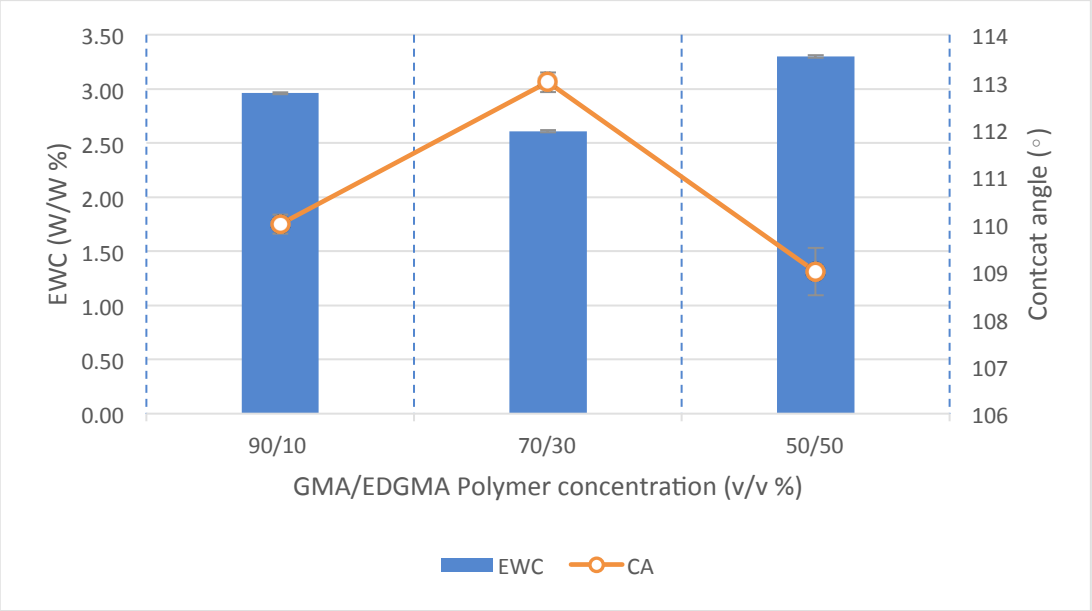

Figure 3.9: Equilibrium water content (%) and contact angle for GMA polymer co-polymerised with cross-linker (EDGMA) results are expressed as mean ± SD, (n=3).

There was a pattern amongst two polymers MAA-EDGMA and MMA-EDGMA, which is displayed in Figures 3.7, and 3.8 that with decrease in the polymer concentration %, whole CLs are formed, however with high polymer concentration % rings or loops are formed.

HEMA, MAA & GMA polymers displayed adverse results where increase in polymer concentration % resulted in whole clear CLs as well as an increase in EWC%. Both HEMA and GMA possess strong hydrophilic characteristics thus when used to prepare CLs it would improve water absorbance. There are several factors that affect the EWC%; the hydrophilic functional groups arranged on the polymers, the quantity of crosslinking agent used and finally

pore morphology of the polymer (49). Polymers with strong polar functional groups such carboxylic acid, hydroxyl or ether groups allows enhanced interaction with water molecules forming hydrogen bonding, ion-dipole or dipole-dipole bonding. The crosslinking agent is vital in the process of keeping the polymer chain intact. The addition and quantity of the crosslinking agent (EGDMA) dictates the swelling ratio as well as the rigidity of CL. Therefore, with increase of EGDMA concentration %, densely cross-linked polymeric hydrogels are formulated, initiating a decrease in swelling degree within the polymer thus a decrease in EWC% (132). *Mohammed et al,* studied the effect of crosslinking concentration (EDGMA) on hydrogels. They discovered that with increase addition of EDGMA EWC of the hydrogels decreased. Decline in EWC% would essentially lead to a reduction in oxygen permeability of the CLs, as oxygen passes through water pockets rather than the polymer material itself as reported by *Maldonado-Codina et al* (54). EDGMA concentration increase would generally increase the YM, making the CLs stronger/ stiff with decrease in ECW%, however with decrease in EDGMA the CLs would obtain poor mechanical properties making it very soft and very hard to handle (132). Thus, it is important to establish the right concentration of crosslinking agent in order to prepare SCLs with an ideal YM, optical transparency, and EWC% as well as oxygen permeability.

There are two types of pore morphology homogenous and heterogeneous. Homogeneous hydrogels the pore volume is relative to the cross-linked polymer chains and heterogeneous hydrogels have a relatively high pore

volume to polymer chain. Increase in crosslinking density causes a decrease in pore volume, which leads to decline in the amount of water content absorbed (133,134). Therefore, with decrease in EGDMA within the polymer systems the EWC increases, loosely cross-linked polymers are able to swell increasing water absorption.

3.3.4. Thermal analysis

Figure 3.10 shows the differential scanning calorimetry for HEMA, MMA, MAA and GMA. HEMA (Figure 3.10, curve A) presents a sharp exothermic peak at roughly 158°C. *Bolbukh et al,* carried out a thermal investigation of HEMA polymer filled with modified silicas, from DSC results presented similar endothermic curve at 106°C and suggested this was due to the decrease in low mobility of polymer molecules (135). *Ning et al*, analysed the thermal reaction of HEMA with benzyl peroxide and polymethacrylate via DSC. The DSC thermogram of butyl-methacrylate with HEMA a small endothermic peak was present (from 50-110°C) which suggested that the heat initiates the polymerisation reaction of HEMA (exothermic peak) beginning at 100°C and ending at 150°C (136). This is very much similar to the DSC curves (Figure 3.10, curve A) obtained in this study.

GMA (Figure 3.10, curve C) displays an initial polymerisation at 105°C and ending with broad exothermic peak at 130°C (137). *Guo et al*, studied formula optimization of GMA modified with waterborne acrylic resin, using amniopropyltriethoxysilane (KH-550) as cross-linking agent. From the DSC thermogram results, the initial polymerisation temperature decreased when

combining KH-550 in GMA polymer mixture. Lower polymerisation temperature indicates a more effective and straightforward polymerisation process to form a three-dimensional network structure (exothermic peak at 108°C for polymerisation of GMA-KH550). They also suggested increase in the amount GMA polymer has similar effects on the polymerisation temperature (138). The polymerisation peak obtained in this study is higher than that of *Guo et al*, due different concentrations of GMA polymer and different cross-linking agent being used.

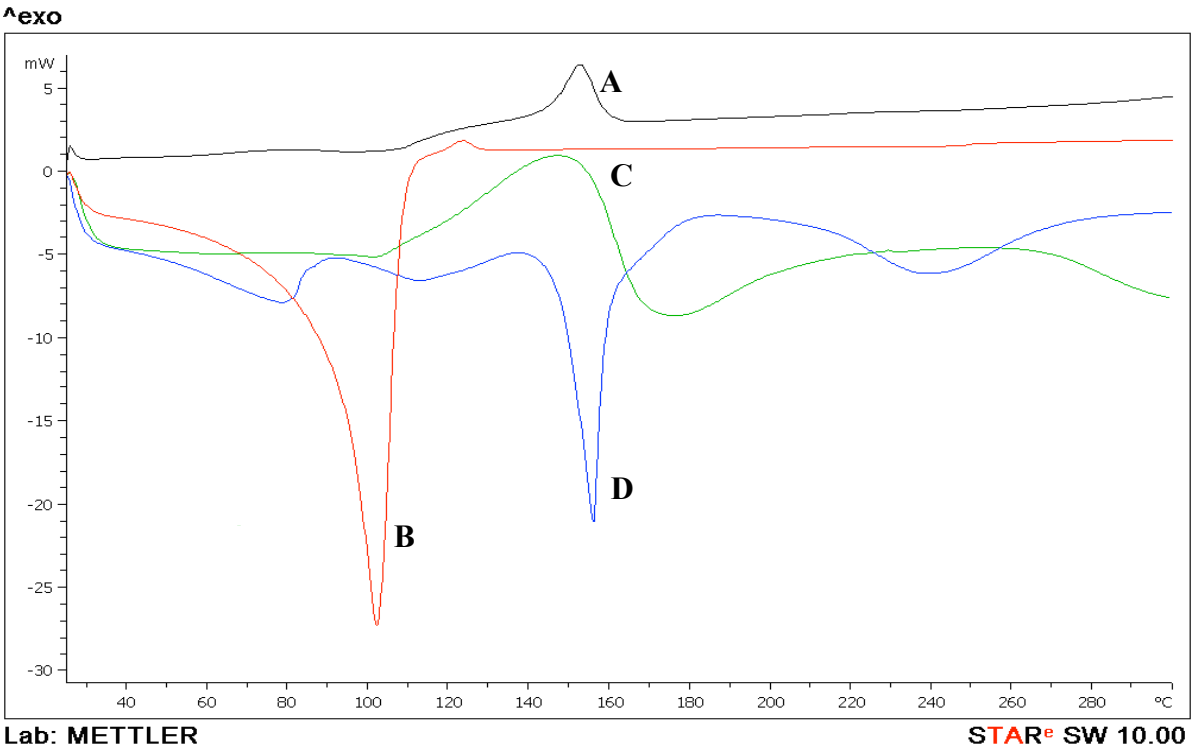

Figure 3.10: DSC analysis of all polymers used HEMA (A), MMA(B), GMA(C) and MAA(D).

MMA and MAA display sharp endothermic peaks at 100°C and 158°C (Figure 3.11, curve B and D) due to the evaporation of unreacted polymers, followed by degradation of MAA at 240°C (D) (139). *Polacco et al*, investigated the thermal behaviour of poly(methacrylic acid) and poly(N-vinyl-2-pyrrolidone) complexes. From DSC thermal analysis *Polacco et al,*

summarised that PMAA displayed suitable thermal stability until reaching 180°C, and from 180-240°C presented endothermic peak suggesting first degradation process. The 2nd endothermic peak at 420°C corresponds to the decomposition of PMAA (140).

Figure 3.11 shows DSC curves for MMA at various different concentrations starting with 99% MMA. An endothermic peak at 100°C is related to the evaporation of unreacted MMA polymer. With increase in cross-linking agent MMA concentration decreases, increasing the intensity of the exothermic peaks with a shift to 120°C-140°C this could be due to increase in polymerisation between MMA and EGDMA (cross-linking agent) causing the peaks to become increasingly broad (141). *Kim et al*, studied the effect of cross-linking agent on the morphology of MMA polymer. Their thermal analysis of MMA/EGDMA (cross-linking agent) suggested that their thermal stability was reduced with decrease in EGDMA, hence increase in initial and end decomposition temperature with increase in EGDMA(142,143).

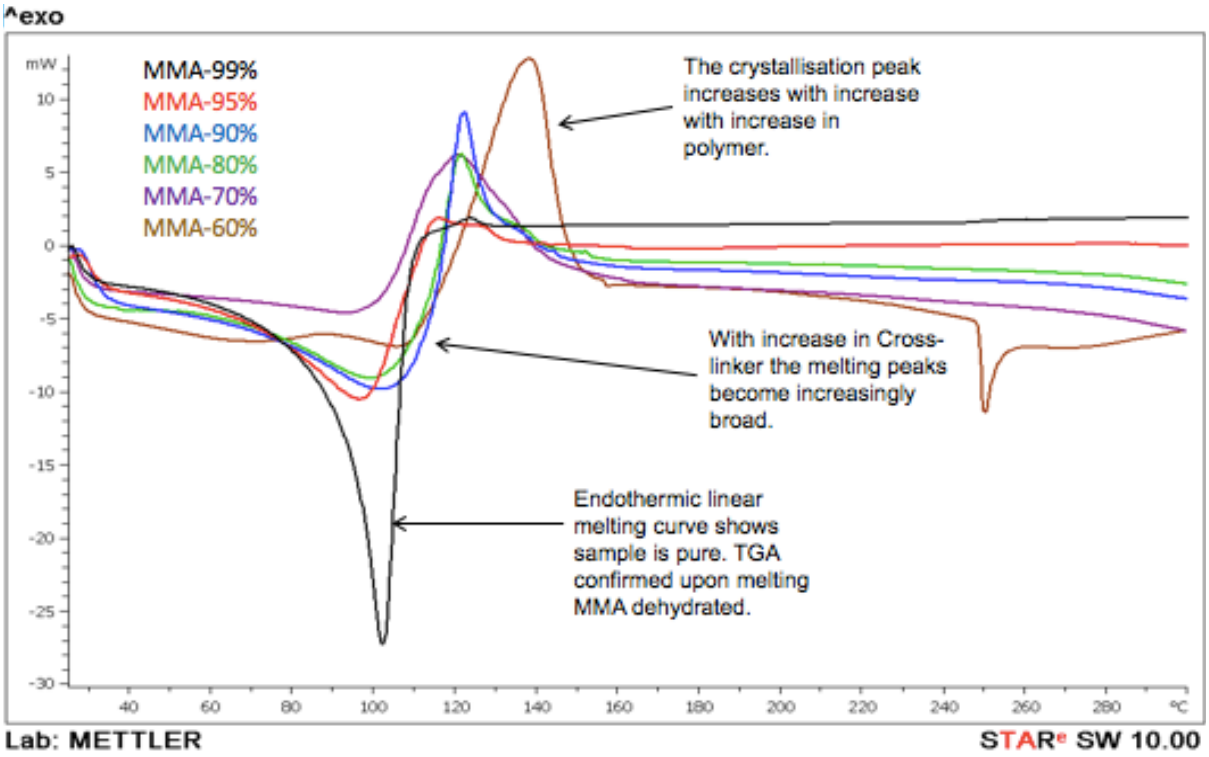

Figure 3.11: Deferential scanning calorimetry (DSC) analysis of MMA at various compositions.

The two amorphous polymers HEMA were further investigated by measuring the glass transition temperature (Tg) at 3 different concentration % 99, 95 and 90% using thermos mechanical analysis (TMA). The Tg value helps represent the mobility of the polymer backbone. The energy required to rotate bonds is linked to the Tg the lower the Tg value indicates a highly flexible backbone (71,145). Table 3.5 below displays the Tg figures and it can be observed that with decrease in polymer concentration % of HEMA the Tg increases suggesting decreased mobility as the polymer chains are linked together by cross-links. According to *Schut et al*, there are several factors that affect the mobility of the chain and impact Tg, molecular weight, chemical structure, cross-linking agent and crystallization (both of which reduce chain mobility) (144).

Table 3.5: Glass transitions of HEMA.

Polymer concentration %	HEMA (Tg)
99	82.29°C ±0.21
95	83.63°C ±0.22
90	93.92°C ±0.18

HEMA polymer was further analysed by measuring its Young's modulus (YM) and the coefficient of thermal expansion (CTE), the results are demonstrated in Figure 3.12. The reason for this would be because HEMA polymer possessed the highest EWC% at increased concentration as well as low CA values suggesting increased surface wettability, not to mention the CLs prepared at concentration % 99-90% (v/v) displayed as most transparent. Making HEMA polymer desirable to be further used and prepare SCLs. *Wang et al,* described some of the basic concepts of CTE, where by the size and volume of the polymer material will vary with increase in temperature (145). CTE is an essential application requirement when optimising and designing polymer material for ocular drug delivery. *Wang et al,* listed the two different types of CTE, positive CTE are known as "hot expansion and cold shrinkage" and negative CTE are known as "hot shrinkage and cold expansion" (145). The CTE therefore depends on the components of the polymer material and Young's modulus (145). Thermo-mechanical analysis (TMA) was used to measures the change in height of the sample, from which the CTE is calculated, (137).

Figure 3.12 showed that decreasing HEMA concentration and increasing the concentration of EDGMA, the YM values increases suggesting a more tightly linked polymer chain with limited space for expansion hence decline in CTE values (128,146). *Lawrence et al,* studied the effect of crosslinking agent on the physical properties of polymers, and discovered that not only does crosslinking agents effects the Tg of polymers (Table 3.5), but also has a great effect on the swelling volume within polymers and CTE (128), this is illustrated in Figure 3.12.

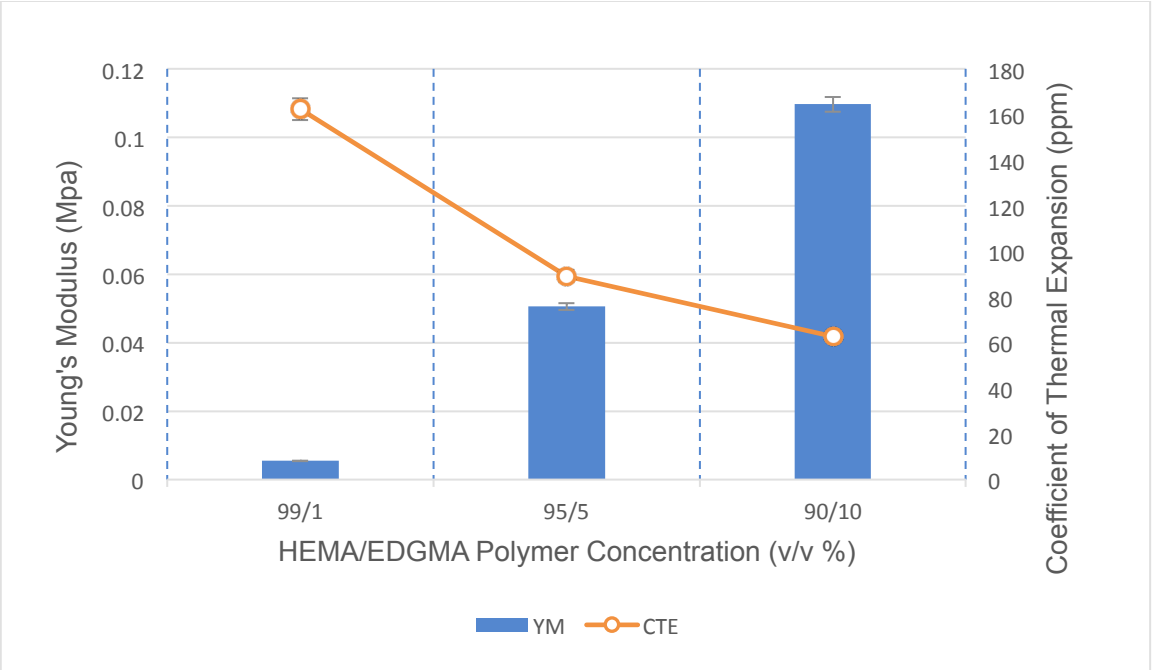

Figure 3.12: Young's modulus (Mpa) and coefficient of thermal expansion (ppm) for HEMA/EGDMA at different concentration, results are expressed as mean ± SD, (n=3).

The concentration of cross-linking agent EDGMA, could affect water absorption within CLs as illustrated in Figures 3.4, 3.6 and 3.7. Decreasing EDGMA concentration decreases the YM values but increased the CTE (Figure 3.12), as the polymers are loosely packed and allowing more space for expansion (146). Polymer backbone has a unique molecular architecture,

the energy required for bond rotation equates to flexibility of the polymer. The energy required to rotate bonds is linked to the glass transition temperature (Tg), low Tg values indicates the polymer having flexible backbone. Polymer flexibility, chain stiffness and chain length all help determine Tg of polymer. Low Tg suggests that the polymers are not tightly linked together and more flexible thus their able to expand more (71). High Tg polymers would not be ideal for SCL formulation, as previously mentioned tightly linked polymer chains suggests poor flexibility thus low EWC%, CA.

3.4. Effect of co-polymers on SCL formulated using HEMA

Results and Discussion

From previous data collected above, it is clear that HEMA works best at higher concentration therefore we further understand how MMA, MAA and GMA polymers would work when copolymerised with HEMA at different concentration ranging from 90-40% (v/v).

Table 3.6: Represents the different concentration % of HEMA Vs MMA, HEMA Vs MAA and HEMA Vs GMA.

SCLs	Polymer concentration % (v/v)		
HEMA (88.4) EDGMA (1) BP (0.6)	MMA – 10	MAA – 10	GMA – 10
HEMA (78.4) EDGMA (1) BP (0.6)	MMA – 20	MAA – 20	GMA – 20
HEMA (63.4) EDGMA (1) BP (0.6)	MMA – 35	MAA – 35	GMA – 35
HEMA (48.4) EDGMA (1) BP (0.6)	MMA – 50	MAA – 50	GMA – 50
HEMA (38.40) EDGMA (1) BP (0.6)	MMA – 60	MAA – 60	GMA – 60

The prepared polymers are then subjected to several characterisation studies such as EWC, CA, transmission and YM. A total of 5 different concentrations were prepared for each polymer.

3.4.1. Preparation SCLs using hydrophilic HEMA copolymerised with MAA at different concentration.

Figure 3.13 shows EWC% and CA results for the copolymerisation of HEMA with MAA using 1% (v/v) of EGDMA (SCL's). HEMA/MAA at 90/10% (v/v) has the highest EWC% 31.12 ± 0.08% and lowest CA of 69.7 ± 2.84°. Increasing the concentration of HEMA caused a rise in EWC% due to the number of hydroxyl and carboxylic acid functional groups all of which forming hydrogen bonding. Both hydroxyl group and carboxylic acid functional group increases the hydrophilicity of the polymer matrix as well as degree of swelling (147)(148). The two concentration that possessed the highest EWC% are HEMA/MAA (90/10) and (80/20) both of which displayed no significant difference within the statistical analysis EWC% *p=0.6362* and CA *p=0.5246.* Figure 3.14 displays Young's Modulus values and transmission %, and it can be observed that increase in MAA within the polymer matrix the Young's modulus (YM) decreases as well as the optical transparency % (TM%). Increase

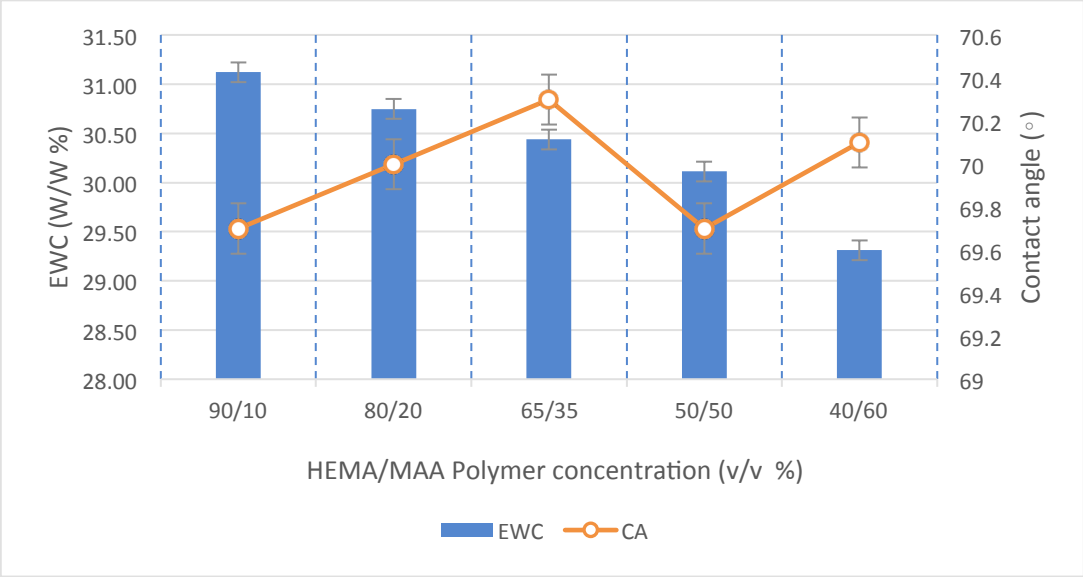

Figure 3.13: Equilibrium water content (%) and contact angle for HEMA/MAA at different concentration, results are expressed as mean ± SD, (n=3).

It can be observed from Figure 3.14 that with increasing MAA concentration the polymer matrix SCL elasticity decreased suggesting lower free movement of the polymer backbone. The polymer matrix with the highest concentration % of HEMA/MAA (90/10%)(v/v) possessed the most elasticity with 7.33E-05 ± 1.04E-05 MPa, compared to HEMA/MAA (50/50) which possessed the lowest YM value of 2.73E-05 ± 5.52E-06 MPa statistical analysis displayed a slight significant difference *p=0.0383*. TM% also decreased with increase in MAA composition, at HEMA/MAA (90/10) and (80/20) (v/v) possessed the highest TM % of 100.40 ± 0.29% and 100.17 ± 0.12% *p=0.3260* respectively. However, when comparing HEMA/MAA (90/10%) Vs (40/60%) (v/v) shows significant difference between the mean data of *p=0.0002.*

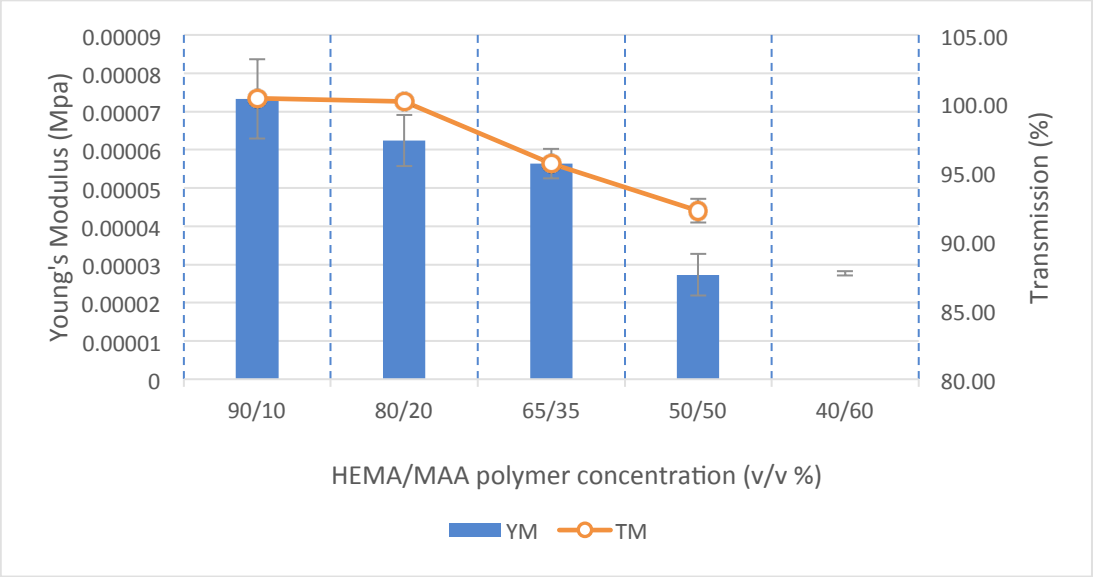

Figure 3.14: Young's modulus (Mpa) and transmission (%) for HEMA/MAA at different concentration, results are expressed as mean ± SD, (n=3).

3.4.2. Preparation of SCLs using hydrophilic HEMA copolymerised with MMA at different concentration %.

Incorporating a hydrophobic polymer such as methyl methacrylate (MMA) into hydrophilic polymer system will aid increase elasticity and provide the SCL with mechanical structure. Figure 3.15 shows that with increase in MMA there is a slight decrease in hydration this is due to the hydrophobic nature of the polymer, thus the hydrophobic interactions amongst the carbonyl groups present become stronger and at the same time inducing the release of water molecules within the polymer matrix resulting in decrease in EWC% (149)(150). Within HEMA/ MMA co-polymerisation the best two concentration % that possessed the highest EWC% were, HEMA/MMA (90/10%) and (80/20%) (v/v) with 35.53 ± 0.18%, 35.41 ± 0.11% and CA 79.4 ± 3.41° and CA 79 ± 3.86° respectively, statistical analysis displayed no significant difference between the two most popular formulations with a $p=0.9441$ for EWC% and $p=0.2698$ for $CA°$.

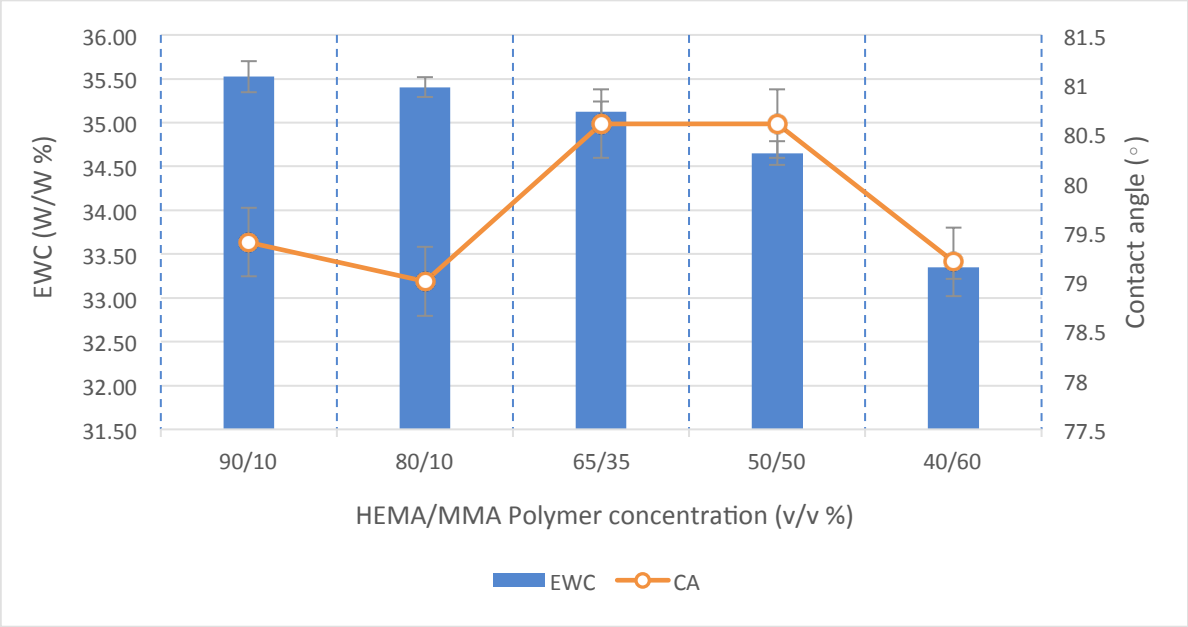

Figure 3.15: Equilibrium water content (%) and contact angle for HEMA/MMA at different concentration; results are expressed as mean ± SD, (n=3).

The Young's modulus and transmission of various concentration % of HEMA/MMA is displayed in Figure 3.16 below, increase in MMA concentration % the Young's modulus deceased suggesting that the contact lenses became increasingly less elastic. MMA is very well known polymer for its use in rigid contact lenses due to their hydrophobic nature(151). HEMA/MMA at (90/10%) and (40/60%) (v/v) the YM is 0.0083±0.002 MPa and 0.0043±0.0003MPa respectively, while the YM was slightly different for both formulations there was not a statistical significance *p=0.1849*. Optical transmission % of HEMA/MMA (90/10%) and (80/20%) (v/v) formulations were 100.24 ± 0.12% and 99.67 ± 0.15% respectively, statistically there was no significant difference between the mean data *p=0.1749.* however, when comparing the TM% of HEMA-MMA (90/10) composition to (40/60) 86.3 ± 0.1% the statistical analysis displayed a significant different with *p=<0.0001.* With increase in MMA in the SCL concentration, transmittance decreases this could be due to crystalline regions within the polymer or phase

separation taking place during polymerisation(82). Figure 3.16 suggests that increased concentration of HEMA yields better TM% values over 90% which is most desired.

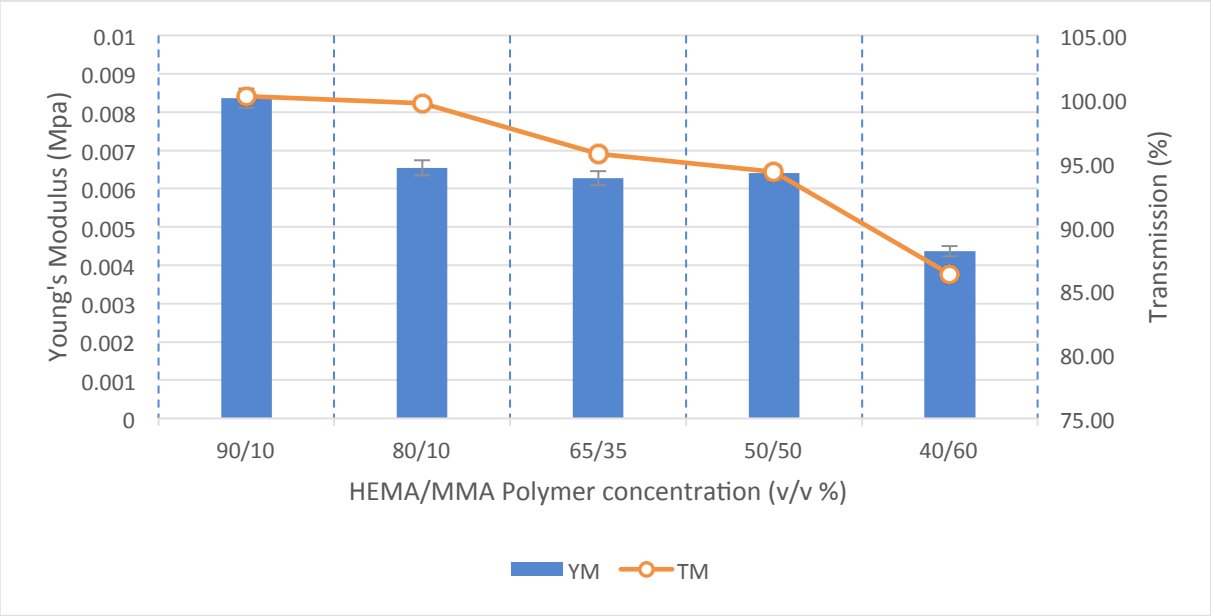

Figure 3.16: Young's modulus (Mpa) and transmission (%) for HEMA-MMA at different concentration, results are expressed as mean ± SD, (n=3).

3.4.3. Preparation of SCLs using hydrophilic HEMA copolymerised with GMA at different concentration.

The final co-polymerisation was between HEMA/GMA this polymer matrix provides hydrophilicity due to the presence of polar epoxy side group and methacrylic acid, it is also used to provide clarity within the lens suggesting that the polymer possesses amorphous regions (152)(153). HEMA/GMA (90:10%) and (80/20%) (v/v) possessed the highest EWC% of 31.69 ± 0.02% and 29.57 ± 0.03% and low CA 66.67 ± 3.37° and 75.2 ± 10.77° respectively, however both sets of results displayed significant statistical difference with $p=0.0054$ for EWC% and $p=<0.0001$ for CA°. Figure 3.17 showed that with increasing the GMA concentration, EWC% decreases, this could be due to the decrease in HEMA concentration (154). Regardless of the hydrophilic polar groups present within GMA, this does not always suggest stronger water binding capacity polymers such as HEMA with slight decrease intensity of polar group, have a higher water-binding capability (156-158).

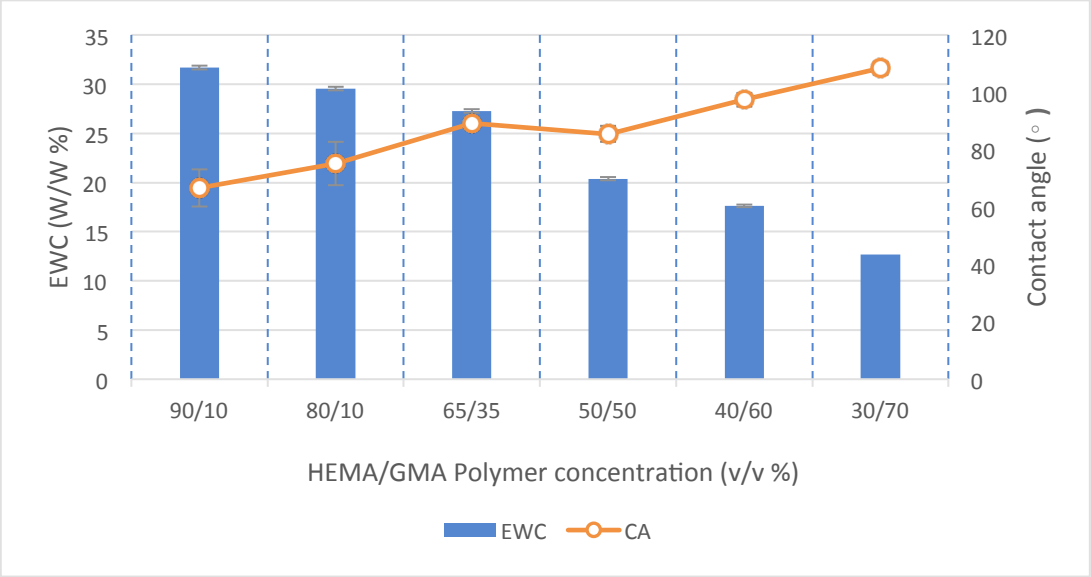

Figure 3.17: Equilibrium water content (%) and contact angle for HEMA/GMA at different concentration; results are expressed as mean ± SD, (n=3).

Figure 3.18 presents TM and YM data for HEMA/GMA concentration %, with increase in GMA concentration, TM% decreased slightly. The two concentration with the highest TM% would be (90/10%) and (80/20%) (v/v) with 90.80 ± 0.17% and 88.60 ± 0.1% respectively, (*p=0.0090).* However, when comparing HEMA/GMA (90/10%) with (40/60%) (v/v) presents a significant statistical difference with *p=<0.0001.*

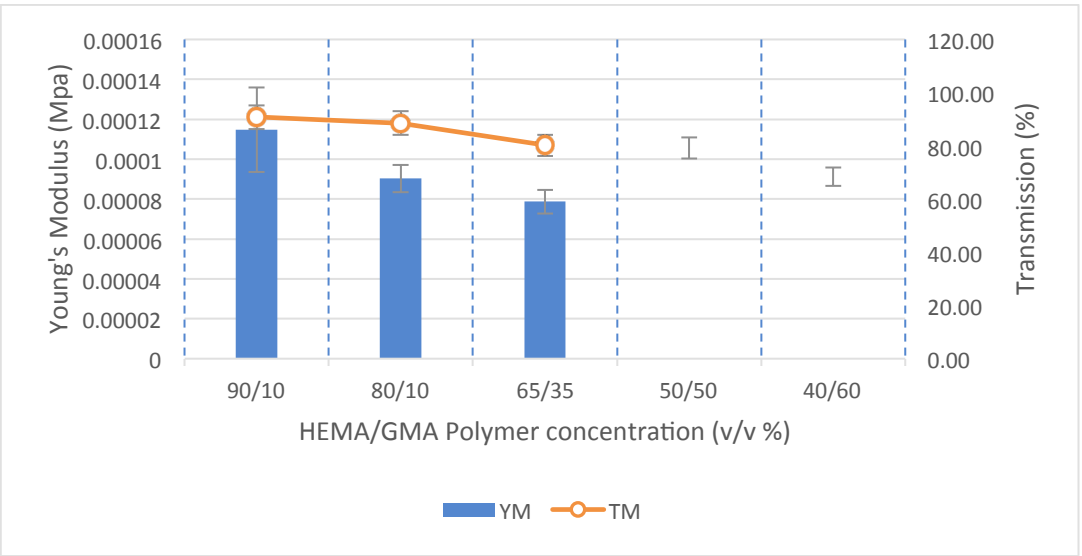

Figure 3.17: Young's modulus (Mpa) and transmission (%) for HEMA/GMA at different concentration, results are expressed as mean ± SD, (n=3).

HEMA/GMA at (50/50%) and (40/60%) (v/v) has shown no YM values in Figure 3.18, this was due to increase in GMA concentration % within the prepared SCLs, which became more ridged like structure this could be very much due to the amorphous properties of the polymer. This is also a good indication that increased concentration of GMA is not ideal for SCL preparations. HEMA/GMA (90/10%) (v/v) has uppermost YM value of 1.14E-03 ± 2.12E-05 MPa compared to (65/35%)(v/v) with YM value of 9.02E-05 ± 6.79E-06 MPa, both sets of data displayed statistically significant difference of $p=<0.0001$.

3.5. Summary

Separation and quantification of DZH using conventional analytical assays such as HPLC was challenging, however a novel analytical assay was developed and validated. This method allowed the quantification of the drug DZH. This assay was found to be stable, accurate and precise.

The polymers used to make the SCLs are categorised into three categories; the hydrophilic polymer that is capable of interacting with water forming basic hydrogel; the hydrophobic polymer producing high mechanical strength lenses; and the cross linking agent that adds both mechanical strength and thermal stability. The results confirmed that hydrophilic polymer increased EWC% within SCLs. High concentration % of HEMA when co-polymerised with EDGMA crosslinking agent displayed the highest EWC% this was the same for MMA polymer. It was also found that crosslinking agent EDGMA

has great influence on the Tg, CTE, YM and EWC%. With increase in crosslinking agent EDGMA the Tg and YM increased, whilst the EWC% and CTE of the polymers decreased suggesting that the polymer chains were tightly linked thus preventing it from expanding and inhibiting water absorption.

GMA at high concentration presented low EWC% within SCLs, due to their hydrophobic nature and interactions. GMA was further investigated and co-polymerised with HEMA, which in turn drastically improved its EWC%, TM% of the SCL. HEMA/MMA (90/10%) and (80/20%) (v/v) possessed the highest EWC%. All concentration of 50% and above of HEMA yielded TM% of 80% and above. With decrease in HEMA concentration it was observed that YM values declined suggesting the CLs became more rigid/stiff, therefore in order to obtain SCLs with an ideal EWC%, TM% and YM values high HEMA concentration should be used.

Contact Lenses Formulated with A Mixture of Hydrogel, Silicone and Fluoro-Silicone

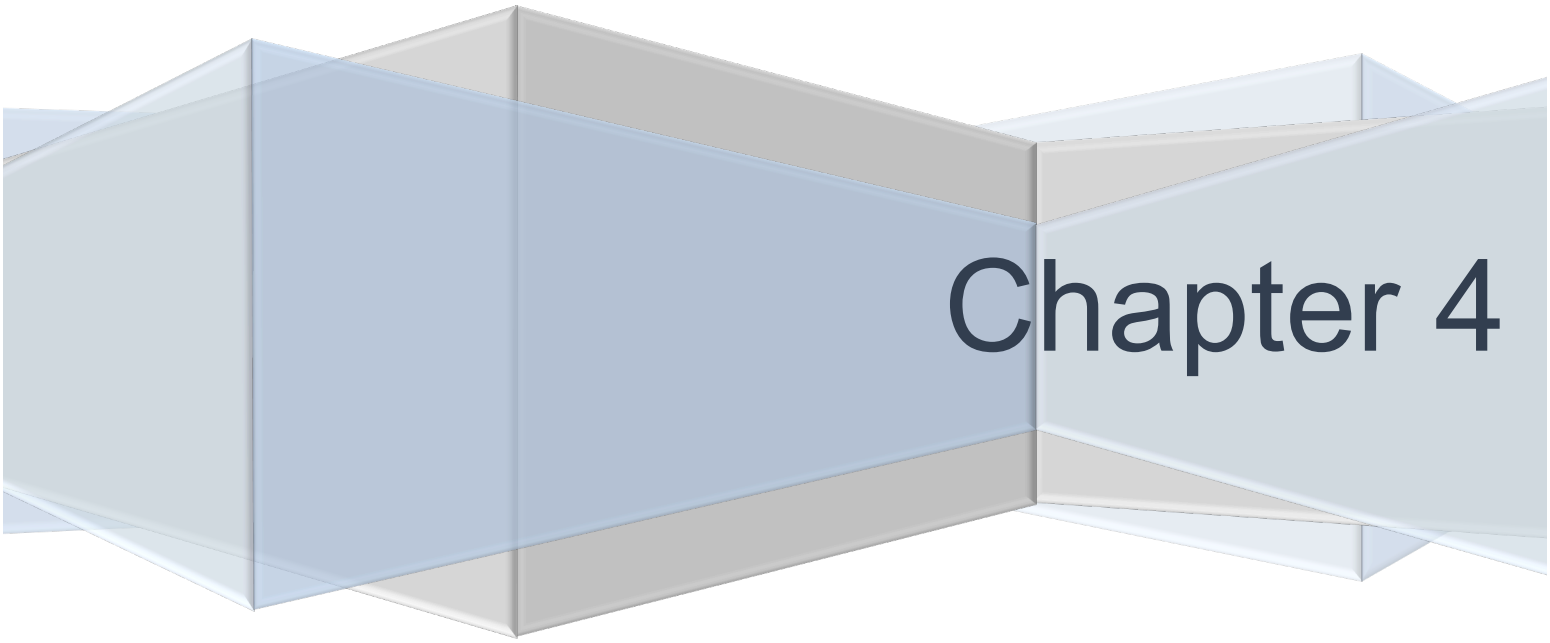

Chapter 4: SCL preparation with a mixture of silicone and fluoro- silicone based polymer

4. Introduction

The structure of hydrogel material is composed of long backbone featuring methacrylic acid with ethylene oxide. The hydroxyl and polar ketone group are responsible for forming strong hydrogen bonding and entrapping high capacity of water within the CLs. HEMA is frequently used as a conventional hydrogel material. Hydrogel and silicone monomers are chemically joined together by crosslinking in a free radical polymerisation process. An ideal contact lens would achieve a balance between oxygen permeability, hydration, material strength and stability (156)(157). Whilst hydrogels are very hydrating (due to hydrophilic hydroxyl functional groups present) and are not oxygen permeable, silicone (siloxane) -polymers possess many beneficial factors such as their high oxygen permeability, provide stability, low glass transition temperature (Tg), and low surface tension which is very important for surface wettability, none the less silicone possess hydrophobic properties (156). Before silicon-hydrogels (Si-Hy) CLs became available wearers wearing SCLs were very much prone to contact lens-induced hypoxia on corneal physiology (158). Si-Hy CLs have enhanced oxygen permeability as oxygen is soluble within the silicone polymer however in conventional hydrogel oxygen is more soluble within the water rather than in the hydrogel polymer.

The pervious chapter investigated the effect of cross-linker on hydrogel monomers used to formulate soft contact lenses (CLs) as well as the effect

of HEMA when co-polymerised with different co-polymers. The results generated from chapter 3 showed that utilising HEMA within CLs formulation was very promising, and that HEMA polymer enhances hydration and optical clarity when used at higher concentrations. However, these CLs lacked oxygen permeability to the ocular surface and possessed low elasticity, these findings will be further addressed and investigated in this chapter. Therefore, formulating silicone-hydrogel (Si-Hy) SCL would hopefully improve oxygen permeability as well as CL elasticity.

Silicone based polymers are the basis of numerous applications in the medical industry thanks to their popularity for prevailing biocompatibility and physiochemical properties (156). Over the last four decades, its evolution has paved the way for pharmaceutical industries to further develop the quality of the contact lenses that are suitable for optical applications. Si-Hy SCLs are one of the most common types of lenses used in the market due to the high oxygen permeability (162,163). There is a wide range of silicone monomers out there in the market and despite their popularity they have not been fully explored in making CLs (160). 3,3,3-trifluoromethoxysilane is one example where despite its increasing oxygen permeability properties; there is very little literature out there that supports its use for preparing SCLs.
High water content hydrogels tend to cause corneal desiccation(72,155). Therefore, there are many researches in the mission for high oxygen permeability. Researchers developed siloxane-hydrogels for SCLs, one common functional group all the silicone polymers have is polysiloxanes, the main reason for its hydrophobic properties. PDMS-vinyl terminated has 1

siloxane group whilst TRIS has 3 siloxane groups, which typically have high oxygen diffusion (Figure 4.1). Silanol ($SiO(Me)_2$) materials are highly hydrophobic and very prone to lipid deposition, silane (SiH4) and methane (CH4) are stable tetrahedral groups with increasing the chain length, and weaken the bonds (161). These silicone polymers encompass a siloxane backbone surrounded by aliphatic hydrocarbons non-covalently bonded creating hydrophobic layer (161). In order to offset the stated shortcomings the silicone polymers were copolymerised with hydrophilic HEMA polymer into hydrogels that offer high oxygen transmission as well as hydration for comfortable wear (162). Siloxane moieties require further treatment for extended wear contact lenses (167,168).

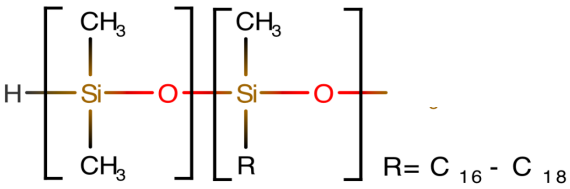

PDMS-Co-Alkylmethyl Siloxane

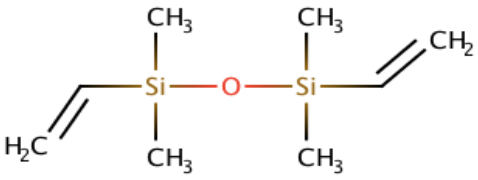

PDMS-Vinyl Terminated

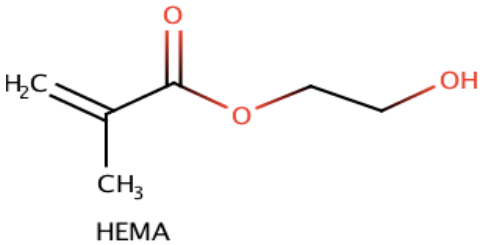

HEMA

3,3,3-Trifluoromethoxysilane

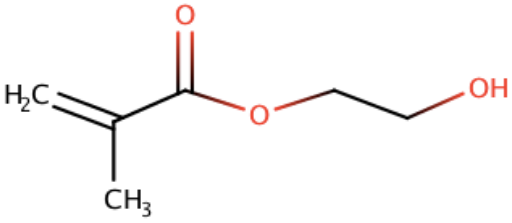

2-Hydroxyethyl methacrylate

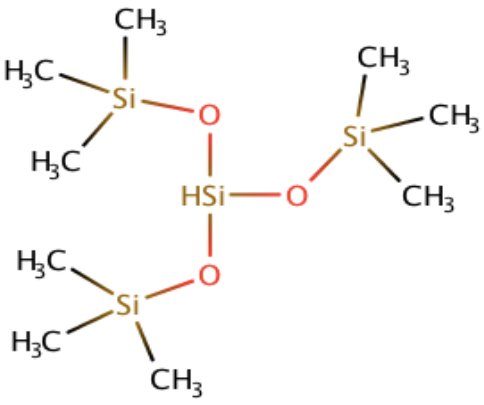

Trimethylsiloxy Silane

Figure 4.1: Silicone-polymers incorporated into hydroxyethyl methacrylate backbone to create novel silicone-hydrogels.

UV- polymerisation was more readily used within chapter 4 onwards, due to the findings in chapter 3, MMA and MAA, showed that they were highly volatile and majority of the polymer evaporated during thermal polymerisation stage. Both polymers have major benefits and were readily used within this study, therefore in order to overcome the drawbacks mentioned UV-polymerisation was used; and for this a photo initiator was used.

4.1. Aim and Objective

To formulate Si-Hy CLs, which are further characterised. The specific objectives include.

- To prepare and optimise SCLs using different concentration of silicone based polymers.
- To understand the influence of silicone based polymers on SCL properties.
- To study the effect of concentration of silicone polymers on the performance of Si-Hy SCLs, and characterise the prepared Si-Hy SCLs for their; EWC, CA, TM and YM.

4.2. Equilibrium water content (EWC%) of silicone-based SCLs

Results and discussion

In this chapter (4) different types of silicone-polymers will be studied, (PDMS-co-alkyl siloxane (PDMS-AS), PDMS-VT (PDMS-vinyl terminated), 3,3,3 trifluoromethoxysilane and TRIS((trimethylsiloxy)saline) (Tris)) (Figure 4.1) all of which originate from poly(dimethylsiloxane) (PDMS) that has been significantly used as biomaterials in ophthalmic applications (164) such as intraocular lenses (170,171), artificial cornea (164,172) and contact lenses (173-175). Originally soft contact lenses were made from hydrophilic polymers, however Si-Hy CLs have been a popular addition to the contact lens market (168), they were formulated to improve oxygen permeability to the ocular surface.

Table 4.1: Percentage composition used for the preparation of Si-Hy SCLs.

Material		% Composition
Set 1 formulation	HEMA, PDMS-VT HMPP TEGDMA	97, 95, 93, 90, 88 1, 3, 5, 8, 10 1 1
Set 2 formulation	HEMA, TRIS HMPP TEGDMA	97, 95, 93, 90, 88 1, 3, 5, 8, 10 1 1
Set 3 formulation	HEMA, PDMS-AS, HMPP TEGDMA	97, 95, 93, 90, 88 1, 3, 5, 8, 10 1 1
Set 4 formulation	HEMA, TFMS HMPP TEGDMA	97, 95, 93, 90, 88 1, 3, 5, 8, 10 1 1

Equilibrium water content of different silicone-based polymers were obtained and displayed in Figure 4.2, formulation containing 1% of any silicone-based polymer the measured EWC% was above 30%, this is due to the 97% HEMA composition this hydrophilic monomer provides the hydrogen bonding within water molecules. However, with increasing the silicone-based polymers the EWC% slightly decreases, indicating a more hydrophobic formulation compared to the formulations without silicone-based polymers.

With PDMS-co-alkyl siloxane and 3,3,3 trifluoromethoxysilane the EWC% remained more or less constant with increase in percentage volume of

silicone-based polymers as displayed in Figure 4.2. Figure 4.2 showed that the EWC% of PDMS-co-alkylsiloxane (PDMS-AS) remained above 30% with increase in silicone polymer (1%, 3%, 5%, 8% and 10%), PDMS-AS also displayed the highest EWC% due to the R= C_{16}-C_{18} present within the chemical structure making the C and H more electronegative and forming hydrogen bond when hydrated(169)(170). Whilst 3,3,3 trifluoromethoxysilane (TFMS) remained at 30% EWC% (1%, 3%, 5%, 8% and 10%). This could be due to an achieved balance between the hydrophilic-hydrophobic polymers, with gradual decrease in hydrophilic HEMA and increase in hydrophobic silicone-based polymer (171).

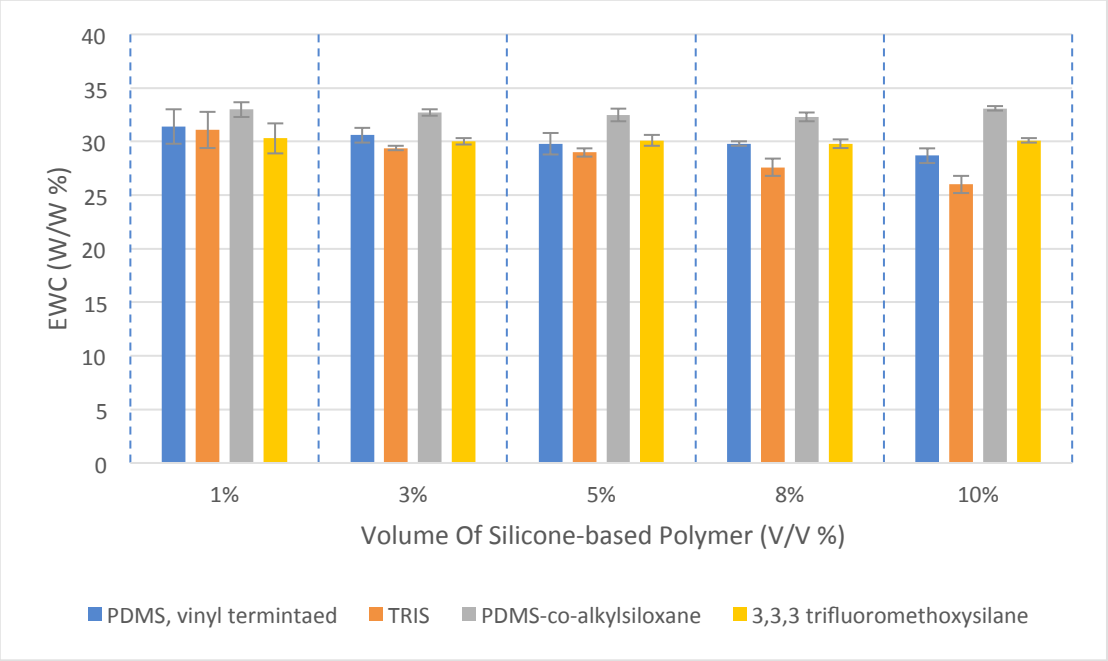

Figure 4.2: EWC (%) against percentage volumes silicone-based polymers results are expressed as mean ± SD, (n=3).

Smaller volumes of PDMS-VT possessed similar EWC% values to that of TFMS shown in Figure 4.2. Siloxane based polymers have high thermal stability, low Tg, low surface tension with high oxygen permeability; due to strong stretching vibrations within the Si-O bonds creating permeable

channels within the polymer complex, as well as providing lens stability and material strength (71,159,179,180).

The hydrophobic properties of TRIS((trimethylsiloxy)saline) and PDMS-VT (PDMS-vinyl terminated) polymers have shown a reduction on EWC% with decrease in HEMA polymer. With EWC% of PDMS-VT from 1% to 10% (v/v) there was a statistical significant with p=0.0169. With silicone polymer TRIS, there was a statistical significance in EWC% from 1%-10% with p=0.0005. PDMS-VT yielded higher EWC% with increase in silicone polymer in comparison to TRIS this is very much related to their chemical structures as already mentioned above TRIS possess 3 polysiloxane groups making it more hydrophobic whilst PDMS-VT only possess one.

4.3. Contact angle (°) of silicone-based SCLs

Surface contact angle (CA) is a parameter used to measure wetting ability of the SCL. The smaller the CA the greater the wetting ability. Good wettability within SCLs indicates comfort and lens stability preventing change of the SCL between the corneal surface and eyelids for CL wearers. Poor wettability suggests a hydrophobic surface making it more prone to lipid adherence on surface of SCL (161,181). Figure 4.3 displays the CA of all the Si-Hy SCLs with increase in silicone percentage volume there was an increase CA suggesting a more hydrophobic surface.

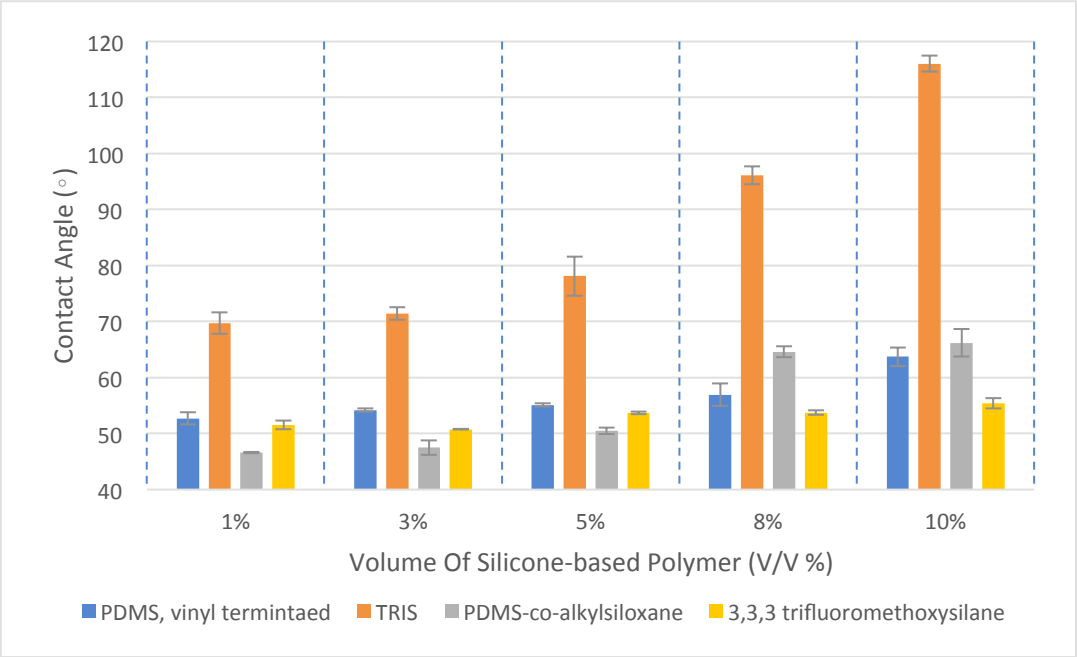

Figure 4.3: Surface Contact Angle against percentage volumes of silicone-based polymers results are expressed as mean ± SD, (n=3).

PDMS-AS showed the smallest CA from 1-5% with PDMS-VT from 1-8% and TFMS 1- 10% volume of silicone-based polymer. Figure 4.3 represents PDMS-AS at 1, 3 and 5% (v/v) with CA of 46.6 ± 0.1°, 47.5 ± 1.3° and 50.5 ± 0.6° respectively, also the data presents slight statistical significance of

P=<0.0001. CLs made of PDMS-VT at 1, 3, 5 and 8% (v/v) showed CA of 52.7 ± 1.1°,54.2 ± 0.3°, 55.1 ± 0.3° and 56.9 ± 2.0° respectively and TFMS at 1-10% (v/v) with CA 51.5 ± 0.8°,50.8 ± 0.1°, 5% 53.7 ± 0.3°, 53.7 ± 0.4° and 55.4 ± 0.9° both PDMS-VT and TFMS displayed statistical significance of *P=<0.0001.* The low CA of the Si-Hy CL surface is believed to be due to the hydrophilic moieties of HEMA enclosing that of the silicone polymers making the overall SCL material hydrophilic (172). Polysiloxane polymers have high thermal and oxidative stability, PDMS is essentially non-toxic and non-irritant hence therefore PDMS is highly exploited for ocular purposes.

TRIS had the highest CA values CLs made of 8% TRIS had CA 96.1 ± 1.6° while 10% TRIS CLs had CA of 116 ± 1.4° *P=<0.0001.* These are due to the surface hydrophobicity as well as the surface roughness of the Si-Hy SCL (173). The structure of TRIS is one of the main reasons for the increase in hydrophobicity of the CL surface, as already mentioned TRIS polymer possess 3 siloxane groups, the silanol bonds are longer and flexible compared to carbon-carbon bond, and due to its innate mobility the silanol chains will easily make its way to the surface of the lens (174) hence the increase CA with increased volume of TRIS polymer. Manufactured contact lenses formulated with TRIS polymer possess a surface tension of 71.0-71.9 mN/m (172). Another factor that could affect the CA is the physical forms of the Si-Hy SCLs shown in Figure 4.5, TRIS SCLs appeared milky with absence of smoothness (173). The images are Post-polymerisation with no modification such as polishing made.

4.4. Optical properties of silicone-based SCLs

Optical transparency is an essential characteristic of SCLs in order to determine the materials suitability for optical applications (175). Based on the literature the acceptable light transmittance percentage (%) ranged from 90-99% (186,187), the obtained results are shown in Figure 4.4. Figure 4.5 displays prepared SCLs containing different percentage volumes of silicone-based polymers and their effect on transparency of the lens. As presented the transparency of SCLs ranged from 58.4 ± 1.1% to 94.7 ± 0.8%. TRIS has the lowest transmission values ranging from 86.6 ± 3.3% for 1% to 58.4 ± 1.1% for 10% TRIS % with *p=0.0001*. It is clear with increase percentage volume of all silicone polymers optical transparency percentage decreases. The significant difference in transparency percentage could be due to the occurrence of phase separation during the polymerisation process as well as incompatibility of the materials within the formulation (82). Guidi et al investigated the effect Si-Hy composition on drug dexamethasone release; optical transparency of the Si-Hy was studied. It was found that with HEMA-co-TRIS (OH)-co-PDMS hydrogel possessed minimal transparency % due to phase separation taking place in the polymerisation stage as HEMA/ PDMS was not be compatible with polysiloxane causing opacity, this particular composition also possessed the lowest EWC% (82).

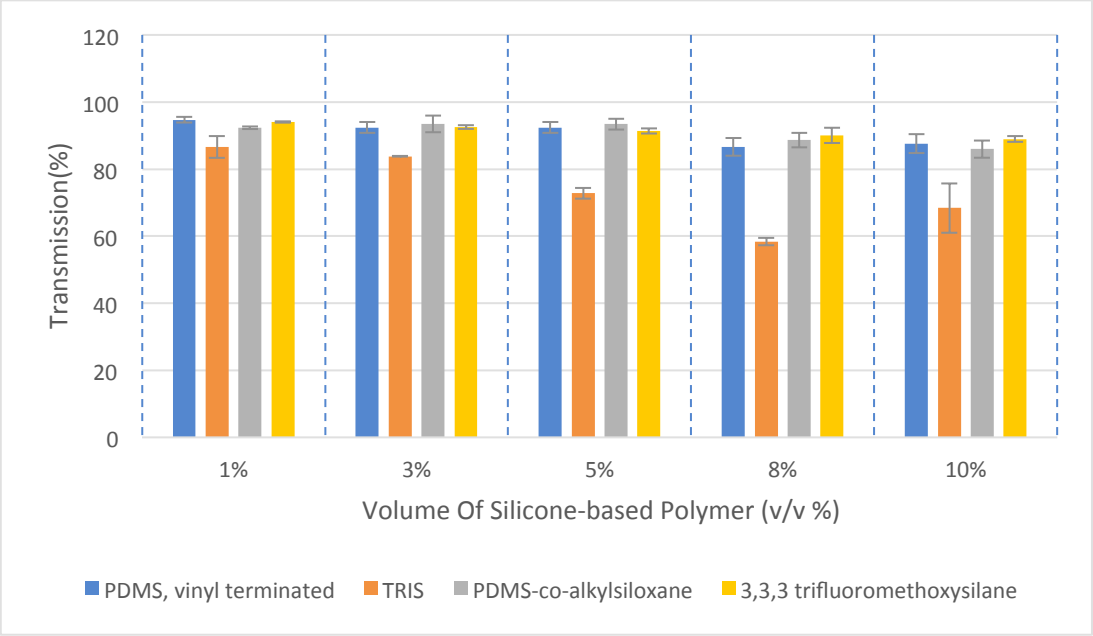

Figure 4.4: Light Transmittance against percentage volumes of silicone-based polymers results are expressed as mean ± SD, (n=3).

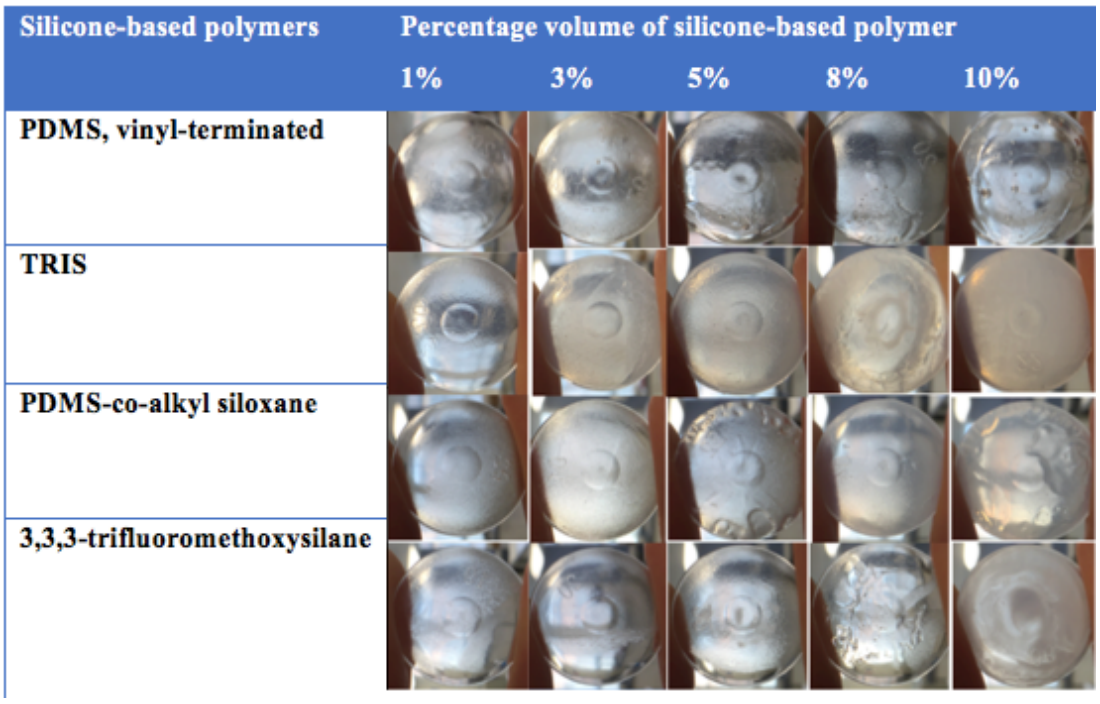

Figure 4.5: Images of SCLs containing different percentage volumes of silicone based polymers.

Both PDMS-VT and PDMS-AS exhibited transparencies that fell within the range of 90% and above(176,177), for 1-5%(v/v) volume of polymer. However, from 8-10% (v/v) percentage transparency dropped below the range. Transmission% of PDMS-VT and PDMS-AS at 8 and 10% (v/v) displayed 86.6 $\pm$ 2.6%, 87.6 $\pm$ 2.8% and 88.7 $\pm$ 2.2%, 86.0 $\pm$ 2.6% respectively, this could be due to phase separation caused by the incompatibility of the materials used resulting in reduced transparency percentage (159). Statistically PDMS-VT and PDMS-AS has shown no significant difference for 8 and 10% (v/v) with *P=0.9461* and *P=0.4804* respectively.

Amongst all the silicone-based polymers TFMS had the most consistent transparency percentage values. TFMS percentage volume of 1% vs 10% (v/v) showed no statistical significance with *p=0.5158*. However, when comparing PDMS-VT and TMFS the results shown that they both possessed the highest transparency value at 1% volume 94.7 $\pm$ 0.8% and 94.0 $\pm$ 0.2 (*p=>0.9999*) respectively.

4.5. Young's modulus of silicone-based SCLs

Young's modulus (YM) helps determine the elasticity of the Si-Hy SCLs. SCL with Young's modulus value below 1.4 MPa have the ability to align with corneal surface of the eye and still be able to resist deformation under tension (178,179). If the YM value is too high it could lead to induced ocular pathology such as superior epithelial arcuate lesions (SEAL) and with low YM value SCL induced papillary conjunctivitis (CLPC) as well as difficulty handling and discomfort could be caused (72,189).

The value of YM was calculated and the results were shown in Figure 4.6. With an increase volume of PDMS-VT, PDMS-AS, FTMS and TRIS this caused an increase in YM value, this was due to the influence of siloxane moiety within all the formulation. Incorporation of silicone into hydrogels (such as HEMA) improves the elasticity of the CLs and prevents deformation when eyelid comes into contact with the contact lens (174). The silicone polymers provide material strength when polymerised with hydrogels this complex helps offset the stated shortcoming.

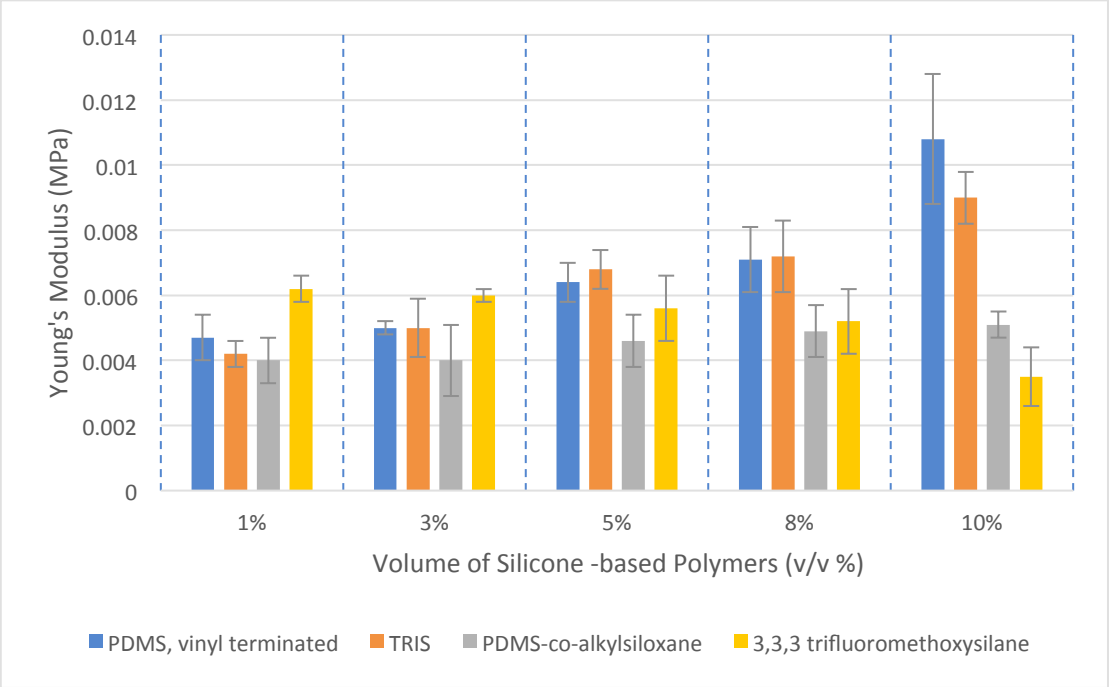

Figure 4.6: Young's Modulus against percentage volumes of silicone-based polymers results are expressed as mean ± SD, (n=3).

However, with increase in TFMS polymer concentration the YM value decreased, as the SCLs became very brittle. Possibly the incorporation of fluorine into the carbon-carbon backbone chain causes a decline in chain flexibility as well as mobility (180)(181). When comparing TFMS at 1% vs 10% (v/v) the results did not present any statistical significance with *P=0.5158.* A study by filipecka et al was carried out they studied a variety of current contact lenses and used middle infrared spectroscopy (MIR) to investigate the internal structure of the materials. The MIR spectra of rigid gas permeable CLs (Conflex-Air and Boston ES) displayed stretching vibrations of C-F bonds appearing to reduce backbone mobility and obtaining inflexible structures (180,191).

4.6. Summary

Hydration measurement indicated that modification of hydrogel structure by siloxane moieties leads to a decrease in EWC% with increasing their volume %. PDMS-AS displayed the highest EWC% as shown in Figure 4.2, this was followed by TFMS this was due to the attractive force present between the hydrogen atom covalently bonded to the fluorine atom within the silicone-polymer. Smaller volumes of PDMS-VT possessed similar EWC% values to that of TFMS.

TRIS polymer possessed the lowest EWC% with increase in polymer concentration, which caused an incline in CA value, thus increasing the hydrophobicity of the SCL surface. Asides from the presence of siloxane moieties, another factor that may have had an effect on the CA value, could be surface roughness of CL as they're not subjected to any surface (polishing) modification. With increase in polymer concentration of PDMS-VT and TFMS small CA values were observed due to their low Tg and surface tension.

TFMS and PDMS-VT possessed the highest TM% values amongst all silicone-based polymers, with increase in these silicones based polymers the TM% dropped slightly. TRIS obtained the lowest TM% values; this was believed to be due to phase separation and incompatibility between the materials. There was a general pattern amongst the TM and YM values, with increase in percentage volume of silicone polymer both TM and YM values

increased. However, within F-S/A silicone based polymer increase in percentage volume resulted in a decrease in YM value, due to the fluorine atom causing a decline in polymer flexibility.

All of these silicones based polymers possess a unique quality that we could benefit from when preparing SCLs, F-S/A polymer proved to be most transparent, whilst PDMS-AS had the highest EWC%, at lower volumes. Combining the silicone based polymers with HEMA hydrogel, forming Si-Hy complex will help eliminate lens-induced hypoxia for SCL wearers, due to the highly oxygen permeable nature of siloxane, at the same time the hydrophilic HEMA hydrogel will provide hydration and comfort for SCL wearers.

Polyacrylic Acid Nanoparticle (PAA-NPs) Formulation, Optimisation And Incorporation Into Si-Hy SCL

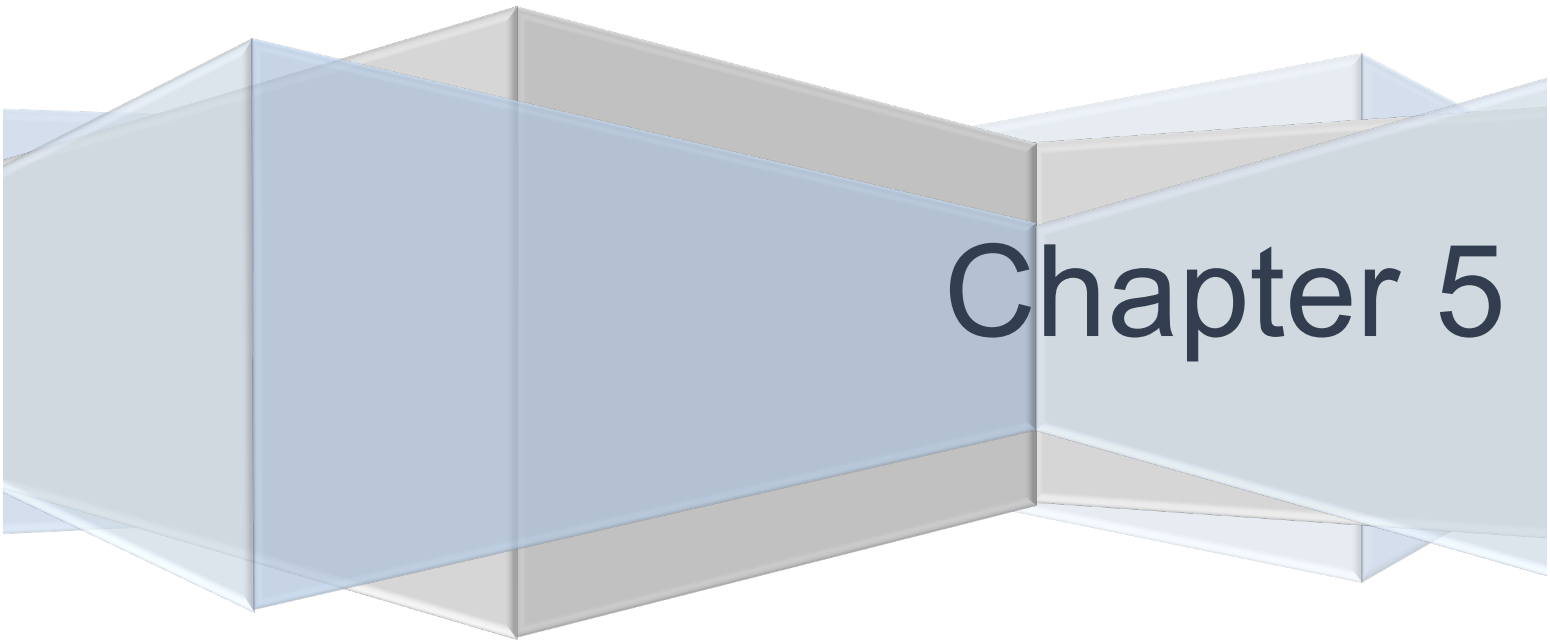

Chapter 5: PAA Nanoparticle

5. Introduction

Based on the results from the previous chapter it was clear that PDMS-AS/HEMA (95/3% v/v) possessed the highest EWC% of 30% this could be due to the high concentration of HEMA being used. Overall PDMS-AS/HEMA proved to be most promising. Siloxane based polymers have high thermal stability, with low value Tg, low surface tension with high oxygen permeability; due to strong stretching vibrations within the Si-O bonds creating permeable channels within the polymer complex, as well as providing lens stability and material strength (17,39,56,61). PDMA-AS was selected to be co-polymerised with HEMA, as it will aid eradicate lens-induced hypoxia for SCL wearers, due to its favourable oxygen permeable nature, whereas the hydrophilic hydrogel HEMA will increase hydration hence providing more comfort for the wearers (41).

There is always room for further improvement when it comes to SCLs, a concentration of HEMA 95% + PDMS 3% would be suitable carrier for nanoparticle laden SCLs (PAA-NP). This is because PDMS-AS displayed the highest EWC% and TM%, at the same time the hydrophilic HEMA hydrogel will provide hydration and comfort for SCL wearers. This chapter assess the effect of DZH nanoparticles (DZH-NPs) on Si-Hy SCLs, and to see whether or not EWC%, CA, TM and YM would be compromised. Due to the complex nature of the human eye, most drugs administered topically must have the ability to pass through the cornea before reaching the aqueous humour. With topical administration, almost 90% of the drug is lost due to a number of

reasons, such as high tear turnover and drug loss via the nasolacrimal drainage, and into systemic circulation (63). Nanoparticle encapsulated SCLs describes particles of 10-1000 nm, used as carriers. NPs are used to encapsulate active pharmaceutical ingredient (API) pre- dispensing via SCLs matrix, protecting the drug from interacting with the active polymers as well as enhancing prolonged drug release (15,45).

Chen et al, encapsulated methazolamide into calcium phosphate nanoparticles (CaP-NP), in *vitvo* release studies demonstrated methazolamide release from CaP-NP over a period of 4 hours. However In *vivo* studies indicated intraocular pressure lowering due to methazolamide release from CaP-NP over a period of 18 hours compared to 1% brinzolamide eye drops that only lasted 6 hours (182).

Yang et al, used hybrid hydrogel poly(lactic-co-glycolic acid) (PLGA) nanoparticles to deliver two anti-glaucoma drugs (Brimonidine and Timolol maleate) that displayed no cytotoxic effect to corneal epithelial cells. *In vitro* studies demonstrated prolonged residence time through slow drug release of 28-35 days and displayed anti-glaucoma effects (40). Thus, this new platform has shown to improve drug bioavailability (40,183–185).

PAA is of particular significance for ocular drug delivery, due to the following properties; high EWC within their structure making them soft and mucoadhesive properties (64,65). These properties enhance the biocompatibility and control of drug release hence they are important in the pharmaceutical industry as form of drug delivery systems(64). PAA is currently used in the market as topical eye drops and eye gels (Lubritha™

and Optrex®) to treat dry eyes.

Muter, studied the effect of acrylic acid (AA) on EWC HEMA hydrogels, and discovered that addition of AA results in increased water absorption due to conversion of carboxyl group into carboxylate anion (more hydrophilic ionised form)(186). Thakur et al, agrees that PAA polymer has the ability to absorb substantial quantities of water due to their hydrophilic nature, making them potential applicants for drug delivery systems (187).

Calixto et al, studied the mucoadhesive properties of PAA intended for topical drug delivery. PAA was prepared at 0.5, 1.0 and 1.5% (w/v). The results showed that with increase in PAA concentration, generated the strongest bioadhesive characteristics. In order to benefit from mucoadhesive properties of PAA and NP delivery systems used to prolong drug release. *Greindl et al,* developed a novel method for preparation of thiolated PAA NPs via ionic gelation. Various cross-linking agents were used including Ca^{+2}, Mg^{+2}, Zn^{+2}, Al^{+2} and Fe^{+2}. *In vitro* characterisation results of the particle size, zeta potential and size distribution suggested that Ca^{+2} was most promising. A particle size from about 220 – 295nm and zeta potential from about -7 up to -20 mV was generated (65).

Within this chapter, PAA NPs will be formulated, optimised and then incorporated into Si-Hy SCL. Optimisation of the NPs is carried out by formulating NPs at various different concentrations of PAA at 0.1, 0.5, 1 and 2%, the mean particle size and polydispersity index (PDI) was assessed. Based on PDI and particle size of the formed PAA nanoparticles the ideal concentration of PAA would be determined. The next step will be to study the

effect of different volumes of Calcium chloride ($CaCl_2$) (0.5%) solution as a cross-linker on the particle size of PAA-NP. Together this will help formulate the right PAA- NP with desired properties.

5.1. Aims and Objectives

To formulate Si-Hy SCLs incorporating PAA NPs to modulate the release of DZH. The specific objectives are:

- To prepare polyacrylic acid (PAA) nanoparticles using ionic gelation ($CaCl_2$ as a crosslinking agent).
- To characterise the prepared PAA nanoparticles for their particle size, zeta potential, polydispersity index, entrapment efficiency and *in vitro* release.
- To study the factors that would affect the performance of PAA nanoparticles such as particle size, zeta potential, polydispersity index
- To investigate the possibility of incorporating PAA-NP into HEMA/PDMS-AS and examine *in vitro* drug release from PAA-NPs.
- To study the effect of PAA-NP on the following properties EWC, CA, TM and YM of SCLs.
- To Investigate corneal irritation potential and to study any corneal damage of the prepared SCLs via examination of the bovine cornea within the BCOP assays.
- To investigate the corneal irritation effect of the prepared PAA nanoparticles.
- To further examine the effects of the prepared PAA nanoparticles on the conjunctiva of the eye via HET-CAM assay.

Results and Discussion

The first part of the discussion focuses on the optimisation study of PAA NPs, investigating the effect of various concentrations of PAA and $CaCl_2$ cross-linking agent on the particle size and surface charge of the formulated NPs. Once the concentrations of PAA and $CaCl_2$ cross-linking agent were optimised, 3 different formulations are selected, control SCL, DZH NPS in SCL and DZH in SCL matrix. The characterisation of all 3 formulations is conducted to study their effect on the SCL properties.

Table 5.1: Percentage composition used for the optimisation of PAA NPs.

Material		Composition (%)(mL)
Group 1 formulation	PAA	0.1%, 0.5%, 1%, 2 %
Group 2 formulation	$CaCl_2$	2mL, 4mL, 8mL, 10mL

Table 5.2: Percentage composition used for the preparation of control SCL, DZH NP in SCLs and DZH in SCL matrix.

Material		Composition (%)
Set 1 formulation SCL CONTROL	HEMA, PDMS-AS, HMPP, TEGDMA	95, 3, 1, 1%
Set 2 formulation DZH NP in SCL	HEMA, PDMS-AS, HMPP, TEGDMA DZH, $CaCl_2$, PAA- NP	93.7, 3, 1, 1, 1, 0.2, 0.1%
Set 3 formulation DZH in SCL matrix	HEMA, PDMS-AS, HMPP, TEGDMA DZH	94.06, 2.97 0.99, 0.99 0.99%

5.2. Characterisation of the formulated PAA nanoparticles (NP's)

Incorporation of hydrophilic drug (DZH) within PAA NPs was a challenging process. Ionic gelation technique was employed for the encapsulation of the hydrophilic drug DZH within the PAA NPs. Refer to chapter 2 section 2.4 for the preparation of NPs.

5.2.1. Particle size, zeta potential and morphology of the nanoparticles

Particle size has a great effect on the bioavailability of the drug when encapsulated within nanoparticles, as smaller NP size suggests greater surface area which means it will have a more enhanced interaction with the release medium and much better release (188). Polydispersity index (PDI) of the NPs provides information on how homogenous the formulation is, a lower PDI value indicates a more homogenous system. The effect of different concentrations of PAA on the PDI of NPs was examined via zetasizer.

Figure 5.1 below shows the effect of different concentrations of PAA on mean particle size and PDI. The average particle size of NPs increases with increase in PAA concentration. A study by Lee *et al,* (2013) showed that increase in PAA induced increase in nanoparticle size (189). Another study panacek *et al,* (2014) showed that the size of silver NPs were very dependent on the concentration of PAA, NPs synthesised without PAA possessed an average size of 28 nm and with presence of PAA that

increased to 77 nm. Suggesting that the presence of PAA has an influence the NP growth stage (61). The findings of these studies suggest that PAA concentration determines the size of the formulated NPs. Therefore, it is important to optimise the concentration of PAA used to formulate NPs.

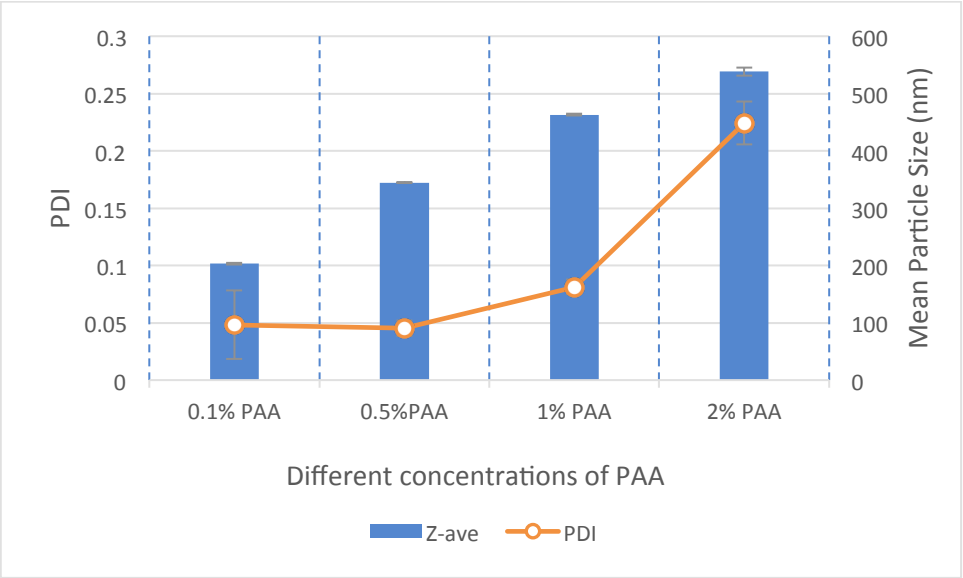

Figure 5.1: Mean particle size and PDI values of various concentrations of PAA. Data presented as a mean ± SD, n=3.

Figure 5.1 presents the mean particle size of PAA NPs prepared using: 0.1, 0.5, 1 and 2% PAA. The smallest particle size was exhibited by 0.1% PAA was 202.9 ± 1.24 nm, followed by 0.5% PAA 344.4 ± 0.63nm, 1% at 463.2 ± 1.31 nm and 2% yielded the highest particle size at 538.5 ± 3.43 nm. 0.1% PAA possessed the most desirable mean particle size for ocular drug delivery as well as showing the most uniformity in size difference (15). Within this study, it is clear that particle size of the nanoparticles is very much dependent on the addition of PAA (61,199). The variations in the mean particle size were statistically significant ($p<0.0001$) between 0.1% and 2% (v/w) PAA concentrations. This indicates change in PAA concentration has a great effect on particle size of the NPs. The measured PDI was found to be

0.048 ± 0.03, 0.045 ± 0.007, 0.081 ± 0.0062 and 0.224 ± 0.019, for 0.1%, 0.5%, 1% and 2% PAA NPs respectively. The different PDI results displayed were statistically significant between 0.1% and 2% (w/v) PAA concentrations (*p<0.0001)*. The results (Figure 5.1) suggest that with increase in PAA there was an increase in PDI value which could suggest diverse population in size or possible aggregation thus decreasing particle stability. 0.1% (w/v) PAA NPs not only yielded the lowest particle size but also the lowest PDI and was seen to be the most monodispersed from all the other NPs formulated.

Figure 5.2 displays mean particle size of PAA nanoparticles against different volumes of Calcium chloride ($CaCl_2$) (0.1%) solution was used as a cross-linker. The effect of different volumes of $CaCl_2$ were studied, the results shows that $CaCl_2$ had significant effect on the mean particle size of NPs.

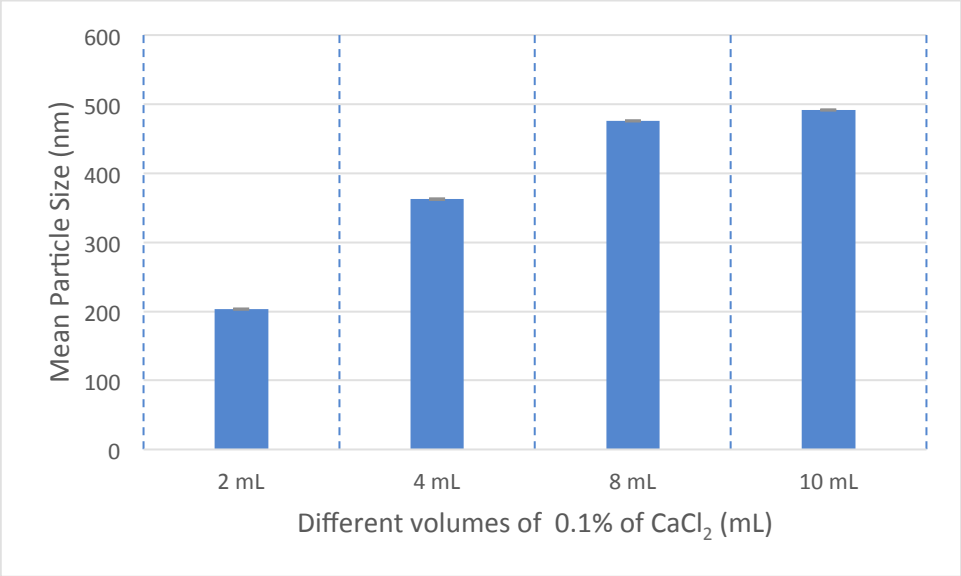

Figure 5.2: Displays the mean particle size for different volumes of $CaCl_2$. Data presented as a mean ± SD, n=3.

The measured particle size of the NPs was shown as 202.9 ± 1.24 nm, 362.4 ± 7.59 nm, 476 ± 8.71 nm and 491.3 ± 4.03 nm, for 0.1%PAA at 2 mL, 4 mL,

8 mL and 10 mL $CaCl_2$ respectively. From Figure 5.2 its observed that 2 mL of $CaCl_2$ results in the smallest particle size of PAA NPs at 200 nm ± 1.24, with increase in $CaCl_2$ volume it is shown to increase particle size of NPs. Statistical analysis displayed a significant difference with increase in $CaCl_2$ at *p<0.0001.* Therefore, the it was suggested to use 2 mL $CaCl_2$ as we obtained the lowest Ca-PAA particle size amongst all the other different $CaCl_2$ volume. This is likely improve particle size and surface charge of nanoparticles that affect ocular penetration, particle size of 400 nm and below increases membrane permeability (38,194,200-201).

Figure 5.3 demonstrates the effect of DZH encapsulation has on particle size, PDI and surface charge of the NPs compared to control NPs. The results presented in Figure 5.3 shows an increase in mean particle size between the control NPs (202.9 ± 1.24 nm) and DZH loaded NPs (1551 ±4.320 nm). The measured zeta-potential of the formulated NPs were negatives with a mean value ranging from -6.24 ± 1.00 (mV), and -17.15 ± 1.12 (mV), for control NP and DZH loaded NP. Statistical analysis between the control and the DZH loaded NPs were significant (p>0.0114), indicating that loading of the DZH into NPs had influence on the zeta potential of the formulated NPs. The negative nature of NPs displays moderately more mucoadhesive properties (65), PAA were responsible for the negative charges displayed as these properties are necessary for enhancing permeation properties (65,202-203).

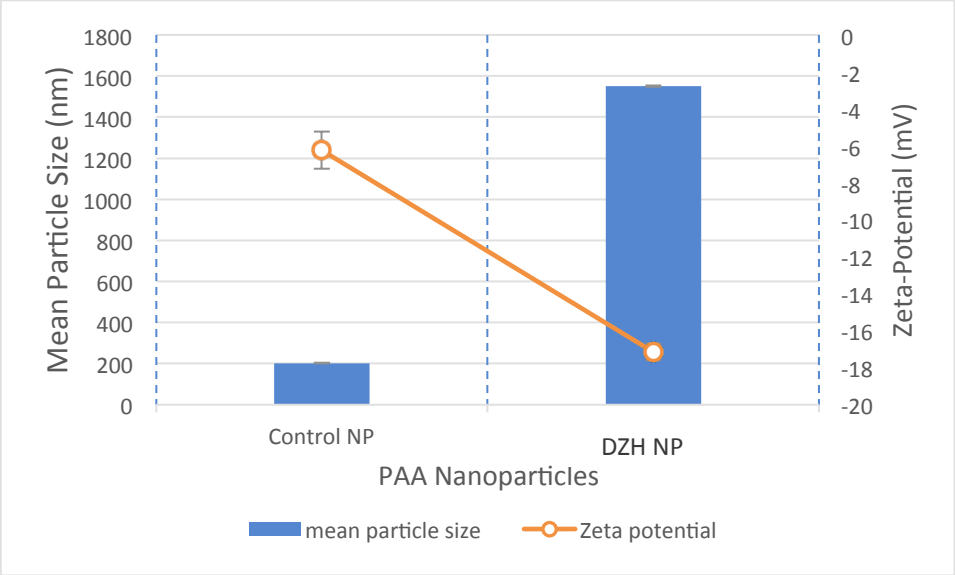

Figure 5.3: A Mean particle size and surface charge of control and DZH loaded NPs. Data presented as a mean ±SD, n=3.

5.2.2. Scanning electron microscopy (SEM)

The morphology of the formulated NP's was investigated using SEM Figure 5.4 displayed SEM micrographs of 0.1%PAA (2 mL-$CaCl_2$) NP's. From the micrograph, it can be noted that the formulated NPs were spherical in shape well dispersed with a smooth surface; furthermore the micrograph showed that the formulated nanoparticles displayed limited aggregation. Moreover, the SEM micrograph showed that the formulated 0.1% PAA NPs had a size below 400 nm (200 nm). The NP's were monodispersed due to the low polydispersity index (PDI) values. The SEM micrograph images display a more spherical, uniform in shape and highly dispersed NP's due to high surface charge and particle size. When comparing the particle size of DZH loaded NPs via zeta- sizer (1551 ± 4.320 nm) and SEM (200 nm) the increase in size could be due to aggregates forming during measurements via the zeta-sizer.

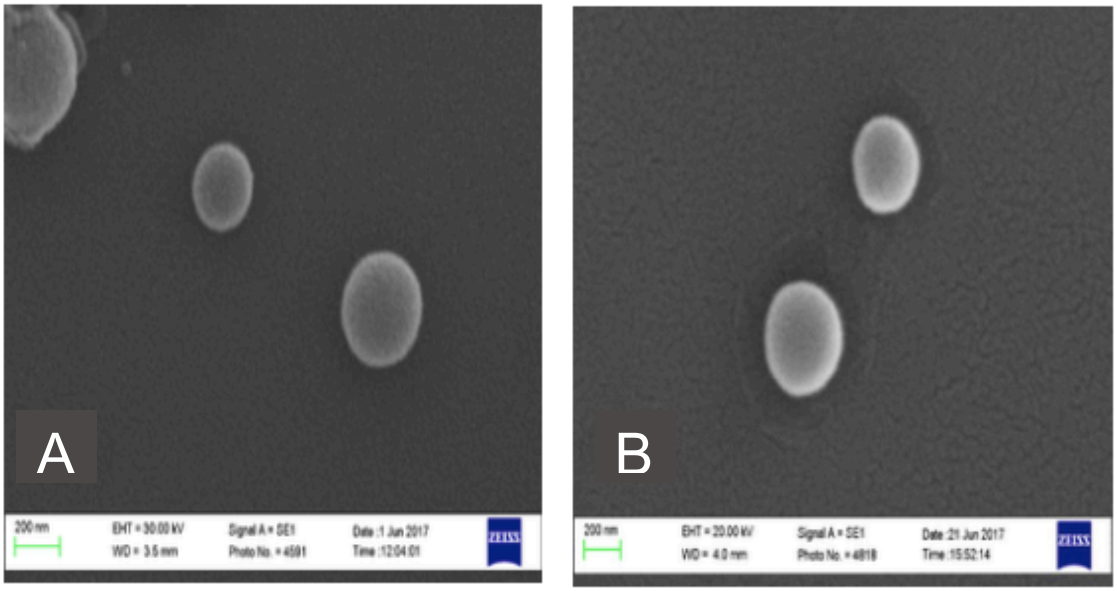

Figure 5.4: SEM micrograph images of 0.1% PAA-NP's high magnification (A). DZH encapsulated PAA-NP's high magnification (B).

The entrapment efficiency (EE) for this technique used was reported to be effective and the particle size generated was as desired (200 nm). Entrapment efficiency of DZH was 81 ± 0.23% this is a relatively high value could be credited to the use of $CaCl_2$ ion, which is a cross-linking agent (65). The total amount of DZH used was 1 mg/ mL while free drug discovered in the solution was 0.2 mg/ mL.

5.2.3. Differential scanning calorimetry (DSC)

Differential scanning calorimetry (DSC) can be used to determine many thermal and physical properties via measuring the energy transfer of the DZH, as well as analysing the characteristics of the NP loaded SCLs at its solid state as well as their polymorphism and phase behaviour. Figure 5.5 below displays the DSC thermogram for DZH, DZH loaded PAA-NPs within

SCL. DZH (A) exhibited a small endothermic peak at 287 °C suggesting a more crystalline form of the drug (Figure 5.5) (193). However, DZH loaded PAA-NP SCL (B) showed endothermic peak starting at 260 °C that could possibly represent melting region and ending at 400 °C. Control SCLs (D) also displayed an endothermic peak at 400 °C, both of which are displaying a form of crystalline nature due to the presence of the following polymers that the SCL material is formulated from (HEMA/PDMA-AS). DZH laden SCL (C) displayed an endothermic peak at 360 °C. Peaks within the 400 °C region corresponds to degradation of PAA (194).

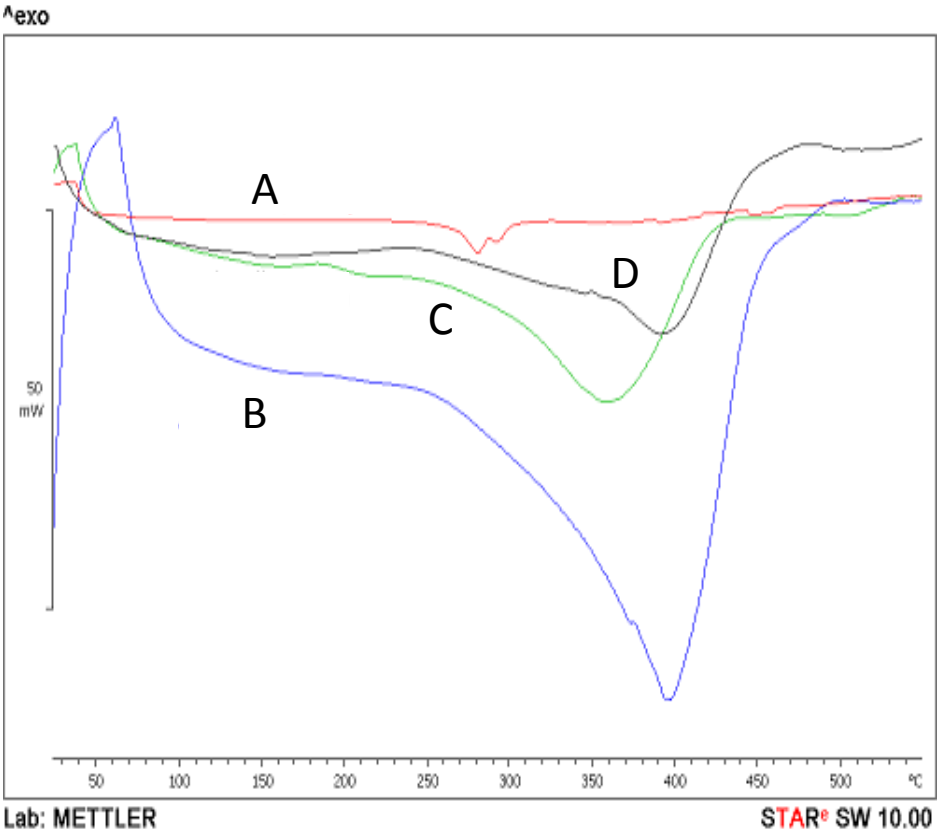

Figure 5.5: DSC of DZH (DZH) (A), DZH loaded NPs within CL (B), DHZ within the CL matrix (C) and control CL (D).

5.3. Equilibrium water content (EWC%) and surface wettability of PAA-NP encapsulated SCLs

Increase in hydration also known as the equilibrium water content (EWC) was introduced by Caló *et al* (195). High EWC within a SCL suggests enhanced flexibility and oxygen permeability. EWC is an important property within CL as it will ensure comfort for wearers. EWC of SCL's is very much associated with other properties such oxygen permeability and surface contact angle (CA). CA helps study the surface wettability of SCL, CA helps determine the balance between cohesive and adhesive forces of the SCL surface, where cohesive forces occur between molecules alike and adhesive forces occur between different molecules (196).

Figure 5.6 shows the change in EWC% and contact angle for three formulations; control SCL, SCL containing DZH NP and DZH in SCL matrix and the EWC % was: 43.9 ± 2.5%, 41.4 ± 0.99% and 46.6 ± 1.9% respectively. DHZ within the SCL matrix possessed the highest EWC% due to the hydrophilic nature of the drug compared to DZH loaded NP within SCLs this could be due to the fact that they are incorporated and shielded within the NPS and not free within the matrix (6). However, there was a decrease in hydration by 2% of DZH loaded NP within CLs when compared to the control. Statistically the results were insignificant with $p=0.0867$ and the NPs did not affect the EWC%. A typical hydrogel SCL has an EWC of about 38% this increases flexibility and increases oxygen permeability (29). These results further confirmed that DZH NP loaded into SCLs does not affect the EWC % of CLs.

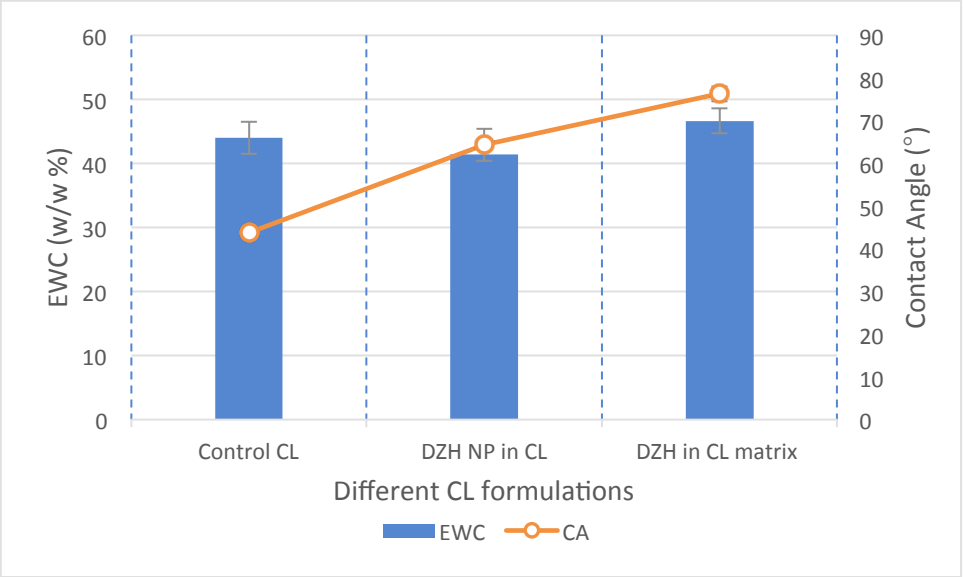

Figure 5.6: Equilibrium water content (%) and contact angle (°) for different types of formulated SCLs with and without DZH loaded PAA-NP. Data presented as a mean ± SD, n=3.

Surface CA is another major property of SCL as it determines the hydrophobicity of the surface. The main objective of this study was to formulate SCLs with more hydrophilic surface by obtaining a lower CA thus potentially preventing bacterial/ lipid adhesion to the surface lens (208,209) By incorporating PAA NPs in SCL matrix this is more likely to enhance surface wettability of SCL due to its hydrophilic nature (64). *Ademovic et al,* used PAA to modify the hydrophobic surface of silicon CLs. The characterisation studies displayed increase surface wettability after graft-polymerisation of PAA (29 ± 2°) (198). A study by Campbell *et al* (2013), suggested that contact angle with a value of 90° and above describes a hydrophobic surface (199), thus preventing bacterial growth and lipid adhesion to the SCL. All the CA recorded were below 90° suggesting a more hydrophilic surface (Figure 5.7). CA for control CL, DZH in CL matrix and DHZ NP in CL were 43.76 ± 0.54°, 64.36 ± 3.81° and 76.3 ± 1.77°

respectively. Although there were slight changes in CA values the changes were insignificant (*p=0.0064).* Therefore, the results displayed in Figure 5.7 have shown that incorporation of DZH helps enhance EWC% within SCLs either in encapsulated within NPs or freely dispersed within material.

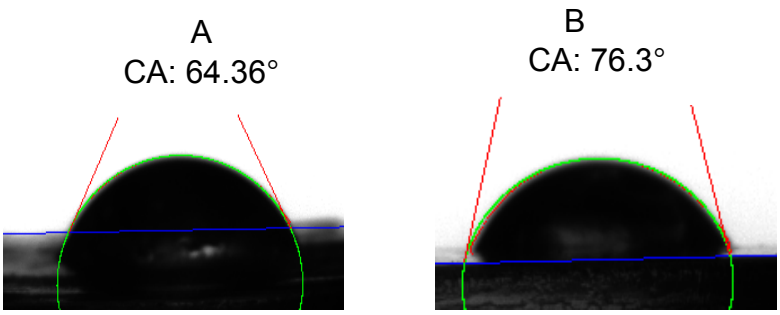

Figure 5.7: Images of CA measurement of DZH in CL matrix and DHZ NP in CL using sessile drop assay.

5.4. Optical properties of PAA-NP encapsulated SCLs

Light transmittance is a vital property that's measured using UV-Vis spectroscopy, by comparing the values this helps determine the level of optical clarity of the SCL. The results are shown in Figure 5.8. Transmittance is among the most desired properties such as EWC, CA and lens elasticity within SCLs (188). For both DZH in SCL matrix and DHZ NP in SCL, the results in Figure 5.8 displays a transmittance range of 80% and above. A study by Gause *et al (2016),* showed that silicone-hydrogel SCLs loaded with NPs are great UV blockers with a transparency range of 60% (200). Gulsen *et al (2005) and ElShaer et al (2016) reported that* incorporation of NPs into SCLs decreased transmittance from 94% to 83% (45,198).

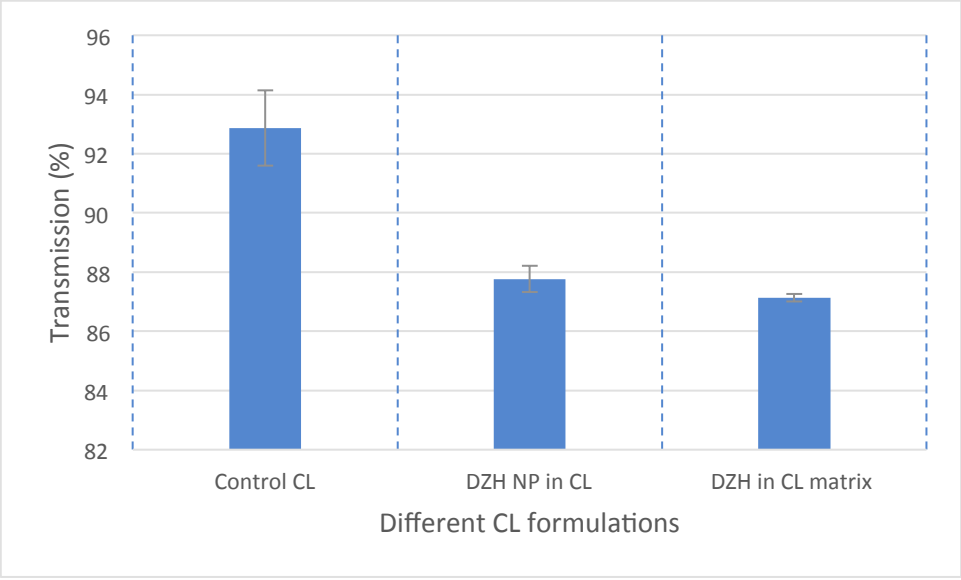

Figure 5.8: Light transmittance (%) for different types of formulated CLs with and without DZH loaded NP. Data presented as a mean ± SD, n=3.

The results in Figure 5.8 displayed transmission % of 92.8% ± 1.2, 87.7% ± 0.44 and 87.13% ± 0.12 for Control SCL, DHZ NP in SCL and DZH within the SCL material respectively. Size and the NPs volume does have an effect on

the opacity of SCL, Gulsen *et al (2005),* reported that NP size effects the transparency of the SCL, with increase in NP size transmittance decreases (46). Also, ElShaer *et al (2016)*, showed the amount of NP incorporated into the SCLs is every important to avoid lack of transmittance (188).

5.5. Young's Modulus (MPa) of NP encapsulated SCL's

Analysing the mechanical characteristics of SCL is essential in ensuring SCL quality. Physical strength is the ability to maintain shape and dimensions of the SCLs post application of external forces (201). Ideal elasticity within SCLs ensures comfort for wearers. Young's Modulus (YM) is calculated by dividing stress (MPa) over strain (% elongation). A higher YM indicates a more rigid material. Hydrophilicity of CLs has been shown to determine the strength of the lens (201). SCLs with a more hydrophilic lens matrix will possess increased EWC% with low YM values, as a result these SCLs will have low stability in holding shape and will be very difficult to handle due to their delicate status (188). Figure 5.9 shows with addition of DZH and DZH NPs the young's modulus has slightly increased. The average value of DZH and DZH NPs and control SCL are 0.99 ± 0.01 MPa, 0.98 ± 0.008 MPa and 0.96 ± 0.02 MPa respectively. Although there were slight changes in YM values the changes were insignificant (*p= 0.2866)*. Therefore, incorporation of PAA NPs displayed no significant effect on the YM of SCLs and as such are unlikely to affect patient acceptability of wears. The values of Young's Modulus within the current study are comparatively lower than the values presented in literature. However, a point to highlight is that the values in literature are not standardised therefore different assay's may have been used to quantify the Young's Modulus of SCL (49,201). Nevertheless, it is demonstrated that the formulated SCLs have small YM values suggesting a flexible material suitable for a more comfortable longer wear.

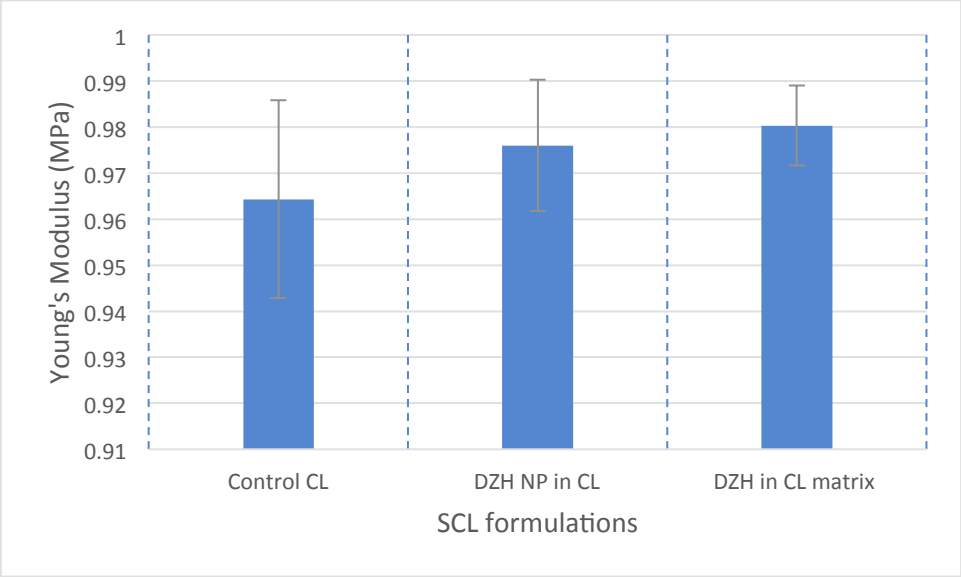

Figure 5.9: Young's modulus (MPa) against HEMA/PDMS-AS SCL some of which are encapsulated with DZH NP and DZH within CL material. Data presented as a mean ± SD, n=3

5.6. Drug release study of NP encapsulated SCL's

In vitro drug release of DZH from the NP loaded SCLs and DZH dispersed into the SCL material, the results (Table 5.3) displayed a two-phase process. Table 5.3 displays initial release for both samples: The total percentage of DZH released over 24 hours from the NP-loaded SCLs and DZH in SCL matrix were 22 ± 0.0047% and 6.34 ± 0.022% after 24 hours.

Table 5.3: DZH release from DZH NPs SCL and DZH freely dispersed into SCL matrix. Data presented as a mean ± SD, n=3

	Percentage Drug Release (%)	
Time (hour)	**DZH NPs in SCL**	**DZH in SCL matrix**
1 hour	9.63 ± 0.0082%	0.7 ± 0.023%
24 hour	22.42 ± 0.0047%	6.34 ± 0.022%

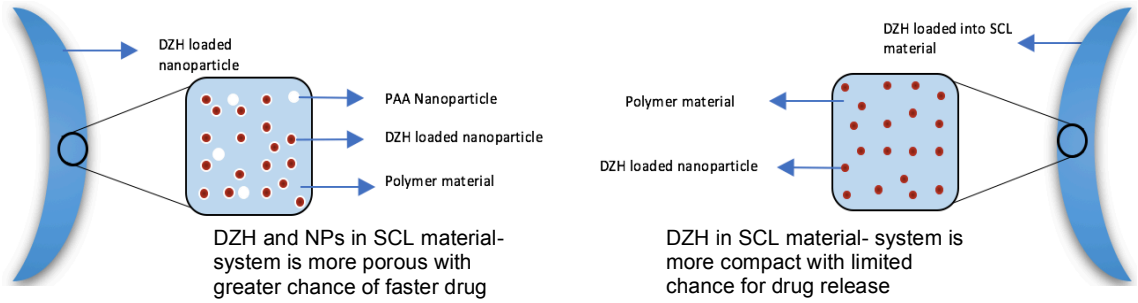

Figure 5.10: Ocular drug release through the use of drug-eluting soft contact lenses.

This could be ascribed to DZH was required to diffuse from both the NP as well as the SCL material, (from the DZH NP IN SCL) forming double barriers (Figure 5.10). As for the DZH dispersed into the SCL material, there was reduced drug release % the reason for this would be that the lens material

could be less porous hence preventing drug diffusion. The initial fast release could be due to the entrapped DZH to the surface of SCLs. The slow release is associated with DZH entrapped within the core of NP (198,214). Within DZH NP in SCLs, in order for the drug to be released into the tear fluid and onto the ocular surface, the tear fluid is required to penetrate into the particles dissolving DZH which is further required to diffuse through the NP as well as the SCL material into the dissolution media, thus contributing to a slower release. It is interesting as both forms of SCL loaded with DZH in matrix or with DZH NPs could be used to tailor sustained drug delivery for specific patients depending on the dosage required with 24 hours, DZH in SCL matrix tend to deliver slow drug release. By incorporating drugs into NP this aids drug release for days or even weeks (188). A study by Li *et al (2017),* NPs exhibited sustained drug release for up to 90 days *in vitro* (203). Another study by Manchanda *et al (2017),* analysed the drug release of encapsulated carbonic anhydrase inhibitor within NPs versus the drug on its own. The results showed that almost all the drug (98.72 ± 4.55%) diffused into the release medium within 4 hours whereas the NPs released 44.08 ± 2.38% within 8 hours (204). Gupta *et al,* discovered that commercial formulations released the drug within 6 hours, whilst that NPs released the drug within 24 hours (205). The findings of these studies support the data obtain in this study with regards to nanoparticles used as a platform for delivering anti-glaucoma drug (DZH) by sustaining a slow drug release.

5.7. *In vitro* Ocular Tolerability study

5.7.1. Hen's Egg test-chorioallantoic membrane (HET-CAM)

The CAM is composed of vascularised respiratory system that surrounds the embryo, this is very similar to conjunctival tissue within the eye (111). The irritation effect was examined at 0.5, 2 and 5 minutes' post exposure. A positive and negative controls were used (NaOH and saline solution) providing bases for assessing prepared SCLs with and without PAA nanoparticle systems. Figure 5.11 illustrates four signs of vascular responses recorded at 4 different time points, for strong irritant NaOH once administered onto the CAM. At 0.5 min, hyperaemia it was noticed within CAM blood vessels, and at 2 min development of haemorrhage within small areas of the CAM and finally at 5 mins this further increased into coagulation, demonstrating a strong irritant. Figure 5.11 also shows the effects of saline solution (negative control) on the CAM. The CAM maintained its normal morphology with no sign of vascular irritation. The positive (NaOH) and negative (saline solution) act as criteria for analysing the test materials on the CAM.

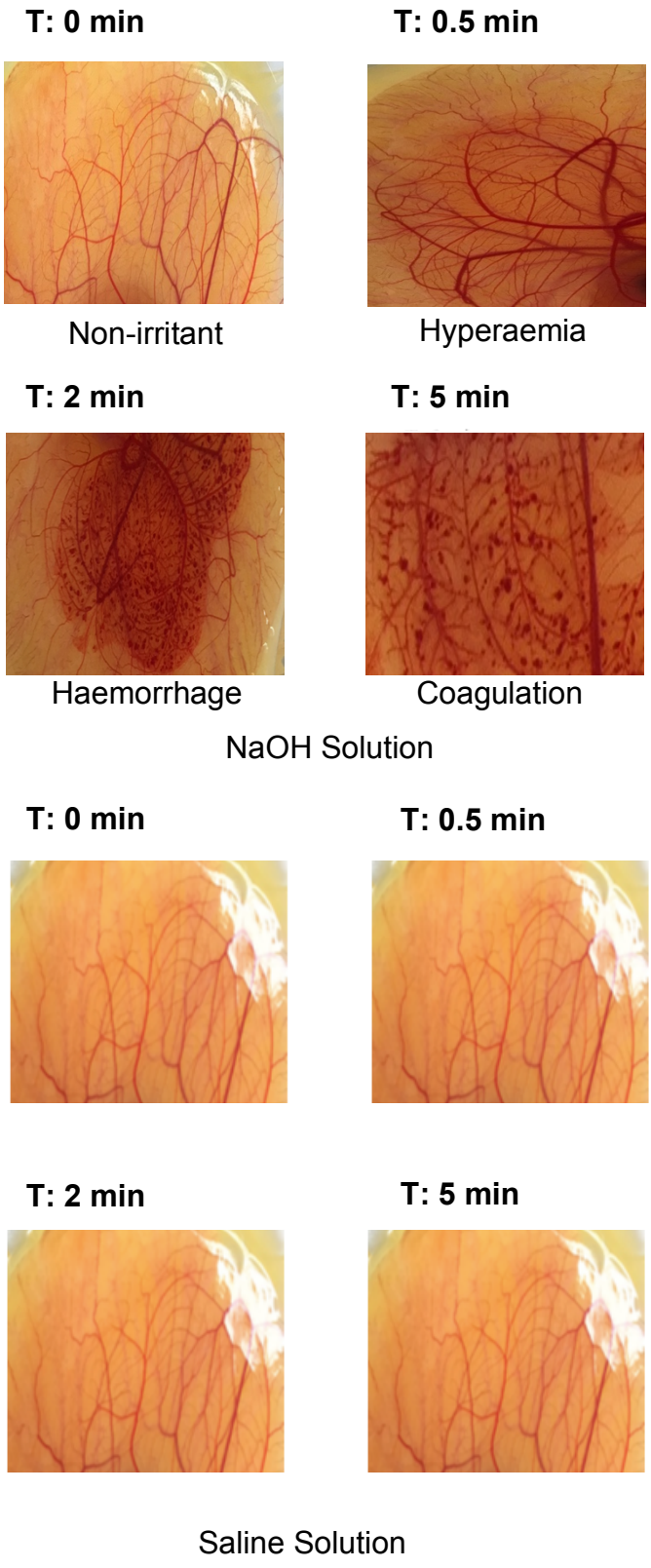

Figure 5.11: CAM Vascular end points to NaOH (0.5 M) strong irritant (+VE control) and saline solution (0.9%) (-VE control) score irritation within the current formulations at 0,0.5, 2 and 5 mins.

Figure 5.12 displays HET-CAM images post application of NP solution, DZH solution and DZH loaded NP in SCL, all images show no sign of irritation on the CAM at all time points (0.5, 2 and 5 minutes). Suggesting that DZH NP in SCLs to be non-irritants (cumulative score 0.0; n=3) thus confirming both formulation to be biocompatible to the conjunctiva (6,206).

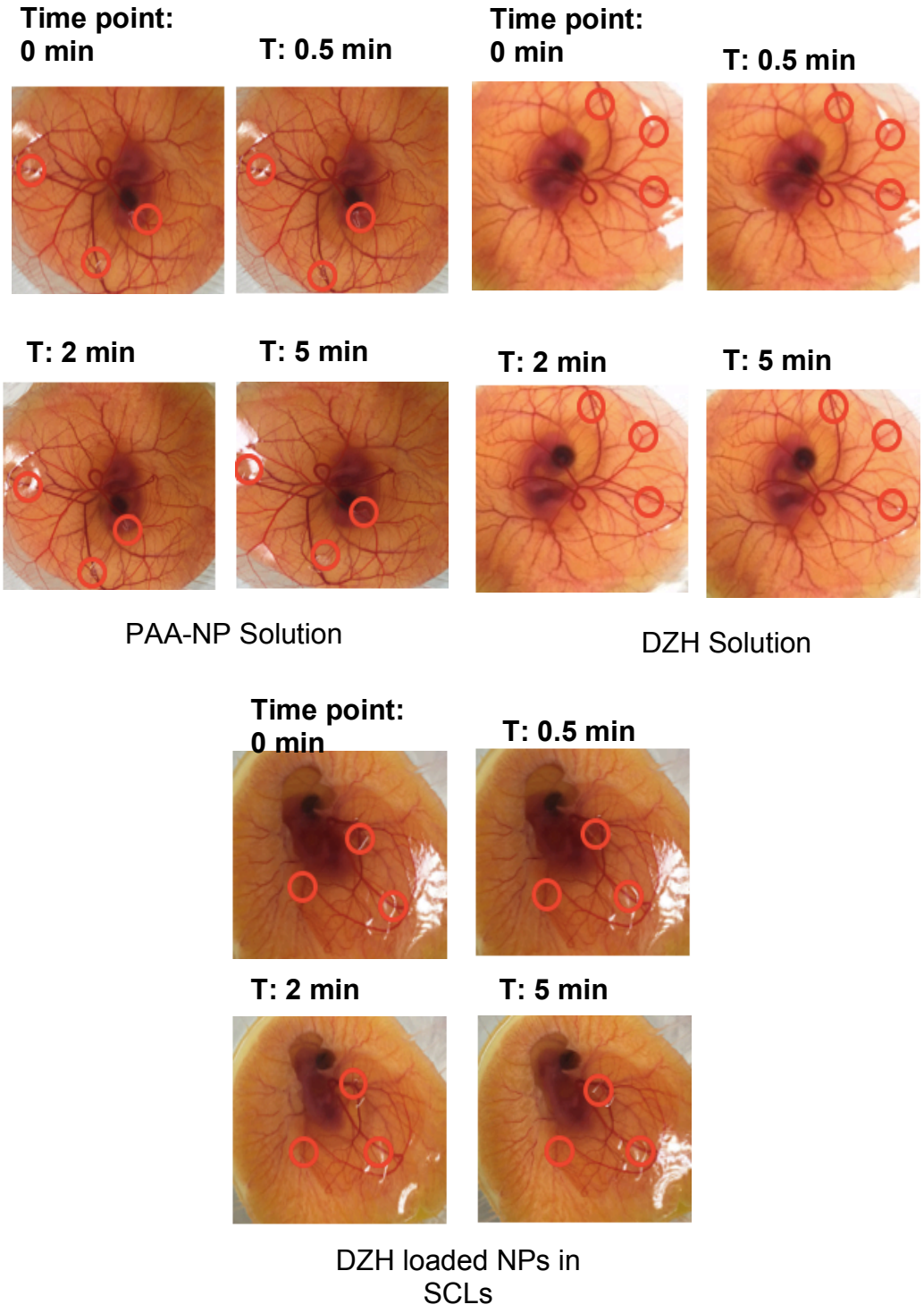

Figure 5.12: HET-CAM images of vascular response to PAA-NP solution, DZH solution and DZH-NP in SCL.

5.8. Bovine corneal opacity and permeability (BCOP) for prepared SCLs.

The BCOP assay is able to measure corneal irritation via corneal opacity and permeability. The corneal opacity determines the level of protein denaturation damages caused to the epithelial cell layers as well as swelling and vascularisation (108). The fluorescein dye indicates the level of corneal damage, as the dye is normally impermeable to a healthy cornea. Slightly irritant material is likely to damage the corneal epithelial layer, and stronger irritants are more likely to damage and penetrate through to the endothelial layer of the cornea. Figure 5.13 below demonstrates the effect of test materials including controls and SCLs on the bovine cornea. From the images in Figure 5.13 it is clear that positive control NaOH is a sever irritant as it caused the most damage to the cornea this is displayed in opacity around the inside of the silicone ring. And normal saline was used as a negative control which displayed no sign of damage to the cornea. When comparing the results gained from the prepared SCLs with the controls, it is clear that none of materials used to prepare the SCLs displayed any indication of damage to the cornea. Suggesting that the formulated SCLs are will not cause irritation and safe for use.

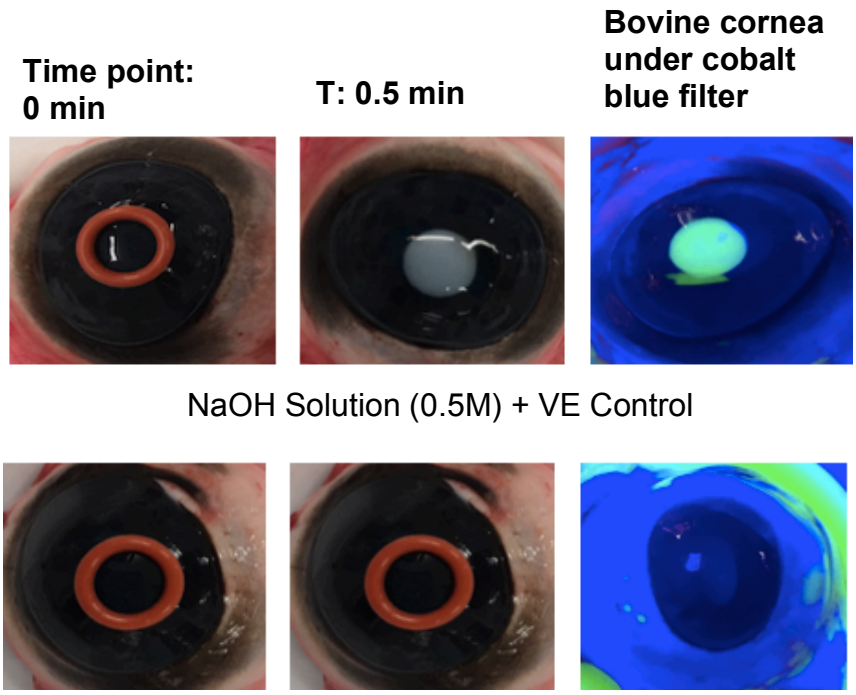

Figure 5.13: BCOP images with corresponding fluorescence images of freshly excised bovine cornea treated with positive control and negative control.

The integrity of the corneal epithelial layer was studied under cobalt blue filter post application of fluorescein dye. Figures 5.14 shows the intensity of the fluorescence permeability through bovine cornea post NaOH application with prominent staining. This indicates sever damage to the corneal epithelial cells as the dye starts to permeate through the cornea. However, when comparing the negative control to the positive control there was no sign of fluorescein staining to the bovine cornea. Figure 5.14 displayed no sign of staining when bovine cornea was treated with PAA-NP solution, DZH solution and DZH loaded NP SCLs. This demonstrates that the formulated SCLs are safe and biocompatible for use.

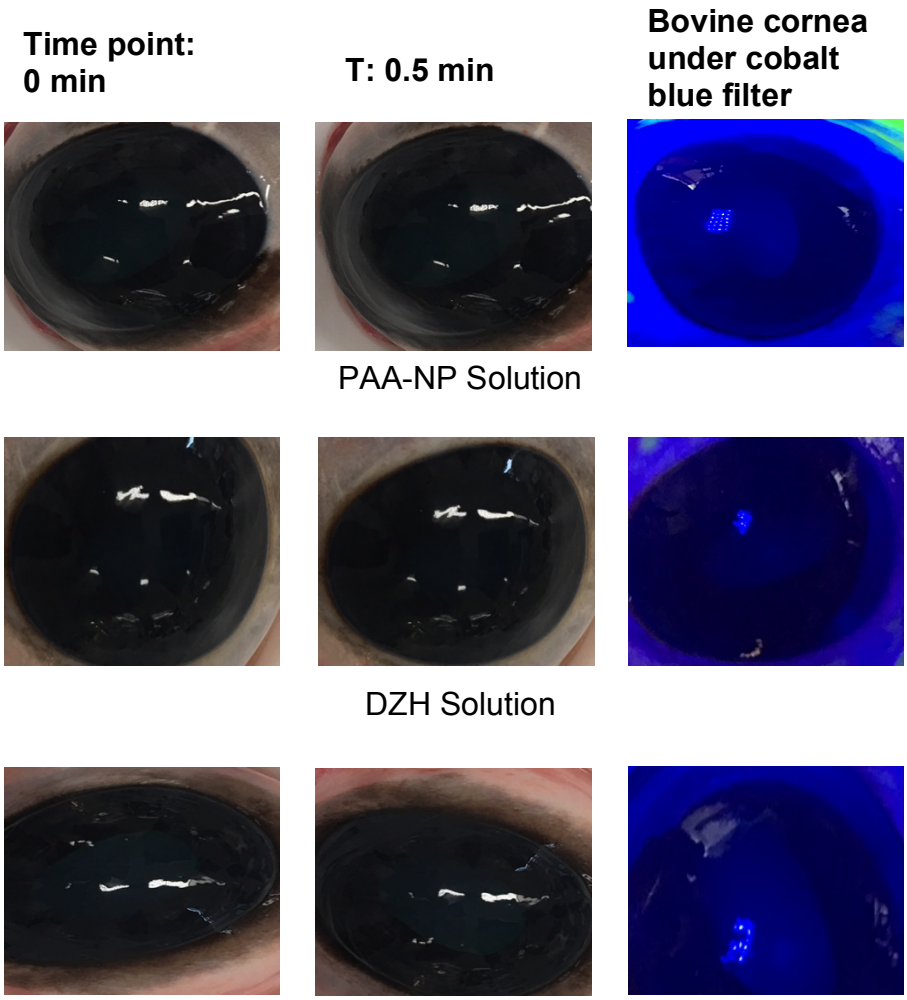

Figure 5.14: BCOP images with corresponding fluorescence images of freshly excised bovine cornea treated with PAA-NP solution, DZH solution and DZH loaded NPs in SCLs.

5.9. Summary

The main purpose of incorporating DZH NPs into SCL is to prolong drug release over a long period of time in return lowering intraocular pressure (IOP) within glaucoma patients. It was discovered that PAA polymer concentration affects the NP size, and at 0.1% PAA concentration proved to be the most ideal as we obtained the lowest particle size and PDI values, which was seen to be the most monodispersed from all the other PAA-NPs formulated. Addition of DZH into NPs, increased mean particle size of NP was displayed. The measured zeta-potential of the formulated NPs were negatives with a mean value, PAA were responsible for the negative charge displayed enhancing permeation properties.

Entrapment efficiency of DZH was 81% this is a relatively high value could be credited to the use of $CaCl_2$ ion (cross-linking agent). The EWC & CA results had shown that incorporation of DZH helps enhance EWC% as well as surface wettability of SCLs within encapsulated NPs or freely dispersed into the matrix, demonstrating that loading of DZH NP into SCL will not compromise the properties of SCL. Similar transmittance was obtained for DZH in NP and DZH in SCL material. When analysing the mechanical properties of all the formulated SCLs their YM values were small suggesting a flexible material suitable for a more comfortable longer wear. *In vitro* tolerability studies *(*HET-CAM and BCOP) results demonstrated that the formulated DZH NP in SCL displayed no sign of vascular response, and are biocompatible with ocular surface. *In vitro* drug release studies has demonstrated that this new platform of incorporating drugs into NPs/ SCL

matrix is an efficient way of enhancing drug bioavailability as well as sustaining low IOP over a long period of time. Both formulations could be used as a drug delivery system, this way you can tailor the mode of delivery based on the requirement of the patients. Drug delivery via SCL could aid reduce dosing of topical applications, thus reducing economic costs as well as enhancing better patient compliance. Not to mention that these SCLs could also be used to correct Myopia, Hyperopia and Astigmatism, the future of these lenses is very promising.

Surfactant Laden Soft Contact Lens To Prevent Microbial Keratitis

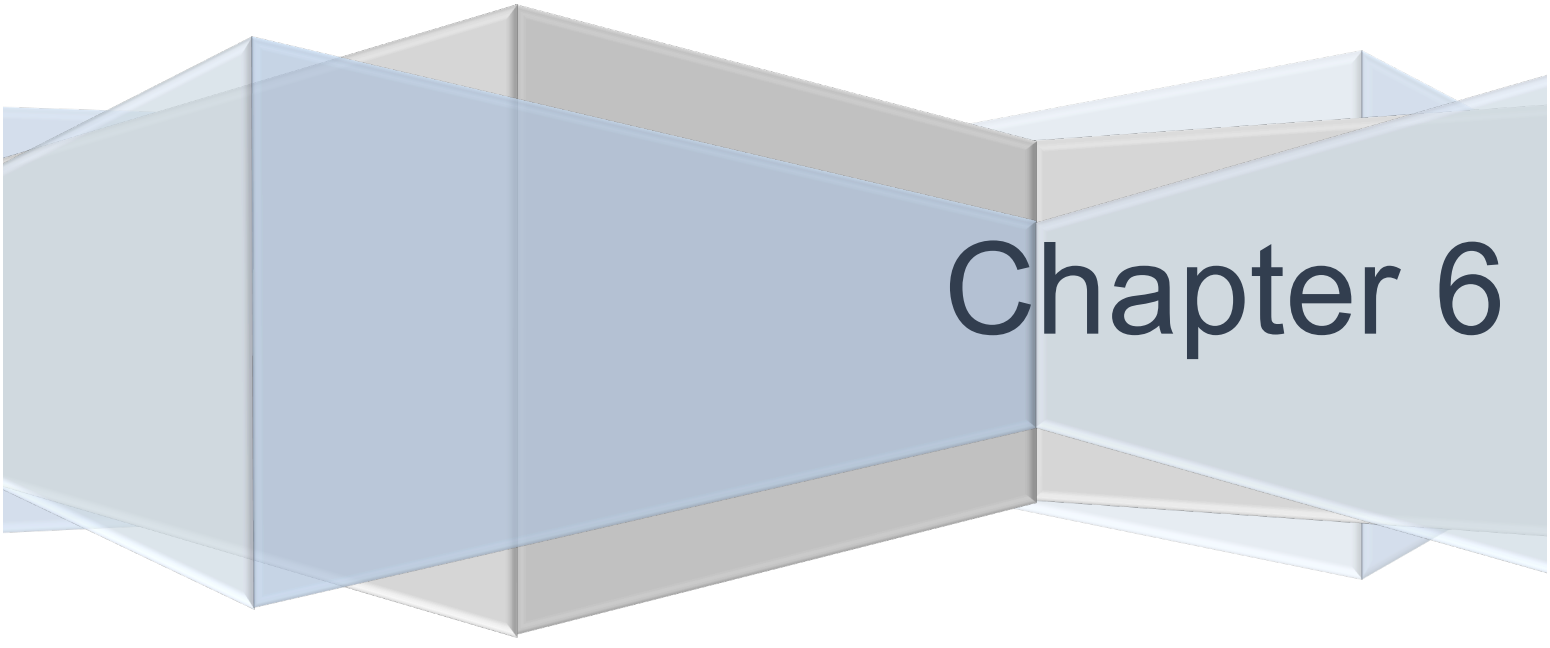

Chapter 6: Bacterial adherence assay

6. Introduction:

The results generated within chapter 5 revealed that DZH-NPs SCLs were able to sustain drug release for 24 hours. PAA-NP assay proved to be much effective with an entrapment efficiency of 81% for DZH. The next and final step of this study was to prepare SCLs using poloxamer (P407), and investigate the effect of different concentration P407 on EWC%, transmittance, young's modulus and surface contact angle. As well as the effect of P407 on the bacterial adhesion of *Pseudomonas aeruginosa* and *Staphylococcus epidermidis* to SCLs.

Microbial Keratitis/ contact lens Microbial Keratitis (CLMK) is severe condition also known as infection of the cornea, which is most common amongst CL wearers (84). CLMK could lead to irritation, pain and even impaired vision (85). According to research bacteria such as *Pseudomonas aeruginosa* is the main causative microorganism, as its most likely to adhere onto the corneal surface via van der waals forces which is followed by irreversible adhesion, by forming biofilms further growing on the ocular surface (86,87). Surfactants were introduced within this study to prevent CLMK, surfactants are mainly used to minimise discomfort (lubricant), allowing tear fluid to spread evenly over the lens thus acting as a buffer between finger and lens (88).

Non-ionic surfactant (P407) was chosen, as they are known to possess low irritation and toxicity, making them very popular within ocular drug delivery

systems. Poloxamers are composed of triblock polymers poly (ethylene oxide) (PEO) that's hydrophilic and poly (propylene oxide) (PPO) hydrophobic (63,89). Scientific research was conducted on the use of poloxamers to modify the surface of marketed SCLs, and discovered that not only does it increases surface wettability and EWC, it also prevented bacterial adhesion (90).

A total of 22 sterile contact lenses were used throughout this study, 4 different formulations were prepared using a mixture of Hydrogel and silicone based polymers with different concentrations of poloxamer 407. All formulations contained hydrophilic HEMA monomer co-polymerised with either hydrophobic GMA or silicone-based polymers (PDMS /F-S/A). The cross-linker and the photo-initiator (TEGDMA and HMPP) were both used at 1% composition. Summary of percentage composition used in preparing the CLs are displayed in table 12.

Pseudomonas aeruginosa is a common gram-negative (gram –ve), rod-shaped bacterium that can cause disease in plants and animals, including humans. It is found in soil, water, skin flora *Staphylococcus epidermidis* is a gram-positive (gram +ve) coccal bacterium that is a member of the Firmicutes, and is frequently found in the nose, respiratory tract, and on the skin. A clinical isolate of *Pseudomonas aeruginosa* NCTC00950 was kindly provided by the microbiology department, Kingston University, London.

6.1. Aims and objective

To formulate SCLs treated with and without surfactant P407, and study bacterial adhesion to the surface of SCLs. The specific objectives are:

- To prepare SCLs using surfactant P407 at several different concentrations.
- To investigate the effect of different concentrations of P407 on the following properties EWC, CA, TM and YM.
- To study the effect of P407 surfactant on the bacterial adhesion of *Pseudomonas aeruginosa and Staphylococcus epidermidis* to the surface of SCLs.
- To investigate any possible corneal and conjunctival irritation from the prepared SCLs via examination of the bovine cornea BCOP and HET-CAM assay.

6.2. Equilibrium water content (EWC) and surface contact angle (°) of P407-SCL

Results and discussion

Two polymers were used in the formulations, hydrogels and silicone based polymers. Two different types of hydrogels were used, hydrophilic 2-hydroxyethyl methacrylate (HEMA) and amphiphilic glycidyl-methacrylate (GMA), two different types of silicone-based polymers were used, PDMS-co-alkyl siloxane (PDMS-AS) and 3,3,3-trifluoropropyltrimethoxysilane (F/S-A). The surfactant used a hydrophilic non-ionic Poloxamer 407 (F127). Cross-linker and photo initiator was, the different types of concentration % are listed in table 6.1.

Table 6.1: Percentage composition used for the preparation of contact lens.

Material		% Composition
Formulation	HEMA, GMA, F-S/A HMPP, TEGDMA	87.97, 9.78, 0.29 0.98, 0.98%
Formulation	HEMA, PDMS-AS, F-S/A, HMPP, TEGDMA	94.82, 2.93, 0.29 0.98, 0.98%
Surfactant	Poloxamer (P407)	1, 0.5, 0.25%

High equilibrium water content (EWC) is vital for an ideal contact lens. A typical hydrogel composed of solely 2-hydroxyethyl methacrylate (pHEMA) has an EWC of 38%, which results in increase in oxygen permeability(29).

Results in Figure 6.1 shown an increase in EWC % when contact lenses are formulated with surfactant (poloxamer P407).

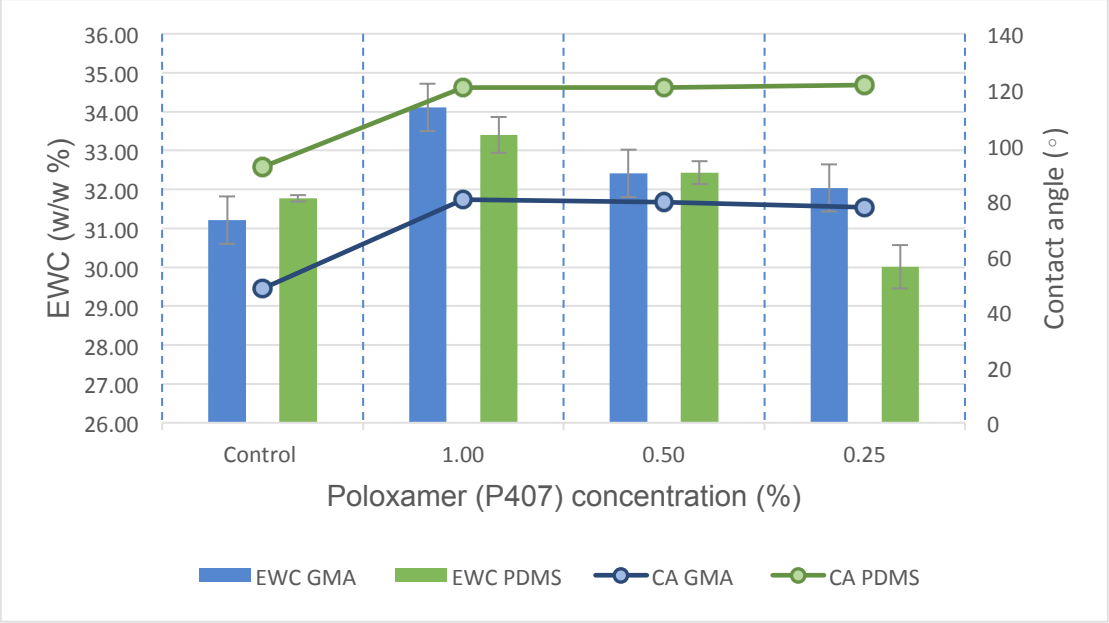

Figure 6.1: Equilibrium water content (%) and surface contact angle (°C) for different types of contact lenses and with and without P407. Data presented as a mean ± SD, n=3.

One type of surfactant was used at 3 different concentrations P407 at 1%, 0.5% and 0.25% for both contact lens formulation (GMA and PDMS). Both hydrogel and silicone-hydrogel lenses formulated with surfactant P407 yielded higher EWC %. All formulations with the highest % of P407 yielded EWC of 30% and above (see Figure 6.1), GMA/P407 at 1% displayed an increase EWC from 32.04 ± 0.54% to 34.10 ± 0.81% (*p=0.0016)*. PDMS/P407 at 1% yielded the highest EWC of 33.40 ± 0.46% compared to PDMS/P407 at 0.5% and 0.25%, 32.43 ± 0.29% and 30.02 ± 0.56% respectively.

There was an increase in water capacity as the concentration of P407 increased this could be very much due to the length of hydrophilic moiety present within P407. The hydrophilic PEO surrounding hydrophobic PPO of the surfactant allows additional –OH groups to form hydrogen boding (207). *Schafer et al* (207), evaluated the surface water characteristics of 3 daily disposable contact lens materials and discovered that Biotrue ONEday® (Nesofilcon A) was able to maintain 78% water content throughout. Nesofilcon A is a traditional hydrogel lens that exploited the amphiphilic properties of P407 enabling the lens surface to retain water mimicking the natural tear film at the same time preventing water evaporation. Kapoor et al (47), investigated the use of surfactant Brij within hydrogels EWC%. Briji 700 at 8% w/v had the highest EWC of 17.4% compared to pure p-HEMA. Both studies support present study findings.

Oxygen permeability, surface contact angle and hydration are among the important characteristics required for an ideal contact lens. Within hydrogel contact lens (p-HEMA) oxygen permeability is very much proportional to the EWC and lens thickness. The pores within hydrogel material expands as the hydrophilic phase increases the uptake of water causing the polymer matrix as a whole to swell resulting in improved oxygen transport (208).

However, changes with silicon-hydrogel (Si-Hy) SCLs such, as oxygen permeability is no longer dependent upon the EWC. Figure 6.2 below displays a representation of water contained within hydrogel and Si-Hy matrices where water is directly bound to the hydrophilic sites via hydrogen-

bonding, van der waals forces and free water. Within Si-Hy material hydrophilic and hydrophobic phases are formed separately but are frequently linked; the oxygen mainly travels through siloxane phase (hydrophobic) due to reduced resistance (208).

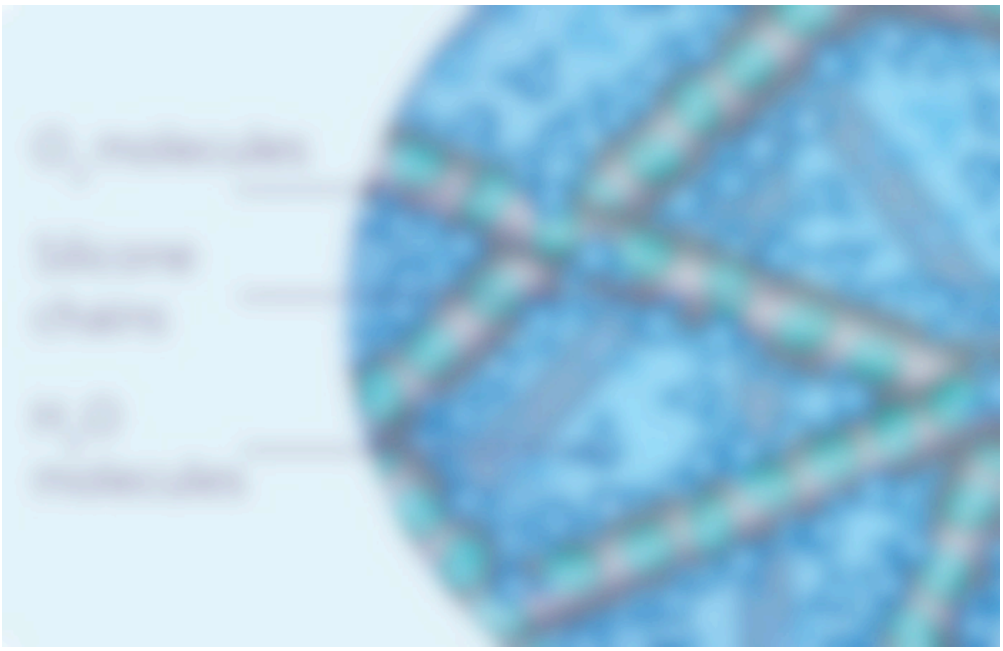

Figure 6.2: Oxygen and water molecules bound to silicone channels. Credit: Coopervision.co.uk (42).

Waiting for copyright permission.

Surface contact angle is another major property that analyses the surface wettability of contact lenses. Surface wettability is best explained through Cohesive and adhesive forces acting on the surface of the contact lens. When a liquid droplet is added onto a hydrophilic surface the inter-molecular forces between the liquid/ solid (contact lens) is far stronger than the cohesive forces between the liquid droplet causing it to spread and resulting a low contact angle. Therefore, the degree of wetting is determined by force balance between the adhesive and cohesive forces (196).

Surface contact angle is another major property that represents the surface wettability of contact lenses. Surface wettability is best explained through cohesive and adhesive forces acting on the surface of the contact lens. When a liquid/liquid droplet is added onto a hydrophilic surface the inter-molecular forces between the liquid/ solid (contact lens) is far stronger than the cohesive forces between the liquid droplet causing it to spread and resulting a low contact angle. Therefore, the degree of wetting is determined by force balance between the adhesive and cohesive forces (196). Surface contact angle is very important, as its able to point out if the surface is hydrophilic/ hydrophobic. Contact angles below 90° suggests high surface wettability and above 90° are considered to possess low wettability.

Bacterial adhesion to SCLs depends on the hydrophobicity and hydrophilicity of the polymer type used. Many studies have shown that hydrophobicity is one of the key factors stimulating bacterial binding (208,209). An increase in EWC is associated with high wettability as well as hydrophilic surface. Within this study, the CA values for the control groups (HEMA/GMA and HEMA/PDMS) were higher than the surfactant incorporated SCLs. This directly correlates with the equilibrium water content (EWC) and the contact angle of the polymers used. With an increase in P407 concentration there is a decrease in contact angle for both PDMS and GMA at 1% and 0.25% P407, 40.24 ± 0.053° - 44.16 ± 0.058° ($p<0.000$) and 80.42 ±0.37° – 77.53 ± 0.50° ($p<0.0001$); this is due to the hydrogen bonding at the ether oxygen site of the PEO groups therefore with increase in P407 there is a general increase in hydration (209).

6.3. Optical properties of the prepared P407-SCL

Spectral transmittance properties of contact lenses are a vital measure for visual performance, it is necessary to analyse these properties and compare the values after the contact lenses have been hydrated for 24 hours. The optical quality of the contact lens is dependent on the absorption characteristics (177). The results are interoperated in Figure 6.3.

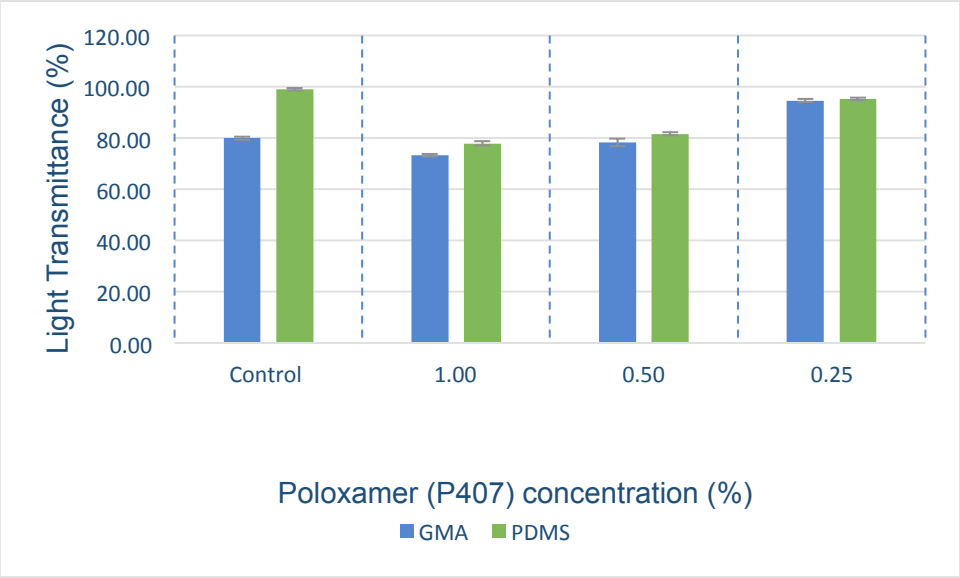

Figure 6.3: Light transmittance (%) for hydrogel and silicone-hydrogel contact lenses some of which are treated with P407. Data presented as a mean ± SD, n=3.

SCLs are used for vision correction or as a drug delivery system, transparency is one of the most important properties, where desired transparency value of 95% (210). Both GMA and PDMS, display a transmittance range of 70-99% for both hydrogel and silicon-hydrogel lenses (Figure 6.3). With decrease in P407 concentration, was associated with increase in light transmission.

Kapoor et al, carried out a study on surfactant laden soft contact lenses for extended drug delivery, their results were similar to those of the current study displayed a transmittance of 98% for pure HEMA hydrogel, and above 99% for non-ionic Brij surfactant laden contact lens. These findings are similar to of those current studies. Looking at the different formulation GMA-P407 1% has a transmission of 73.33 ± 0.58%compared to 94.67 ± 0.58% for 0.25% P407. PDMS-P407 1% 77.90 ± 0.79% and at 0.25% P407 95.33 ± 0.58%. As the majority of the contact lenses have transparency of 70% and above we can conclude that with the addition of surfactant the transparency of the SCL's are not compromised however lower concentration of the P407 is desired in this case as it yields better transmission %.

6.4. Young's modulus of the prepared P407-SCL

An important characteristic within SCL material is its ability to maintain its physical dimensions after are applied external forces of SCLs. Good mechanical property provides a better comfort for the wearer. Young's Modulus is calculated by dividing stress (Mpa) over strain (%). A higher YM indicates a more rigid material.

With increase in P407 concentration Young's Modulus decreased to 0.00738±0.00088 MPa in GMA (1% V 0.25% P=0.0506) and similar results were observed for PDMS 0.00911 ± 0.00143 MPa (1% V 0.25% P=0.0413) (Figure 6.4). A general pattern is noticed with addition of higher concentration of surfactant P407 a lower value of Young's Modulus is generated. These results are ruled by the interaction between the non-ionic surfactant and the hydrophilic polymeric structure, these hydrophilic moieties have a great influence upon the mechanical properties of SCL. The values of Young's Modulus within the current study are comparatively lower than the values presented in literature. However, a point to highlight is that the values in literature are not standardised therefore different assay's may have been used to quantify the Young's Modulus of SCL.

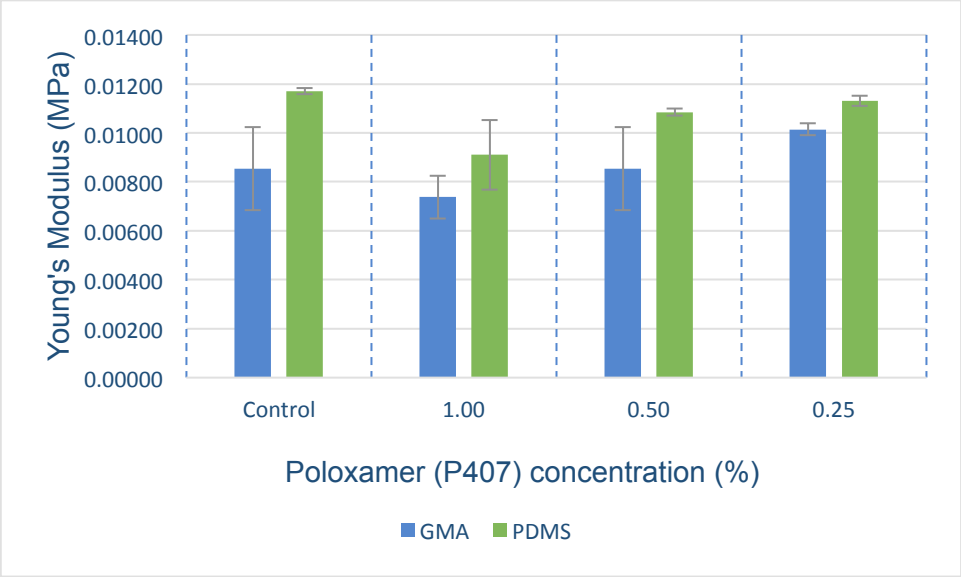

Figure 6.4: Young's modulus (MPa) for hydrogel and silicone-hydrogel contact lenses some of which are treated with P407. Data presented as a mean ± SD, n=3.

6.5 Bacterial adhesion

6.5.1 Bioluminescence ATP calibration curve

Bioluminescence is a quantitative assay developed to measure microbial contamination on surfaces. ATP bioluminescence requires optical biosensors with a detection measurement of luminescence or fluorescence emissions. This assay is one of the most effective and widespread method for pathogen detection due to high sensitivity and non-damaging way. This assay mainly relies on the on the chemical reaction between the bacterial ATP and luciferase enzyme, catalysis forming oxyluciferin, adenosine monophosphate (AMP) and pyrophosphate (PP_i) also resulting light emission at 562 nm (equation 5) (211)[adapted from ATP Bioluminescence assay] (212). The light emitted was recorded as relative light unit (RLU). Figure 6.5 shows a liner log RLU –log ATP concentration calibration curve plotted with regression coefficient (R^2) of 0.98321.

$$\mathrm{ATP + D-Luciferin + O_2} \xrightarrow[Mg^{2+}]{Luciferase} \mathrm{Oxyluciferin + PP_i + AMP + CO_2 + light}$$

Equation 4

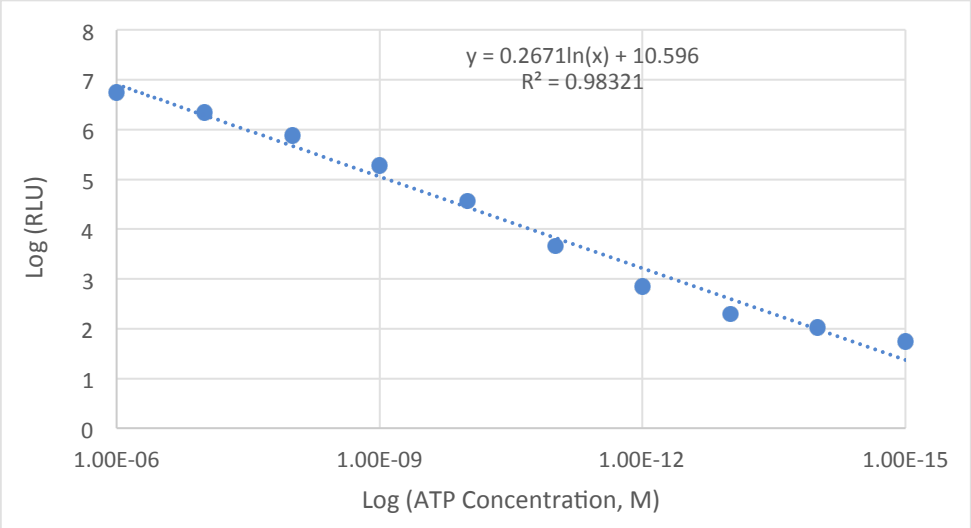

Figure 6.5: ATP calibration curve displaying Log- RLU bioluminescence intensity against Log-ATP concentration (M).

6.5.2. Bacterial optical density (OD_{600})

A consistent bacterial concentration of 2×10^8 CFU/mL was used throughout the bacterial adhesion assay, as formerly suggested by *Kodjikian et al* (211). The CFU was calculated from the number of ATP-bacteria via linear regression curve using logarithmic value of CFU and optical density (OD^{600}). This was possible through a serial dilution measurement of viable bacteria (Figure 6.6).

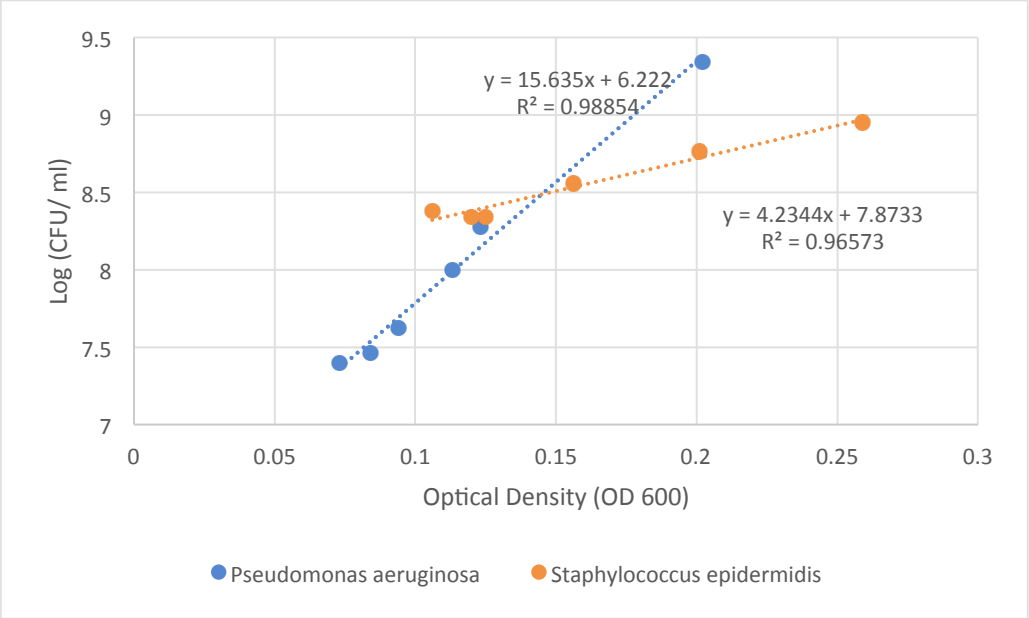

Figure 6.6: Bacterial calibration curve count (Log CFU/mL) versus Optical Density (OD $_{600}$) of Pseudomonas aeruginosa and Staphylococcus epidermidis to determine the desired OD and attaining bacterial concentration of 2.0x 108 CFU/mL).

The standard curve for *pseudomonas aeruginosa and Staphylococcus epidermidis* shown in Figure 6.6 displays the slope and coefficient of determination (R^2) of y = 15.635x + 6.222, R^2= 0.98854 and y = 4.2344x + 7.8733, R^2= 0.96573, respectively where y is log CFU/mL and x is optical density (OD^{600}). The results were presented as $\log^{10}$ CFU/mL ± SD. Also, quantification of cellular ATP corresponds to a valuation of cell activity within biofilm, as not every bacterium has the same metabolic activity, the bacteria located within greater layers of the biofilm expressed reduced metabolic activity therefore the results are expressed as pM of ATP instead of CFU per CL (213).

6.6 Pseudomonas aeruginosa and staphylococcus epidermidis

SCL wears are at risk of developing microbial infections such as microbial keratitis especially with *P. aeruginosa* which is a Gram -ve bacterium, composed of a complex genetic makeup aiding its survival in a wide diversity of environments (214). Additions within the bacteria such as the pili and flagella promote adhesion to SCL. The pili are small protein subunits that provides the hydrophobic bacterial surface (215).

Bioluminescence assay is a simple yet very frequently used method of quantification for bacterial adherence to CL surfaces. This technique provides a precise assay for quantifying ATP with a detection limit as low as 10^{-16} moles, making it 10,000 times more sensitive than your average spectroscopy measurement (104). Therefore, bioluminescences assay a precise way of quantifying the number of bacteria on the surface of SCLs when compared to bacterial counting. This technique is not only highly sensitive but also cost effective as only small amount of the reagent is required.

Figure 6.7 displays bacterial adhesion of *P. aeruginosa* on SCL, a general pattern is present over time there was a general increase in bacterial ATP concentration. However, least bacteria were bound to surfactant treated SCL's. PDMS-P407 had less bacteria on the surface of the lens compared to the control (0.5hr p= 0.1, 6hr p=0.003, 16hr p= <0.0001). PDMS-P407bacterial ATP concentration of $1.08\times10^{-3} \pm 1.08\times10^{-4}$ compared to

GMA-P407 possessed the least bacterial adhesion to the lens compared to the control (0.5hr *p*= 0.03, 6hr *p*=0.001, 16hr *p*= <0.0001). GMA-P407 has bacterial ATP concentration of $5.76\times10^{-4} \pm 1.18\times10^{-4}$pM in comparison with the control $1.77\times10^{-3} \pm 1.32\times10^{-4}$.

P. aeruginosa is one of the main causes of MK (223,228), due to its ability to adhere tightly to the surface of CL. As previously stated pili are responsible for the hydrophobic surface of the bacteria (227,229) and the flagella provides the means of transport to the surface of CL (230-231). When *P. aeruginosa* adheres to the surface of CL it starts to produce biofilm with the aid of the bacterial DNA, *P. aeruginosa* is also able to quorum sense, which enables the biofilm to avoid the detection of the immune system (217).

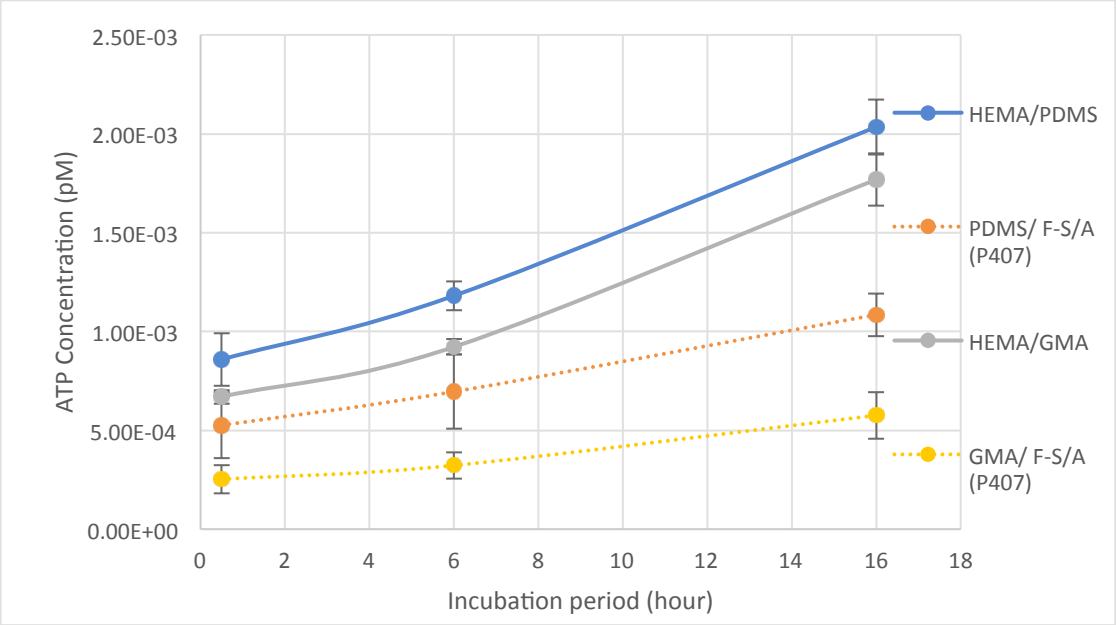

Figure 6.7: Bioluminescence measured at three different time points (0.5h, 6h, and 16h) bacterial adhesion of pseudomonas aeruginosa on contact lenses some of which treated with Poloxamer 407. Data presented as a mean ± SD, n=3.

Within the two main formulations GMA-P407 had the least bacterial adhesion when compared to PDMS-P407. At 0.5hr majority of the formulations had very similar bacterial ATP concentrations (pM). At 6hr mark the surfactant treated contact lenses (GMA-P407 and PDMS-P407) had less bacterial binding with a statistical significance (p=0.05). at 16hr there was a statistically significant decrease in bacterial ATP concentration between the two formulations GMA-P407 and PDMS-P407 ($p=0.0023$).

S. epidermis is also among the bacterial microorganisms responsible for MK. This gram-positive bacterium has the ability to form biofilm which helps it latch onto biomaterials surface (218), which contributes towards the virulence factor. Therefore, initial adhesion of *S. epidermis* to the biomaterial surface is a focal step in the colonization of SCL's (219).

Adhesion of *S. epidermis* to SCLs are presented in Figure 6.8 Initially (at 0.5hr) there was no significant difference in *S. epidermis* adherence within all formulations, with increase in incubation period bacterial adherence increases. A study by *Marshall et al*, demonstrates bacterial adhesion consists of two phases, reversible sorption is where instantaneous attraction of the bacteria to the surface of biomaterial occurs involving van der waals forces, that can be removed by rinsing the surface with 2.5% NaCl. And irreversible sorption which involves firm bacterial adhesion to the surface that can no longer be washed with 2.5% NaCl (220) this is where the bacteria then grow to colonize (90). The findings of Marshall's study support the present study in which there is increased number of bound bacteria on the surface of the SCLs after 16hr incubation period.

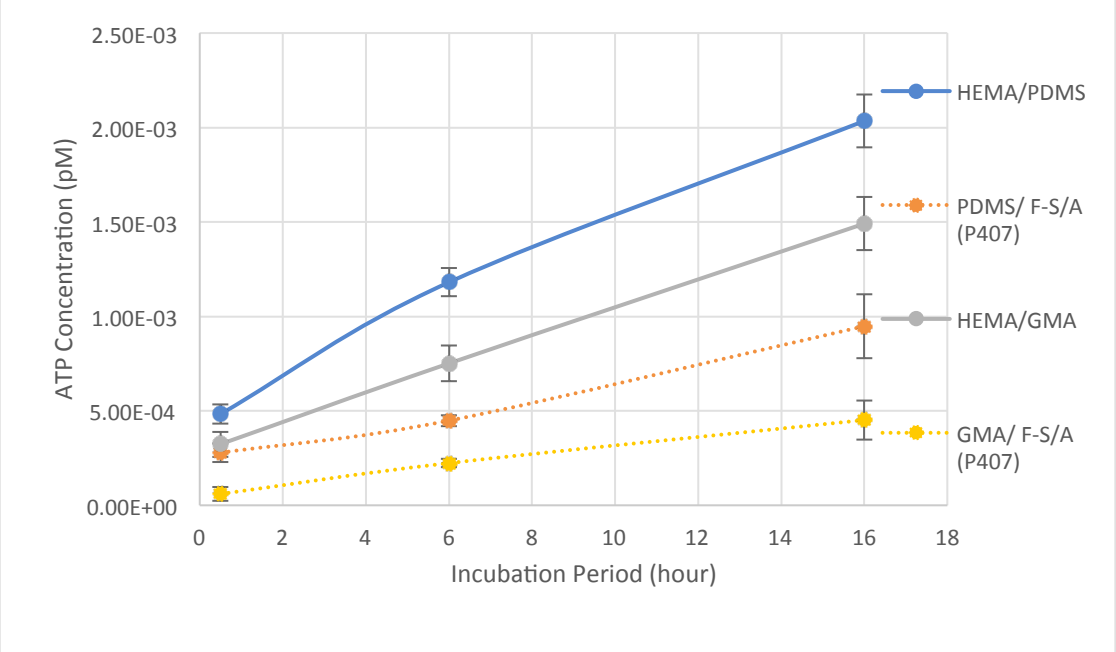

Figure 6.8: Bioluminescence measured at three different time points (0.5h, 6h, and 16h) bacterial adhesion of Staphylococcus epidermidis on contact lenses some of which treated with Poloxamer 407. Data presented as a mean ± SD, n=3.

The two treated SCLs GMA-P407 and PDMS-P407 possessed less bacteria on the surface of the lens compared to the controls at 0.5hr both formulations had lower number of bacterial adhesion however not statistically significant (GMA-P407, 0.5hr *P*=0.0747 and PDMS-P407, 0.5hr *P*=0.302). At 6 and 16hr time point both formulations possessed less binding bacteria to the SCLs surface with a statistical significance of GMA-P407, 6hr *p*= <0.0001, 16hr *p*= <0.0001, PDMS-P407, 0.5hr *P*=0.302, 6hr *p*= <0.0001, 16hr *p*= <0.0001.

However, comparing the two surfactants treated formulations against one another displayed not statistical significance at 0.5hr (*p*=0.223) and 6hr (*p*=0.193). But at 16hr there was a statistical difference (GMA-P407 Vs PDMS-P407 *p*=<0.0001). GMA-P407 possessed ATP bacterial concentration of $4.51\times10^{-4} \pm 1.04\times10^{-4}$ pM in comparison with PDMS-P407 $9.48\times10^{-4} \pm 1.69\times10^{-4}$ pM.

Kodjikian et al, studied the adhesion of clinically relevant bacteria to conventional hydrogel and silicone-hydrogel CLs, and discovered that hydration and the physical environment such as hydrophobicity, as well as the chemical compositions of CLs are all important properties that govern the level of bacterial adhesion to the surface of the CL. It was discovered that initial adhesion of *P. aeruginosa* occurs much faster than that of *S. epidermis,* this is mainly due to biofilm formation, hydrophobicity promotes bacterial binding and is directly related to the EWC and surface CA, it was discovered that bacterial binding decreased with increase in EWC, and

increase in surface wettability decrease lipid deposition. Silicone-hydrogel lenses promotes oxygen permeability however have hydrophobic areas, and standard hydrogel CL showed more resistance to bacterial adhesion. These findings support the findings of this current study.

Both *P. aeruginosa* and *S. epidermis* recorded a deceasing attachment strength in the following order, GMA-P407(EWC 32.04 ± 0.54%), PDMS-P407 (EWC 30.02 ± 0.56%), HEMA-GMA (EWC 31.21 ± 0.05%) and HEMA-PDMS (EWC 31.77 ± 0.08%). The hydrogel P407 treated SCL has the lowest number of bacterial adhesion compared to the silicone-hydrogel contact lens, this could be due to hydrophobic areas present on the surface of the SCL, that form tightly bound noncovalent interactions with the bacteria (221).

As shown in Figure 6.7 and 6.8, the bacterial adherence of *P. aeruginosa* was slightly above than that of *S. epidermis* for both treated SCLs (GMA-P407 and PDMS-P407 0.5hr 0.0012, 6hr p= 0.001, p= <0.0001). GMA-P407 is composed of 90% HEMA which is a hydrophilic and increases the EWC of the CL, and increase surface wettability, this will not only prevent lipid deposits (222) forming but also prevent bacterial adherence to the CL. A study by *Aswad et al,* found *P. aeruginosa* showed significant adherence to CL, also the extent of bacterial adherence was proportional to focal deposits (214). PDMS-P407 is composed of 97% HEMA and 3% PDMS, PDMS is readily used by CL manufactures due to its high optical transmission, and oxygen permeability, however its hydrophobic due to siloxane (Si-O-Si)

bonds present that restricts the formation of hydrogen bonds on the matrix (223), hence its combined with HEMA to overcome the stated limitation.

P407 used due to its antimicrobial properties and adhesive effects on both gram-negative and gram-positive bacteria (96,237), with addition of P407 in *P. aeruginosa* there was reduced bacterial adherence by 12% for PDMS-P407 and 17% GMA-P407. And within *S. epidermis* bacterial adherence was reduced by 6% for PDMS-P407 and 16% GMA-P407.
P. aeruginosa is one of the main causes of MK (223,228), due to its ability to adhere tightly to the surface of CL. As previously stated pili are responsible for the hydrophobic surface of the bacteria (227,229) and the flagella provides the means of transport to the surface of CL (230,231). When *P. aeruginosa* adheres to the surface of CL it starts to produce biofilm with the aid of the bacterial DNA, *P. aeruginosa* is also able to quorum sense, which enables the biofilm to avoid the detection of the immune system (217).

S. epidermis is another significant microbe that's also associated with MK, this bacterium is able to form biofilm with polysaccharide adhesion (PS/A) on the surface of the CL. based on the strain *S. epidermis* some are able to produce biofilm and some don't non the less they're still able to colonize the surface of CL after adhesion(100,238).

6.7. *In vitro* Ocular Tolerability study

6.7.1. Hen's Egg test chorioallantoic membrane (HET-CAM)

The irritation effect of SCLs treated with and without P407 was examined at 0.5, 2 and 5 minutes' post exposure (Figure 6.9). Positive and negative controls were used (NaOH and saline solution) providing bases for assessing prepared SCLs with and without P407 surfactant as well as PAA nanoparticle systems. Figure 6.9 displays CAM images post application of SCL material with and without P407, and the images displayed no sign of irritation on the CAM at all time points. Thus, the use of P407 within SCL matrix has proven to be non-irritant making them biocompatible to the conjunctiva. Similar results were obtained by *Chen et al,* ocular irritation HET-CAM assay displayed no irritation for glyceryl monooleate P407 nanoparticles, also there was no sign of ocular damage, or abnormal signs in the cornea, conjunctiva or iris of the albino rabbits (225,226).

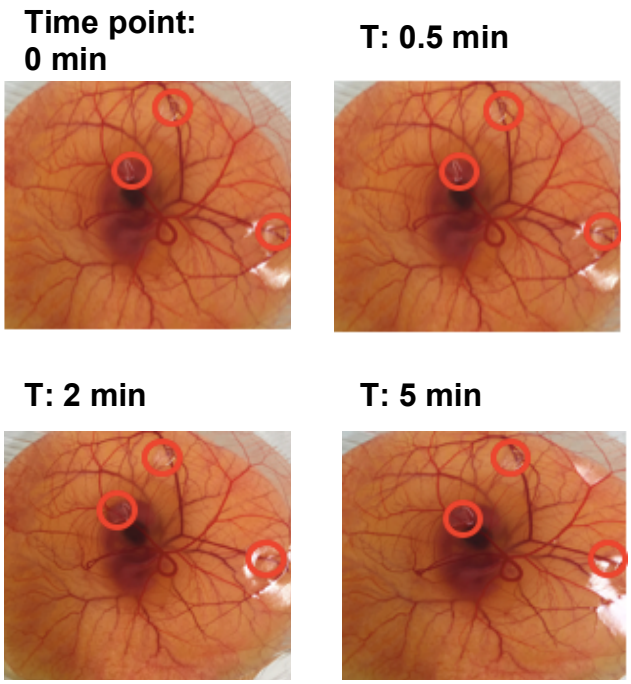

Figure 6.9: HET-CAM images of vascular response to, HEMA-PDMS-F-S/A-P407 and HEMA-PDMS-F-S/A-P407 SCL's.

6.7.2. Bovine corneal opacity and permeability (BCOP) for prepared SCLs.

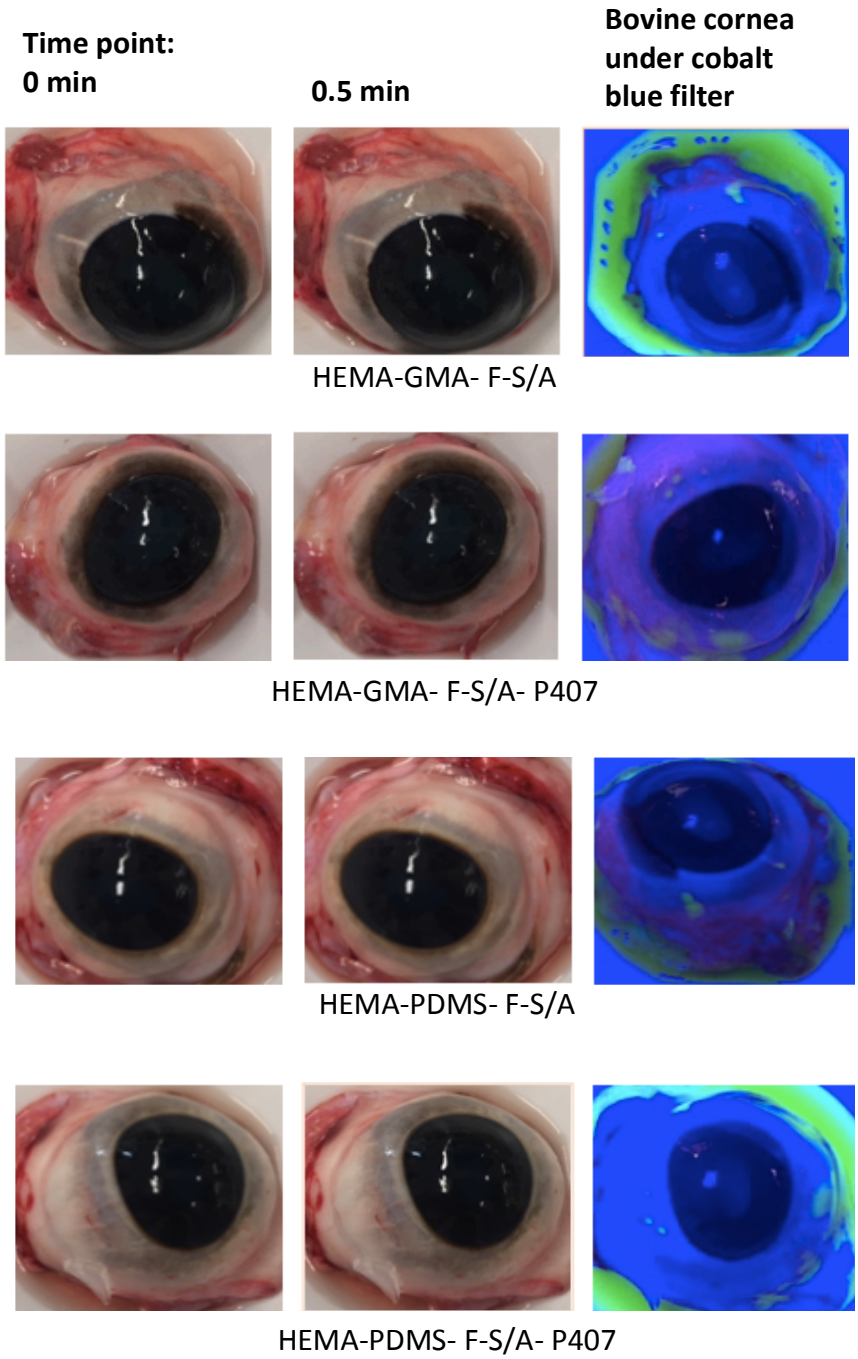

Figure 6.10: BCOP images with corresponding fluorescence images of freshly excised bovine cornea treated with prepared SCLs with and without surfactant (P407

As previously mentioned in chapter 5 BCOP assay is used to measure corneal irritation. Fluorescein dye is used to indicate the level of corneal damage as the dye will permeate through a damaged endothelial layer of the cornea. BCOP assay was used to study the irritation effects of the prepared SCLs with and without P407 surfactant. Figure 5.13 (in chapter 5) displays the positive control NaOH is a sever irritant causing damage to the cornea; BCOP images display opacity around the inside of the silicone ring. And for the negative control normal saline was used which displayed no sign of damage to the cornea. Figure 6.10 displays images of bovine corneas post treatment of SCLs with and without P407 surfactant. The integrity of the corneal epithelial layer was studied under blue cobalt filter post application of fluorescein dye, BCOP images displayed no sign of staining suggesting no damage was caused by the test material.

6.8. Summary:

S. epidermis and *P. aeruginosa* are two of the most common microorganisms responsible for bacterial keratitis in contact lens wearers. Both ATP per unit amounts are indirectly proportional to the number of bound bacteria for the bioluminescence represented in Figure 6.7 and 6.8. By means of ATP (M) counts for bacterial adherence was statistically lower for P-407 treated SCL for both *S. epidermis* and *P. aeruginosa*. Also, ANOVA (Graph Pad) showed that there was a significant difference between the 4 groups of SCLs.

Bacterial adherence is very much related to biofilm production on the surface of the SCL. Thus, some surfaces of SCL are more resistant (GMA-P407) than others, PDMS-P407 had slightly lower resistance to bacterial adherence compared to GMA-P407, due to the hydrophobic areas within the silicone-hydrogel. The silicone component within PDMS-P407 SCL provides many beneficial properties to the lens such as increasing oxygen permeability, while the hydrogel provides flexibility and increasing water capacity within the SCL.

Nonetheless incorporation P407 aided the resistance to bacterial adherence of both gram-negative and gram-positive bacteria when compared to the controls. We believe that MK related to contact lenses could very well decrease with the basis of our results. Both formulations contain high percentages of 90-97% HEMA, and P407 which are highly hydrophilic, increasing EWC and surface wettability, and having antimicrobial properties, these contact lenses could reduce the risk of corneal infection.

HET-CAM and BCOP assays were used to investigate the level of irritation and the cytotoxic effects of the prepared SCLs treated with and without surfactant P407. *In vitro* results obtained from both irritation assays (HET-CAM and BCOP assay) were well correlated with one another and demonstrated no sign of irritation to the corneal epithelial cells or conjunctiva.

General Conclusion and Future Studies

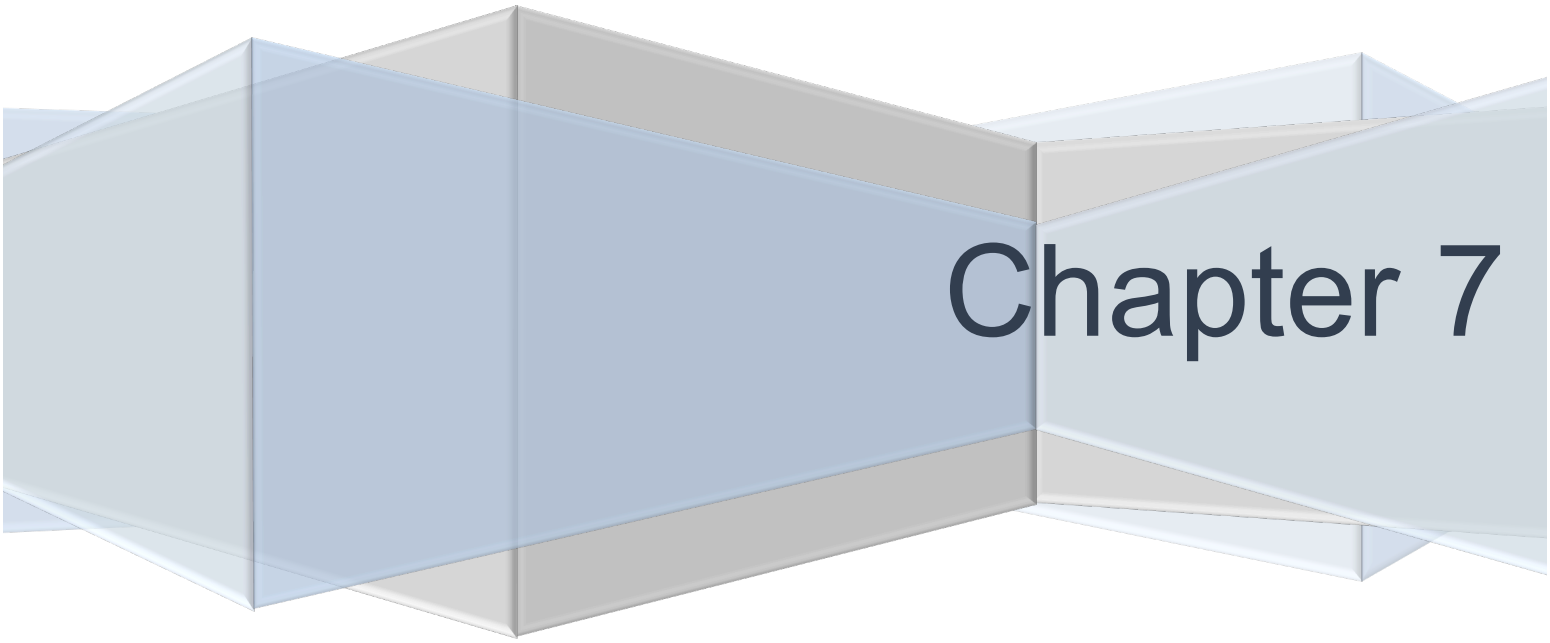

CHAPTER 7

7. General Conclusion and Future Studies

With Glaucoma being one of the leading causes of vision loss, there are many challenges when trying to develop new ways of delivering carbonic anhydrase inhibitors (DZH) to the eye. Surgery such as laser trabeculoplasty and topical drug administrations are the current treatments available. The main limiting factor to surgery is this form of treatments would not be available to more developing countries due to the costs. Also, there are many current topical applications within the market, Lumigan® (prostaglandin analogs), Timolol (beta-blockers), Trusopt® (carbonic anhydrase inhibitors) etc. topical administration accounts for 90% of ocular drug delivery within the market. This is because it is widely preferred by both medical practitioners and patients due to its easy application. However, these anti-glaucoma eye drops require multiple administration (up to twice a day), leading to poor patient compliance, short residence time and limited bioavailability due to major drug loss post application via rapid tear flow and nasolacrimal drainage. Hence the increase in desire to develop an alternative way of treating patients with glaucoma. Nanotechnology has become increasingly popular within ocular drug delivery. Integrating nanotechnology into SCLs as this will enhance therapeutic outcomes and improve patient compliance.

One of the main reasons for Glaucoma is blocked trabecular meshwork located between the cornea and the iris. This prevents the outflow of the circulating aqueous fluid, which in turn increases resistance and intra-ocular pressure within the eye and if left untreated could cause damage to the optic nerve and result in irreversible loss of sight. DZH is a carbonic anhydrase inhibitor used to treat patients with glaucoma. DZH works by preventing formation of hydrogen and bicarbonate ions from carbon dioxide and water and promotes renal excretion of sodium, potassium, bicarbonate and water.

The main purpose of chapter 3 was to develop and validate a simple, selective and sensitive HPLC method for the quantification of DZH drug and optimise the right concentrations of hydrogel polymers and cross-linking agent used to prepare SCLs. Identify the different parameters according to the different characterisation studies to assess various properties of the SCL matrix, which potentially can determine the ideal concentration for SCL. An analytical assay for the separation and quantification of DZH was essential. HPLC validation method for the simultaneous determination of DZH was adopted as per ICH-guidelines. The separation of DZH was successful and was achieved in fewer than 2 mins. HPLC method was fast, accurate, precise and reliable with LLOD and LLOQ of 2.00 and 6.05 µg/ mL respectively. The permeated DZH through dialysis tube was also quantified using this HPLC method.

SCLs along with nanotechnology have shown increase interest within current research. HEMA is one of the most extensively studied polymers used for the

preparation of SCLs due to its unique properties, high EWC%, low surface wettability, high optical clarity and its hydrophilic nature as well as being non-toxic. The effect of EDGMA (cross-linking agent) against different concentration % of HEMA polymer was studied. And it was discovered that when high concentrations of HEMA used the SCL possessed the highest EWC, CA and TM values however the YM value was low suggesting a soft lens. In order to improve the SCL a variety of hydrophilic and hydrophobic polymers were used to copolymerise with HEMA polymer. The effect of different concentrations of MMA, MAA and GMA against HEMA polymer was studied. HEMA/MAA (90/10% v/v) followed by HEMA/GMA (90/10% v/v) both MMA and GMA are hydrophobic polymers that could help enhance the mechanical strength increasing the YM values of the SCL. These concentration % yielded TM% of 80% and above, with improved EWC%, CA values.

EWC% and TM% was one of the most important properties within SCL, and once we discovered the correct concentration% for SCL with increased EWC and TM%. The next step was to target some of the most common complaints amongst lens wearers, such as experiencing discomfort due to hypoxia and induced dry lens as well as burning sensation due to contaminated SCLs. The main objectives behind chapter 4 were to optimise and prepare SCLs using different volumes of various different silicone-based polymers. In order to understand the level of influence the silicone based polymers possess over SCL properties. SCLs were prepared using different concentrations of silicone-based polymers against HEMA polymer. Si-Hy SCLs are one of the

most popular types of lenses used in the market at the moment due to high oxygen permeability. We wanted to prepare an ideal SCL with a balance between oxygen permeability, EWC%, material strength and stability. The hydrogel polymer (HEMA) contributes hydration due to the hydrophilic hydroxyl functional groups present, however they lack in oxygen permeability, whilst the silicone based polymers provided oxygen permeability. Both PDMS-AS and TMFS exhibited transparency of 90% and above, optical clarity is one of the major components towards and ideal SCL. Both silicone polymers also displayed a constant high EWC% with increase in silicone polymer suggesting a more stable polymer. Along with high EWC% these polymers displayed a low surface wettability with low CA values suggesting a more hydrophilic SCL material, this is due the combination of HEMA/PDMS-AS.

Silicone based polymers are known to improve elasticity by providing material strength to the lens as well as preventing deformation when the eyelids come into contact with SCLs. A general pattern noticed with increase in silicone-based polymers the YM values increased, making the CL material more tough. TMF polymer was the only one that was different increasing in polymer concentration % the YM value decreased, as the SCLs became more brittle like in texture, due to incorporation fluorine into the carbon-carbon backbone. Siloxane based polymers have high thermal stability, low Tg, low surface tension with high oxygen permeability; due to strong stretching vibrations within the Si-O bonds creating permeable channels within the polymer complex and providing stability and material strength.

PDMS have high thermal and oxidative stability, and is non-toxic and non-irritant which is why they are highly used for ocular purposes.

Once we developed an ideal SCL that possessed the ideal properties consisting of adequate percentages of EWC, TM, YM and CA, the next step was looking at pharmaceutical approaches based on nanotechnologies and development of drug loaded nanoparticles (NPs), using mucoadhesive polymer PAA. The main objectives of chapter 5 was to optimise the formulation of PAA nanoparticle, in order to load DZH. And quantify the *in vitro* drug release from the DZH NP loaded SCL. The effect of various variables on the formulation outcome was examined via particle size and surface charge of PAA NP. PAA polymer is extensively used to prepare nanoparticles due to its hydrophilic nature and high water capacity absorption, making the polymer structure soft and flexible. For a prolong residence time and sustained drug release it is important to use mucoadhesive polymers to prepare nanoparticles. Another advantage of PAA polymer is that its non-toxic and biocompatible. Ionic gelation method was used to prepare PAA nanoparticles, this is a simple assay, and however there are several factors known to influence the properties of the nanoparticles. For optimisation of prepared PAA nanoparticles, three potential variables were identified, PAA, $CaCl_2$ and DZH concentrations. All of which had an effect on the particle size of PAA nanoparticle. Formulated PAA nanoparticles resulted in small particle size, good polydispersity values with well DZH entrapment. The *in vitro* release study of DZH loaded PAA nanoparticles was investigated via dialysis bag immersed in PBS for 24

hours at 37 °C. There was increase release of DZH loaded PAA nanoparticles in SCL compared to DZH loaded into SCL material. Both formulations could be used to tailor DZH delivery based on the patient requirement.

Silicone based SCLs are very much prone to bacterial adherence due to their hydrophobic nature, resulting in ocular infections such as microbial keratitis. Surfactants work by improving the hydrophilicity, wettability and the biocompatibility of the SCLs. The main aim behind chapter 6 was to prepare SCLs treated with different volumes of P407 surfactant and to examine the effect of P407 on the bacterial adhesion of *Pseudomonas aeruginosa (P.aeruginosa) and Staphylococcus epidermidis (S.epidermis)* on SCL surface. The effects of P407 were studied to further understand and prevent it from compromising SCL properties. P407 surfactant was used to treat silicone based SCLs (PDMS/HEMA/P407) as well as hydrogel based SCLs (GMA/HEMA/P407). These SCLs are characterised based on EWC%, TM%, YM and CA. All SCLs displayed an increase in EWC% and decrease in CA values with increase in P407 concentration. However, the YM value decreased with increase in P407 concentration, this is due to increased EWC%, making the material of the SCL softer thus decreasing in mechanical strength. TM% values of 90% and above were displayed for PDMS/HEMA/P407 and GMA/HEMA/P407 at 0.25% P407, high transparency is most desired for SCLs.

Bacterial adhesion assay of both *P.aeruginosa* and *S.epidermis* for both sets of SCLs was carried out using bioluminescence ATP assay at several time points (0.5, 6 and 16 hours). A general pattern was notice, surfactant treated SCLs displayed a lower bacterial ATP concentration for both *P.aeruginosa* and *S.epidermis.* Despite limited research studies on bacterial adherence of SCLs, however the results presented in this study suggests the use of surfactant P407 enhanced the resistance of bacterial adherence to the SCL surface.

It is essential for new formulation proposed for topical application to studied for potential toxicity/ irritation effects on the eye. Most topically administered drugs are faced with barriers at the cornea and conjunctiva. *In vitro* ocular toxicity study was carried out to investigate the irritation level of the prepared SCL with and without surfactant P407 as well as DZH loaded PAA nanoparticles. The results presented from the BCOP and HET-CAM assay were promising, the prepared SCLs with and without P407 as well as the DZH loaded PAA nanoparticles were well tolerated on the ocular surface with no sign of irritation.

In conclusion, this doctoral research has shown that carbonic anhydrase inhibitor (DZH) can be loaded into PAA nanoparticles and then placed into SCL material for a sustained drug release. Thus, SCL demonstrated can be suitable for drug delivery not only to treat glaucoma but the potential to treat other chronic or acute eye disorders. P407 surfactant has proved to be essential for resistance of bacterial adherence preventing MK.

The future studies:

- Further investigate the permeation using *ex vivo* trans-corneal permeation

- Investigating the effect of the prepared ocular delivery system using an appropriate glaucoma animal mode

The main aim of this doctoral research was to prevent one of the main causes of irreversible blindness. The idea of drug loaded SCL topical application could be the future for glaucoma treatment as well as many other ocular conditions, without compromising their vision. These contact lenses could also be used to correct refractive errors such as myopia and hyperopia. I believe that this thesis is the start of a very long journey with a promising future.

References

1. Hiatt KL, Braithwaite MG, Crowley JS, Rash CE, van de Pol C, Ranchino DJ, et al. The effect of a monocular helmet-mounted display on aircrew health: A cohort study of Apache AH MK1 pilots initial report. US Army Aeromed Res Lab Rep No 2002-4. 2002;(May 2015).
2. Remington LA. Clinical anatomy of the visual system. Elsevier; 2005. 292 p.
3. Al-Ebini Y. Investigations into Drug Delivery to the Eye: Nanoparticle Comparisons [Internet]. 2014 [cited 2018 Aug 25]. Available from: https://pdfs.semanticscholar.org/268c/f4f237974a59104dc7d2e2739dfc54f82715.pdf
4. Watson C. Visual System. The Mouse Nervous System. 2012. 646–652 p.
5. Fekrat S, Weizer JS. All about your eyes [Internet]. Duke University Press; 2006 [cited 2018 Jun 5]. 199 p. Available from: https://books.google.co.uk/books/about/All_about_Your_Eyes_PB.html?id=zJES898fXJYC&redir_esc=y
6. Bachu RD, Chowdhury P, Al-Saedi ZHF, Karla PK, Boddu SHS. Ocular Drug Delivery Barriers-Role of Nanocarriers in the Treatment of Anterior Segment Ocular Diseases. Pharmaceutics [Internet]. 2018 Feb 27 [cited 2018 May 31];10(1). Available from: http://www.ncbi.nlm.nih.gov/pubmed/29495528
7. Dartt DA. Regulation of mucin and fluid secretion by conjunctival epithelial cells. Prog Retin Eye Res [Internet]. 2002 Nov [cited 2018 Nov 22];21(6):555–76. Available from: http://www.ncbi.nlm.nih.gov/pubmed/12433377
8. Cholkar K, Patel SP, Vadlapudi AD, Mitra AK. Novel strategies for anterior segment ocular drug delivery. J Ocul Pharmacol Ther [Internet]. 2013 Mar [cited 2018 Nov 23];29(2):106–23. Available from: http://www.ncbi.nlm.nih.gov/pubmed/23215539
9. Dey S, Patel J, Anand BS, Jain-Vakkalagadda B, Kaliki P, Pal D, et al.

Molecular evidence and functional expression of P-glycoprotein (MDR1) in human and rabbit cornea and corneal epithelial cell lines. Invest Ophthalmol Vis Sci [Internet]. 2003 Jul [cited 2018 Nov 23];44(7):2909–18. Available from: http://www.ncbi.nlm.nih.gov/pubmed/12824231

10. Scherz W, Doane MG, Dohlman CH. Tear volume in normal eyes and keratoconjunctivitis sicca. Albrecht Von Graefes Arch Klin Exp Ophthalmol [Internet]. 1974 [cited 2018 Nov 23];192(2):141–50. Available from: http://www.ncbi.nlm.nih.gov/pubmed/4548323
11. Gaudana R, Ananthula HK, Parenky A, Mitra AK. Ocular drug delivery. AAPS J [Internet]. 2010 Sep [cited 2018 Nov 23];12(3):348–60. Available from: http://www.ncbi.nlm.nih.gov/pubmed/20437123
12. Hornof M, Toropainen E, Urtti A. Cell culture models of the ocular barriers. Eur J Pharm Biopharm [Internet]. 2005 Jul [cited 2018 Nov 23];60(2):207–25. Available from: http://www.ncbi.nlm.nih.gov/pubmed/15939234
13. Mantelli F, Mauris J, Argüeso P. The ocular surface epithelial barrier and other mechanisms of mucosal protection: from allergy to infectious diseases. Curr Opin Allergy Clin Immunol [Internet]. 2013 Oct [cited 2018 Nov 23];13(5):563–8. Available from: http://www.ncbi.nlm.nih.gov/pubmed/23974687
14. Diecke FPJ, Ma L, Iserovich P, Fischbarg J. Corneal endothelium transports fluid in the absence of net solute transport. Biochim Biophys Acta [Internet]. 2007 Sep [cited 2018 Nov 23];1768(9):2043–8. Available from: http://www.ncbi.nlm.nih.gov/pubmed/17597578
15. ElShaer A, Ghatora B, Mustafa S, Alany RG. Contact lenses as drug reservoirs & delivery systems: the successes & challenges. Ther Deliv [Internet]. 2014;5(10):1085–100. Available from: http://www.ncbi.nlm.nih.gov/pubmed/25418268
16. Dr Nguyen D. Dan Nguyen is a consultant eye surgeon (ophthalmologist) operating in Cheshire and South Manchester in the UK. As well as dealing with the full range of general ophthalmic conditions, Mr. Nguyen has [Internet]. [cited 2019 Jan 30]. Available from: https://www.dannguyen.co.uk/glaucoma/

17. Claouè charles. Private Glaucoma Treatment London | Prof. Charles Claoué [Internet]. [cited 2019 Mar 3]. Available from: http://www.thelondoneyespecialists.co.uk/conditions/glaucoma/
18. Schacknow PN, Samples JR. The Glaucoma Book: A Practical, Evidence-Based Approach to Patient Care. [cited 2018 Jun 5]; Available from: http://www.glaucomasampaolesi.com/files/ebooks/The-Glaucoma-Book.pdf
19. Phelps CD, Corbett JJ. Migraine and low-tension glaucoma. A case-control study. Invest Ophthalmol Vis Sci [Internet]. 1985 Aug [cited 2018 Jun 5];26(8):1105–8. Available from: http://www.ncbi.nlm.nih.gov/pubmed/4019101
20. Mckinnon SJ, Peeples P, Walt Allergan JG. Article in The American Journal of Managed Care [Internet]. 2008 [cited 2018 Dec 13]. Available from: https://www.researchgate.net/publication/5568490
21. National Eye Research Centre | Glaucoma [Internet]. [cited 2018 Dec 13]. Available from: https://www.nerc-charity.org.uk/glaucoma
22. keyser PD. Glaucoma : its symptoms, diagnosis, and treatment : Keyser, Peter Dirck, 1835-1897 : Free Download, Borrow, and Streaming : Internet Archive [Internet]. Philadelphia : Lindsay & Blakiston. Philadelphia ; [cited 2018 Jun 5]. Available from: https://archive.org/details/101191505.nlm.nih.gov
23. Gieser DK, Tracy Williams R, O??Connell W, Pasquale LR, Rosenthal BP, Walt JG, et al. Costs and Utilization of End-stage Glaucoma Patients Receiving Visual Rehabilitation Care: A US Multisite Retrospective Study. J Glaucoma [Internet]. 2006 Oct [cited 2018 Dec 13];15(5):419–25. Available from: http://www.ncbi.nlm.nih.gov/pubmed/16988605
24. Neelima A, Vishal A, Sagar R, Sreenivas V, Rathi A, Kumar S, et al. Investigative ophthalmology & visual science. [Internet]. Vol. 53, Investigative Ophthalmology & Visual Science. [Association for Research in Vision and Ophthalmology, etc.]; 2012 [cited 2018 Dec 13]. 6365–6365 p. Available from: https://iovs.arvojournals.org/article.aspx?articleid=2360063
25. Rowe S, MacLean CH, Shekelle PG. Preventing Visual Loss From

Chronic Eye Disease in Primary Care. JAMA [Internet]. 2004 Mar 24 [cited 2018 Dec 13];291(12):1487. Available from: http://www.ncbi.nlm.nih.gov/pubmed/15039416

26. Kwon YH, Fingert JH, Greenlee EC, Heffron E, Duffel P. A patient's guide to glaucoma [Internet]. F.E.P. International; 2008 [cited 2018 Dec 13]. 164 p. Available from: https://www.saera.eu/libreria/home/510-a-patient-s-guide-to-glaucoma.html
27. Salopek-Rabatić J, Pavan J, Kastelan S, Rabatić L. Glaucoma patients and contact lenses--how to fit--how to treat? Coll Antropol [Internet]. 2013 Apr [cited 2018 Dec 13];37 Suppl 1:195–8. Available from: http://www.ncbi.nlm.nih.gov/pubmed/23837243
28. Hadrill marilyn, Slonim C. Glaucoma Treatment: Eye Drops and Other Medications - AllAboutVision.com [Internet]. allaboutvision.com. 2018 [cited 2018 Dec 13]. Available from: https://www.allaboutvision.com/conditions/glaucoma-3-treatment.htm
29. ElShaer A, Ghatora B, Mustafa S, Alany RG. Contact lenses as drug reservoirs & delivery systems: the successes & challenges. Ther Deliv [Internet]. 2014 Oct [cited 2017 Dec 15];5(10):1085–100. Available from: http://www.ncbi.nlm.nih.gov/pubmed/25418268
30. Trope GE. Glaucoma : a patient's guide to the disease [Internet]. [cited 2018 Jun 5]. 97 p. Available from: https://books.google.co.uk/books?id=uUvW4dQtJwwC&pg=PT3&lpg=PT3&dq=4th+ed.+Toronto+Buffalo+London:+University+of+Toronto+Press;+2011&source=bl&ots=MAUUFOfc6-&sig=Ilf2RPtaAcW2Fn_3ZBwnAng-SWU&hl=en&sa=X&ved=0ahUKEwjSrem5mrvbAhVqL8AKHRF_BPwQ6AEISzAD#v=onepage&q=4th ed. Toronto Buffalo London%3A University of Toronto Press%3B 2011&f=false
31. Trusopt (Dorzolamide Hydrochloride Ophthalmic Solution): Side Effects, Interactions, Warning, Dosage & Uses [Internet]. [cited 2018 Jun 5]. Available from: https://www.rxlist.com/trusopt-drug.htm
32. Mohammadi S, Jones L, Gorbet M. Extended Latanoprost Release from Commercial Contact Lenses: In Vitro Studies Using Corneal

Models. Eniola-Adefeso O, editor. PLoS One [Internet]. 2014 Sep 10 [cited 2018 Jun 5];9(9):e106653. Available from: http://dx.plos.org/10.1371/journal.pone.0106653

33. Brooks AMV, Gillies WE. Ocular beta-Blockers in Glaucoma Management. Drugs Aging [Internet]. 1992 [cited 2018 Dec 13];2(3):208–21. Available from: http://www.ncbi.nlm.nih.gov/pubmed/1351412
34. Linden C, Alm A. Prostaglandin Analogues in the Treatment of Glaucoma. Drugs Aging [Internet]. 1999 May [cited 2018 Dec 13];14(5):387–98. Available from: http://www.ncbi.nlm.nih.gov/pubmed/10408738
35. TIMOPTIC-XE ® 0.25% AND 0.5% (TIMOLOL MALEATE OPHTHALMIC GEL FORMING SOLUTION) [Internet]. 1993 [cited 2019 Jan 30]. Available from: https://www.merck.com/product/usa/pi_circulars/t/timoptic/timoptic_xe_pi.pdf
36. Apătăchioae I, Chiseliţă D. [Alpha-2 adrenergic agonists in the treatment of glaucoma]. Oftalmologia [Internet]. 1999 [cited 2018 Dec 13];47(2):35–40. Available from: http://www.ncbi.nlm.nih.gov/pubmed/10641099
37. Holló G. Carbonic Anhydrase Inhibitors. Glaucoma [Internet]. 2015 Jan 1 [cited 2018 Dec 13];559–65. Available from: https://www.sciencedirect.com/science/article/pii/B9780702051937000546
38. Pfeiffer N. Dorzolamide: development and clinical application of a topical carbonic anhydrase inhibitor. Surv Ophthalmol [Internet]. [cited 2018 Jun 5];42(2):137–51. Available from: http://www.ncbi.nlm.nih.gov/pubmed/9381367
39. Patel A, Cholkar K, Agrahari V, Mitra AK. Ocular drug delivery systems: An overview. World J Pharmacol [Internet]. 2013 [cited 2018 Jun 5];2(2):47. Available from: http://www.ncbi.nlm.nih.gov/pubmed/25590022
40. Yang H, Tyagi P, Kadam RS, Holden CA, Kompella UB. Hybrid Dendrimer Hydrogel/PLGA Nanoparticle Platform Sustains Drug

Delivery for One Week and Antiglaucoma Effects for Four Days Following One-Time Topical Administration. ACS Nano [Internet]. 2012 Sep 25 [cited 2018 Aug 29];6(9):7595–606. Available from: http://www.ncbi.nlm.nih.gov/pubmed/22876910

41. Xu J, Li X, Sun F. *In vitro* and *in vivo* evaluation of ketotifen fumarate-loaded silicone hydrogel contact lenses for ocular drug delivery. Drug Deliv [Internet]. 2011 Feb 3 [cited 2017 Nov 5];18(2):150–8. Available from: http://www.tandfonline.com/doi/full/10.3109/10717544.2010.522612
42. Ciolino JB, Stefanescu CF, Ross AE, Salvador-Culla B, Cortez P, Ford EM, et al. In vivo performance of a drug-eluting contact lens to treat glaucoma for a month. 2014 [cited 2018 Dec 14]; Available from: http://dx.doi.org/10.1016/j.biomaterials.2013.09.032
43. How Contact Lenses Work | CooperVision UK [Internet]. cooper vision . [cited 2018 Dec 14]. Available from: https://coopervision.co.uk/about-contacts/how-contact-lenses-work
44. Keirl A, Christie C. Clinical optics and refraction : a guide for optometrists, contact lens opticians, and dispensing opticians. Baillière Tindall Elsevier; 2007. 338 p.
45. Gulsen D, Li C-C, Chauhan A. Dispersion of DMPC Liposomes in Contact Lenses for Ophthalmic Drug Delivery. Curr Eye Res [Internet]. 2005 Jan 2 [cited 2017 Nov 5];30(12):1071–80. Available from: http://www.tandfonline.com/doi/full/10.1080/02713680500346633
46. Gulsen D, Chauhan A. Dispersion of microemulsion drops in HEMA hydrogel: A potential ophthalmic drug delivery vehicle. Int J Pharm. 2005;292(1–2):95–117.
47. Kapoor Y, Thomas JC, Tan G, John VT, Chauhan A. Surfactant-laden soft contact lenses for extended delivery of ophthalmic drugs. Biomaterials. 2009;30(5):867–78.
48. Maulvi FA, Soni TG, Shah DO. A review on therapeutic contact lenses for ocular drug delivery. Drug Deliv [Internet]. 2016 Oct 12 [cited 2017 Nov 5];23(8):3017–26. Available from: https://www.tandfonline.com/doi/full/10.3109/10717544.2016.1138342
49. ElShaer A, Ghatora B, Mustafa S, Alany RG. Contact lenses as drug

reservoirs & delivery systems: the successes & challenges. Ther Deliv. 2014;5(10):1085–100.

50. J. L. Creech †, A. Chauhan and, Radke* CJ. Dispersive Mixing in the Posterior Tear Film Under a Soft Contact Lens. 2001 [cited 2018 Nov 10]; Available from: https://pubs.acs.org/doi/abs/10.1021/ie000596z
51. Schultz CL, Poling TR, Mint JO. A medical device/drug delivery system for treatment of glaucoma. Clin Exp Optom [Internet]. 2009 Jul [cited 2018 Nov 10];92(4):343–8. Available from: http://www.ncbi.nlm.nih.gov/pubmed/19389129
52. Jung HJ, Abou-Jaoude M, Carbia BE, Plummer C, Chauhan A. Glaucoma therapy by extended release of timolol from nanoparticle loaded silicone-hydrogel contact lenses. J Control Release [Internet]. 2013 Jan 10 [cited 2018 Nov 13];165(1):82–9. Available from: http://www.ncbi.nlm.nih.gov/pubmed/23123188
53. Jung HJ, Chauhan A. Temperature sensitive contact lenses for triggered ophthalmic drug delivery. Biomaterials [Internet]. 2012 Mar [cited 2018 Nov 13];33(7):2289–300. Available from: http://www.ncbi.nlm.nih.gov/pubmed/22182750
54. Maldonado-Codina C, Efron N. Hydrogel Lenses – Materials and Manufacture : A Review. Optom Pract. 2003;4:101–15.
55. Refractive Index of Polymers by Index « scientificpolymer.com [Internet]. [cited 2018 Jun 5]. Available from: http://scientificpolymer.com/technical-library/refractive-index-of-polymers-by-index/
56. Jones L. Contact Lens Spectrum - Modern Contact Lens Materials: A Clinical Performance Update. Contact Lens Spectr [Internet]. 2002 [cited 2018 Nov 19]; Available from: https://www.clspectrum.com/issues/2002/september-2002/modern-contact-lens-materials-a-clinical-performa
57. Guidi G. Silicone Hydrogels and their use as Ophthalmic Drug Delivery Systems. 2013 [cited 2018 Jun 11]; Available from: https://macsphere.mcmaster.ca/handle/11375/13129
58. Morgan PB, Brennan noel. The decay of DK? Optician. 2004;227(5937).

59. Malaekeh-Nikouei B, Vahabzadeh SA, Mohajeri SA. Preparation of a Molecularly Imprinted Soft Contact Lens as a New Ocular Drug Delivery System for Dorzolamide. Curr Drug Deliv. 2013;
60. Hiratani H, Alvarez-Lorenzo C. Timolol uptake and release by imprinted soft contact lenses made of N,N-diethylacrylamide and methacrylic acid. J Control Release. 2002;
61. Panáček A, Prucek R, Hrbáč J, Nevečná T, Šteffková J, Zbořil R, et al. Polyacrylate-Assisted Size Control of Silver Nanoparticles and Their Catalytic Activity. Chem Mater [Internet]. 2014 Feb 11 [cited 2018 May 28];26(3):1332–9. Available from: http://pubs.acs.org/doi/10.1021/cm400635z
62. Glycidyl methacrylate 97%, contains 100 ppm monomethyl ether hydroquinone as inhibitor | Sigma-Aldrich [Internet]. [cited 2018 Jun 5]. Available from: https://www.sigmaaldrich.com/catalog/product/aldrich/151238?lang=en&region=GB
63. Sharma RK, Lalita, Singh AP, Chauhan GS. Grafting of GMA and some comonomers onto chitosan for controlled release of diclofenac sodium. Int J Biol Macromol. 2014;
64. Calixto G, Yoshii AC, Rocha e Silva H, Stringhetti Ferreira Cury B, Chorilli M. Polyacrylic acid polymers hydrogels intended to topical drug delivery: preparation and characterization. Pharm Dev Technol [Internet]. 2015 May 19 [cited 2018 Nov 14];20(4):490–6. Available from: http://www.ncbi.nlm.nih.gov/pubmed/25975700
65. Greindl M, Bernkop-Schnürch A. Development of a Novel Method for the Preparation of Thiolated Polyacrylic Acid Nanoparticles. Pharm Res [Internet]. 2006 Sep 9 [cited 2018 Mar 25];23(9):2183–9. Available from: http://www.ncbi.nlm.nih.gov/pubmed/16952008
66. Singh J, Agrawal KK. Polymeric Materials for Contact Lenses. J Macromol Sci Part C Polym Rev [Internet]. 1992 Aug [cited 2018 Nov 20];32(3–4):521–34. Available from: http://www.tandfonline.com/doi/abs/10.1080/15321799208021431
67. Ribeiro AM, Figueiras A, Veiga F. Improvements in Topical Ocular Drug Delivery Systems: Hydrogels and Contact Lenses. J Pharm

Pharm Sci [Internet]. 2015 [cited 2018 Nov 21];18(5):683–95. Available from: http://www.ncbi.nlm.nih.gov/pubmed/26670365

68. Tateishi Y, Kai N, Noguchi H, Uosaki K, Nagamura T, Tanaka K. Local conformation of poly(methyl methacrylate) at nitrogen and water interfaces. Polym Chem [Internet]. 2010 Apr 13 [cited 2018 Jun 5];1(3):303–11. Available from: http://xlink.rsc.org/?DOI=B9PY00227H
69. Monis C. Hydrogel Contact Lenses. 2002;
70. Karlgard CCS, Wong NS, Jones LW, Moresoli C. In vitro uptake and release studies of ocular pharmaceutical agents by silicon-containing and p-HEMA hydrogel contact lens materials. Int J Pharm. 2003;
71. Owen MJ, Emeritus S. Why Silicones Behave Funny - M. J. Owen. [cited 2018 Jan 19]; Available from: https://www.dowcorning.com/content/publishedlit/01-3078-01.pdf
72. Nicolson PC, Vogt J. Soft contact lens polymers: an evolution. Biomaterials [Internet]. 2001 Dec 15 [cited 2018 Jan 19];22(24):3273–83. Available from: https://www.sciencedirect.com/science/article/pii/S014296120100165X
73. Luensmann D, Heynen M, Liu L, Sheardown H, Jones L. The efficiency of contact lens care regimens on protein removal from hydrogel and silicone hydrogel lenses. Mol Vis. 2010;16:79–92.
74. Friends GD, Kunzler JF, Ozark RM. Recent advances in the design of polymers for contact lenses. Macromol Symp [Internet]. 1995 Jul 1 [cited 2018 Nov 21];98(1):619–31. Available from: http://doi.wiley.com/10.1002/masy.19950980153
75. Montero Iruzubieta J, Nebot Ripoll JR, Chiva J, Fernández OE, Rubio Alvarez JJ, Delgado F, et al. Practical experience with a high Dk lotrafilcon A fluorosilicone hydrogel extended wear contact lens in Spain. CLAO J [Internet]. 2001 Jan [cited 2018 Jan 19];27(1):41–6. Available from: http://www.ncbi.nlm.nih.gov/pubmed/11215605
76. Tris(trimethylsiloxy)silane ≥98% | Sigma-Aldrich [Internet]. [cited 2018 Jun 5]. Available from: https://www.sigmaaldrich.com/catalog/product/aldrich/370908?lang=en&region=GB
77. Hu X, Hao L, Wang H, Yang X, Zhang G, Wang G, et al. Hydrogel

Contact Lens for Extended Delivery of Ophthalmic Drugs. Int J Polym Sci [Internet]. 2011 Jun 7 [cited 2018 Jun 5];2011:1–9. Available from: https://www.hindawi.com/journals/ijps/2011/814163/

78. Xu J, Li X, Sun F. In vitro and in vivo evaluation of ketotifen fumarate-loaded silicone hydrogel contact lenses for ocular drug delivery. Drug Deliv. 2011;
79. Kang P, Swarbrick H. Peripheral Refraction in Myopic Children Wearing Orthokeratology and Gas-Permeable Lenses. Optom Vis Sci [Internet]. 2011 Apr [cited 2018 Nov 1];88(4):476–82. Available from: https://insights.ovid.com/crossref?an=00006324-201104000-00007
80. Kakisu K, Matsunaga T, Kobayakawa S, Sato T, Tochikubo T. Development and efficacy of a drug-releasing soft contact lens. Investig Ophthalmol Vis Sci. 2013;54(4):2551–61.
81. Xinming L, Yingde C, Lloyd AW, Mikhalovsky S V., Sandeman SR, Howel CA, et al. Polymeric hydrogels for novel contact lens-based ophthalmic drug delivery systems: A review. Contact Lens Anterior Eye [Internet]. 2008 Apr [cited 2018 Nov 1];31(2):57–64. Available from: http://www.ncbi.nlm.nih.gov/pubmed/17962066
82. Guidi G, Hughes TC, Whinton M, Brook MA, Sheardown H. The effect of silicone hydrogel contact lens composition on dexamethasone release. J Biomater Appl [Internet]. 2014 Aug 20 [cited 2018 Jan 19];29(2):222–33. Available from: http://www.ncbi.nlm.nih.gov/pubmed/24556362
83. Kim SW, Bae YH, Okano T. Hydrogels: swelling, drug loading, and release. Pharm Res [Internet]. 1992 Mar [cited 2018 Nov 2];9(3):283–90. Available from: http://www.ncbi.nlm.nih.gov/pubmed/1614957
84. Stapleton F, Carnt N. Contact lens-related microbial keratitis: how have epidemiology and genetics helped us with pathogenesis and prophylaxis. Eye (Lond). 2012;26(2):185–93.
85. Zimmerman A, Nixon A, Rueff E. Contact lens associated microbial keratitis: practical considerations for the optometrist. Clin Optom. 2016;8:1–12.
86. Egan DJ, Dyavaiah M. Microbial Keratitis in Contact Lens Wearers INTRODUCTION AND EPIDEMIOLOGY. JSM Ophthalmol [Internet].

2015 [cited 2018 Jul 11];3(3). Available from: https://www.jscimedcentral.com/Ophthalmology/ophthalmology-spid-eye-contact-lenses-1036.pdf

87. Bourcier T, Thomas F, Borderie V, Chaumeil C, Laroche L. Bacterial keratitis: predisposing factors, clinical and microbiological review of 300 cases. Br J Ophthalmol. 2003;87(7):834–8.
88. Teo L, Lim L, Tan DTH, Chan T-K, Jap A, Ming LH. A survey of contact lens complications in Singapore. Eye Contact Lens. 2011 Jan;37(1):16–9.
89. Elhanan MM, Nabi A, Tayara F, Alsharhan M. Bacterial Keratitis Risk Factors, Pathogens and Antibiotic Susceptibilities: A 5- Year Review of Cases at Dubai hospital, Dubai. J Clin Exp Ophthalmol [Internet]. 2016 Aug 15 [cited 2018 Jul 18];07(04):1–5. Available from: https://www.omicsonline.org/open-access/bacterial-keratitis-risk-factors-pathogens-and-antibiotic-susceptibilities-a-5year-review-of-cases-at-dubai-hospital-dubai-2155-9570-1000591.php?aid=79459
90. Bruinsma GM, van der Mei HC, Busscher HJ. Bacterial adhesion to surface hydrophilic and hydrophobic contact lenses. Biomaterials [Internet]. 2001 Dec [cited 2017 Dec 15];22(24):3217–24. Available from: http://www.ncbi.nlm.nih.gov/pubmed/11700793
91. Dutta D, Cole N, Willcox M. Factors influencing bacterial adhesion to contact lenses. Mol Vis [Internet]. 2012 [cited 2017 May 3];18:14–21. Available from: http://www.ncbi.nlm.nih.gov/pubmed/22259220
92. Tran VB, Sung YS, Copley K, Radke CJ. Effects of aqueous polymeric surfactants on silicone-hydrogel soft- contact-lens wettability and bacterial adhesion of Pseudomonas aeruginosa. Cont Lens Anterior Eye [Internet]. 2012 Aug [cited 2018 Jun 6];35(4):155–62. Available from: http://www.ncbi.nlm.nih.gov/pubmed/22456099
93. Singh Sekhon B. Surfactants: Pharmaceutical and Medicinal Aspects [Internet]. Vol. 1, Journal of Pharmaceutical Technology. 2013 [cited 2018 Nov 2]. Available from: https://pdfs.semanticscholar.org/1d86/e51fed2e9d07388a28b1872a2e3c9203076c.pdf
94. Mishra M, Muthuprasanna P, Prabha KS, Rani PS, Babu IAS,

Chandiran IS, et al. Basics and potential applications of surfactants - A review. Int J PharmTech Res. 2009;1(4):1354–65.

95. Portolés M, Refojo MF, Leong F-L. Poloxamer 407 as a bacterial abhesive for hydrogel contact lenses. J Biomed Mater Res [Internet]. 1994 Mar [cited 2017 Dec 15];28(3):303–9. Available from: http://www.ncbi.nlm.nih.gov/pubmed/8077245
96. Dumortier G, Grossiord JL, Agnely F, Chaumeil JC. A Review of Poloxamer 407 Pharmaceutical and Pharmacological Characteristics. Pharm Res [Internet]. 2006 Nov 29 [cited 2018 Nov 22];23(12):2709–28. Available from: http://link.springer.com/10.1007/s11095-006-9104-4
97. Gan L, Han S, Shen J, Zhu J, Zhu C, Zhang X, et al. Self-assembled liquid crystalline nanoparticles as a novel ophthalmic delivery system for dexamethasone: Improving preocular retention and ocular bioavailability. Int J Pharm [Internet]. 2010 Aug 30 [cited 2018 Nov 22];396(1–2):179–87. Available from: http://www.ncbi.nlm.nih.gov/pubmed/20558263
98. El-Kamel AH. In vitro and in vivo evaluation of Pluronic F127-based ocular delivery system for timolol maleate. Int J Pharm. 2002;241(1):47–55.
99. Garcia-Saenz MC, Arias-Puente A, Fresnadillo-Martinez MJ, Paredes-Garcia B. Adherence of two strains of Staphylococcus epidermidis to contact lenses. Cornea [Internet]. 2002 Jul [cited 2017 Dec 15];21(5):511–5. Available from: http://www.ncbi.nlm.nih.gov/pubmed/12072728
100. Cook AD, Sagers RD, Pitt WG. Bacterial adhesion to poly(HEMA)-based hydrogels. J Biomed Mater Res [Internet]. 1993 Jan [cited 2018 Nov 22];27(1):119–26. Available from: http://www.ncbi.nlm.nih.gov/pubmed/8420997
101. Miller MJ, Ahearn DG. Adherence of Pseudomonas aeruginosa to hydrophilic contact lenses and other substrata. J Clin Microbiol [Internet]. 1987 Aug [cited 2018 Nov 22];25(8):1392–7. Available from: http://www.ncbi.nlm.nih.gov/pubmed/3114317
102. Miller MJ, Wilson LA, Ahearn DG. Effects of protein, mucin, and human

tears on adherence of Pseudomonas aeruginosa to hydrophilic contact lenses. J Clin Microbiol [Internet]. 1988 Mar [cited 2018 Nov 22];26(3):513–7. Available from: http://www.ncbi.nlm.nih.gov/pubmed/3128579

103. Garhwal R, Shady SF, Ellis EJ, Ellis JY, Leahy CD, McCarthy SP, et al. Sustained Ocular Delivery of Ciprofloxacin Using Nanospheres and Conventional Contact Lens Materials. Investig Opthalmology Vis Sci [Internet]. 2012 Mar 13 [cited 2018 Apr 6];53(3):1341. Available from: http://iovs.arvojournals.org/article.aspx?doi=10.1167/iovs.11-8215
104. Ludwicka A, Jansen B, Wadström T, Switalski LM, Peters G, Pulverer G. Attachment of Staphylococci to Various Synthetic Polymers. In: Polymers as Biomaterials [Internet]. Boston, MA: Springer US; 1984 [cited 2017 Jun 20]. p. 241–55. Available from: http://link.springer.com/10.1007/978-1-4613-2433-1_17
105. Wilson SL, Ahearne M, Hopkinson A. An overview of current techniques for ocular toxicity testing. Toxicology [Internet]. 2015 Jan 2 [cited 2018 Sep 6];327:32–46. Available from: https://www.sciencedirect.com/science/article/pii/S0300483X14002157#bib0595
106. Oecd. OECD/OCDE 405 OECD GUIDELINE FOR THE TESTING OF CHEMICALS Acute Eye Irritation/Corrosion INTRODUCTION [Internet]. 2012 [cited 2018 Sep 6]. Available from: https://ntp.niehs.nih.gov/iccvam/suppdocs/feddocs/oecd/oecd-tg405-2012-508.pdf
107. Steiling W, Bracher M, Courtellemont P, de Silva O. The HET–CAM, a Useful In Vitro Assay for Assessing the Eye Irritation Properties of Cosmetic Formulations and Ingredients. Toxicol Vitr [Internet]. 1999 Apr 1 [cited 2018 Sep 6];13(2):375–84. Available from: https://www.sciencedirect.com/science/article/pii/S0887233398000915#BIB4
108. Barile FA. Validating and troubleshooting ocular invitro toxicology tests. J Pharmacol Toxicol Methods [Internet]. 2010 Mar 1 [cited 2018 Sep 11];61(2):136–45. Available from: https://www.sciencedirect.com/science/article/pii/S1056871910000031

109. Parish WE. Ability of in vitro (corneal injury—eye organ— and chorioallantoic membrane) tests to represent histopathological features of acute eye inflammation. Food Chem Toxicol [Internet]. 1985 Feb [cited 2018 Sep 11];23(2):215–27. Available from: http://linkinghub.elsevier.com/retrieve/pii/0278691585900201
110. Tufan A, Satiroglu-Tufan N. The Chick Embryo Chorioallantoic Membrane as a Model System for the Study of Tumor Angiogenesis, Invasion and Development of Anti-Angiogenic Agents. Curr Cancer Drug Targets [Internet]. 2005 Jun 1 [cited 2018 Sep 12];5(4):249–66. Available from: http://www.eurekaselect.com/openurl/content.php?genre=article&issn=1568-0096&volume=5&issue=4&spage=249
111. Nowak-Sliwinska P, Segura T, Iruela-Arispe ML. The chicken chorioallantoic membrane model in biology, medicine and bioengineering. Angiogenesis [Internet]. 2014 Oct [cited 2018 Sep 13];17(4):779–804. Available from: http://www.ncbi.nlm.nih.gov/pubmed/25138280
112. Alany RG, Rades T, Nicoll J, Tucker IG, Davies NM. W/O microemulsions for ocular delivery: Evaluation of ocular irritation and precorneal retention. J Control Release [Internet]. 2006 Mar 10 [cited 2018 Apr 7];111(1–2):145–52. Available from: http://www.ncbi.nlm.nih.gov/pubmed/16426694
113. GAUTHERON P, DUKIK M, ALIX D, SINA JF. Bovine Corneal Opacity and Permeability Test: An *in Vitro* Assay of Ocular Irritancy. Toxicol Sci [Internet]. 1992 Apr 1 [cited 2018 Sep 12];18(3):442–9. Available from: https://academic.oup.com/toxsci/article-lookup/doi/10.1093/toxsci/18.3.442
114. Chiou GCY. Ophthalmic toxicology [Internet]. Taylor & Francis; 1999 [cited 2018 Sep 12]. Available from: https://books.google.co.uk/books?id=Xo8ZKwCm-2sC&pg=PA89&lpg=PA89&dq=Species+specificity:+Factors+affecting+the+interpretation+of+species+differences+in+toxic+responses+of+ocular+tissues&source=bl&ots=ht9EQ2z9qZ&sig=GHPlXNHW7Ga2pCn-

Ly2TzLU4Qzg&hl=en&sa=X&ved=2ahUKEwjYqrLl6rXdAhVGSsAKHfONCpsQ6AEwAXoECAgQAQ#v=onepage&q=Species specificity%3A Factors affecting the interpretation of species differences in toxic responses of ocular tissues&f=false

115. A Elshanawane A. Development and Validation of HPLC Method for Simultaneous Estimation of Brimonidine Tartrate and Timolol Maleate in Bulk and Pharmaceutical Dosage Form. J Chromatogr Sep Tech [Internet]. 2014 [cited 2018 Aug 3];05(03). Available from: http://omicsonline.org/open-access/development-and-validation-of-hplc-method-for-simultaneous-estimation-of-brimonidine-tartrate-and-timolol-maleate-in-bulk-and-pharmaceutical-dosage-form-2157-7064.1000230.php?aid=29720
116. Abdul Rasool Hassan B. HPLC Uses and Importance in the Pharmaceutical Analysis and Industrial. 2012 [cited 2018 Aug 3]; Available from: https://www.omicsonline.org/hplc-uses-and-importance-in-the-pharmaceutical-analysis-and-industrial-field-2153-2435.1000e133.pdf
117. Ashfaq M, Khan IU, Asghar MN. High‐Performance Liquid Chromatography Determination of Latanoprost in Pharmaceutical Formulations using UV Detection. Anal Lett [Internet]. 2006 Aug [cited 2018 Aug 3];39(11):2235–42. Available from: http://www.tandfonline.com/doi/abs/10.1080/00032710600755330
118. Nikolin B, Imamović B, Medanhodžić-Vuk S, Sober M, Sober M. High performance liquid chromatography in pharmaceutical analyses. Bosn J Basic Med Sci [Internet]. 2004 May 20 [cited 2018 Aug 3];4(2):5. Available from: http://www.bjbms.org/ojs/index.php/bjbms/article/view/3405
119. Mathrusri Annapurna M, Narendra A, Deepika D. DEVELOPMENT AND VALIDATION OF RP-HPLC METHOD FOR SIMULTANEOUS DETERMINATION OF DORZOLAMIDE AND TIMOLOL MALEATE IN PHARMACEUTICAL DOSAGE FORMS. J Drug Deliv Ther [Internet]. 2012 Mar 15 [cited 2018 Aug 3];2(2). Available from: http://jddtonline.info/index.php/jddt/article/view/120

120. Narendra A, Deepika D, Annapurna MM. Validated LC Method for the Estimation of Dorzolamide HCl (Carbonic Anhydrase Inhibitor) in Ophthalmic Solutions. E-Journal Chem [Internet]. 2012 [cited 2018 Aug 4];9(3):1238–43. Available from: http://www.hindawi.com/journals/jchem/2012/258261/
121. A. R. Polawar MCD. Development and Validation of Rp-Hplc Method for estimation of lurasidone hydrochloride in bulk and pharmaceutical dosage form. Int J Res Pharm Chem. 2014;4(2):327–32.
122. Waghule SN, Jain NP, Patani CJ, Patani AC. Method development and validation of HPLC method for determination of azithromycin. Pharma Chem [Internet]. 2013;5(4):166–72. Available from: http://derpharmachemica.com/archive.html
123. INTERNATIONAL CONFERENCE ON HARMONISATION OF TECHNICAL REQUIREMENTS FOR REGISTRATION OF PHARMACEUTICALS FOR HUMAN USE ICH HARMONISED TRIPARTITE GUIDELINE VALIDATION OF ANALYTICAL PROCEDURES: TEXT AND METHODOLOGY Q2(R1) [Internet]. [cited 2018 Aug 9]. Available from: https://www.ich.org/fileadmin/Public_Web_Site/ICH_Products/Guidelines/Quality/Q2_R1/Step4/Q2_R1__Guideline.pdf
124. Moorthy GS, Norris RE, Adamson PC, Fox E. A liquid chromatography/tandem mass spectrometry method for determination of obatoclax in human plasma. J Chromatogr B Analyt Technol Biomed Life Sci [Internet]. 2014 Nov 15 [cited 2018 Aug 10];971:30–4. Available from: http://www.ncbi.nlm.nih.gov/pubmed/25261914
125. Ruzette A-VG, Mayes AM. A Simple Free Energy Model for Weakly Interacting Polymer Blends. [cited 2018 Feb 22]; Available from: https://www.ncnr.nist.gov/programs/sans/pdf/publications/0140.pdf
126. Kogej K, Ksenija. Thermodynamic Analysis of the Conformational Transition in Aqueous Solutions of Isotactic and Atactic Poly(Methacrylic Acid) and the Hydrophobic Effect. Polymers (Basel) [Internet]. 2016 Apr 28 [cited 2018 Feb 23];8(12):168. Available from: http://www.mdpi.com/2073-4360/8/5/168
127. Sonia TA, Sharma CP, Sonia TA, Sharma CP. Polymers in oral insulin

delivery. Oral Deliv Insul [Internet]. 2014 Jan 1 [cited 2018 Aug 14];257–310. Available from: https://www.sciencedirect.com/science/article/pii/B9781907568473500069

128. Lawrence E N. CROSSLINKING-EFFECT ON PHYSICAL PROPERTIES OF POLYMERS [Internet]. monsanto/ Washington university; 1968 [cited 2018 Aug 17]. Available from: http://www.dtic.mil/dtic/tr/fulltext/u2/834683.pdf
129. Kopeček J. HYDROGELS FROM SOFT CONTACT LENSES AND IMPLANTS TO SELF-ASSEMBLED NANOMATERIALS. J Polym Sci A Polym Chem [Internet]. 2009 Nov 15 [cited 2018 Aug 15];47(22):5929–46. Available from: http://www.ncbi.nlm.nih.gov/pubmed/19918374
130. Findik F. A Case Study on the Selection of Materials for Eye Lenses. ISRN Mech Eng [Internet]. 2011 Apr 12 [cited 2018 Aug 14];2011:1–4. Available from: https://www.hindawi.com/archive/2011/160671/
131. Proença M, Carrilho F. Effect of Composition on the Drug Release Behaviour and Properties of Hydrogels for Contact Lenses [Internet]. 2016 [cited 2018 Nov 28]. Available from: https://fenix.tecnico.ulisboa.pt/downloadFile/1689244997255793/Extended Abstract_Magda Carrilho.pdf
132. Mohammed AH, Ahmad MB, Ibrahim NA, Zainuddin N. Effect of crosslinking concentration on properties of 3-(trimethoxysilyl) propyl methacrylate/N-vinyl pyrrolidone gels. Chem Cent J [Internet]. 2018 Feb 13 [cited 2018 Aug 16];12(1):15. Available from: http://www.ncbi.nlm.nih.gov/pubmed/29442180
133. Amsden B. Solute Diffusion within Hydrogels. Mechanisms and Models. 1998 [cited 2018 Aug 16]; Available from: http://vip.gatech.edu/wiki/images/b/bb/Solute_diffusion_within_hydrogels.pdf
134. Zhang X-Z, Wu D-Q, Chu C-C. Effect of the crosslinking level on the properties of temperature-sensitive poly(N-isopropylacrylamide) hydrogels. J Polym Sci Part B Polym Phys [Internet]. 2003 Mar 15 [cited 2018 Aug 16];41(6):582–93. Available from: http://doi.wiley.com/10.1002/polb.10388

135. Bolbukh Y, Tertykh V, Klonos P, Pissis P. DSC study of polyhydroxyethylmethacrylate filled with modified silicas. J Therm Anal Calorim [Internet]. 2012 Jun 16 [cited 2018 Nov 29];108(3):1111–9. Available from: http://link.springer.com/10.1007/s10973-011-2030-7
136. Ning L, Xu N, Xiao C, Wang R, Liu Y. Analysis for the Reaction of Hydroxyethyl Methacrylate/Benzoyl Peroxide/Polymethacrylate Through DSC and Viscosity Changing and Their Resultants as Oil Absorbent. J Macromol Sci Part A [Internet]. 2015 Dec 2 [cited 2018 Nov 29];52(12):1017–27. Available from: http://www.tandfonline.com/doi/full/10.1080/10601325.2015.1095605
137. Achilias D, Siafaka P. Polymerization Kinetics of Poly(2-Hydroxyethyl Methacrylate) Hydrogels and Nanocomposite Materials. Processes [Internet]. 2017 Apr 24 [cited 2018 Mar 1];5(4):21. Available from: http://www.mdpi.com/2227-9717/5/2/21
138. Guo X, Ge S, Wang J, Zhang X, Zhang T, Lin J, et al. Waterborne acrylic resin modified with glycidyl methacrylate (GMA): Formula optimization and property analysis. Polymer (Guildf) [Internet]. 2018 May 9 [cited 2018 Nov 29];143:155–63. Available from: https://www.sciencedirect.com/science/article/pii/S0032386118303070
139. PerkinElmer, Inc. Differential Scanning Calorimetry (DSC) PerkinElmer's DSC Family A Beginner's Guide. [cited 2018 Mar 1]; Available from: http://www.perkinelmer.co.uk/CMSResources/Images/44-74542GDE_DSCBeginnersGuide.pdf
140. Polacco G, Cascone MG, Petarca L, Peretti A. Thermal behaviour of poly(methacrylic acid)/poly(N-vinyl-2-pyrrolidone) complexes [Internet]. [cited 2018 Nov 29]. Available from: http://www1.diccism.unipi.it/Polacco_Giovanni/articoli/A20.pdf
141. Wanis Elshereksi N, Hamd Mohamed S, Arifin A, Arifin Mohd Ishak Z. Thermal Characterisation of Poly(Methyl Methacrylate) Filled with Barium Titanate as Denture Base Material. J Phys Sci [Internet]. 2014 [cited 2018 Mar 2];25(2):15–27. Available from: http://web.usm.my/jps/25-2-14/25-2-2.pdf
142. Kumar M, Chung J, Hur S. Controlled atom transfer radical

polymerization of MMA onto the surface of high-density functionalized graphene oxide. Nanoscale Res Lett [Internet]. 2014 [cited 2018 Nov 29];9(1):345. Available from: http://www.ncbi.nlm.nih.gov/pubmed/25114639

143. Kim D, Lee Y, Lee K, Choe S. Effect of Crosslinking Agents on the Morphology of Polymer Particles Produced by One-Step Seeded Polymerization [Internet]. Vol. 17, Macromolecular Research. 2009 [cited 2018 Nov 29]. Available from: https://www.cheric.org/PDF/MMR/MR17/MR17-4-0250.pdf
144. Schut J, Bolikal D, Khan I, Pesnell A, Rege A, Rojas R, et al. Glass transition temperature prediction of polymers through the mass-per-flexible-bond principle. Polymer (Guildf) [Internet]. 2007 Sep 21 [cited 2018 Aug 16];48(20):6115–24. Available from: http://www.ncbi.nlm.nih.gov/pubmed/18813337
145. Wang R-M, Zheng S-R, Zheng Y-P, Wang R-M, Zheng S-R, Zheng Y-P. Other properties of polymer composites. Polym Matrix Compos Technol [Internet]. 2011 Jan 1 [cited 2018 Nov 30];513–48. Available from: https://www.sciencedirect.com/science/article/pii/B9780857092212500114
146. Ogata M, Kinjo N, Kawata T. Effects of crosslinking on physical properties of phenol–formaldehyde novolac cured epoxy resins. J Appl Polym Sci [Internet]. 1993 Apr 20 [cited 2018 Aug 17];48(4):583–601. Available from: http://doi.wiley.com/10.1002/app.1993.070480403
147. Hogt AH, Gregonis DE, Andrade JD, Kim SW, Dankert J, Feijen J. Wettability and ζ potentials of a series of methacrylate polymers and copolymers. J Colloid Interface Sci [Internet]. 1985 Aug [cited 2018 Mar 2];106(2):289–98. Available from: http://linkinghub.elsevier.com/retrieve/pii/S0021979785800023
148. Klinger D. Light-Sensitive Polymeric Nanoparticles Based on Photo-Cleavable Chromophores [Internet]. Cham: Springer International Publishing; 2013 [cited 2018 Mar 3]. (Springer Theses). Available from: http://link.springer.com/10.1007/978-3-319-00446-4
149. Milichovsky M. Water—A Key Substance to Comprehension of Stimuli-

Responsive Hydrated Reticular Systems. J Biomater Nanobiotechnol [Internet]. 2010 Oct 30 [cited 2018 Mar 3];01(01):17–30. Available from: http://www.scirp.org/journal/doi.aspx?DOI=10.4236/jbnb.2010.11003

150. Justin Bergin. Contact Lens Polymers. In New York: State University of New York at Buffalo; 2000 [cited 2018 Feb 22]. Available from: http://wwwcourses.sens.buffalo.edu/ce435/2001ZGu/Contact_Lens/ContactLensReport.htm
151. Davis TP, Huglin MB. Effect of crosslinking on the properties of poly(2-hydroxyethyl methacrylate) hydrogels. Angew Makromol Chemie [Internet]. 1991 May 1 [cited 2018 Mar 4];189(1):195–205. Available from: http://doi.wiley.com/10.1002/apmc.1991.051890118
152. Seidel JM, Malmonge SM. Synthesis of polyHEMA hydrogels for using as biomaterials. Bulk and solution radical-initiated polymerization techniques. Mater Res [Internet]. 2000 Jul [cited 2018 Mar 3];3(3):79–83. Available from: http://www.scielo.br/scielo.php?script=sci_arttext&pid=S1516-14392000000300006&lng=en&tlng=en
153. Luo D, Li Y, Yang M. Preparation and characterization of novel crosslinked poly[glycidyl methacrylate-poly(ethylene glycol) methyl ether methacrylate] as gel polymer electrolytes. J Appl Polym Sci [Internet]. 2011 Jun 5 [cited 2018 Mar 3];120(5):2979–84. Available from: http://doi.wiley.com/10.1002/app.33363
154. Li Q-L, Gu W-X, Gao H, Yang Y-W. Self-assembly and applications of poly(glycidyl methacrylate)s and their derivatives. Chem Commun [Internet]. 2014 May 19 [cited 2018 Mar 3];50(87):13201–15. Available from: http://xlink.rsc.org/?DOI=C4CC03036B
155. Tranoudis I, Efron N. Water properties of soft contact lens materials. Contact Lens Anterior Eye. 2004;27(4):193–208.
156. Klykken P, Servinski M, Thomas X. Silicone Film-Forming Technologies for Health Care Applications. [cited 2018 Jan 18]; Available from: http://citeseerx.ist.psu.edu/viewdoc/download?doi=10.1.1.578.7746&re

p=rep1&type=pdf

157. Tighe, Brian. Brennan, Noel. Coles C. Chapter 5 Silicone Hydrogels - What are they and how should they be used in everyday practice? Optician. 1999;218(5726):161–219.
158. Stapleton F, Stretton S, Papas E, Skotnitsky C, Sweeney DF. Silicone Hydrogel Contact Lenses and the Ocular Surface. Ocul Surf [Internet]. 2006 Jan 1 [cited 2018 Jan 17];4(1):24–43. Available from: https://www.sciencedirect.com/science/article/pii/S1542012412702628
159. Lin C-H, Yeh Y-H, Lin W-C, Yang M-C. Novel silicone hydrogel based on PDMS and PEGMA for contact lens application. Colloids Surfaces B Biointerfaces [Internet]. 2014 Nov 1 [cited 2018 Jan 19];123:986–94. Available from: http://www.ncbi.nlm.nih.gov/pubmed/25465755
160. Lin MC, French HM, Graham AD, Sanders TL. Effects of Daily Irrigation on Corneal Epithelial Permeability and Adverse Events With Silicone Hydrogel Contact Lens Continuous Wear. Investig Opthalmology Vis Sci [Internet]. 2014 Feb 10 [cited 2018 Feb 1];55(2):776. Available from: http://iovs.arvojournals.org/article.aspx?doi=10.1167/iovs.13-13508
161. Spaeth V, Lecomte JP, Delplancke MP, Orlowsky J, Büttner T. Impact of Silane and Siloxane Based Hydrophobic Powder on Cement-Based Mortar. Adv Mater Res [Internet]. 2013 Apr [cited 2018 Jan 15];687:100–6. Available from: http://www.scientific.net/AMR.687.100
162. Kutz M. Applied plastics engineering handbook processing, materials, and applications. Willam Andrew; 2017.
163. Zeigler JM, Fearon FWG, American Chemical Society. Division of Polymer Chemistry., International Topical Workshop “Advances in Silicon-Based Polymer Science” (1987 : Makaha H. Silicon-based polymer science : a comprehensive resource [Internet]. Washington, DC: American Chemical Society; 1990 [cited 2018 Jan 8]. 801 p. Available from: https://catalyst.library.jhu.edu/catalog/bib_3900914
164. Abbasi F, Mirzadeh H, Simjoo M. Hydrophilic interpenetrating polymer networks of poly(dimethyl siloxane) (PDMS) as biomaterial for cochlear implants. J Biomater Sci Polym Ed [Internet]. 2006 Jan [cited 2018 Feb 1];17(3):341–55. Available from:

http://www.tandfonline.com/doi/abs/10.1163/156856206775997287

165. Dimitriya Bozukova †, Christophe Pagnoulle ‡, Marie-Claire De Pauw-Gillet §, Simon Desbief ‖, Roberto Lazzaroni ‖, Nadia Ruth ⊥, et al. Improved Performances of Intraocular Lenses by Poly(ethylene glycol) Chemical Coatings. 2007 [cited 2018 Feb 1]; Available from: http://pubs.acs.org/doi/abs/10.1021/bm0701649
166. Lin R-R, Mao X, Yu Q-C, Tan B-H. Preparation of bioactive nano-hydroxyapatite coating for artificial cornea. Curr Appl Phys [Internet]. 2007 Apr 1 [cited 2018 Feb 1];7:e85–9. Available from: https://www.sciencedirect.com/science/article/pii/S1567173906002318
167. Martín-Montañez V, López-Miguel A, Arroyo C, Mateo ME, González-Méijome JM, Calonge M, et al. Influence of environmental factors in the *in vitro* dehydration of hydrogel and silicone hydrogel contact lenses. J Biomed Mater Res Part B Appl Biomater [Internet]. 2014 May 1 [cited 2018 Feb 1];102(4):764–71. Available from: http://doi.wiley.com/10.1002/jbm.b.33057
168. van Beek M, Weeks A, Jones L, Sheardown H. Immobilized hyaluronic acid containing model silicone hydrogels reduce protein adsorption. J Biomater Sci Polym Ed [Internet]. 2008 Jan [cited 2018 Feb 1];19(11):1425–36. Available from: http://www.tandfonline.com/doi/abs/10.1163/156856208786140364
169. Polysiloxanes - by Lachelle Sussman [Internet]. [cited 2018 Jan 15]. Available from: http://wwwcourses.sens.buffalo.edu/ce435/Polysiloxanes/
170. Poly(dimethylsiloxane-co-alkylmethylsiloxane) | Sigma-Aldrich [Internet]. [cited 2018 Jan 19]. Available from: https://www.sigmaaldrich.com/catalog/product/aldrich/457655?lang=en&region=GB
171. Yui N, Mrsny RJ, Park K. Reflexive polymers and hydrogels : understanding and designing fast responsive polymeric systems [Internet]. CRC Press; 2004 [cited 2018 Jan 8]. 452 p. Available from: https://books.google.co.uk/books?id=UNHLaj90Jd0C&pg=PA190&lpg=PA190&dq=when+a+hydrophilic+and+hydrophobic+balance+is+reach

ed+the+equilibrium+water+content+will+no+longer+increase+within+contact+lenses&source=bl&ots=NsYi3oED4r&sig=yvMTf64WgXyBAFifuBCyd-LeuTA&hl=en&sa=X&ved=0ahUKEwjD8tWan8nYAhVHDMAKHXKmAGEQ6AEIKTAA#v=onepage&q=when a hydrophilic and hydrophobic balance is reached the equilibrium water content will no longer increase within contact lenses&f=true

172. Maldonado-Codina C, Morgan PB. In vitro water wettability of silicone hydrogel contact lenses determined using the sessile drop and captive bubble techniques. J Biomed Mater Res Part A [Internet]. 2007 Nov 1 [cited 2018 Jan 18];83A(2):496–502. Available from: http://doi.wiley.com/10.1002/jbm.a.31260
173. Quéré D. Wetting and Roughness. Annu Rev Mater Res [Internet]. 2008 Aug 8 [cited 2018 Jan 18];38(1):71–99. Available from: http://www.annualreviews.org/doi/10.1146/annurev.matsci.38.060407.132434
174. Tighe BJ. A Decade of Silicone Hydrogel Development. Eye Contact Lens Sci Clin Pract [Internet]. 2013 Jan [cited 2018 Jan 18];39(1):1. Available from: http://www.ncbi.nlm.nih.gov/pubmed/23292050
175. Park J, Kim J, Kim S-Y, Cheong WH, Jang J, Park Y-G, et al. Soft, smart contact lenses with integrations of wireless circuits, glucose sensors, and displays. Sci Adv [Internet]. 2018 Jan 24 [cited 2018 Aug 23];4(1):eaap9841. Available from: http://advances.sciencemag.org/lookup/doi/10.1126/sciadv.aap9841
176. Harris MG, Chamberlain MD. Light transmission of hydrogel contact lenses. Am J Optom Physiol Opt [Internet]. 1978 Feb [cited 2018 Jan 19];55(2):93–6. Available from: http://www.ncbi.nlm.nih.gov/pubmed/677252
177. Fuentes R, Fernández E, Pascual I, García C. UV-visible transmittance of silicone-hydrogel contact lenses measured with a fiber optic spectrometer. 2013;8785:8785AZ.
178. Explanation of contact lens properties and features [Internet]. [cited 2018 Jan 19]. Available from: https://www.jnjvisioncare.co.uk/education/balance-of-

properties/explanation-of-contact-lens-properties-and-features
179. Mechanical Properties of Contact Lenses: The Contribution of Measurement 1 Techniques and Clinical Feedback to 50 Years of Materials Development [Internet]. 2016 [cited 2019 Feb 21]. Available from: http://creativecommons.org/licenses/by-nc-nd/4.0/2
180. Filipecka K, Budaj M, Chamerski K, Miedziński R, Sitarz M, Miskowiak B, et al. PALS, MIR and UV–vis–NIR spectroscopy studies of pHEMA hydrogel, silicon- and fluoro-containing contact lens materials. J Mol Struct [Internet]. 2017 Nov 15 [cited 2018 Jan 19];1148:521–30. Available from: https://www.sciencedirect.com/science/article/pii/S002228601731027X
181. Pasquet C, Longuet C, Hamdani-Devarennes S, Ameduri B, Ganachaud F. Comparison of Surface and Bulk Properties of Pendant and Hybrid Fluorosilicones. In Springer, Dordrecht; 2012 [cited 2018 Jan 19]. p. 115–78. Available from: http://www.springerlink.com/index/10.1007/978-94-007-3876-8_5
182. Chen R, Qian Y, Li R, Zhang Q, Liu D, Wang M, et al. Methazolamide calcium phosphate nanoparticles in an ocular delivery system. Yakugaku Zasshi [Internet]. 2010 Mar [cited 2018 Aug 29];130(3):419–24. Available from: http://www.ncbi.nlm.nih.gov/pubmed/20190526
183. Wadhwa S, Paliwal R, Paliwal SR, Vyas SP. Nanocarriers in ocular drug delivery: an update review. Curr Pharm Des [Internet]. 2009 [cited 2018 Dec 6];15(23):2724–50. Available from: http://www.ncbi.nlm.nih.gov/pubmed/19689343
184. Xu Q, Kambhampati SP, Kannan RM. Nanotechnology approaches for ocular drug delivery. Middle East Afr J Ophthalmol [Internet]. 2013 [cited 2018 Aug 25];20(1):26–37. Available from: http://www.ncbi.nlm.nih.gov/pubmed/23580849
185. Silva MM, Calado R, Marto J, Bettencourt A, Almeida AJ, Gonçalves LMD. Chitosan Nanoparticles as a Mucoadhesive Drug Delivery System for Ocular Administration. Mar Drugs [Internet]. 2017 Dec 1 [cited 2018 Sep 24];15(12). Available from: http://www.ncbi.nlm.nih.gov/pubmed/29194378
186. Muter MA. Synthesis and Biocompatibility of New Contact Lenses

Based On Derivatives of 2-Hydroxy Ethyl Meth Acrylate and 2-Ethyl Hexyl Methacrylate. Int J Res Stud Biosci [Internet]. 2015 [cited 2018 Dec 6];3(3):152–60. Available from: www.arcjournals.org

187. Thakur A, Wanchoo RK SP. Chemical and biochemical engineering quarterly. Chem Biochem Eng Q [Internet]. 2011 Jan 22 [cited 2018 Dec 6];25(4):471–82. Available from: https://hrcak.srce.hr/76440?lang=en
188. El Shaer A, Mustafa S, Kasar M, Thapa S, Ghatora B, Alany RG. Nanoparticle-laden contact lens for controlled ocular delivery of prednisolone: Formulation optimization using statistical experimental design. Pharmaceutics. 2016;8(2).
189. Lee KD, Jeong Y-I, Kim DH, Lim G-T, Choi K-C. Cisplatin-incorporated nanoparticles of poly(acrylic acid-co-methyl methacrylate) copolymer. Int J Nanomedicine [Internet]. 2013 [cited 2018 May 27];8:2835–45. Available from: http://www.ncbi.nlm.nih.gov/pubmed/23966778
190. Amrite AC, Kompella UB. Size-dependent disposition of nanoparticles and microparticles following subconjunctival administration. J Pharm Pharmacol [Internet]. 2005 Dec [cited 2018 Aug 25];57(12):1555–63. Available from: http://www.ncbi.nlm.nih.gov/pubmed/16354399
191. Ban J, Zhang Y, Huang X, Deng G, Hou D, Chen Y, et al. Corneal permeation properties of a charged lipid nanoparticle carrier containing dexamethasone. Int J Nanomedicine [Internet]. 2017 [cited 2018 Aug 25];12:1329–39. Available from: http://www.ncbi.nlm.nih.gov/pubmed/28243093
192. Peppas NA, Buri PA. Surface, interfacial and molecular aspects of polymer bioadhesion on soft tissues. J Control Release [Internet]. 1985 Nov 1 [cited 2018 May 29];2:257–75. Available from: https://www.sciencedirect.com/science/article/pii/0168365985900501
193. Katiyar S, Pandit J, Mondal RS, Mishra AK, Chuttani K, Aqil M, et al. In situ gelling dorzolamide loaded chitosan nanoparticles for the treatment of glaucoma. Carbohydr Polym [Internet]. 2014 Feb 15 [cited 2018 May 30];102:117–24. Available from: https://www.sciencedirect.com/science/article/pii/S0144861713011089?via%3Dihub

194. Moharram MA, Allam MA. Study of the interaction of poly(acrylic acid) and poly(acrylic acid-poly acrylamide) complex with bone powders and hydroxyapatite by using TGA and DSC. J Appl Polym Sci [Internet]. 2007 Sep 15 [cited 2018 May 31];105(6):3220–7. Available from: http://doi.wiley.com/10.1002/app.26267
195. Caló E, Khutoryanskiy V V. Biomedical applications of hydrogels: A review of patents and commercial products. Eur Polym J [Internet]. 2015 Apr [cited 2017 Nov 3];65:252–67. Available from: http://linkinghub.elsevier.com/retrieve/pii/S0014305714004091
196. Alderson A. Soft Contact Lens Material Properties. Acad Vis Care. 1999;1–10.
197. Cerca N, Pier GB, Vilanova M, Oliveira R, Azeredo J. Quantitative analysis of adhesion and biofilm formation on hydrophilic and hydrophobic surfaces of clinical isolates of Staphylococcus epidermidis. Res Microbiol [Internet]. 2005 May [cited 2017 Oct 19];156(4):506–14. Available from: http://www.ncbi.nlm.nih.gov/pubmed/15862449
198. Ademović Z, Marić S, Kingshott P, Iličković Z. HYDROGELS FROM POLYACRYLIC ACID FOR REDUCTION OF BIOADHESION ON SILICONE CONTACT LENSES. Contemp Mater [Internet]. 2014 Sep 26 [cited 2018 Dec 6];1(5):95–100. Available from: http://doisrpska.nub.rs/index.php/conterporarymaterials3-1/article/view/1504
199. Campbell D, Carnell SM, Eden RJ. Applicability of contact angle techniques used in the analysis of contact lenses, part 1: comparative methodologies. Eye Contact Lens. 2013;39(3):254–62.
200. Gause S, Chauhan A. Incorporation of ultraviolet (UV) absorbing nanoparticles in contact lenses for Class 1 UV blocking. J Mater Chem B [Internet]. 2016 Dec 23 [cited 2018 Jun 1];4(2):327–39. Available from: http://xlink.rsc.org/?DOI=C5TB01532D
201. Tranoudis I, Efron N. Tensile properties of soft contact lens materials. Contact Lens Anterior Eye. 2004;27(4):177–91.
202. Vasita R, Mani G, Agrawal CM, Katti DS. Surface hydrophilization of electrospun PLGA micro-/nano-fibers by blending with Pluronic® F-

108. Polymer (Guildf) [Internet]. 2010 Jul 22 [cited 2018 Jun 4];51(16):3706–14. Available from: https://www.sciencedirect.com/science/article/pii/S0032386110004763?via%3Dihub
203. Joseph RR, Venkatraman SS. Drug delivery to the eye: what benefits do nanocarriers offer? Nanomedicine [Internet]. 2017 Mar 10 [cited 2018 Jun 4];12(6):683–702. Available from: http://www.futuremedicine.com/doi/10.2217/nnm-2016-0379
204. Manchanda S, Sahoo PK. Topical delivery of acetazolamide by encapsulating in mucoadhesive nanoparticles. Asian J Pharm Sci [Internet]. 2017 Nov 1 [cited 2018 Jun 4];12(6):550–7. Available from: https://www.sciencedirect.com/science/article/pii/S1818087616302902
205. Gupta P, Vermani K, Garg S. Hydrogels: From controlled release to pH-responsive drug delivery. Drug Discov Today. 2002;7(10):569–79.
206. M.A. Fathalla Z, Vangala A, Longman M, Khaled KA, Hussein AK, El-Garhy OH, et al. Poloxamer-based thermoresponsive ketorolac tromethamine in situ gel preparations: Design, characterisation, toxicity and transcorneal permeation studies. Eur J Pharm Biopharm [Internet]. 2017 May [cited 2018 Sep 18];114:119–34. Available from: http://www.ncbi.nlm.nih.gov/pubmed/28126392
207. Schafer J, Steffen R, Reindel W, Chinn J. evaluation of surface water characteristics of novel daily disposable contact lens materials, using refractive index shifts after wear. 2015 [cited 2017 Sep 21]; Available from: https://www.ncbi.nlm.nih.gov/pmc/articles/PMC4622526/pdf/opth-9-1973.pdf
208. Pozuelo J, Compañ V, González-Méijome JM, González M, Mollá S. Oxygen and ionic transport in hydrogel and silicone-hydrogel contact lens materials: An experimental and theoretical study. J Memb Sci [Internet]. 2014 [cited 2017 Sep 28];452:62–72. Available from: https://ac.els-cdn.com/S0376738813008107/1-s2.0-S0376738813008107-main.pdf?_tid=d14c618e-a46e-11e7-8f0e-00000aab0f26&acdnat=1506618333_8988a860bb8ceb1677fe3f6c4fc10e86
209. Wu J, Xu Y, Dabros T, Hamza H. Effect of EO and PO positions in

nonionic surfactants on surfactant properties and demulsification performance. Colloids Surfaces A Physicochem Eng Asp. 2005;252(1):79–85.

210. Caló E, Khutoryanskiy V V. Biomedical applications of hydrogels: A review of patents and commercial products. Eur Polym J. 2015;65:252–67.
211. Kodjikian L, Casoli-Bergeron E, Malet F, Janin-Manificat H, Freney J, Burillon C, et al. Bacterial adhesion to conventional hydrogel and new silicone-hydrogel contact lens materials. Graefe's Arch Clin Exp Ophthalmol. 2008;246(2):267–73.
212. ATP Bioluminescence Assay Kit HS II [Internet]. Mannheim, Germany ; 2014 [cited 2017 Nov 16]. Available from: https://www.sigmaaldrich.com/content/dam/sigma-aldrich/docs/Roche/Bulletin/1/11699709001bul.pdf
213. Le Magrex E, Brisset L, Jacquelin LF, Carquin J, Bonnaveiro N, Choisy C. Susceptibility to antibacterials and compared metabolism of suspended bacteria versus embedded bacteria in biofilms. Colloids Surfaces B Biointerfaces [Internet]. 1994 Mar [cited 2017 Sep 8];2(1–3):89–95. Available from: http://linkinghub.elsevier.com/retrieve/pii/0927776594800227
214. Aswad MI, John T, Barza M, Kenyon K, Baum J. Bacterial adherence to extended wear soft contact lenses. Ophthalmology [Internet]. 1990 Mar [cited 2017 Nov 24];97(3):296–302. Available from: http://www.ncbi.nlm.nih.gov/pubmed/2110642
215. Hahn HP. The type-4 pilus is the major virulence-associated adhesin of Pseudomonas aeruginosa - A review. In: Gene [Internet]. Elsevier; 1997 [cited 2017 Nov 20]. p. 99–108. Available from: http://www.sciencedirect.com/science/article/pii/S0378111997001169?via%3Dihub
216. de Kerchove AJ, Elimelech M. Impact of alginate conditioning film on deposition kinetics of motile and nonmotile Pseudomonas aeruginosa strains. Appl Environ Microbiol [Internet]. 2007 Aug 15 [cited 2017 Dec 15];73(16):5227–34. Available from: http://www.ncbi.nlm.nih.gov/pubmed/17574995

217. Robertson DM, Parks QM, Young RL, Kret J, Poch KR, Malcolm KC, et al. Disruption of Contact Lens–Associated *Pseudomonas aeruginosa* Biofilms Formed in the Presence of Neutrophils. Investig Opthalmology Vis Sci [Internet]. 2011 Apr 27 [cited 2017 Dec 15];52(5):2844. Available from: http://www.ncbi.nlm.nih.gov/pubmed/21245396
218. Shida T, Koseki H, Yoda I, Horiuchi H, Sakoda H, Osaki M. Adherence ability of Staphylococcus epidermidis on prosthetic biomaterials: an in vitro study. Int J Nanomedicine [Internet]. 2013 [cited 2017 Dec 14];8:3955–61. Available from: http://www.ncbi.nlm.nih.gov/pubmed/24143100
219. Batzilla CF, Rachid S, Engelmann S, Hecker M, Hacker J, Ziebuhr W. Impact of the accessory gene regulatory system (Agr) on extracellular proteins,codY expression and amino acid metabolism inStaphylococcus epidermidis. Proteomics [Internet]. 2006 Jun [cited 2017 Dec 14];6(12):3602–13. Available from: http://www.ncbi.nlm.nih.gov/pubmed/16691552
220. Marshall KC, Stout R, Mitchell R. Mechanism of the Initial Events in the Sorption of Marine Bacteria to Surfaces. J Gen Microbiol [Internet]. 1971 [cited 2017 Dec 14];68(3):337–48. Available from: http://www.microbiologyresearch.org/docserver/fulltext/micro/68/3/mic-68-3-337.pdf?expires=1513266501&id=id&accname=guest&checksum=D266A1A46CCC6541F8D7241EC42871E2
221. Sousa C, Teixeira P, Oliveira R. Influence of Surface Properties on the Adhesion of Staphylococcus epidermidis to Acrylic and Silicone. Int J Biomater [Internet]. 2009 Jan 25 [cited 2017 Oct 19];2009:718017. Available from: http://www.ncbi.nlm.nih.gov/pubmed/20126579
222. Carney FP, Nash WL, Sentell KB. The Adsorption of Major Tear Film Lipids In Vitro to Various Silicone Hydrogels over Time. Investig Opthalmology Vis Sci [Internet]. 2008 Jan 1 [cited 2017 Dec 15];49(1):120. Available from: http://iovs.arvojournals.org/article.aspx?doi=10.1167/iovs.07-0376
223. Sulym IY, Borysenko MV, Goncharuk OV, Terpilowski K, Sternik D, Chibowski E, et al. Structural and hydrophobic–hydrophilic properties

of nanosilica/zirconia alone and with adsorbed PDMS. Appl Surf Sci [Internet]. 2011 Oct 15 [cited 2017 Dec 15];258(1):270–7. Available from: https://www.sciencedirect.com/science/article/pii/S0169433211012736

224. Dutta D, Science V. A Laboratory Assessment of Factors That Affect Bacterial Adhesion to Contact Lenses. Biology (Basel). 2013;2:1268–81.
225. M.A. Fathalla Z, Vangala A, Longman M, Khaled KA, Hussein AK, El-Garhy OH, et al. Poloxamer-based thermoresponsive ketorolac tromethamine in situ gel preparations: Design, characterisation, toxicity and transcorneal permeation studies. Eur J Pharm Biopharm [Internet]. 2017 May [cited 2018 Nov 1];114:119–34. Available from: https://linkinghub.elsevier.com/retrieve/pii/S0939641117301017
226. Chen Y, Lu Y, Zhong Y, Wang Q, Wu W, Gao S. Ocular delivery of cyclosporine A based on glyceryl monooleate/poloxamer 407 liquid crystalline nanoparticles: preparation, characterization, *in vitro* corneal penetration and ocular irritation. J Drug Target [Internet]. 2012 Dec 11 [cited 2018 Dec 11];20(10):856–63. Available from: http://www.tandfonline.com/doi/full/10.3109/1061186X.2012.723214

P